UDC 502/504; 57; 63

SCIENTIFIC REPORTS OF THE NATIONAL UNIVERSITY OF LIFE AND ENVIRONMENTAL SCIENCES OF UKRAINE

Founder:
National University of Life and Environmental Sciences of Ukraine

Year of foundation: 2005

Recommended for printing and distribution via the Internet by the Academic Council of National University of Life and Environmental Sciences of Ukraine (Minutes No. 11 of April 23, 2026)

State Registration:
Media identifier - R40-02082.
Decision of the National Council of Television and Radio Broadcasting of Ukraine No. 1471, Minutes No. 28, dated 23.11.2023.

The journal is included in the list of Professional Scientific Publications of Ukraine
Category “B”. Specialties: 0511 – Biology, 0521 – Environmental Sciences, 0522 – Natural Environments and Wildlife, 0512 – Biochemistry, 0811 – Crop and Livestock Production, 0821 – Forestry, 0812 – Horticulture, 0841 – Veterinary (Order of the Ministry of Education and Science of Ukraine No. 409 of 14 March 2020), 0715 – Mechanics and Metal Trades, 0716 – Motor Vehicles, Ships and Aircraft (Order of the Ministry of Education and Science of Ukraine No. 886 of 02 July 2020).

The journal is presented international scientometric databases, repositories and scientific systems:
Google Scholar, Vernadsky National Library of Ukraine, BASE, AGRIS, Ulrichsweb, ERIH PLUS, Dimensions, University of Oslo Library, OUCI (Open Ukrainian Citation Index), Polska Bibliografia Naukowa, DOAJ, CABI, Litmaps, EBSCO, J-Gate, Research4Life

Editors office address:
National University of Life and Environmental Sciences of Ukraine
03041, 15 Heroiv Oborony Str., Kyiv, Ukraine
E-mail: sr@scireports.com.ua
https://scireports.com.ua/en

УДК 502/504; 57; 63

НАУКОВІ ДОПОВІДІ НАЦІОНАЛЬНОГО УНІВЕРСИТЕТУ БІОРЕСУРСІВ І ПРИРОДОКОРИСТУВАННЯ УКРАЇНИ

Засновник:
Національний університет біоресурсів і природокористування України

Рік заснування: 2005

*Рекомендовано до друку та поширення
через мережу Інтернет Вченою радою
Національного університету біоресурсів і природокористування України
(протокол № 11 від 23 квітня 2026 р.)*

Державна реєстрація:
Ідентифікатор медіа – R40-02082.
Рішення Національної Ради України з питань телебачення і радіомовлення
№ 1471, протокол № 28 від 23.11.2023 р.

Журнал входить до переліку
наукових фахових видань України
Категорія «Б». Спеціальності: 091 – Біологія, 101 – Екологія, 162 – Біотехнології та біоінженерія, 201 – Агрономія, 204 – Технологія виробництва і переробки продукції тваринництва, 205 – Лісове господарство, 206 – Садово-паркове господарство, 211 – Ветеринарна медицина, 212 – Ветеринарна гігієна, санітарія і експертиза (наказ МОН України № 409 від 14 березня 2020 року),
131 – Прикладна механіка, 133 – Галузеве машинобудування
(наказ МОН України № 886 від 02 липня 2020 року).

Журнал представлено у міжнародних наукометричних базах даних,
репозитаріях та пошукових системах:
Google Scholar, Національна бібліотека України імені В. І. Вернадського, BASE, AGRIS, Ulrichsweb, ERIH PLUS, Dimensions, University of Oslo Library, OUCI (Open Ukrainian Citation Index), Polska Bibliografia Naukowa, DOAJ, CABI, Litmaps, EBSCO, J-Gate, Research4Life

Адреса редакції:
Національний університет біоресурсів і природокористування України
03041, вул. Героїв Оборони, 15, м. Київ, Україна
E-mail: sr@scireports.com.ua
https://scireports.com.ua/uk

Contents

Зміст

Received 14.11.2025 Revised 20.02.2026 Accepted 23.04.2026 Published: 30.04.2026

Vol. 22, No. 2
2026

Scientific Reports of the National University of Life and Environmental Sciences of Ukraine

Journal homepage: https://scireports.com.ua/en e-ISSN 2223-1609

UDC 581.15:547.97:634.11613.2(477) DOI: 10.31548/dopovidi/2.2026.07

Bioactive compounds in red-fleshed apple germplasm

Dmytro Pyshcholka
Postgraduate Student
National University of Life and Environmental Sciences of Ukraine
03041, 15 Heroiv Oborony Str., Kyiv, Ukraine
http://orcid.org/0009-0001-9025-4463

Volodymyr Mezhenskyj*
Doctor of Agricultural Sciences, Senior Researcher
National University of Life and Environmental Sciences of Ukraine
03041, 15 Heroiv Oborony Str., Kyiv, Ukraine
https://orcid.org/0000-0002-3154-1120

Abstract. Red-fleshed apple cultivars of the *Malus domestica* Niedzwetzkyana Group have attracted increasing attention due to their distinctive pigmentation and elevated levels of health-promoting phytochemicals. This study aimed to evaluate the biochemical composition and variability of major bioactive compounds in red-fleshed apple cultivars grown in the forest-steppe zone of Ukraine. Eleven cultivars were investigated over three growing seasons (2023-2025). The content of ascorbic acid, total polyphenols, anthocyanins, flavonols, and chalcones was determined using standard spectrophotometric and titrimetric methods. The results revealed substantial biochemical diversity among the studied genotypes. The content of ascorbic acid ranged from 5.06 to 11.41 mg/100 g fresh weight and did not differ significantly among cultivars. In contrast, pronounced differences were observed in the accumulation of phenolic compounds. The highest total polyphenol concentrations were recorded in cultivars 'Jurgen' (636.50 mg/100 g) and 'Firecracker' (621.63 mg/100 g). Anthocyanin and chalcone contents showed considerable variation, with the highest values detected in 'Dr Campbell' (31.86 mg/100 g and 22.20 mg/100 g, respectively). Statistical analysis yielded a coefficient of determination ($R^2 = 0.81$), suggesting that chalcone concentration accounts for 81% of the observed variability in anthocyanin levels. The cultivars 'Era' and 'Jurgen' demonstrated the highest flavonol accumulation (79.10 mg/100 g and 65.90 mg/100 g, respectively). Overall, 'Dr Campbell', 'Cranberry', and 'Jurgen' were identified as the most promising genotypes due to their favourable combination of

Suggested Citation:
Pyshcholka, D., & Mezhenskyj, V. (2026). Bioactive compounds in red-fleshed apple germplasm. *Scientific Reports of the National University of Life and Environmental Sciences of Ukraine*, 22(2), 7-19. doi: 10.31548/dopovidi/2.2026.07.

**Corresponding author*

high phenolic content and pigment accumulation. The results highlight the significant nutritional and breeding potential of red-fleshed apple cultivars and support their wider introduction into horticultural production and functional food development in Ukraine

Keywords: *Malus domestica* Niedzwetzkyana Group; ascorbic acid; polyphenols; anthocyanins; flavonols; chalcones

Introduction

Apples (*Malus domestica* (Suckow) Borkh.) are among the most widely cultivated and consumed fruit crops in the world and represent an important component of a healthy human diet. According to the Food and Agriculture Organization of the United Nations (FAO) (2025), global apple production exceeds 97 million tonnes annually, while Ukraine produces more than 1 million tonnes. Apples are the most popular fruit in Ukraine and are valued not only for their taste but also for their nutritional and biological properties.

The health-promoting value of apples is largely associated with their rich content of biologically active compounds, including polyphenols, flavonoids, and vitamin C. These substances contribute to fruit colour, flavour, and aroma while exhibiting strong antioxidant activity (Asma *et al.*, 2023). Polyphenols and related compounds have been associated with anti-inflammatory, cardioprotective, and other health-promoting effects (Catalán *et al.*, 2022). In apples, many of these compounds are concentrated in the peel; however, because consumers generally eat more flesh than peel, their intake of beneficial compounds may be limited (Juhart *et al.*, 2022).

A special group of apple cultivars accumulates anthocyanins not only in the peel but also in the fruit flesh (Bu *et al.*, 2025). These red-fleshed apples belong to *Malus domestica* f. *niedzwetzkyana* (Dieck) Mezhenskyj, commonly referred to as the Niedzwetzkyana Group (Mezhenskyj *et al.*, 2024). They attract increasing interest because of their unique pigmentation and high content of bioactive compounds. The presence of anthocyanins in the flesh significantly increases the content of flavonoids, making these cultivars of particular interest for both nutrition and breeding. Studies by J. Juhart *et al*. 2022) have shown that red-fleshed cultivars may contain higher levels of anthocyanins, flavonols, and dihydrochalcones compared with traditional white-fleshed varieties such as ‘Golden Delicious’. The red coloration of apple flesh is determined by the anthocyanin biosynthetic pathway. Genomic studies by Z. Li *et al*. (2023) and S. Keller-Przybylkowicz *et al*. (2025) have identified numerous regulatory genes, particularly transcription factors of the MYB family, which, together with other structural genes, control anthocyanin accumulation in the fruit. Flavonoids formed through this pathway also play an important role in plant protection and stress resistance, while demonstrating antioxidant and antibacterial properties, as stated by Y. Chen *et al*. (2023). These bioactive compounds specifically exhibit hepatoprotective effects by reducing oxidative stress and modulating the composition of intestinal microorganisms. In particular, the study demonstrated that these extracts effectively reduce the levels of malondialdehyde in liver tissues, thereby preventing lipid peroxidation and cellular damage. Furthermore, the researchers observed that the flavonoids promote the growth of beneficial probiotic bacteria, such as *Lactobacillus*, which reinforces the host’s overall immunological resilience.

In the 2020’s, interest in red-fleshed apples has increased significantly due to their distinctive appearance and potential health benefits. Many cultivars are marketed internationally under collective trademarks such as Redlove®, Lucy™, Kissabel®, and Red Moon®. Despite this growing popularity, such varieties are not yet included in the State Register of Plant Varieties of Ukraine, although they are already cultivated by some farms and private growers (Pyshcholka & Mezhenskyj, 2026).

The Forest-Steppe region provides a unique environmental matrix for studying secondary metabolism in *Malus* species. The interplay between specific soil compositions and fluctuating temperature regimes during the ripening phase plays a crucial role in the phenotypic expression of genetic traits. Eleven cultivars were investigated over three growing seasons (2023-2025). This study provided a multi-year evaluation of bioactive compounds in red-fleshed apple cultivars under Ukrainian Forest-Steppe conditions. This multi-year approach was essential to mitigate the influence of seasonal climatic anomalies and to establish a reliable baseline for the nutraceutical profiling of these genotypes. To achieve this, the research focused on several interrelated tasks: first, to quantify and compare the concentrations of primary antioxidants, including ascorbic acid and various phenolic fractions, across eleven distinct cultivars. Furthermore, the study aimed to evaluate the environmental stability and interannual variability of these phytochemicals over the 2023-2025 growing seasons to identify the most resilient genotypes. Finally, a detailed analysis was conducted to establish the correlations between different flavonoid groups, specifically investigating the metabolic dependence of anthocyanin accumulation on chalcone concentrations within the fruit mesocarp.

Materials and Methods

The study used 11 cultivars: 'Cranberry', 'Dr Campbell' ('Simontornya Veralma'), 'Era' (Redlove®Era), 'Firecracker', 'Jurgen', 'Marisa' (Baya®Marisa), 'Maypole', 'Mott`s Pink', 'Red Katty', 'Sirena' (Redlove®Sirena), and 'Weirouge' (Fig. 1). Trees were grown in the collection orchard of the Educational, Research and Production Laboratory of Genetic Resources, Introduction and Breeding of Rare Fruits and Ornamental Plants at the Professor V.L. Symyrenko Department of Horticulture of the National University of Life and Environmental Sciences of Ukraine (NULES). This orchard is located at the Agronomic Research Station of the NULES in Pshenychne village, Bila Tserkva district, Kyiv region, Ukraine (50°05'24.6"N 30°12'55.1"E). It is part of the Forest-Steppe natural zone. According to the Köppen climate classification system, the region is characterised by a typical warm-summer humid continental climate (Dfb). The research was conducted on soil classified as meadow chernozem. The adult trees were cultivated at a spacing of 5 × 4 m, with care involving standard horticultural practices such as inter-row cultivation and mechanical weed control. Irrigation was not used. Notably, the study complied with the ethical principles of the Convention on Biological Diversity (1992) and the Convention on the Trade in Endangered Species of Wild Fauna and Flora (1976). Fruit harvesting was performed in mid-September in 2023-2025, with the fruits being picked upon reaching the stage of technical maturity. The analysis was carried out by the Laboratory of Fruit Storage and Processing Technology at the Institute of Horticulture of the National Academy of Agricultural Sciences of Ukraine. Ascorbic acid was determined by grinding samples in a porcelain mortar with glass and transferring them to a 100 ml volumetric flask containing a 2% oxalic acid : 1% HCl mixture (80:20, v/v). The extract was filtered and titrated with 2.6-dichlorophenolindophenol using Tillman's method. Results were expressed as mg/100 g fresh mass. Total polyphenol content was determined using the Folin–Denis method. Samples were macerated with ethanol, filtered through a Büchner funnel, and washed with ethanol until colorless. Extracts reacted with Folin-Denis reagent, followed by saturated sodium carbonate. Optical density was measured at 640 nm after 1 hour. Calibration was done using chlorogenic acid standards, and results were expressed as mg/100 g fresh mass. Anthocyanin and chalcone content were determined by spectrophotometry using alcoholic extracts from 3.5% HCl-acidified homogenates, measured at 530 nm and 364 nm, respectively. Results were expressed as mg/100 g raw mass. Flavonol content was measured by absorption spectrophotometry using a flavonol complex with a 3% aluminium chloride solution. The absorption was measured at 410 nm using a ULAB 102UV spectrophotometer. Data were expressed as mg/100g raw weight. Statistical analysis involved descriptive statistics such as mean values, standard deviation (SD), and coefficient of variation (CV, %). Microsoft Excel 2019 was used for statistical analyses and chart construction. ANOVA was used to test differences among means, and Pearson correlation coefficients were calculated for normally distributed data. Fisher's least significant difference (LSD) test identified significant differences between means at a 95% confidence level ($p \leq 0.05$).

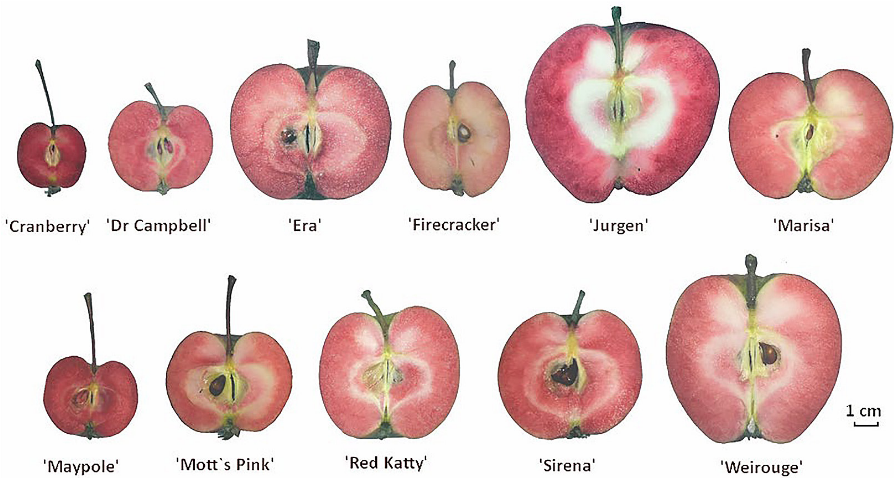

Figure 1. *Red-fleshed cultivars of Malus domestica Niedzwetzkyana Group*

Source: developed by the authors

Results and Discussion

The analysis of the biochemical composition of the cultivars is a key step in identifying their unique properties and potential. The content of the main bioactive compounds is presented in Table 1. The ascorbic acid content of red-fleshed apples varied from 5.06 mg/100 g in 'Red Katty' to 11.41 mg/100 g in 'Cranberry', with an average value of 7.12 mg/100 g. No statistically significant differences were detected among the cultivars for this trait. When comparing these red-fleshed cultivars with modern Ukrainian apple cultivars, the latter contain an average of 5.7 mg/100 g of ascorbic acid, according to L. Shevchuk *et al.* (2021). Only the cultivar 'Harant' shows a comparable level to 'Cranberry' in terms of ascorbic acid content. In general, apples are not considered a major dietary source of this vitamin. As shown by J. Juhart *et al.* (2022), the ascorbic acid content in the traditional, white-fleshed apple cultivar 'Golden Delicious' is only 0.9 mg/100 g, compared to 2.6 mg/100 g in the red-fleshed 'Marisa'. The relative stability of ascorbic acid across the 11 cultivars suggests that this vitamin serves as a basal antioxidant component, likely regulated by highly conserved metabolic pathways. However, the lack of significant differences between cultivars ($P > 0.05$) does not diminish their importance; rather, it indicates that the health benefits of red-fleshed apples are consistently supported by a reliable vitamin C base, regardless of the intensity of red pigmentation. This finding is crucial for processors who require a predictable nutritional profile for standardised juice or dried fruit production.

Table 1. *The phytochemicals of red-fleshed apple (2023-2025, x̄ ± SD, mg/100 g)*

Cultivar	Ascorbic acid	Total polyphenols	Anthocyanins	Flavonols	Chalcones
'Cranberry'	11.41 ± 3.44	428.13 ± 141.01c	21.98 ± 8.09b	27.05 ± 12.09fg	15.47 ± 4.45bc
'Dr Campbell'	6.32 ± 1.38	582.73 ± 36.17ab	31.86 ± 5.72a	46.01 ± 14.57cde	22.20 ± 7.83a
'Era'	5.89 ± 1.34	216.73 ± 44.46d	4.70 ± 2.23c	79.10 ± 12.73a	6.60 ± 1.49d
'Firecracker'	7.78 ± 2.84	621.63 ± 50.52a	4.87 ± 4.37c	40.20 ± 3.56def	10.07 ± 4.45cd
'Jurgen'	6.05 ± 1.05	636.50 ± 96.99a	9.07 ± 5.26c	65.90 ± 6.08ab	8.30 ± 2.08d
'Marisa'	8.33 ± 1.50	212.73 ± 29.01d	9.08 ± 2.39c	14.50 ± 0.85g	6.40 ± 2.44d
'Maypole'	6.74 ± 0.40	487.43 ± 30.99bc	22.75 ± 10.82b	26.40 ± 4.53fg	16.60 ± 10.47b
'Mott's Pink'	7.12 ± 0.89	189.67 ± 29.60d	6.18 ± 2.10c	61.05 ± 14.78bc	5.33 ± 1.50d
'Red Katty'	5.06 ± 2.60	175.43 ± 33.95d	4.10 ± 1.74c	20.40 ± 2.97g	5.33 ± 2.15d
'Sirena'	8.04 ± 1.94	186.53 ± 17.84d	5.24 ± 1.97c	57.65 ± 10.25bc	5.50 ± 1.57d
'Weirouge'	5.56 ± 3.90	187.57 ± 38.58d	6.15 ± 1.13c	31.30 ± 13.29efg	5.03 ± 0.90d
Average	7.12 ± 2.51	356.83 ± 195.36	11.45 ± 9.72	42.70 ± 21.66	9.73 ± 6.78
CV, %	35.2	54.7	84.9	50.7	69.7

Note: different letters within a column indicate statistically significant differences according to the LSD test ($p \leq 0.05$)
Source: compiled by the authors

While ascorbic acid levels are relatively modest, red-fleshed apples stand out significantly in terms of their polyphenolic profile. In contrast, as noted by D. Bars-Cortina *et al.* (2017) and S. Yuste *et al.* (2022), apples are an important source of total polyphenols with strong antioxidant properties. While modern Ukrainian apple cultivars contain an average of 206 mg/100 g of total polyphenols in their fruits, according to L. Shevchuk *et al.* (2021), the red-fleshed cultivars examined in this study contain, on average 356.83 mg/100 g, which is approximately 1.5 times higher. The cultivars 'Jurgen', 'Firecracker', and 'Dr Campbell' exhibited the highest accumulation of total polyphenols, containing 636.50 mg/100 g, 621.63 mg/100 g, and 582.73 mg/100 g, respectively. These values are higher than those reported by M. Jalali *et al.* (2024) for red-fleshed apples in Iran and D. Bars-Cortina *et al.* (2017) for red-fleshed apples in Europe.

Apple peel colour is determined by pigments such as chlorophyll, carotenoids, and anthocyanins (Ban *et al.*, 2007; Liu *et al.*, 2013). Differences in pigment composition and their regulatory mechanisms explain the wide colours observed among apple cultivars, ranging from green to deep purple (Bu *et al.*, 2025). In red-skinned apples, anthocyanins accumulate in large quantities in the peel, whereas in other cultivars their content is negligible. Studies have shown that in red apples, anthocyanins are mainly localised in several epidermal and hypodermal cell layers, while the mesocarp usually remains unpigmented (van Nocker *et al.*, 2012). In contrast, red-fleshed apples are characterised by anthocyanin accumulation within the fruit flesh, which is associated with the activity of specific regulatory genes controlling anthocyanin biosynthesis (Espley *et al.*, 2007).

Researchers who have studied red-fleshed apples report considerable variation in anthocyanin content in both the peel and the flesh. According to X. Wang *et al.* (2015), anthocyanin content in the peel ranges from 22.7 mg/100 g to 120.3 mg/100 g, and in the flesh from 0.8 mg/100 g to 38.1 mg/100 g, depending on the genotype. P. Bouillon *et al.* (2024) reported values ranging from 0.2 mg/100 g to 30.9 mg/100 g of anthocyanins in the fruit flesh. Among the cultivars examined in this study, 'Dr Campbell' showed the highest anthocyanin content, averaging 31.86 mg/100 g, which corresponds closely to the upper values reported by X. Wang *et al.* (2015) and P. Bouillon *et al.* (2024). 'Dr Campbell' is followed by the cultivars 'Maypole' and 'Cranberry' with anthocyanin contents of 22.75 mg/100 g and 21.98 mg/100 g, respectively. All other studied cultivars formed a third group with significantly lower anthocyanin levels, ranging from 4.10 mg/100 g to 9.08 mg/100 g. Overall, the coefficient of variation for anthocyanin content is the highest in this study at 84.9%. This high variability likely reflects their sensitivity to environmental factors and their role as intermediate metabolites in the anthocyanin biosynthetic pathway. Specifically, the accumulation of these compounds is profoundly influenced by the interplay between solar radiation and ambient temperature during the pre-harvest period. High light intensity, particularly in the UV-B spectrum, acts as a primary inducer of the MYB10 transcription factor. According to H. Bu *et al.* (2025), this process is further mediated by a complex network of transcription factors, such as MdHY5 and MdBBX20, which enhance anthocyanin accumulation by binding to MYB promoters specifically under conditions of high UV radiation and low temperatures. Furthermore, the thermal regime plays a decisive role: while moderate day temperatures combined with cool nights significantly stimulate anthocyanin synthesis, prolonged periods of high heat (above 30°C) are known to inhibit pigment accumulation or even trigger their degradation. In the context of the Ukrainian Forest-Steppe, the interannual fluctuations in precipitation and temperature during August and September create a diverse environmental pressure that explains the instability of chalcone and anthocyanin concentrations across different seasons.

M. Jalali *et al.* (2024) reported that red-fleshed genotypes in Iran exhibit significant variability in anthocyanin content, ranging from 2.1 mg/100 g to 18.9 mg/100 g. In Spain, D. Bars-Cortina *et al.* (2017) found that four red-fleshed cultivars contained from 0.93 mg/100 g to 4.93 mg/100 g of anthocyanins. A. Ceci *et al.* (2021) reported an anthocyanin content of 7.5 mg/100 g. Given the significant differences in eco-geographical growing conditions and the heterogeneity of plant material across various studies, a direct comparison of absolute metabolite concentrations appears problematic. A more objective approach involves analysing general trends and patterns of trait variability.

As noted by R. Tsao *et al.* (2003), chalcones represent one of the common groups of flavonoids. They serve as primary precursors in the biosynthesis of anthocyanins (Lautenbach *et al.*, 2025). Apples are considered a major dietary source of these compounds (Bars-Cortina *et al.*, 2018). Chalcones generally account for approximately 2-6% of the total polyphenols (Vrhovsek e*t al.*, 2004). In the mesocarp of commercial apple cultivars with white flesh, their average content is 19 mg/100 g (Tsao *et al.*, 2003). In contrast, M. Jalali *et al.* (2026) reported lower chalcone content in the mesocarp of red-fleshed apples, averaging 5.63 mg/100 g. In the red-fleshed cultivars examined in this study, the average content was 9.73 mg/100 g, ranging from 5.03 mg/100 g to 22.20 mg/100 g in 'Dr Campbell', which also showed the highest anthocyanin concentration.

According to X. Zhang *et al.* (2020), flavonols constitute a relatively high proportion of the polyphenolic compounds in red-fleshed apples. Regarding the flavonoid profile, Y. Ren *et al.* (2026) identified eight distinct classes of flavonoids based on their chemical structures. In terms of structural diversity, the most abundant class was flavonols, accounting for 40.29% of the identified compounds, followed by flavones (9.42%), flavanones (12.23%), chalcones (9.35%), flavanols (7.19%), flavonoid carbonosides (5.76%), flavanonols (5.04%), and anthocyanidins (0.72%). In studies by X. Wang *et al.* (2015), it was shown that the highest content of flavonols (mainly quercetin derivatives) is found in the peel of red-fleshed apples, ranging from 18.2 mg/100 g to 89.8 mg/100 g, while their content in the mesocarp ranges from 5.3 mg/100 g to 14.5 mg/100 g. In the red-fleshed cultivar 'XJ4', the most abundant flavonol (quercetin) was 23.087 mg/100 g. Research by M. Jalali *et al.* (2026) reported an average flavonol content of 4.21 mg/100 g, with a maximum value of 24.55 mg/100 g. In the present study, the highest flavonol content was observed in the cultivar 'Era' (79.10 mg/100 g), followed by 'Jurgen' and 'Mott's Pink', with values of 65.90 mg/100 g and 61.05 mg/100 g, respectively. Such variations in absolute flavonol concentrations compared to international studies may be attributed to the complex nature of genotype × environment interactions. This is consistent with the findings of B.T. Geleta *et al.* (2025), who demonstrated that while the genotype is the primary driver of variance for fruit weight and total phenolic content, the environment exerts a more profound influence on the total flavonoid content and vitamin C levels. In the present study, the relatively higher level of flavonols in cultivars such as 'Era' and 'Jurgen' suggests a strong genetic determination of this trait. Conversely, the high variability of anthocyanins (CV = 84.9%) compared to flavonols aligns with the observation that certain flavonoid classes are more susceptible to environmental shifts, reflecting the cumulative impact of specific hydrothermal conditions during the ripening period in the Ukrainian Forest-Steppe. Flavonols, mainly represented by quercetin glycosides, are known for their high thermal stability compared to anthocyanins. The fact that flavonol levels did not correlate with the red pigment concentration implies that these two groups of flavonoids can be enhanced independently. To better identify relationships among the studied traits, data from different years were pooled to increase the sample size for correlation analysis (Table 2).

Table 2. *Pearson correlation coefficients between traits (r)*

Trait	Ascorbic acid	Total polyphenols	Anthocyanins	Chalcones	Flavonols
Ascorbic acid	1				
Total polyphenols	0.036	1			
Anthocyanins	0.178	**0.495**	1		
Chalcones	0.160	**0.591**	**0.904**	1	
Flavonols	-0.109	0.117	-0.172	-0.128	1

Note: significant coefficients ($p \leq 0.05$) are shown in bold ($n = 33$)
Source: compiled by the authors

A strong and highly significant correlation was observed between anthocyanins and chalcones ($r = 0.904$), confirming the pivotal role of chalcones as essential biosynthetic precursors. This relationship aligns with the metabolic model proposed by X. Wang *et al.* (2024), which suggests that the efficiency of the conversion from chalcones to downstream flavonoids is a limiting factor for intense fruit pigmentation. The correlation coefficients between total polyphenols and their components (anthocyanins and chalcones) are lower, but remain statistically significant. In contrast, flavonols behaved as a relatively independent group of compounds, the accumulation of which did not show a relationship with other polyphenols. Similarly, the ascorbic acid content was not correlated with pigments or total polyphenol content, suggesting that this trait is largely genetically determined. The observed peak concentration in 'Dr Campbell' likely reflects a high metabolic flux through the flavonoid pathway, ensuring a consistent supply of substrates for anthocyanin synthesis even under fluctuating environmental conditions. Furthermore, the discrepancy between these results and the lower averages reported by M. Jalali *et al.* (2026) may be attributed to the specific genetic background of the investigated cultivars and their differential response to the hydrothermal regime of the Ukrainian Forest-Steppe. Such findings support the hypothesis that high chalcone accumulation is a prerequisite for achieving superior anthocyanin levels in red-fleshed genotypes, providing a biochemical marker for selecting high-pigment varieties. The comparison of coefficients of variation for the main antioxidant compounds revealed significant cultivar differences (Fig. 2).

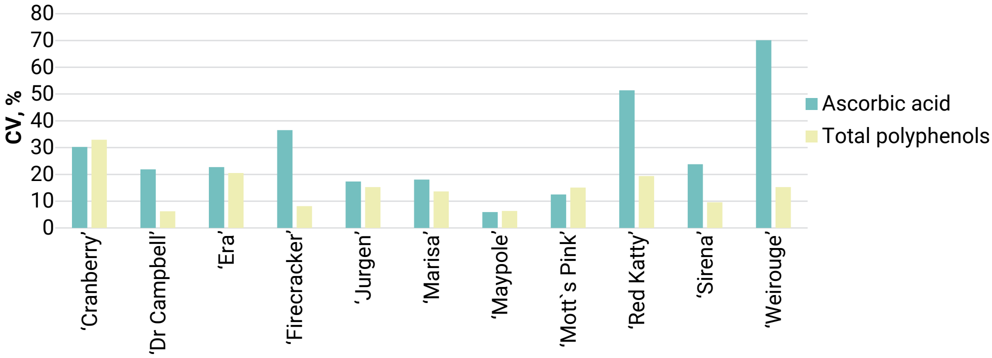

Figure 2. *Variability (CV, %) of ascorbic acid and total polyphenol content in apple fruits (2023-2025)*
Source: compiled by the authors

The 'Maypole' proved to be the most stable in terms of ascorbic acid and total polyphenol content. This indicates a low dependence of antioxidant accumulation on the weather conditions of a specific year. The cultivars 'Mott's Pink' and 'Marisa' also showed relatively low variability in these traits. 'Dr Campbell' was characterised by high antioxidant accumulation while maintaining relatively stable polyphenol levels. Total polyphenols were generally more stable than ascorbic acid, the content of which showed greater sensitivity to environmental conditions, with CV values ranging from approximately 6% in 'Maypole' to 70% in 'Weirouge'. A comparative analysis of the coefficients of variation revealed differences in the stability of secondary metabolite accumulation among the studied cultivars (Fig. 3).

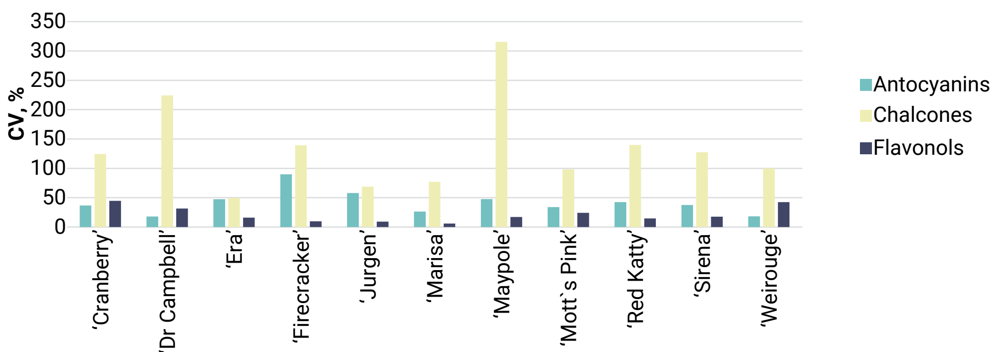

Figure 3. *Stability of anthocyanin, chalcone, and flavonol accumulation across different growing seasons*
Source: compiled by the authors

Among the components of the pigment complex, flavonols exhibited the highest stability, showing the lowest coefficients of variation, which indicates a lower dependence on annual weather conditions. In contrast, anthocyanins showed moderate variability, whereas chalcones demonstrated the highest instability, with coefficients of variation exceeding 100% in several cultivars. This high variability likely reflects their sensitivity to environmental factors and their role as intermediate metabolites in the anthocyanin biosynthetic pathway. It is hypothesised that such instability in these parameters is driven by the dynamics of temperature and humidity, as well as their interaction with other abiotic environmental factors. The higher variability of anthocyanins compared to their precursors, chalcones, may be attributed to the cumulative effect of environmental conditions on the final stages of biosynthesis throughout the fruit ripening period. Among the studied cultivars, 'Dr Campbell' combined high anthocyanin accumulation with relatively stable expression of this trait, whereas 'Era' showed a more balanced profile, with similar variability of anthocyanins, chalcones, and flavonols (about 40-50%). Overall, the results indicate that different groups of flavonoids differ in environmental stability: flavonols are the most stable, anthocyanins show moderate variability, and chalcones are the most sensitive to interannual environmental changes. Figure 4 illustrates a strong proportional relationship between chalcone and anthocyanin content, confirming chalcones as the metabolite precursors in the anthocyanin biosynthetic pathway, which supports the findings of J. Lautenbach *et al.* (2025).

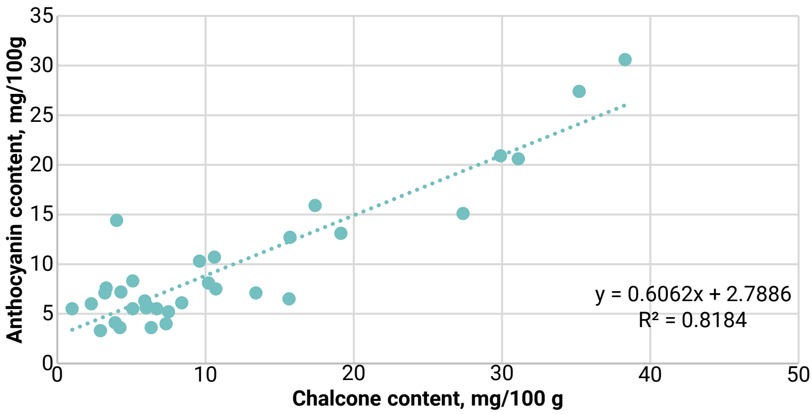

Figure 4. *Correlation between chalcone and anthocyanin content in red-flesh apples (2023-2025)*

Note: the dashed line represents the linear regression equation ($R^2 = 0.81$)

Source: compiled by the authors

These two groups of pigments function as a single mechanism. The calculated coefficient of determination ($R^2 = 0.81$) indicates that approximately 81% of the variation in anthocyanin content can be explained by the differences in chalcone concentration. The dashed line in Figure 4 represents the linear regression model, confirming that the anthocyanin accumulation is closely associated with chalcone concentration in the fruit mesocarp.

Thus, flavonols demonstrated the highest stability among the components of the pigment complex, showing minimal variability, which indicates that they are less affected by weather conditions. Anthocyanins showed moderate variability, whilst chalcones proved to be the most unstable, likely due to their sensitivity to environmental factors and their role in the anthocyanin biosynthesis pathway. The high variability of chalcones and anthocyanins is influenced by temperature, humidity and other abiotic factors, with this effect being most pronounced during fruit ripening. The 'Dr Campbell' variety showed high anthocyanin accumulation with stable expression, whilst the 'Era' variety demonstrated more balanced variability among different types of flavonoids. The strong correlation between the content of chalcones and anthocyanins supports the hypothesis that chalcones are precursors in the anthocyanin biosynthesis pathway.

Conclusions

The primary objective of this study was to evaluate the biochemical diversity and nutritional potential of red-fleshed apple cultivars of the Niedzwetzkyana Group under the environmental conditions of the Ukrainian Forest-Steppe. Through a comprehensive analysis of secondary metabolites, the research aimed to identify genotypes with superior antioxidant properties and establish the metabolic relationships between key flavonoid classes. The results obtained fully confirm the achievement of this goal, providing a detailed characterisation of the phytochemical profiles of eleven specialised cultivars. The study involved a systematic quantification of ascorbic acid, total polyphenols, anthocyanins, chalcones, and flavonols over multiple growing seasons. It was found that red-fleshed apples significantly outperform traditional white-fleshed cultivars in terms of total phenolic content, with an average concentration of 356.83 mg/100 g.

The analysis revealed that 'Jurgen', 'Firecracker', and 'Dr Campbell' are the most promising genotypes for functional food production, exhibiting peak polyphenol levels exceeding 580 mg/100 g. A critical finding of the research was the extreme variability of anthocyanin accumulation (CV = 84.9%), which was shown to be highly sensitive to interannual hydrothermal fluctuations. In contrast, flavonol concentrations remained relatively stable, with 'Era' and 'Jurgen' consistently maintaining high levels of quercetin glycosides. Correlation analysis established a robust positive link between chalcones and anthocyanins (r = 0.904), while the coefficient of determination ($R^2 = 0.81$) confirmed that chalcone availability is the decisive factor for intense flesh pigmentation. Conceptualising these results, the data suggest that the biosynthetic pathway in red-fleshed apples is driven by a high metabolic flux from chalcone precursors to downstream anthocyanins, which is both genetically determined and environmentally regulated. This implies that while the maximum pigment potential is fixed by the genotype, the actual expression of the "red-flesh" trait is a result of complex genotype-by-environment interactions. Such findings deepen the understanding of flavonoid metabolism in niche fruit crops and provide a clear biochemical rationale for the selection of parent material in breeding programmes. The identified independence of flavonol and ascorbic acid accumulation further indicates that these traits can be improved simultaneously without pleiotropic constraints.

Future research should focus on evaluating the stability of these bioactive compounds during long-term storage and industrial processing to ensure the delivery of high-quality functional products to consumers.

Acknowledgements

None.

Funding

The study was not funded.

Conflict of Interest

None.

References

[1] Asma, U., Morozova, K., Ferrentino, G., & Scampicchio, M. (2023). Apples and apple by-products: Antioxidant properties and food applications. *Antioxidants*, 12(7), article number 1456. doi: 10.3390/antiox12071456.

[2] Ban, Y., Honda, C., Hatsuyama, Y., Igarashi, M., Bessho, H., & Moriguchi, T. (2007). Isolation and functional analysis of a MYB transcription factor gene that is a key regulator for the development of red coloration in apple skin. *Plant & Cell Physiology*, 48(7), 958-970. doi: 10.1093/pcp/pcm066.

[3] Bars-Cortina, D., Macià, A., Iglesias, I., Garanto, X., Badiella, L., & Motilva, M.J. (2018). Seasonal variability of the phytochemical composition of new red-fleshed apple varieties compared with traditional and new white-fleshed varieties. *Journal of Agricultural and Food Chemistry*, 66(38), 10011-10025. doi: 10.1021/acs.jafc.8b03950.

[4] Bars-Cortina, D., Macià, A., Iglesias, I., Romero, M.P., & Motilva, M.J. (2017). Phytochemical profiles of new red-fleshed apple varieties compared with traditional and new white-fleshed varieties. *Journal of Agricultural and Food Chemistry*, 65(8), 1684-1696. doi: 10.1021/acs.jafc.6b02931.

[5] Bouillon, P., Fanciullino, A.-L., Belin, E., Bréard, D., Boisard, S., Bonnet, B., Hanteville, S., Bernard, F., & Celton, J.-M. (2024). Image analysis and polyphenol profiling unveil red-flesh apple phenotype complexity. *Plant Methods*, 20, article number 71. doi: 10.1186/s13007-024-01196-1.

[6] Bu, H., Gu, G., Hu, Y., Yang, Y., Yang, L., Yuan, H., & Yu,W. (2025). Research advances in the synthesis and regulation of apple anthocyanins. *Biology*, 14(10), article number 1322. doi: 10.3390/biology14101322.

[7] Catalán, Ú., *et al.* (2022). Red-fleshed apples rich in anthocyanins and white-fleshed apples modulate the aorta and heart proteome in hypercholesterolaemic rats: The AppleCOR Study. *Nutrients*, 14(5), article number 1047. doi: 10.3390/nu14051047.

[8] Ceci, A.T., Bassi, M., Guerra, W., Oberhuber, M., Robatscher, P., Mattivi, F., & Franceschi, P. (2021). Metabolomic characterization of commercial, old, and red-fleshed apple varieties. *Metabolites*, 11(6), 378. doi: 10.3390/metabo11060378.

[9] Chen, Y., Wang, Y., Jiang, S., Xu, J., Wang, B., Sun, X., & Zhang, Y. (2023). Red-fleshed apple flavonoid extract alleviates CCl4-induced liver injury in mice. *Frontiers in Nutrition*, 9, article number 1098954. doi: 10.3389/fnut.2022.1098954.

[10] Convention on Biological Diversity. (1992, June). Retrieved from https://www.cbd.int/doc/legal/cbd-en.pdf.

[11] Convention on the Trade in Endangered Species of Wild Fauna and Flora. (1976, March). Retrieved from https://treaties.un.org/doc/publication/unts/volume%20993/volume-993-i-14537-english.pdf.

[12] Espley, R.V., Hellens, R.P., Putterill, J., Stevenson, D.E., Kutty-Amma, S., & Allan, A.C. (2007). Red colouration in apple fruit is due to the activity of the MYB transcription factor, MdMYB10. *The Plant Journal*, 49(3), 414-427. doi: 10.1111/j.1365-313X.2006.02964.x.

[13] Food and Agriculture Organization (FAO). (2025). Retrieved from https://www.fao.org/faostat/.

[14] Geleta, B.T., Abebe, A.M., & Heo, J.-Y. (2025). Effect of genotype × environment interactions on apple fruit characteristics in a high latitude region of Korea. *Applied Fruit Science*, 67, article number 14. doi: 10.1007/s10341-024-01243-0.

[15] Jalali, M., Abedi, M., Tabarsa, M., & Moreno, D.A. (2024). Morphological and biochemical characteristics of wild red-fleshed apples (*Malus sieversii* f. *niedzwetzkyana*) in the North and Northeast of Iran. *BMC Plant Biology*, 24, article number 899. doi: 10.1186/s12870-024-05608-1.

[16] Jalali, M., Abedi, M., Tabarsa, M., & Moreno, D.A. (2026). Superior phytochemical composition and antioxidant potential of wild red-fleshed apples: A comparative analysis across humid and dry ecosystems. *LWT – Food Science and Technology*, 239, article number 118950. doi: 10.1016/j.lwt.2025.118950.

[17] Juhart, J., Medic, A., Veberic, R., Hudina, M., Jakopic, J., & Stampar, F. (2022). Phytochemical composition of red-fleshed apple cultivar "Baya Marisa" compared to traditional, white-fleshed apple cultivar "Golden Delicious". *Horticulturae*, 8(9), article number 811. doi: 10.3390/horticulturae8090811.

[18] Keller-Przybylkowicz, S., Oskiera, M., Liu, X., Song, L., Zhao, L., Du, X., Kruczynska, D., Walencik, A., Kowara, N., & Bartoszewski, G. (2024). Transcriptome analysis of white- and red-fleshed apple fruits uncovered novel genes related to the regulation of anthocyanin biosynthesis. *International Journal of Molecular Sciences*, 25(3), article number 1778. doi: 10.3390/ijms25031778.

[19] Lautenbach, J., Abbas, Q., Brajkovic, S., Sieberer, T., Neumüller, M., Kuster, B., & Poppenberger, B. (2025). Unraveling the proteomic landscape of red-fleshed apples to identify regulators of anthocyanin accumulation. *Journal of Proteomics*, 319, article number 105470. doi: 10.1016/j.jprot.2025.105470.

[20] Li, Z., Liu, W., Chen, Q., Zhang, S., Mei, Z., Yu, L., Wang, C., Mao, Z., Chen, Z., Chen, X., & Wang, N. (2023). Mdm-miR858 targets MdMYB9 and MdMYBPA1 to participate anthocyanin biosynthesis in red-fleshed apple. *The Plant Journal*, 113(6), 1295-1309. doi: 10.1111/tpj.16111.

[21] Liu, Y., Zhang, X., & Zhao, Z. (2013). Effects of fruit bagging on anthocyanins, sugars, organic acids, and color properties of 'Granny Smith' and 'Golden Delicious' during fruit maturation. *European Food Research and Technology*, 236(2), 329-339. doi: 10.1007/s00217-012-1896-3.

[22] Mezhenskyj, V.M., Pyshcholka, D.V., Mezhenska, L.O., & Havryliuk, O.S. (2024). An overview of the red-fleshed apple: History and its importance for horticulturists, gardeners, nurserymen, and consumers. *Biosystems Diversity*, 32(1), 158-167. doi: 10.15421/012416.

[23] Pyshcholka, D., & Mezhenskyj, V.M. (2026). Biochemical composition and nutritional value of red-fleshed apple cultivars in the Ukrainian forest-steppe. *Plant and Soil Science*, 17(1), 9-19. doi: 10.31548/plant1.2026.09.

[24] Ren, Y., Guan, Y., Ma, Y., Fang, Z., Ding, Y., & Ao, P. (2026). Metabolic profiling of red-fleshed apple and functional characterization of MdERF072 in anthocyanin biosynthesis. *BMC Plant Biology*, 26, article number 158. doi: 10.1186/s12870-025-07987-5.

[25] Shevchuk, L., Grynyk, I., Levchuk, L., Babenko, S., Podpriatov, H., & Kondratenko, P. (2021). Fruit quality indicators of apple (*Malus domestica* Borkh.) cultivars bred in Ukraine. *Journal of Horticultural Research*, 29(2), 95-106. doi: 10.2478/johr-2021-0019.

[26] Tsao, R., Yang, R., Young, J. C., Zhu, H. (2003). Polyphenolic profiles in eight apple cultivars using high-performance liquid chromatography (HPLC). *Journal of Agricultural and Food Chemistry*, 51(21), 6347-6353. doi: 10.1021/jf0346298.

[27] van Nocker, S., Berry, G., Najdowski, J., Michelutti, R., Luffman, M., Forsline, P., Alsmairat, N., Beaudry, R., Nair, M.G., & Ordidge, M. (2012). Genetic diversity of red-fleshed apples (Malus). *Euphytica*, 185(2), 281-293. doi: 10.1007/s10681-011-0579-7.

[28] Vrhovsek, U., Rigo, A., Tonon, D., & Mattivi, F. (2004). Quantitation of polyphenols in different apple varieties. *Journal of Agricultural and Food Chemistry*, 52(21), 6532-6538. doi: 10.1021/jf049317z.

[29] Wang, X., Li, C., Liang, D., Zou, Y., Li, P., & Ma, F. (2015). Phenolic compounds and antioxidant activity in red-fleshed apples. *Journal of Functional Foods*, 18, 1086-1094. doi: 10.1016/j.jff.2014.06.013.

[30] Yuste, S., Ludwig, I.A., Romero, M.-P., Motilva, M.-J., & Rubió, L. (2022). New redfleshed apple cultivars: A comprehensive review of processing effects, (poly)phenol bioavailability and biological effects. *Food and Function*, 13(9), 4861-4874. doi: 10.1039/D2FO00130F.

[31] Zhang, X., Xu, J., Xu, Z., Sun, X., Zhu, J., & Zhang, Y. (2020). Analysis of antioxidant activity and flavonoids metabolites in peel and flesh of red-fleshed apple varieties. *Molecules*, 25, article number 1968. doi: 10.3390/molecules25081968.

Біоактивні сполуки в генетичному матеріалі яблук з червоним м'якушем

Дмитро Пищолка
Аспірант
Національний університет біоресурсів і природокористування України
03041, вул. Героїв Оборони, 15, м. Київ, Україна
http://orcid.org/0009-0001-9025-4463
Володимир Меженський
Доктор сільськогосподарських наук, старший науковий співробітник
Національний університет біоресурсів і природокористування України
03041, вул. Героїв Оборони, 15, м. Київ, Україна
https://orcid.org/0000-0002-3154-1120

Анотація. Сорти *Malus domestica* Niedzwetzkyana Group з червоним м'якушем привертають все більше уваги завдяки своєму характерному забарвленню та підвищеному вмісту фітохімічних речовин, корисних для здоров'я. Метою цього дослідження було оцінити біохімічний склад і мінливість основних біоактивних сполуку червоном'якушних сортів яблук, вирощених у лісостеповій зоні України. Протягом трьох вегетаційних періодів (2023-2025 рр.) було досліджено 11 сортів. Уміст аскорбінової кислоти, загальних поліфенолів, антоціанів, флавонолів та халконів визначали за допомогою стандартних спектрофотометричних і титрометричних методів. Результати виявили значне біохімічну різноманітніття серед вивчених генотипів. Уміст аскорбінової кислоти коливався від 5,06 до 11.41 мг/100 г свіжої маси і не відрізнявся істотно між сортами. Натомість спостерігалися суттєві відмінності в накопиченні фенольних сполук. Найвищі концентрації загальних поліфенолів зафіксовано в сортах 'Jurgen' (636,50 мг/100 г) та 'Firecracker' (621,63 мг/100 г), що с відчить про їхній сильний антиоксидатний потенціал. Уміст антоціанів і халконів демонстрував значну варіабельність, причому найвищі значення виявлено в сорту 'Dr Campbell' (відповідно 31,86 мг/100 г і 22,20 мг/100 г). Статистичний аналіз показав коефіцієнт детермінації (R^2 = 0,81), який свідчить про те, що концентрація халконів пояснює 81 % спостережуваної мінливості рівнів антоціанів. Сорти 'Era' і 'Jurgen' продемонстрували найвище накопичення флавонолів (відповідно 79,10 мг/100 г і 65,90 мг/100 г). Загалом, сорти 'Dr Campbell', 'Cranberry' та 'Jurgen' були визначені як найперспективніші генотипи завдяки поєднанню високого вмісту фенолів і накопиченню пігментів. Отримані результати підкреслюють значний харчовий та селекційний потенціал червоном'якушних сортів яблук та підтверджують доцільність їх ширшого впровадження у садівництво та розробку функціональних продуктів харчування в Україні

Ключові слова: *Malus domestica* Niedzwetzkyana Group; аскорбінова кислота; поліфеноли; антоціани; флавоноли; халкони

Received 15.12.2025 Revised 11.03.2026 Accepted 23.04.2026 Published: 30.04.2026

Vol. 22, No. 2
2026

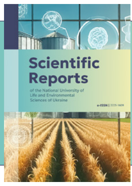

Scientific Reports of the National University of Life and Environmental Sciences of Ukraine

Journal homepage: https://scireports.com.ua/en e-ISSN 2223-1609

UDC 630*56:633.877(477.82) DOI: 10.31548/dopovidi/2.2026.20

Radial tree growth in Scots pine stands of Volyn Polissia

Oleksandr Lesnik*
PhD in Agricultural Sciences, Associate Professor
Education and Research Institute of Forestry and Landscape-Park Management
National University of Life and Environmental Sciences of Ukraine
03041, 19 Horikhuvatskyi Shliakh Str., Kyiv, Ukraine
https://orcid.org/0000-0002-4287-3454

Maksym Fesiuk
Postgraduate Student
Education and Research Institute of Forestry and Landscape-Park Management
National University of Life and Environmental Sciences of Ukraine
03041, 19 Horikhuvatskyi Shliakh Str., Kyiv, Ukraine
https://orcid.org/0009-0008-7474-0913

Oleksandr Sizhuk
State Enterprise Forestry Innovation and Analytical Centre
State Forest Resources Agency of Ukraine
01013, 1 Derevoobrobna Str., Kyiv, Ukraine
https://orcid.org/0009-0008-4607-3447

Abstract. This study examines the patterns of radial growth in Scots pine (*Pinus sylvestris* L.) stands within the Volyn Polissia region, with particular reference to the influence of climatic variables. The research aimed to characterise the seasonal structure of climatic sensitivity in Scots pine radial growth and to identify the key climatic factors that drive the interannual variability of tree-ring width. The analysis was based on tree-ring width series obtained from nine temporary sample plots. To remove age-related growth trends, detrending was applied, converting raw measurements into ring-width indices. The relationships between radial growth dynamics and climatic parameters were evaluated through correlation analysis using monthly mean air temperature and total precipitation for both the current and preceding years. The results indicated that the radial growth of Scots pine is most sensitive to temperature conditions during the winter-to-early-spring period of the current year, particularly in February and March. Significant climatic lag effects were also identified: precipitation levels in July and

Suggested Citation:
Lesnik, O., Fesiuk, M., & Sizhuk, O. (2026). Radial tree growth in Scots pine stands of Volyn Polissia. *Scientific Reports of the National University of Life and Environmental Sciences of Ukraine*, 22(2), 20-35. doi: 10.31548/dopovidi/2.2026.20.

*Corresponding author

August of the previous year positively influence growth in the following year. The analysis confirmed the substantial impact of these climatic factors on interannual growth variability. The absence of significant spatial random effects suggests a coherent common climate signal across the study area. These findings extend current understanding of the seasonal climatic sensitivity of pine stands in Volyn Polissia and can be utilised to assess the resilience of forest ecosystems and to inform adaptive forest management strategies in the face of contemporary climate change

Keywords: *Pinus sylvestris* L.; radial growth dynamics; ring-width indices; climatic factors; dendrochronology

Introduction

The Volyn Polissia is a region characterised by high forest cover and a widespread distribution of Scots pine (*Pinus sylvestris* L.), which is the dominant species in the forest stands of the study area (Fesiuk & Lesnik, 2025). The forests of this region have significant ecological and resource value. Investigating the dynamics of their radial growth enables not only an assessment of the current state of the stands but also the identification of their developmental trends in the context of climate change and forest management.

Tree radial growth is a key indicator that characterises growth processes in forest stands and reflects the interaction between the biological traits of the tree species and external environmental factors. Growth dynamics are directly related to stand productivity, physiological state, and resilience to adverse factors. Furthermore, they determine the potential for providing ecosystem services, particularly carbon sequestration (Bilous *et al.*, 2022; Lesnik *et al.*, 2022).

In modern dendrochronological research, radial growth is considered not only as an indicator of productivity but also as a sensitive archive of climatic information. Tree-ring analysis allows the tracking of interannual growth variability and the identification of the seasonal structure of climatic influence, provided that age-related trends are removed in advance. Applying detrending and converting measurements to ring-width indices (RWI) are necessary prerequisites for the accurate assessment of the climate sensitivity of trees of different ages and from various site conditions (McPartland *et al.*, 2020; Druckenbrod *et al.*, 2024). Recent research by Y. Prokopuk *et al.* (2024) indicates that radial growth sensitivity is primarily driven by precipitation from the dormant season to the early growing season, with site-specific factors such as topography further modulating this response. This finding underscores the need to evaluate the seasonal climate sensitivity of Scots pine (*Pinus sylvestris* L.) in Volyn Polissia, where annual growth fluctuations reflect the complex interplay between environmental change and site-specific conditions.

The significance of local environmental factors is further emphasised by studies focusing on specific forest health issues within the region. For instance, I. Koval & O. Andreeva (2022) analysed changes in the radial growth of Scots pine in epicentres of the pine shoot beetle following clear sanitary felling within the Polissia natural-climatic zone. They found that illuminated areas are characterised by a higher growth sensitivity to hydrothermal conditions, with a negative response to moisture deficits, whereas control plots exhibited a positive correlation with integrated hydrothermal indices. These results indicate a significant impact of microclimatic changes induced by clear-cutting on the growth dynamics of pine stands.

Ukrainian studies have paid considerable attention to determining the response of the main forest-forming tree species in Ukraine to climate change. Specifically, I. Koval *et al.* (2025) examined changes in the radial growth of Japanese larch (*Larix leptolepis* Gord.) under conditions of climate change in the Left-Bank Forest-Steppe of Ukraine. The study developed local chronologies of earlywood, latewood, and total ring width for three periods: 1979-1993, 1994-2008, and 2009-2022. The results showed that, during the third period, the sensitivity of radial growth to climatic fluctuations increased, leading to stand weakening due to rising temperatures. Earlywood was identified as the most sensitive component to climatic change.

Beyond coniferous species, climate sensitivity has also been documented for deciduous stands in the region. I. Ivanyuk & Y. Fuchylo (2020) analysed the impact of meteorological factors on the radial growth of artificial stands of pedunculate oak in the Central Polissia of Ukraine from 1946 to 2018. Optimal values of the hydrothermal coefficient that ensure maximum growth were determined. The study found that oak stands on fresh loamy soils are more sensitive to climatic fluctuations than stands on moist soils.

The patterns observed in Ukraine align with broader European trends regarding the physiological mechanisms of tree growth. For example, a large-scale study by S. Etzold *et al.* (2022), conducted across 47 sites in Switzerland over eight years using automated dendrometers, analysed the daily dynamics of radial stem growth in 160 trees belonging to seven temperate species. The study demonstrated that growth occurs only during a limited number of days within the growing season, with most of these days occurring before the summer solstice. The key driver of annual growth formation is the number of active growth days, whereas the overall length of the growing season is of secondary importance.

While growth duration is a key internal driver, the external regulation of growth by specific meteorological parameters remains equally decisive. This is illustrated by the study of A. Kastridis *et al.* (2022), which analysed the dependence of Greek fir (*Abies borisii-regis* Mattf.) radial growth on climatic factors in the forests of Central Greece over a 60-year period (1961-2020). The results showed that the main growth regulator is precipitation, especially in May-July, while air temperature plays a secondary role. The most negative impact was caused by high June temperatures, which increased evaporation and reduced moisture availability.

Therefore, a review of the scientific literature demonstrates that tree radial growth is a sensitive indicator of the impact of climatic and environmental factors, and in the case of Scots pine, it serves as a key metric of stand resilience and productivity. However, the seasonal structure of the climate sensitivity of radial growth in pine stands within Volyn Polissia, particularly with consideration of climatic lag effects and the removal of age-related trends, remains insufficiently studied. In this regard, the present study aimed to assess the interannual variability of Scots pine radial growth in the stands of Volyn Polissia and to identify the key climatic drivers and seasonal periods that determine growth formation under contemporary climate change conditions.

Materials and Methods

The research was carried out in Scots pine stands during the 2021 and 2023 field seasons within the Kamin-Kashyrske FMU (Branch "Poliskyi Forest Office", SFE "Forests of Ukraine"). In 2021 and 2023, five temporary sample plots were established, and 64 tree cores were extracted in the Dobrenske Forest District. In 2023, four additional sample plots were established in the Nuynivske Forest District, from which 75 tree cores were collected (Fig. 1). To collect wood samples during the field surveys, circular sample plots (CSPs) were established in the most representative areas of the forest subcompartments, following the guidelines of SOU 02.02-37-476:2006 (Ministry of Agrarian Policy of Ukraine, 2006). The plot radius varied depending on stand age, with plot areas ranging from 100 to 500 m^2. Tree diameters at breast height (DBH, 1.3 m) were measured using a tree calliper in two mutually perpendicular directions, and the average value was recorded to the nearest

0.1 cm. The heights of the sample trees were measured using a Haglöf EC-II-D hypsometer. A measuring tape was used to demarcate the plot boundaries (radii).

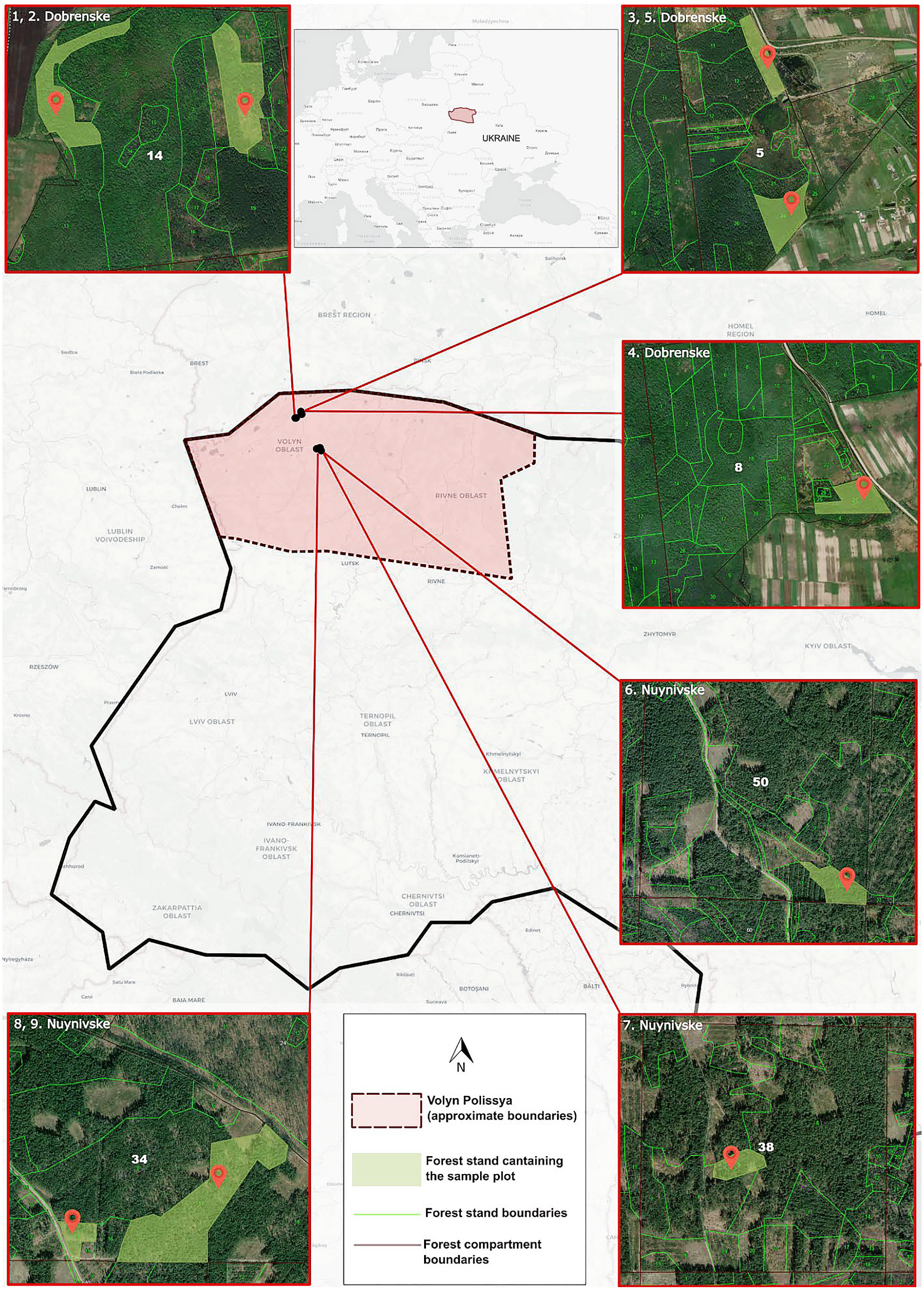

***Figure 1.** Location of the temporary sample plots*

Source: compiled by the authors based on the database of the Geoinformation System of Forest Resources Management of Ukraine (Ukrainian State Forest Management Planning Association, n.d.)

Tree cores were extracted from the sample trees at breast height (1.3 m) using a Haglöf increment borer, with boring performed perpendicular to the longitudinal axis of the stem. The extracted cores were mounted on wooden supports for safe transportation and subsequent laboratory preparation, which involved progressively sanding and scanning the samples for tree-ring dating. Each core was uniquely coded to ensure accurate identification of its sampling location. Tree-ring dating and radial growth measurements were performed using ImageJ software equipped with the ObjectJ plugin. Subsequent data processing was conducted using MS Excel. This laboratory processing yielded a comprehensive dataset of annual tree-ring widths. The summary characteristics of the processed dataset are presented in Table 1.

Table 1. *Statistical characteristics of the research data*

No.	Mean increment, mm	Number of rings	Standard deviation	No.	Mean increment, mm	Number of rings	Standard deviation	No.	Mean increment, mm	Number of rings	Standard deviation
1	1.5	89	0.82	48	2.9	41	2.00	95	1.7	61	1.37
2	2.2	78	0.89	49	2.5	43	0.94	96	1.8	66	1.02
3	1.6	90	0.97	50	3.7	21	1.62	97	2.1	66	1.27
4	2.1	77	1.12	51	2.9	20	1.64	98	1.2	66	0.86
5	1.9	85	0.80	52	3.4	20	1.93	99	2.0	68	1.13
6	1.8	78	0.84	53	4.8	20	2.31	100	1.6	58	1.50
7	1.6	86	1.07	54	3.3	19	1.98	101	2.0	63	1.08
8	1.7	89	0.86	55	5.2	20	2.11	102	2.6	50	1.92
9	1.4	79	1.20	56	5.8	18	2.06	103	1.7	61	0.93
10	1.5	79	1.19	57	4.1	21	2.02	104	3.0	66	1.38
11	1.8	82	1.14	58	4.6	18	1.99	105	2.2	64	1.19
12	2.0	88	1.10	59	5.4	18	1.77	106	1.6	66	0.72
13	1.5	75	1.37	60	3.8	21	2.99	17	1.5	63	0.92
14	1.4	69	0.53	61	3.8	21	1.92	108	1.9	59	0.80
15	1.1	90	1.44	62	4.5	20	1.90	109	1.8	61	1.57
16	0.9	87	1.09	63	3.9	17	3.07	110	1.4	52	1.34
17	1.4	83	1.09	64	5.2	20	2.51	111	2.0	64	1.67
18	1.3	89	1.06	65	5.2	17	2.62	112	1.4	67	0.98
19	1.2	90	1.03	66	2.2	19	1.72	113	1.9	59	1.08
20	1.4	88	0.74	67	4.5	19	2.86	114	1.8	64	1.03
21	1.0	76	0.84	68	3.0	17	1.80	115	2.2	66	1.23
22	1.1	88	0.87	69	3.0	16	1.66	116	1.8	61	1.43
23	1.1	90	0.72	70	3.0	17	1.89	117	1.9	62	1.17
24	1.5	81	0.82	71	2.8	19	1.65	118	1.9	60	1.69
25	1.6	71	0.94	72	3.8	18	2.71	119	1.5	50	1.07
26	1.4	81	0.87	73	3.8	20	2.31	120	2.5	58	1.32
27	1.8	95	0.74	74	4.3	21	2.33	121	1.8	60	1.59
28	1.5	97	1.09	75	3.8	18	2.69	122	1.7	59	1.50
29	1.2	92	1.10	76	2.8	19	2.14	123	1.5	64	0.97
30	2.0	93	1.14	77	3.8	19	2.86	124	1.5	81	1.38
31	1.5	98	0.72	78	5.6	18	2.83	125	2.1	81	1.56
32	1.4	97	0.70	79	3.9	17	1.70	126	2.0	83	1.52
33	1.7	87	0.76	80	4.4	17	3.62	127	1.9	77	1.09
34	1.6	98	0.96	81	4.3	18	2.50	128	2.1	83	1.47

Table 1. *Continued*

No.	Mean increment, mm	Number of rings	Standard deviation	No.	Mean increment, mm	Number of rings	Standard deviation	No.	Mean increment, mm	Number of rings	Standard deviation
35	2.2	72	1.04	82	4.8	19	2.35	129	2.2	77	1.29
36	1.3	84	0.60	83	4.6	18	2.43	130	2.3	80	1.00
37	3.7	39	2.31	84	3.6	19	2.08	131	3.2	71	1.35
38	2.5	46	1.46	85	1.7	55	1.01	132	2.5	84	1.93
39	2.5	39	1.41	86	2.5	51	1.62	133	2.1	70	2.22
40	3.1	46	0.95	87	2.5	65	1.54	134	2.4	87	1.66
41	2.7	42	1.97	88	2.6	63	1.61	135	2.5	77	1.68
42	2.3	42	1.47	89	3.6	61	2.34	136	2.3	82	2.12
43	3.4	44	1.07	90	2.3	60	2.10	137	1.8	82	1.66
44	2.6	52	0.82	91	2.4	54	2.21	138	2.0	83	1.23
45	3.0	44	2.04	92	2.1	65	1.71	139	1.5	81	1.60
46	2.8	43	1.20	93	1.9	47	1.43	max	5.8	98	3.6
47	3.2	40	2.41	94	2.1	67	1.40	min	0.9	16	0.5

Source: developed by the authors

All experimental research on plant materials in this study was conducted in accordance with relevant institutional, national, and international guidelines and legislation. The research strictly adheres to the principles of the Convention on Biological Diversity (United Nations, 1992). The dendrochronological sampling was carried out using non-destructive methods (increment borers), ensuring minimal impact on the health of individual trees and the integrity of the forest ecosystem.

To assess the impact of climatic drivers on the annual radial growth of Scots pine, a climate database was compiled, comprising monthly mean air temperatures and total precipitation data from the Kovel meteorological station, the nearest weather station to the study area. The use of data from a single meteorological station is methodologically justified, given the regional scale of the study and the relative climatic homogeneity of the Volyn Polissia. The historical and socio-economic peculiarities of the region – specifically, the inclusion of the territory of the present-day Volyn region within the Volhynian and Polissia Voivodeships of the Second Polish Republic between 1921 and 1939, coupled with the severe infrastructure destruction during the Second World War – resulted in highly fragmented meteorological observations in the first half of the 20th century. Consequently, for subsequent analysis, a complete and continuous climate dataset available from 1946 onwards, obtained from the archival records of the Borys Sreznevsky Central Geophysical Observatory (State Emergency Service of Ukraine, n.d.), was utilised.

To assess the influence of climatic drivers on annual growth formation, climatic variables from both the current year of growth formation and the previous year were used. This approach allowed for the consideration of potential delayed (lag) climatic effects associated with resource accumulation, soil water regimes, and the physiological state of the trees during the previous growing season. The primary processing of the tree-ring width series was performed to remove non-climatic growth trends related to tree age. For this purpose, individual detrending was applied to the radial growth series of each tree using a cubic smoothing spline as a function of age. The smoothing parameter was set at spar = 0.5, which ensured the removal of the long-term age-related trend without loss of interannual growth variability. Following standardisation, ring-width indices were obtained and used in all subsequent analyses of climate sensitivity.

The relationship between radial growth and climatic drivers was evaluated in stages. In the first stage, monthly correlations between the RWI and the climatic variables of air temperature and precipitation were analysed for the months of the current (t) and previous (t-1) years. This approach enabled the identification of critical intra-annual periods with the greatest influence on radial growth formation. To summarise the results of the correlation analysis and visually present the seasonal structure of climate sensitivity, the obtained correlation coefficients were visualised as a heatmap, reflecting the strength and statistical significance of the relationships between the climatic variables and the ring-width indices. All subsequent statistical calculations were performed in the R statistical environment using standard packages.

Results and Discussion

The results of the comprehensive dendroclimatic analysis highlight the environmental context and the specific growth responses of forest stands in the Kamin-Kashyrske FMU. The long-term dynamics of climatic variables (1946-2023) reflect the environmental background of the study region. The calculated air temperature series illustrates both the interannual variability of the mean regime and the intra-annual range between minimum and maximum values (Fig. 2a). Precipitation analysis shows the distribution of annual totals and the relative contribution of different seasons to the water regime (Fig. 2b).

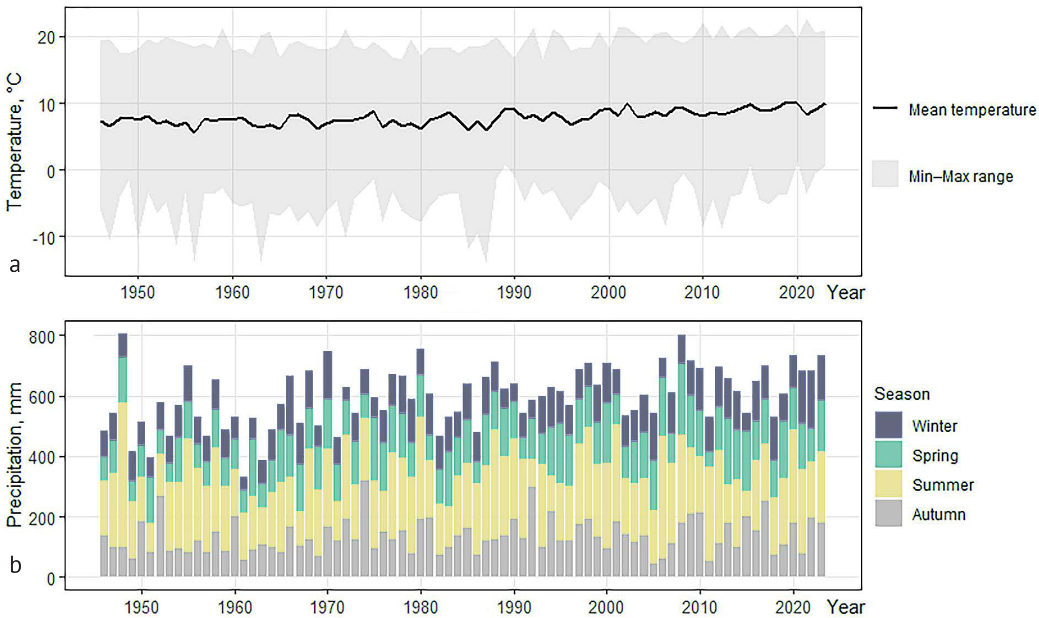

Figure 2. *Long-term characteristics of climatic variables in the study area (1946-2023)*

Note: a – annual minimum, mean, and maximum air temperatures calculated from monthly observations; b – seasonal precipitation

Source: developed by the authors based on the database of the Borys Sreznevsky Central Geophysical Observatory (State Emergency Service of Ukraine, n.d.)

The seasonal structure of climatic conditions is further detailed in the climograph, which visualises the monthly dynamics of temperature and precipitation (Fig. 3). This distribution identifies specific intra-annual periods that potentially act as primary drivers of radial growth formation in the study area. In total, 139 extracted cores were cross-dated, resulting in the measurement of 7,942 tree rings and the determination of their mean width (Table 1). The number of tree rings per core ranged from a minimum of 16 to a maximum of 98. The minimum mean radial growth was 0.9 mm, recorded in tree No. 16 (87 rings), while the maximum was observed in tree No. 56 (18 rings).

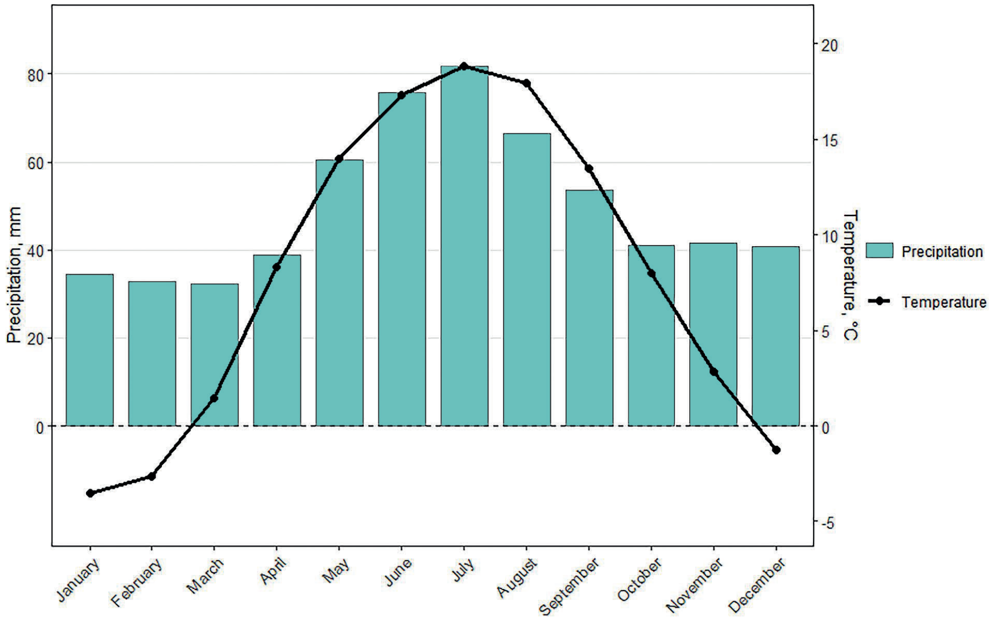

Figure 3. *Long-term monthly mean air temperature and precipitation at the Kovel meteorological station (1946-2023)*

Source: developed by the authors based on the database of the Borys Sreznevsky Central Geophysical Observatory (State Emergency Service of Ukraine, n.d.)

The analysis of individual Scots pine tree-ring chronologies obtained from the nine sample plots indicates a clearly pronounced long-term trend of decreasing radial growth with increasing tree age. The analysis confirms that tree-ring width variability is strictly age-dependent: in young stands, variability is significantly higher due to intensive growth processes, whereas this variability decreases as stand age increases. Such an age-related growth pattern is typical for tree species and can mask interannual growth fluctuations driven by external environmental factors, particularly climate. To isolate the climate-driven interannual variability from this ontogenetic trend, the radial growth series were standardised through detrending. As a result, RWI were calculated for each tree, characterising the relative deviations of growth from the expected age-related baseline. The transition from raw individual tree-ring measurement data to standardised ring-width indices across all sample plots is illustrated in Figure 4. The individual tree-ring chronologies clearly exhibit an age-related trend of decreasing radial growth (Fig. 4a). Following detrending, the ring-width indices for all sample plots (Fig. 4b) fluctuated around a mean of one (RWI ≈ 1), indicating the effective removal of the long-term age-related trend and confirming the validity of the applied standardisation procedure. At the same time, noticeable inter-tree growth variability is observed within each plot, manifested in the differing amplitudes of interannual fluctuations among individual trees.

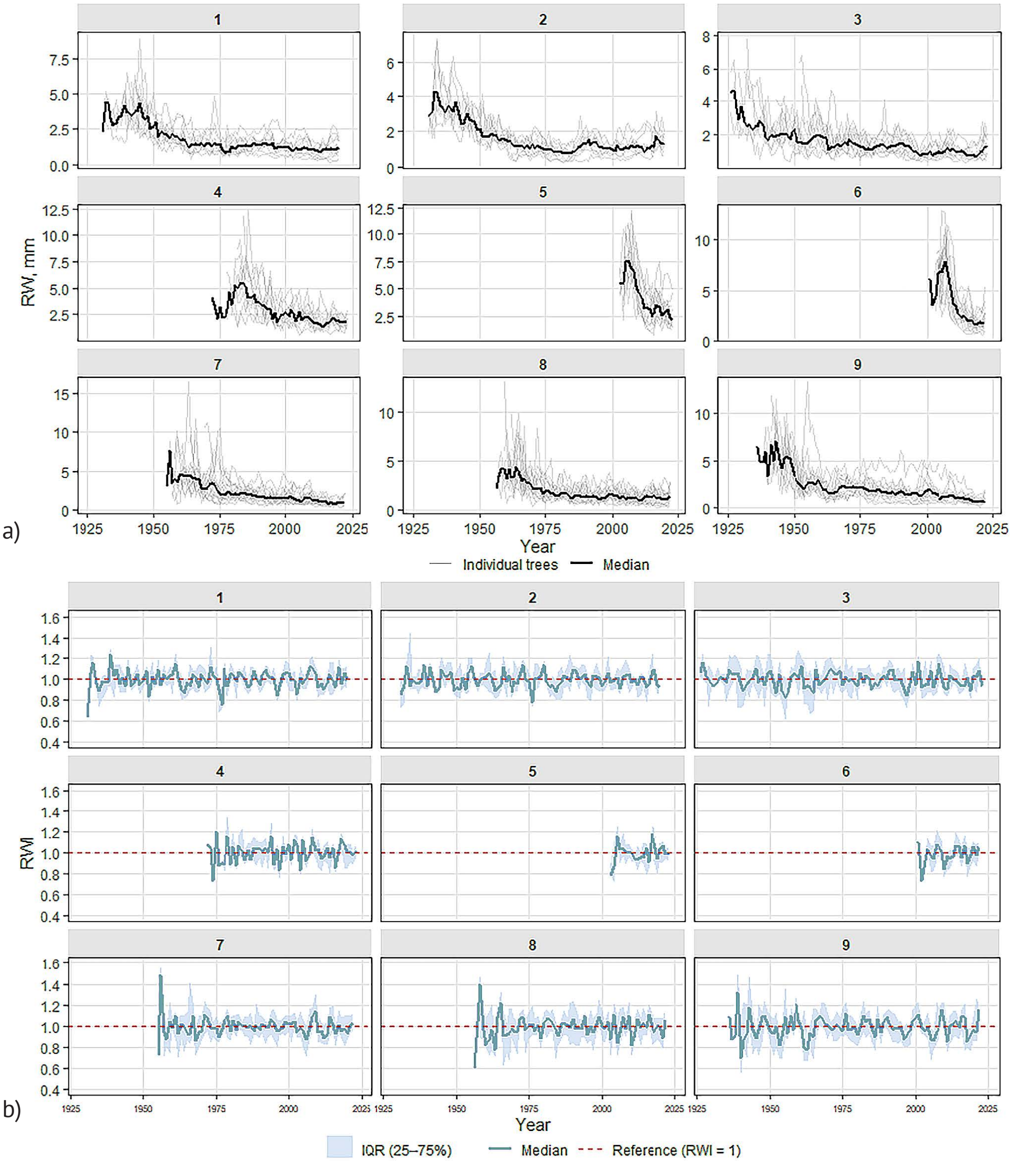

Figure 4. *Individual tree-ring chronologies (a) and standardised ring-width indices (b)*

Source: developed by the authors based on original research data

A comparison of the dynamics of the mean ring-width indices across the sample plots revealed a generally similar pattern of interannual fluctuations, indicating the presence of a common regional growth signal. However, differences in the amplitude and duration of specific phases of enhanced or reduced growth were noted for certain plots, which may be driven by local site conditions. Overall, these results confirm that, following the standardisation of the radial growth series, the RWIs are highly suitable for further analysis of the stands' climate sensitivity, specifically for assessing the relationship between interannual growth variability and climatic drivers of the current and previous years.

To verify the homogeneity of the climate signals, a correlation analysis was conducted between the ring-width indices and climatic variables separately for each of the nine sample plots. The obtained results demonstrate a general coherence in the seasonal structure of climate sensitivity across the sample plot data, despite some differences in statistical significance for specific months. The most stable relationships, in terms of both direction and strength, were observed for air temperature during the winter and early spring of the current year, and for precipitation during the summer months of the previous year. This finding justified the subsequent pooling of data from all sample plots to perform an integrated correlation analysis for the entire dataset of the studied stands.

To assess the seasonal structure of the climate sensitivity of radial growth, monthly correlations between the ring-width indices and the climatic variables of air temperature and precipitation were analysed. The analysis covered the months of the current year of growth formation (t) as well as the previous year (t-1), allowing for the assessment of both direct and delayed (lag) climatic effects. The data from the correlation analysis are presented as a heatmap (Fig. 5).

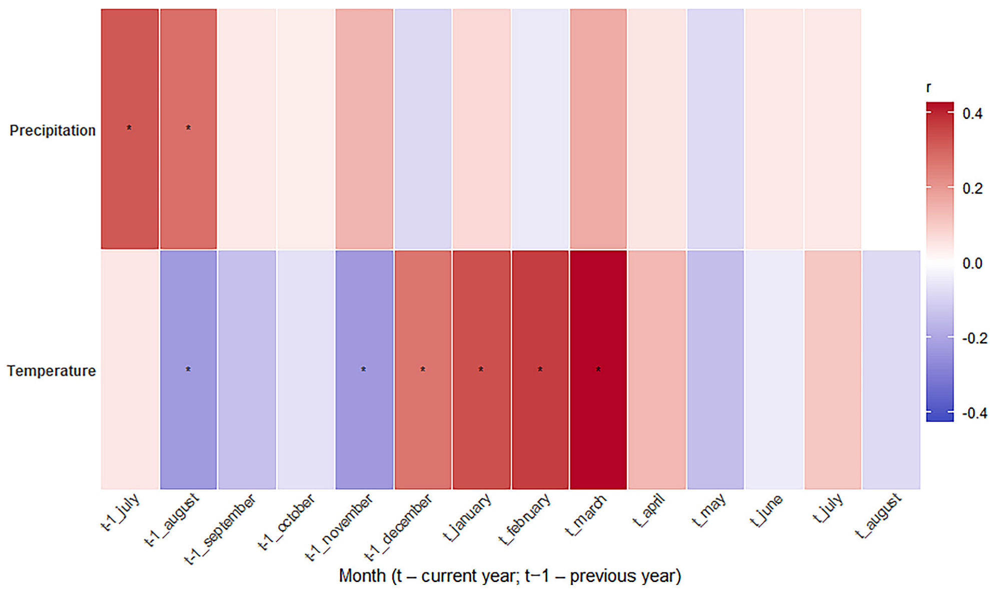

Figure 5. *Correlation analysis of the research data*

Source: developed by the authors based on original research data

The monthly correlation heatmap clearly illustrates the distinct seasonal structure of the climate sensitivity of Scots pine radial growth (Fig. 5). For air temperature, a statistically significant positive correlation with the ring-width indices was established during the winter and early spring of the current year, with maximum correlation coefficients observed from January to March ($r = 0.34$-0.43; $p < 0.01$). During the summer months of the current year, the relationship between temperature and radial growth is weak or absent. For precipitation, a different seasonal impact structure was found: statistically significant positive correlations with the ring-width indices are primarily concentrated in the summer months of the previous year, specifically in July and August ($r = 0.28$-0.32; $p < 0.05$), indicating the presence of delayed (lag) climatic effects. The temperature conditions of the previous year demonstrated both positive and negative correlations depending on the month, reflecting the bidirectional nature of their influence on radial growth formation. Overall, the obtained results confirm the presence of two main types of climate signals in growth formation: the direct impact of temperature conditions at the beginning of the year of growth formation, and the delayed impact of the water regime during the previous growing season. To illustrate the manifestation of the identified climate-growth relationships within the time series, the dynamics of both radial growth and the annual moisture balance were analysed (Fig. 6).

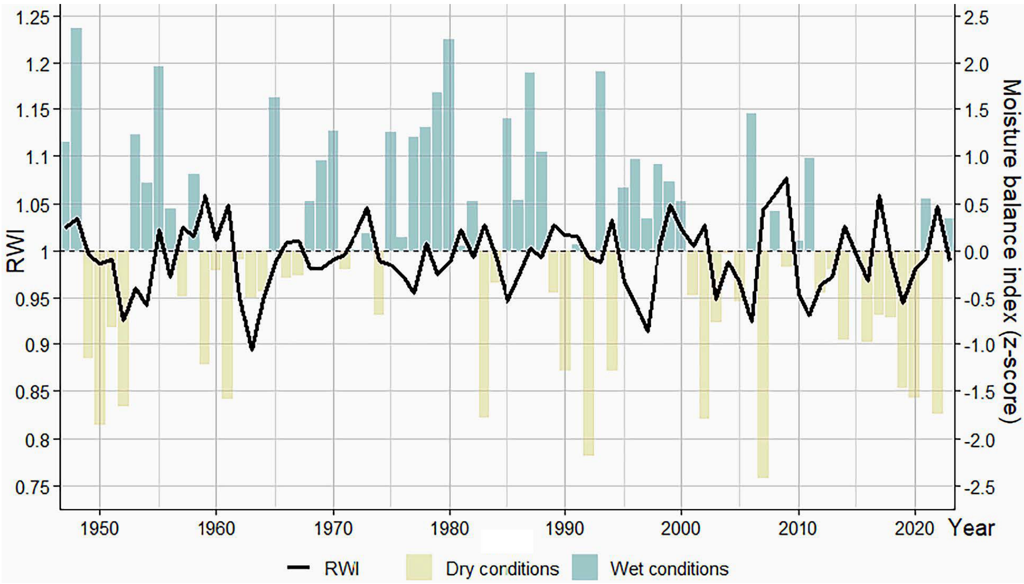

Figure 6. *Relationship between tree radial growth and hydrothermal conditions*

Source: developed by the authors based on original research data and data from the Borys Sreznevsky Central Geophysical Observatory (State Emergency Service of Ukraine, n.d.)

The data analysis (Fig. 6) indicates that negative radial growth anomalies predominantly coincide with years of negative moisture balance, i.e. drought conditions. The most pronounced growth reductions were observed in years when a moisture deficit was combined with elevated temperatures. Since 2000, a clearer synchronisation of negative RWI anomalies with dry periods has been observed, which may indicate the increasing sensitivity of the stands to moisture deficits. The obtained results demonstrate that the radial growth of Scots pine in the stands of the Volyn Polissia is shaped by a combination of long-term ontogenetic processes and seasonally structured climatic drivers. The application of individual detrending and the transition to standardised ring-width indices have enabled the removal of the age-related growth component and facilitated a focus on interannual variability driven by climatic conditions, which is a widely accepted approach in dendroclimatic research.

The identified positive impact of air temperature in February-March of the current year on Scots pine radial growth aligns with the results of numerous dendroclimatic studies, which emphasise the role of thermal conditions at the end of winter and the beginning of the growing season (Koprowski *et al.*, 2012; Janecka *et al.*, 2020; Waszak *et al.*, 2021). Elevated temperatures during this period are critical, as they promote an earlier reduction in soil frost depth. Milder thermal conditions prevent deep soil freezing, which facilitates earlier root water uptake and accelerates the restoration of xylem sap transport in early spring. This, in turn, promotes an earlier resumption of cambial activity and reduces the risk of physiological drought in the early growing season, ultimately ensuring more intensive radial growth.

The positive relationship between precipitation totals in July-August of the previous year and radial growth in the subsequent year indicates the presence of a pronounced lagged climate effect. Sufficient water availability in the second half of the growing season facilitates the accumulation of assimilates and the formation of carbohydrate reserves, which are utilised for growth processes at the beginning of the following year. Similar delayed precipitation effects have been repeatedly noted in dendroclimatic studies (Zeng *et al.*, 2022; Tumajer *et al.*, 2023), which is particularly relevant for pine stands on the sandy and loamy sand soils of the Polissia, where moisture deficit is a primary growth-limiting factor.

The identified sensitivity of Scots pine to shifting hydrothermal conditions in Volyn Polissia aligns with recent studies in adjacent areas. For instance, V. Levchenko *et al.* (2025) demonstrated in the Polissia Nature Reserve that radial growth serves as a primary indicator of both climatic fluctuations and the pathological impact of disease pathogens, which is crucial for assessing forest ecosystem resilience. Furthermore, observations of growth synchronisation with climatic parameters support the conclusions of V.A. Romanenko & S.B. Kovalevskyi (2023) from the Boyarka Forest Research Station. Their retrospective analysis similarly emphasised the importance of monitoring physiological resilience to develop effective forestry adaptation mechanisms for preserving Scots pine stands in Ukraine.

The absence of significant random effects across the sample plots and individual trees indicates the spatial coherence of the climate signal within the study area. This suggests that climatic drivers exert a dominant influence on the interannual variability of radial growth compared with local site conditions. Such spatial coherence of dendroclimatic signals is characteristic of lowland regions with relatively homogeneous climatic conditions (Duchesne *et al.*, 2017). This persistence of the climate signal is further supported by the research of M. Netsvetov *et al.* (2023) in the Chornobyl exclusion zone. Their study demonstrated that even under extreme environmental stressors, such as radiation exposure, pronounced climate signals persist in the growth dynamics of Scots pine.

While the findings emphasise the primary role of climatic drivers, it is important to note that radial growth fluctuations in the region are part of a more complex interaction. As noted by D. Holiaka *et al.* (2026) and V. Myroniuk *et al.* (2026), annual growth dynamics are driven not only by natural factors but also by the intensity of anthropogenic impacts, sanitary conditions, and silvicultural treatments. However, the high spatial coherence of the climate signal observed in this study suggests that under contemporary climate change, these external stressors likely act in synergy with climatic fluctuations (Julio Camarero *et al.,* 2015; Klisz *et al.,* 2023).

The observed synchronisation of negative RWI anomalies with dry periods since 2000 suggests a shift in the stands' adaptive capacity. This trend is likely driven by the increasing intensity and frequency of heatwaves and atmospheric droughts in the 21st century. As temperatures rise, the evaporative demand of the atmosphere increases, meaning that even moderate precipitation deficits now result in more severe physiological stress for the trees than in previous decades. These results are consistent with the findings of A. Debel *et al.* (2021), who analysed Scots pine growth in Bavaria and recorded a significant increase in tree sensitivity to climatic factors over the last few decades. Their study confirms that Scots pine remains one of the most vulnerable European tree species to climate change, with its sensitivity increasing even in relatively moist regions.

In summary, the dendroclimatic analysis of Scots pine stands in Volyn Polissia reveals a robust and spatially coherent climate signal that remains the primary driver of radial growth despite the presence of local environmental stressors. Growth formation depends critically on a specific seasonal window, namely thermal conditions in late winter and moisture availability during the peak of the previous growing season. However, the increasing synchronisation of growth reductions with drought events over the last two decades indicates a potential decline in the adaptive capacity of pine stands. These findings highlight the necessity of integrating seasonally specific climatic responses into forest management strategies to enhance the resilience of Volyn Polissia's forest ecosystems in the face of accelerating climate change.

Conclusions

The study of radial growth in Scots pine stands in the Volyn Polissia, based on tree-ring analysis, has identified several patterns of growth formation under ongoing climate change. The radial growth of Scots pine is characterised by a clearly pronounced age-related decreasing trend, which necessitates the application of detrending for accurate assessment of climate sensitivity. The transition to ring-width indices has allowed the removal of the ontogenetic growth component and enabled a focus on interannual variability driven by external factors. The monthly analysis of climatic variables revealed a distinct seasonal differentiation in the impact of these factors on radial growth formation. The most significant positive impact was exerted by the temperature conditions of the winter and early spring period of the current year, particularly in February and March. The presence of pronounced delayed (lag) climatic effects was also established. Specifically, precipitation totals in July-August of the previous year positively influenced radial growth in the following year, indicating the critical role of water availability at the end of the growing season in forming the resource base for growth. A comparison of the temporal dynamics of the ring-width index with the integrated moisture balance indicator showed that years with reduced growth predominantly coincide with periods of moisture deficit. This confirms the limiting influence of water availability on the formation of interannual radial growth variability and aligns with the results of the correlation analysis. The obtained results emphasise the high sensitivity of the Volyn Polissia pine stands to seasonal and delayed climatic impacts. These findings can be utilised to predict the response of forest ecosystems to further climate change and to justify the implementation of adaptive forest management practices. Future research could be directed towards expanding the range of climatic variables, specifically by incorporating extreme weather events, integrated hydroclimatic indices, and higher-resolution (daily) climate data.

Acknowledgements

The authors would like to thank Stanislav Berezynets and Marharyta Behal for their assistance with field data collection.

Funding

None.

Conflict of Interest

None.

References

[1] Bilous, A., Myroniuk, V., Svynchuk, V., Kashpor, S., & Lesnik, O. (2022). Stem volume by height classes of immature, mature and overmature stands of the main forest-forming species of Ukraine. *Ukrainian Journal of Forest and Wood Science*, 13(3), 7-12. doi: 10.31548/forest.13(3).2022.7-12.

[2] Debel, A., Meier, W.J.-H., & Bräuning, A. (2021). Climate signals for growth variations of *F. sylvatica*, *P. abies*, and *P. sylvestris* in Southeast Germany over the past 50 years. *Forests*, 12(11), article number 1433. doi: 10.3390/f12111433.

[3] Druckenbrod, D.L., Cook, E.R., Pederson, N., & Martin-Benito, D. (2024). Detrending tree-ring widths in closed-canopy forests for climate and disturbance history reconstructions. *Dendrochronologia*, 85, article number 126195. doi: 10.1016/j.dendro.2024.126195.
[4] Duchesne, L., D'Orangeville, L., Ouimet, R., Houle, D., & Kneeshaw, D. (2017). Extracting coherent tree-ring climatic signals across spatial scales from extensive forest inventory data. *PLOS ONE*, 12, article number e0189444. doi: 10.1371/journal.pone.0189444.
[5] Etzold, S., *et al.* (2022). Number of growth days and not length of the growth period determines radial stem growth of temperate trees. *Ecology Letters*, 25(2), 427-439. doi: 10.1111/ele.13933.
[6] Fesiuk, M., & Lesnik, O. (2025). Structure and utilisation of forest resource potential of Scots pine stands in the Volyn Polissya. *Ukrainian Journal of Forest and Wood Science*, 16(3), 57-74. doi: 10.31548/forest/3.2025.57.
[7] Holiaka, D., *et al.* (2026). Estimation of 90Sr and 137Cs activity concentrations in Chornobyl wood: Significance of factors and classical vs. machine learning methods. *Journal of Environmental Radioactivity*, 291, article number 107839. doi: 10.1016/j.jenvrad.2025.107839.
[8] Ivanyuk, I., & Fuchylo, Y. (2020). Influence of meteorological factors on the radial increase of English oak trees in the fresh and moist fairly fertile forest types conditions of the Ukrainian Polissya. *Proceedings of the Forestry Academy of Sciences of Ukraine*, 20, 57-63. doi: 10.15421/412005.
[9] Janecka, K., Harvey, J.E., Trouillier, M., Kaczka, R.J., Metslaid, S., Metslaid, M., Buras, A., & Wilmking, M. (2020). Higher winter-spring temperature and winter-spring/summer moisture availability increase Scots pine growth on coastal dune microsites around the south Baltic Sea. *Frontiers in Forests and Global Change*, 3, article number 578912. doi: 10.3389/ffgc.2020.578912.
[10] Julio Camarero, J., Gazol, A., Sancho-Benages, S., & Sangüesa-Barreda, G. (2015). Know your limits? Climate extremes impact the range of Scots pine in unexpected places. *Annals of Botany*, 116(6), 917-927. doi: 10.1093/aob/mcv124.
[11] Kastridis, A., Kamperidou, V., & Stathis, D. (2022). Dendroclimatological analysis of fir (*A. borisii-regis*) in Greece in the frame of climate change investigation. *Forests*, 13(6), article number 879. doi: 10.3390/f13060879.
[12] Klisz, M., Puchałka, R., Jakubowski, M., Koprowski, M., Netsvetov, M., Prokopuk, Y., & Jevšenak, J. (2023). Local site conditions reduce interspecific differences in climate sensitivity between native and non-native pines. *Agricultural and Forest Meteorology*, 341, article number 109694. doi: 10.1016/j.agrformet.2023.109694.
[13] Koprowski, M., Przybylak, R., Zielski, A., & Pospieszyńska, A. (2012). Tree rings of Scots pine (*Pinus sylvestris* L.) as a source of information about past climate in northern Poland. *International Journal of Biometeorology*, 56(1), 1-10. doi: 10.1007/s00484-010-0390-5.
[14] Koval, I., & Andreeva, O. (2022). Radial increment of Scots pine next to the a place of clear cutting at the center of the ipid bark beetle outbreaks in Polissya. *Proceedings of the Forestry Academy of Sciences of Ukraine*, 24, 56-65. doi: 10.15421/412205.
[15] Koval, I., Maksymenko, N., Cherkashyna, N., Gololobov, V., & Andreieva, O. (2025). Response of Japanese larch (*Larix leptolepis* Gord) radial growth to climate change in the left bank forest-steppe, Ukraine. *Acta Horticulturae et Regiotecturae*, 28(1), 12-20. doi: 10.2478/ahr-2025-0002.
[16] Lesnik, O., Blyshchyk, V., Odruzhenko, A., & Behal, M. (2022). Growth and physiological resilience of pine forests in Ukrainian Polissia. *Ukrainian Journal of Forest and Wood Science*, 13(1), 18-24. doi: 10.31548/forest.13(1).2022.18-24.

[17] Levchenko, V., Tkachenko, M., & Adamovych, B. (2025). Indicators of the impact of climatic factors and pathogen development on the radial growth of Scots Pine in the Polissya Nature Reserve. In *Proceedings of the 7th international scientific and practical online conference* (pp. 19-28). Łomży: MANS w Łomży.
[18] McPartland, M.Y., St. George, S., Pederson, G.T., & Anchukaitis, K.J. (2020). Does signal-free detrending increase chronology coherence in large tree-ring networks? *Dendrochronologia*, 63, article number 125755. doi: 10.1016/j.dendro.2020.125755.
[19] Ministry of Agrarian Policy of Ukraine. (2006). *SOU 02.02-37-476:2006. Forest management sample plots. Establishment method*. Kyiv: Ministry of Agrarian Policy of Ukraine.
[20] Myroniuk, V., Svynchuk, V., Terentiev, A., Matushevych, L., Bala, O., Lesnik, O., Lakyda, I., Domashovets, G., Bondar, H., & Melnyk, O. (2026). Estimating current annual volume increment of pine stands using one-time tree measurements on temporary sample plots. *Journal of Forest Research*, 31(1), 45-53. doi: 10.1080/13416979.2025.2582348.
[21] Netsvetov, M., Prokopuk, Y., Holiaka, D., Klisz, M., Porté, A.J., Puchałka, R., & Romenskyy, M. (2023). Is there Chornobyl nuclear accident signature in Scots pine radial growth and its climate sensitivity? *Science of The Total Environment*, 878, article number 163132. doi: 10.1016/j.scitotenv.2023.163132.
[22] Prokopuk, Y., Sylenko, O., Klisz, M., Annabel, J., & Netsvetov, M. (2024). Terrain's steepness governs sensitivity of urban oak forests to climate variability. *Urban Forestry & Urban Greening*, 102, article number 128586. doi: 10.1016/j.ufug.2024.128586.
[23] Romanenko, V.A., & Kovalevskyi, S.B. (2023). Influence of climate change on the radial growth of Scots pine in Forest Stands of the Boyarka Forest Research Station. *Scientific Bulletin of UNFU*, 33(5), 40-45. doi: 10.36930/40330505.
[24] State Emergency Service of Ukraine. (n.d.). *Borys Sreznevsky Central Geophysical Observatory [Data set]*. Retrieved from http://cgo-sreznevskyi.kyiv.ua/uk/.
[25] Tumajer, J., Altman, J., & Lehejček, J. (2023). Linkage between growth phenology and climate-growth responses along landscape gradients in boreal forests. *Science of The Total Environment*, 905, article number 167153. doi: 10.1016/j.scitotenv.2023.167153.
[26] Ukrainian State Forest Management Planning Association. (n.d.). *Geoinformation System of Forest Resources Management of Ukraine [Data set]*. Retrieved from https://gis.lisproekt.gov.ua/portal/apps/sites/#/gis-lisproekt.
[27] United Nations. (1992). *Convention on Biological Diversity*. Retrieved from https://www.cbd.int/convention/text/.
[28] Waszak, N., Robertson, I., Puchałka, R., Przybylak, R., Pospieszyńska, A., & Koprowski, M. (2021). Investigating the climate-growth response of Scots pine (*Pinus sylvestris* L.) in Northern Poland. *Atmosphere*, 12(12), article number 1690. doi: 10.3390/atmos12121690.
[29] Zeng, X., Evans, M.N., Liu, X., Peltier, D.M.P., Zhan, S., Ni, P., Li, Y., Zhang, L., & Yang, B. (2022). Process representation of conifer tree-ring growth is improved by incorporation of climate memory effects. *Agricultural and Forest Meteorology*, 327, article number 109196. doi: 10.1016/j.agrformet.2022.109196.

Радіальний приріст дерев у соснових насадженнях Волинського Полісся

Олександр Леснік
Кандидат сільськогосподарських наук, доцент
Навчально-науковий інститут лісового та садово-паркового господарства
Національного університету біоресурсів та природокористування України
03041, вул. Горіхуватський шлях, 19, м. Київ, Україна
https://orcid.org/0000-0002-4287-3454
Максим Фесюк
Аспірант
Навчально-науковий інститут лісового та садово-паркового господарства
Національного університету біоресурсів та природокористування України
03041, вул. Горіхуватський шлях, 19, м. Київ, Україна
https://orcid.org/0009-0008-7474-0913
Олександр Сіжук
Державне підприємство «Лісогосподарський інноваційно-аналітичний центр»
Державного агентства лісових ресурсів України
01013, вул. Деревообробна, 1, м. Київ, Україна
https://orcid.org/0009-0008-4607-3447

Анотація. У статті досліджено особливості формування радіального приросту сосни звичайної (*Pinus sylvestris* L.) у насадженнях Волинського Полісся з урахуванням впливу кліматичних показників. Метою дослідження було визначення сезонної структури кліматичної чутливості радіального приросту сосни звичайної та встановлення ключових кліматичних чинників, що зумовлюють міжрічну мінливість ширини річних кілець. Аналіз базувався на рядах ширини річних кілець, отриманих на дев'яти тимчасових пробних площах. Для усунення вікових тенденцій росту застосовано детрендінг з переходом до індексів радіального приросту. Оцінювання зв'язків між динамікою радіального приросту та кліматичними показниками виконано за допомогою кореляційного аналізу з використанням місячних значень температури повітря та атмосферних опадів поточного і попереднього років. У результаті дослідження встановлено, що радіальний приріст сосни звичайної найбільш чутливо реагує на температурні умови зимово-ранньовесняного періоду поточного року, зокрема у лютому-березні. Виявлено також виражені лагові ефекти клімату: кількість опадів у липні-серпні попереднього року позитивно впливає на приріст у наступному році. Результати аналізу підтвердили суттєвий вплив зазначених кліматичних чинників у формуванні міжрічної мінливості приросту. Відсутність істотних просторових випадкових ефектів свідчить про узгодженість кліматичного сигналу в межах досліджуваної території. Отримані результати розширюють уявлення про сезонну структуру кліматичної чутливості соснових насаджень Волинського Полісся та можуть бути використані для оцінки стійкості лісових екосистем і розроблення адаптивних підходів до ведення лісового господарства в умовах сучасних кліматичних змін

Ключові слова: *Pinus sylvestris* L.; динаміка радіального приросту; показники ширини річних кілець; кліматичні фактори; дендрохронологія

Received 28.11.2025 Revised 24.02.2026 Accepted 23.04.2026 Published: 30.04.2026

Vol. 22, No. 2
2026

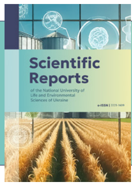

Scientific Reports of the National University of Life and Environmental Sciences of Ukraine

Journal homepage: https://scireports.com.ua/en e-ISSN 2223-1609

UDC 635.15:631.527.53.04](477.4) DOI: 10.31548/dopovidi/2.2026.36

Adaptive potential and breeding value of daikon varieties (*Raphanus sativus* L. *convar. acanthiformis* Sazon.) under different sowing dates in the conditions of the Forest-Steppe of Ukraine

Ivan Fedosiy
PhD in Agricultural Sciences, Associate Professor
National University of Life and Environmental Sciences of Ukraine
03041, 15 Heroiv Oborony Str., Kyiv, Ukraine
https://orcid.org/0000-0002-5044-9960

Oleksandr Komar*
PhD in Agricultural Sciences
National University of Life and Environmental Sciences of Ukraine
03041, 15 Heroiv Oborony Str., Kyiv, Ukraine
https://orcid.org/0000-0001-7511-4190

Iryna Bobos
PhD in Agricultural Sciences, Associate Professor
National University of Life and Environmental Sciences of Ukraine
03041, 15 Heroiv Oborony Str., Kyiv, Ukraine
https://orcid.org/0000-0001-5193-7192

Olena Siedova
Assistant
National University of Life and Environmental Sciences of Ukraine
03041, 15 Heroiv Oborony Str., Kyiv, Ukraine
https://orcid.org/0000-0003-4869-1560

Mykhailo Retman
PhD in Agricultural Sciences, Senior Researcher
Institute of Water Problems and Land Reclamation of the National Academy of Agrarian Sciences of Ukraine
03022, 37 Vasylkivska Str., Kyiv, Ukraine
https://orcid.org/0000-0002-6972-2410

Suggested Citation:
Fedosiy, I., Komar, O., Bobos, I., Siedova, O., & Retman, M. (2026). Adaptive potential and breeding value of daikon varieties (*Raphanus sativus* L. *convar. acanthiformis* Sazon.) under different sowing dates in the conditions of the Forest-Steppe of Ukraine. *Scientific Reports of the National University of Life and Environmental Sciences of Ukraine*, 22(2), 36-50. doi: 10.31548/dopovidi/2.2026.36.

*Corresponding author

Abstract. Global climate change and the shifting of agroclimatic zones in Ukraine necessitate a revision of traditional elements of vegetable crop cultivation technology to ensure stable food security. The aim of the study was to evaluate the adaptive potential of daikon varieties depending on sowing dates in order to achieve stable yields under modern agroclimatic transformations. Analysis of variance (Type III SS) showed that 92.5% of yield variation was determined by the studied factors. The greatest influence was exerted by sowing date (62.6%, $p < 0.001$), which significantly exceeded the effect of variety (15.4%, $p < 0.001$), while the influence of year was minor (4.1%, $p < 0.001$). Among interactions, only the "sowing date × year" combination was statistically significant (7.5%, $p < 0.001$). All varieties were characterised by high relative stability (Sg_i 6.0-14.4%). According to ANOVA and Tukey's HSD test, significant differences between varieties were established for most sowing dates ($p < 0.05$). The variety 'Minowase' outperformed 'Gulliver' in the second ten-day period of July to the first ten-day period of August (50.8-58.9 vs 47.4-54.6 t/ha). The early sowing date (first ten-day period of July) did not provide significant differences between genotypes. All varieties showed high plasticity, except for 'Gulliver' in the early sowing period (b_i = -0.39). Reduced plasticity for 'Minowase' was observed in the first ten-day period of August (b_i = 0.89). The highest sensitivity to environmental conditions was recorded for the second ten-day period of July (b_i = 1.43-2.20). The highest breeding value indices were obtained for sowing in the first ten-day period of August (34.8-40.9), which was associated with high yield (51.0-56.4 t/ha) and stability (2.9-3.1). The results substantiate the expediency of using the variety 'Minowase' and optimising sowing dates (late July – early August) as an effective agrotechnological tool for increasing productivity and stability of daikon cultivation under climate change conditions

Keywords: ecological plasticity; genotype stability; root yield; hydrothermal stress; adaptive capacity

Introduction

Climate change poses a threat to the stability of vegetable crop production. The use of ecologically adaptable genotypes, which are characterised by low sensitivity to adverse abiotic factors and ensure stable yields under various soil and climatic conditions, plays a key role in the adaptation process. At the same time, optimising sowing dates allows the negative impact of stress factors, pests and diseases to be minimised at critical stages of plant development.

According to X. Wang *et al*. (2025), global food security faces a dual challenge. Firstly, demographic expansion – with the population projected to reach 9.7 billion by 2050 and nearly 11 billion by the end of the century – requires a proportional increase in resources. Secondly, the agricultural sector generates around 33% of anthropogenic greenhouse gas emissions. As part of the transition to sustainable food systems, the intensive expansion of vegetable and fruit growing is of critical importance: to provide for the diets of 10 billion people, global fruit and vegetable production must increase by 50-150% by the middle of the century.

Research by E.A. Dumitru *et al*. (2023) has shown that in the future, heat stress and droughts will render many areas that currently have an optimal climate unsuitable for growing vegetable crops in open fields. Research by A. Paul & R. Machavaram (2026) highlighted that the destabilisation of the Indian vegetable market is a direct consequence of weather anomalies. The unpredictability of monsoons and temperature fluctuations not only disrupt the production cycle but also trigger a chain reaction: from logistical disruptions to a sharp rise in product prices. Under such conditions, the adoption of climate-smart agriculture methods becomes a prerequisite for maintaining the sector's profitability. In Ukraine, the average annual temperature, according to V. Vyshnevskyi (2025), has risen by more than 3°C. This has caused a shift in climatic zones of 500 km and, as highlighted by S. Klok *et al*. (2023), led to the expansion of "tropical nights" after 2000, exacerbating soil drought and temperature stress. Such changes have negatively affected traditional cold-tolerant brassica root crops due to impaired assimilation, premature bolting and the development of physiological disorders, in particular, softness, cracking and internal browning of tissues resulting from intensive lignification, disruption of Ca^{2+} transport and the activation of enzymatic oxidation of phenolic compounds. According to R.R. Babu *et al*. (2024), the stable development of the vegetable sector will depend directly on the adaptation of agronomic practices to these changes, in particular through crop diversification and the adjustment of traditional sowing dates.

Analysing the characteristics of daikon cultivation, N. Khusanov *et al*. (2024) established a significant influence of sowing dates on field germination: when sown in July, germination was 97-98%, whereas in August it fell to 76% due to temperature stress, demonstrating the critical importance of adjusting sowing dates to maintain the necessary plant density. A. Kaur & N. Singh (2022) emphasised that the strategic combination of variety selection and sowing date is a critical factor for maximising radish yield under a changing climate. Incorrect variety selection can completely negate the benefits of optimal sowing dates, causing physiological disorders in the root crops. According to a study by I. Fedosiy *et al*. (2025), regulating sowing dates is a strategic method for adapting daikon to hydrothermal challenges, as crop yield and quality depend directly on this. Sowing in the second half of summer not only promotes maximum root mass accumulation but also minimises the risks of pest damage and physiological disorders. S. Parajuli & P. Dhital (2023) argued that optimising plant spacing parameters is also critical for minimising competition for resources, as excessive density inhibits root morphogenesis. The key issue behind low yields lies in the failure to adhere to sowing patterns, which limits vegetative development and the realisation of the crop's biological potential. Rational spatial geometry ensures better sunlight exposure and nutrient uptake, which is crucial for the formation of yield mass and quality.

At the same time, recent studies have confirmed that the limiting factors affecting daikon yield are largely due to soil degradation and an imbalance in mineral nutrition. In particular, Shilpa *et al*. (2023) demonstrated that the systematic application of mineral fertilisers alone, without integrated approaches, leads to a decline in soil fertility, whereas the synergy of organic and microbiological components results in a yield increase of over 10%. This confirmed the advisability of transitioning to sustainable fertilisation systems within the framework of adaptive technologies. An additional destabilising factor is the prolonged cultivation of a single crop in a monoculture. A. Nowak *et al*. (2024) found that the absence of crop rotation leads to a transformation of the soil microbiome structure and a reduction in enzymatic activity, which impairs the bioavailability of nutrients. This highlights the need to implement scientifically grounded crop rotations and strategies for the biologisation of agriculture.

Despite a significant number of studies on the influence of sowing dates and genotypic characteristics on the productivity of *Raphanus* crops, their combined effect on the formation of ecological plasticity and stability of daikon varieties under conditions of climate change remains insufficiently studied. Most existing studies have been conducted in other soil and climate zones and do not account for the specific characteristics of the Ukrainian Forest-Steppe, which limits the possibility of directly extrapolating the results. The lack of generalised data on "genotype × environment" interactions in combination with sowing dates complicates the scientifically grounded selection of varieties and the optimisation of cultivation techniques to ensure stable yields. Thus, the aim of this study was to determine the parameters of ecological plasticity, stability and breeding value of daikon varieties depending on sowing dates under the conditions of the Ukrainian Forest-Steppe in order to optimise cultivation techniques.

Materials and Methods

Field experiments were conducted during 2022-2024 at the experimental fields (educational laboratory "Fruit and Vegetable Garden") of the Department of Vegetable Growing and Protected Cultivation at the National University of Life and Environmental Sciences of Ukraine. The coordinates of the experimental site were 50°22'42.21"N, 30°30'05.17"E, with an altitude of 158 m above sea level. The soils of the experimental plots were soddy-podzolic on loess. The granulometric composition of the soil was light loam. Agrochemical properties were as follows: pH of the salt extract 6.74, organic matter (humus) 2.71%, nitrate nitrogen 6.42 mg/kg, ammonium nitrogen 11.72 mg/kg, available phosphorus 568.83 mg/kg, and available potassium 152.93 mg/kg.

Meteorological conditions during 2022-2024 were characterised by a general trend towards warming and increased moisture relative to long-term averages (LTA) (Fig. 1). On average over the study years, the annual temperature exceeded the norm by 1.6°C, and the annual precipitation total exceeded the LTA by 216.7 mm. Temperature conditions during the crop growing period (July-October) were characterised by an excess over long-term averages by 0.9-2.6°C, with the most pronounced warming observed in August (23°C). The moisture regime during this period was uneven: the average monthly precipitation ranged from 49.2 to 109.9 mm. In particular, July was characterised by anomalously high precipitation (deviation of +41.9 mm from LTA), whereas August and September showed a moisture deficit (-6.8 and -7.8 mm from LTA, respectively), followed by increased precipitation in October (35.5 mm above the norm).

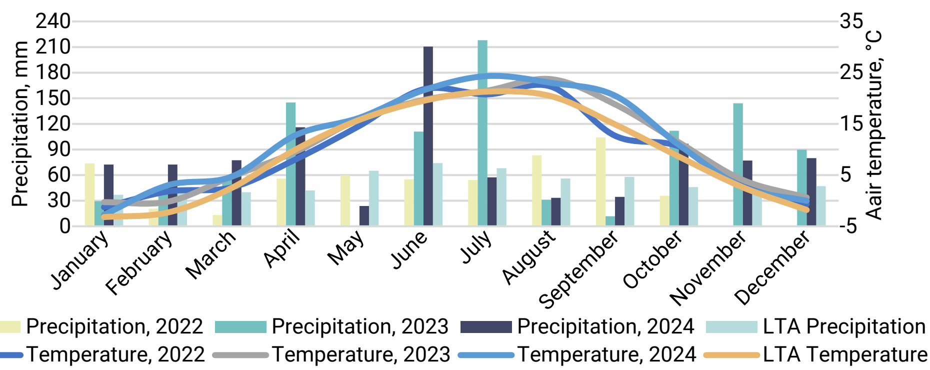

Figure 1. *Monitoring of meteorological indicators in 2022-2024*

Source: developed by the authors based on own research

The research programme was based on a two-factor design. Factor A comprised varietal characteristics of daikon: 'Gulliver' (control, bred in Ukraine) and 'Minowase' (the Netherlands). The variety 'Gulliver' served as the control as a widely distributed Ukrainian variety with high ecological plasticity under the agroclimatic conditions of Ukraine. Factor B included four sowing dates: the first, second (control), and third ten-day periods of July, and the first ten-day period of August. Optimisation of daikon sowing dates was based on consideration of its photoperiodic response as a long-day crop. The selection of a sowing date that ensures active vegetation under shortening daylight conditions is critical for preventing premature bolting. A rationally determined sowing date made it possible to synchronise plant development with periods of low activity of the cabbage root fly, thereby minimising entomological damage to crops. The hydrothermal regime – characterised by decreasing temperatures alongside increasing air and soil moisture – acted as a key factor in preventing physiological disorders such as bitterness accumulation and the development of pithiness in roots. At the same time, the temporal placement of sowing dates, in accordance with the duration of the growing period, limited the harvesting window, ensuring the attainment of marketable weight and high biochemical quality.

The experiment was established using a randomised block design with three replications. The area of the accounting plot was 5 m^2. Sowing was carried out manually to a depth of 4-5 cm, following a planting scheme of 45 × 10 cm. Harvesting was performed differentially, taking into account the duration of the growing period of the varieties: on the 50^{th} day after mass emergence for 'Gulliver' and on the 60^{th} day for 'Minowase'. Records were taken at the onset of phenological stage BBCH 49 (Biologische Bundesanstalt, Bundessortenamt and Chemical Industry), when the root crop had reached the size and shape typical of the variety. This approach allowed the recording of maximum marketable productivity while preventing the risk of physiological overmaturity and tissue coarsening in the roots. The study adhered to the principles of the Convention on Biological Diversity (1992). For a comprehensive evaluation of daikon genotypes, the following traits were analysed: mean yield, coefficient of variation (*CV*), general (GAC_i) and specific (SAC_i) adaptive capacity, relative stability (Sg_i), ecological plasticity (regression coefficient b_i), and breeding value of the genotype (SVG_i). The adaptive response of the studied varieties to growing conditions was assessed through their general and specific adaptive capacity. According to the methodological approaches of A. Tyshchenko *et al*. (2023), GAC_i was defined as the mean value of a quantitative trait based on trials across different environmental gradients, whereas SAC_i was considered as the amplitude of deviation from the mean value in a specific environment. The ability of a genotype to maintain stability of a given phenotype across a wide range of growing conditions due to internal regulatory mechanisms was identified as genetic stability. The parameter of ecological plasticity was calculated using the regression coefficient of the genotype against environmental conditions, allowing a quantitative assessment of the intensity of phenotypic variability in response to changes in external factors. The mathematical determination of the effects of general and specific adaptive capacity was based on the study of a population consisting of *n* genotypes tested in *m* environments with *c* replications. In this case, the number of replications equals *c*:

$$x_{ikr} = U + V_i + d_k + (Vd)_{ik} + e_{ikr}\,, \qquad (1)$$

where x_{ikr} – phenotypic value of the *i*-th genotype grown in the *k*-th environment in the *r*-th replication; *U* – overall mean of the entire set of phenotypes; V_i – effect of the *i*-th genotype; d_k – effect of the *k*-th environment; $(Vd)_{ik}$ – effect of the interaction between the *i*-th genotype and the *k*-th environment; e_{ikr} – effect determined by random factors and attributed to the *eikr* phenotype.

The elements of the model are subject to the following constraints:

$$\sum_i v_i = \sum_k d_k = \sum_k (vd)_{ik} = \\ = \sum_k (vd)_{ik} = \sum e_{ik} = 0 \qquad (2)$$

The evaluation methodology consisted of a preliminary analysis of variance followed by the identification of parameters of adaptability and stability. The value V_i was taken as the effect of general adaptive capacity. Specific adaptive capacity was calculated as a deviation from the sum $U + V_i$ and included both the linear effect of the environment and the non-linear component of the interaction $(Vd)_{ik.}$

The parameters of specific adaptive capacity were determined:

$$\sigma^2\ SAC_i = \frac{\sum_{k=1}^{m}(SAC_{ik})^2}{m-1} - \frac{\sigma_e^2}{c}, \quad (3)$$

where σ^2 SAC$_i$ – variance of specific adaptive capacity of the *i*-th genotype (an indicator of its genetic stability); SAC$_{ik}$ – effect of specific adaptive capacity of the *i*-th genotype in the *k*-th environment, calculated as a deviation from the sum $U+V_i$; *m* – number of environments in the study; σ_e^2 – random variance (mean square error) obtained from the analysis of variance; *c* – number of replications in each environment.

$$\sigma\ SAC_i = \sqrt{\sigma^2\ SAC_i}, \quad (4)$$

where σ SAC$_i$ – the standard deviation of the specific adaptive capacity of the *i*-th genotype.

To assess the variability of traits comparatively, the relative stability coefficient was calculated *(*Sg_i*)*:

$$Sg_i = \frac{\sigma_{SAC_i}}{U+GAC_i} * 100\ \%. \quad (5)$$

The ecological stability of genotypes was assessed using the relative stability index (Sg_i) by classifying the obtained values into five categories: high stability ($0 \leqslant Sg_i \leqslant 25$), stability ($26 \leqslant Sg_i \leqslant 50$), moderate stability ($51 \leqslant Sg_i \leqslant 75$), instability ($76 \leqslant Sg_i \leqslant 100$) and high instability ($Sg_i > 100$).

Varietal plasticity was assessed using the regression coefficient b_i:

$$b_i = \frac{\sum X_{iR} * d_R}{\sum_R d_R^2}. \quad (6)$$

The regression coefficient b_i served as an indicator of the ecological plasticity of genotypes: values of $b_i > 1$ indicated high sensitivity of the variety to improved growing conditions (intensive type); $b_i <$ indicated a low response to agronomic practices and high adaptability to unfavourable factors; at $b_i = 1$, a complete correlation between changes in yield and environmental conditions was observed.

Comprehensive selection of genotypes based on productivity and stability was carried out using the breeding value index (SVG_i):

$$SVG_i = U + GAC_i - p\ \sigma_{SAC_i}. \quad (7)$$

The degree of variability of the studied traits was assessed using the coefficient of variation (*CV*, %), applying the following classification: low variability at $CV \leqslant 10\%$, moderate at $10\% < CV \leqslant 20\%$, and high at $CV > 20\%$.

Statistical analysis of the experimental data was performed using JASP software (Version 0.95.4, JASP Team, 2025). The calculations included a multifactor analysis of variance (ANOVA) to determine the significance of the effects of year, variety, sowing date, and their interactions. Comparison of mean values was carried out using Tukey's HSD post hoc test at a significance level of $p < 0.05$. To quantify the contribution of each factor to the overall variability of the traits, the partial eta-squared (η^2_p) index was calculated. The precision of mean yield values was assessed using the pooled standard error (SE). The applied statistical methods and mathematical models ensured the reliability of the obtained results, allowing conclusions to be drawn regarding the adaptive characteristics of daikon varieties under different sowing dates.

Results and Discussion

Assessment of daikon yield (2022-2024) indicated the dominant importance of cultivation technology elements. According to the results of the three-factor analysis of variance (Table 1), the main factor influencing variability of this trait was the sowing date, for which the effect size (η^2_p) was 0.894 at $p < 0.001$. The influence of the variety factor was also characterised by high statistical significance ($F = 99.2$; $p < 0.001$), although its share in the total variance ($\eta^2_p = 0.674$) was lower compared with sowing dates. The influence of annual weather conditions was the smallest among the studied factors ($\eta^2_p = 0.357$). The three-factor analysis of variance confirmed the high representativeness of the selected model, in which the predominant share of yield variation was determined by the influence of controlled factors with minimal contribution from random error. The sowing date was identified as the key determinant of productivity, with its importance significantly exceeding the contribution of varietal characteristics and annual weather conditions. At the same time, the statistically significant interaction between the sowing date and seasonal meteorological parameters indicates the need for an adaptive approach to cultivation technology in order to fully realise the genetic potential of the varieties. It was established that the total contribution of the studied factors to the variation in daikon yield amounted to 92.5%, whereas only 7.5% was attributable to random deviations (Fig. 2).

Table 1. *Results of the analysis of variance examining the effect of the factors under study on daikon yield (2022-2024)*

Cases	Sum of squares	df	Mean square	F	p	η^2	η^2_p
Variety	256.360	1	256.360	99.205	<0.001	0.154	0.674
Sowing date	1,040.821	3	346.940	134.258	<0.001	0.626	0.894
Year	69.003	2	34.501	13.351	<0.001	0.041	0.357
Variety ✻ Sowing date	30.017	3	10.006	3.872	0.015	0.018	0.195
Variety ✻ Year	1.496	2	0.748	0.289	0.750	8.991×10^{-4}	0.012
Sowing date ✻ Year	123.978	6	20.663	7.996	<0.001	0.075	0.500
Variety ✻ Sowing date ✻ Year	17.825	6	2.971	1.150	0.349	0.011	0.126
Residuals	124.038	48	2.584				

Note: the Type III sum-of-squares method was used. Statistical significance was set at $p < 0.05$. The symbol η^2_p denotes the partial eta-squared (a measure of the strength of the effect)
Source: developed by the authors based on own research

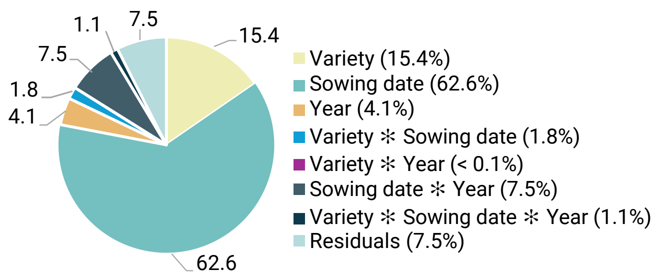

Figure 2. *Structure of the influence of the studied factors on the variability of daikon yield (based on the η^2 coefficient), % (2022-2024)*
Source: developed by the authors based on own research

Graphical visualisation of the data (Fig. 3) made it possible to identify a clear pattern in yield variation. In particular, regardless of variety and year of study, an increase in yield was observed from the first to the third ten-day period of July, followed by a decline in yield in the first ten-day period of August. The high precision of the experiments is confirmed by the small length of the error bars (95% confidence intervals) relative to the mean values, indicating data stability and reliability of the measurements. According to the results of the statistical significance assessment using Tukey's HSD test, the variety 'Minowase', when sown in the third ten-day period of July and the first ten-day period of August, demonstrated significantly higher yields compared with the control variety (Table 2). The increase amounted to 4.3-5.4 t/ha (7.9-10.6%), corresponding to yields of 56.4-58.9 t/ha. Analysis of sowing dates for the variety 'Gulliver' indicates that sowing in the third ten-day period of July and the first ten-day period of August ensured a significant increase in yield to 51.0-54.6 t/ha, which is 3.6-7.2 t/ha (7.6-15.2%) higher than the control (second ten-day period of July). At the same time, when sown in the first ten-day period of July, yield indicators were statistically similar to the control variant. A similar trend was observed for the variety 'Minowase': the maximum yield relative to the control was recorded for sowing in the third ten-day period of July and the first ten-day period of August, with an increase of 5.6-8.1 t/ha (11.0-15.9%).

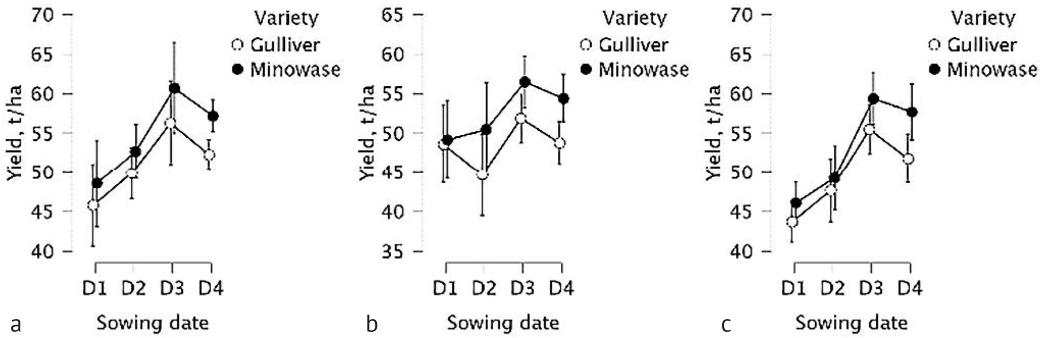

Figure 3. *Comparative characteristics of the yield of daikon varieties depending on sowing dates (2022-2024)*

Note: a – 2022, b – 2023, c – 2024; each point represents the mean value based on three replications (n = 3). Vertical error bars indicate the 95% confidence interval (95% CI). Sowing dates: D1 – first ten-day period of July, D2 – second ten-day period of July, D3 – third ten-day period of July, D4 – first ten-day period of August

Source: developed by the authors based on own research

Table 2. *Parameters of adaptive capacity and stability of daikon varieties under different sowing dates (2022-2024)*

Variety	'Gulliver'*				'Minowase'			
Sowing date	D1	D2*	D3	D4	D1	D2*	D3	D4
Mean, t/ha	46.0^{a}	47.4^{a}	54.6^{c}	51.0^{b}	48.0^{a}	50.8^{b}	58.9^{d}	56.4^{c}
CV, %	5.7	5.7	4.5	3.7	4.5	4.3	4.0	3.3
GAC_i	-5.6	-4.2	2.9	-0.7	-3.7	-0.8	7.2	4.8
SAC_i	6.4	6.8	5.6	3.1	4.1	4.3	5.2	2.9
Sg_i, %	14.0	14.4	10.2	6.0	8.6	8.5	8.9	5.2
b_i	-0.39	2.20	1.23	1.15	0.30	1.43	1.19	0.89
SVGi	12.1	11.4	25.2	34.8	26.2	27.9	31.3	40.9

Note: the table presents mean values for 2022-2024, n = 9 (where n is the total number of observations: 3 years × 3 replications for each treatment). The pooled standard error (SE) for all treatments is 0.54. Values marked with different letters (a, b, c, d) differ significantly at $p < 0.05$ according to Tukey's HSD test. Mean – average yield (t/ha); CV – coefficient of variation (%); *GACi* and *SACi* – general and specific adaptive capacity; Sg_i – relative stability (%); b_i – plasticity (regression coefficient); *SVGi* – breeding value. Sowing dates: D1 – first ten-day period of July, D2 – second ten-day period of July, D3 – third ten-day period of July, D4 – first ten-day period of August. The symbol (*) indicates the control

Source: developed by the authors based on own research

The coefficient of variation in the experiment ranged from 3.3 to 4.5%, indicating low variability of the studied trait ($CV < 10\%$). For a comparative assessment of yield stability, the Sg_i index was also used. As the obtained values ranged from 6.0 to 14.4%, this fully corresponds to the criterion of high genotype stability ($Sg_i < 25\%$).

The ability of genotypes to maximise the expression of economically valuable traits is directly correlated with the magnitude of GAC_i; therefore, the most valuable variants are those with the highest values of this parameter. In particular, sowing in the third ten-day period of July and the first ten-day period of August provided the highest GAC_i effects, while the lowest values of this parameter were observed for sowing in the first ten-day period of July. When assessing variety stability using the SAC_i parameter, it was taken into account that higher values indicate lower stability of the trait under fluctuating environmental conditions. The lowest SAC_i values were recorded for sowing in the third ten-day period of July and the first ten-day period of August, allowing these variants to be characterised as the most stable within the experiment.

When the variety 'Gulliver' was sown in the first ten-day period of July, the linear regression coefficient was $b_i < 1$, indicating a weaker response of the variety to environmental changes compared with the average across all studied variants. This justifies its use under resource-saving conditions, where the genotype ensures high return on inputs at a moderate level of agronomic practice. Conversely, values of $b_i > 1$ for subsequent sowing dates indicate a transition to an intensive type of response. In particular, sowing in the second ten-day period of July proved to be the most sensitive: with an increase in the environmental index by 1 t/ha, productivity increased by 2.20 t/ha. Slightly lower responsiveness was observed for sowing in the third ten-day period of July and the first ten-day period of August (1.1-1.23 t/ha per unit improvement in conditions). According to the calculations, all experimental variants of the variety 'Minowase' exhibited characteristics of an intensive type ($b_i > 1.0$), indicating high sensitivity to improved growing conditions. The minimum bi value (0.30) was recorded for sowing in the first ten-day period of July, while the maximum was observed in the second ten-day period of July ($b_i = 1.43$), after which the indicator gradually decreased with later sowing dates.

Thus, the optimal genotype for the experimental zone is one that combines high general adaptive capacity with maximum productivity and stability. For this reason, an integrated index, SVG_i, was used for comprehensive evaluation, allowing the risks of low productivity in unstable varieties under unfavourable conditions to be minimised. The SVG_i index was highest for the varieties 'Gulliver' and 'Minowase' when sown in the first ten-day period of August (34.8-40.9). In contrast, a decrease in this indicator was observed at earlier sowing dates.

As noted by S. Ali *et al.* (2023), ensuring food security requires careful consideration of the dynamics of environmental factors and an understanding of their impact on specific crops. In recent years, species distribution models have been widely used to assess the effects of climate change on geographical ranges. In particular, the study by Q. Han *et al.* (2023), based on a maximum entropy model, demonstrated that the geographical distribution of wild radish in East Asia is determined by hydrothermal conditions by 93.9%, primarily by precipitation in the driest month and its seasonality. The results of the analysis of variance obtained in this study are fully consistent with this model: the three-factor ANOVA showed that the dominant factor influencing yield variability was the sowing date ($\eta^2_p = 0.894$), which determines the moisture and thermal conditions for crop development.

The high significance of the varietal effect ($F = 99.2$; $p < 0.001$) is consistent with the findings of S.N. Mari *et al.* (2025), where genotype was also identified as a key determinant of radish productivity. In particular, the variety Medium Roasted produced the highest root mass (122.90 g). At the same time, the high coefficient of variation reported in that study indicates considerable intra-varietal variability in root weight, which may be due to the specific agroclimatic conditions of the study region. However, according to the results obtained in the present study, high stability and uniformity of the trait were recorded (coefficient of variation *CV* only 3.3-4.5%), indicating a high adaptive capacity of the varieties 'Gulliver' and 'Minowase'. In the study by A. Manzoor *et al*. (2024) involving 20 radish genotypes, it was also established that heredity, rather than the environment, plays a decisive role in the development of economically valuable traits (>20%).

A strong dependence of crop productivity on agroclimatic conditions and sowing dates is evident. It was established that for the varieties 'Gulliver' and 'Minowase', the optimal sowing period is from the third ten-day period of July to the first ten-day period of August, which ensured yields of 51.0-58.9 t/ha. These values significantly exceed the results of S. Parajuli & P. Dhital (2023), where under lowland conditions in Rupandehi (120 m above sea level, Nepal), early sowing (12 April) resulted in only 24.5 t/ha and late sowing (27 April) in 20.4 t/ha. In comparison with the data of B. Luitel *et al*. (2024) for the mid-hills of Dailekh (1,255 m above sea level), it was found that even the highest result of May sowing in Nepal (24.0 t/ha) remains twice as low as the values obtained in the present study. Such a substantial difference in yield is explained not only by varietal characteristics but also by the conditions under which the experiments were conducted. This supports the scientific assumption that high yields in the third ten-day period of July to the first ten-day period of August due to an optimal combination of daylight hours and temperature conditions, which promotes the intensive growth of root crops and vegetative mass.

At the same time, the results of N. Kamal & H. Kaur (2023) in Punjab (India), where October sowing ensured yields of 41 t/ha, are the closest to the recorded values. High productivity in both cases confirms the expediency of shifting sowing dates to late summer and autumn periods. It also indicates the high effectiveness of the selected sowing window (late July – early August) for the full realisation of the genetic potential of daikon varieties under the conditions of the Forest-Steppe of Ukraine. Moreover, the risks of premature bolting and morphological branching of roots – identified by E. Kim *et al*. (2025) as key factors reducing yield and quality under high-altitude conditions in Bolivia – were minimised in the present experiments through optimisation of sowing dates (third ten-day period of July – first ten-day period of August), which ensured maximum yields for the variety 'Minowase' at the level of 56.4-58.9 t/ha.

In a study of 30 Asian radish genotypes under different sowing dates in Bathinda (India), A. Dhand & N. Garg (2023) found that the contribution of the environment to total variance was highest for root weight, followed by plant weight and rosette weight – 60.2%, 59.6%, and 43.6%, respectively. Although the study's results also confirm the primacy of external factors, it was clarified that the influence of the year's weather conditions is significantly lower ($\eta^2_p = 0.357$) than the effect of sowing dates. This complements the conclusions of L. Mbambalala *et al*. (2025), who showed that sowing date is a decisive factor in determining the forage value of radish: December sowing resulted in maximum protein accumulation due to optimal hydrothermal conditions, whereas March sowing ensured the highest carbohydrate and metabolisable energy content. At the same time, later sowing in May under drought conditions led to a deterioration in biomass quality.

L.N. Dongarwar *et al*. (2024) noted that understanding the relationship between yield and its components is of considerable importance, as this indicator results from the complex interaction of numerous plant morphological traits. Significant progress can be achieved through targeted selection for traits that exhibit strong positive correlations with productivity, including plant height, leaf area, chlorophyll content, root diameter and weight, total biomass, root-to-leaf ratio, and the content of moisture, ascorbic acid, and soluble solids. Analysis of ecological plasticity ($b_i > 1.0$) demonstrated that the studied genotypes belong to an intensive type, capable of fully realising their potential only under improved agronomic conditions. At the same time, the results of H. Hong *et al.* (2023) complement this strategy, indicating that genetic differentiation of radish varieties is closely linked to their adaptability to seasonal growing conditions. Cluster analysis using molecular markers enabled clear differentiation between autumn, spring, and summer/winter varieties, which is an important factor in planning sowing dates. The application of an integrated breeding value index made it possible to establish that August sowing dates provide the best alignment between genotype and environmental conditions of the growing region. In the study by L.M. Dang *et al.* (2023), it was noted that the use of an automated phenotyping system based on the Mask-RCNN algorithm ensures high accuracy in measuring morphological traits of radish (82-100%), which is critically important for evaluating the breeding value of samples under different growing conditions.

The results of the present study demonstrated that the use of classical parameters of stability and adaptive capacity remains a highly reliable method for identifying promising daikon varieties under field conditions. The findings clearly highlight the importance of sowing dates for daikon yield, particularly under the conditions of the Forest-Steppe of Ukraine. Increased yields at the identified sowing dates confirmed the adaptability of the studied varieties to changing climatic conditions, which is essential for ensuring the stability of production.

Conclusions

The conducted research demonstrated that optimising sowing dates is an important element in adapting daikon to current climatic challenges in the Forest-Steppe of Ukraine. The studied factors accounted for 92.5% of yield variation, with sowing dates being dominant (62.6%, $p < 0.001$). The influence of variety and year amounted to 15.4% and 4.1%, respectively. Across all experimental variants, high relative yield stability was observed (Sg_i 6.0-14.4%). According to Tukey's test, the variety 'Minowase' significantly outperformed 'Gulliver' when sown in the second and third ten-day periods of July and the first ten-day period of August, with yields of 50.8-58.9 t/ha. A high coefficient value ($b_i > 1$) in most variants indicates considerable plasticity of the varieties. Such genotypes realise their potential only under intensive cultivation technologies. In contrast, the variety 'Gulliver', when sown in the first ten-day period of July with $b_i < 1$, exhibited lower-than-average sensitivity to environmental changes, characterising this variant as suitable for extensive farming systems, where achieving results with limited resources is essential. The latest sowing dates showed the lowest response to improvements in agronomic conditions within the experiment. With an increase in the overall yield level by 1 t/ha, the yield of genotypes sown in the first ten-day period of August increased by only 0.89-1.15 t/ha. At the same time, sowing in the second ten-day period of July proved to be the most intensive: its response to changes in environmental conditions was the highest, amounting to 1.43-2.20 t/ha for each unit increase in the group mean. The highest breeding value (34.8-40.9) and stability (2.9-3.1) for the studied varieties were ensured by sowing in the first ten-day period of August, with yields of 51.0-56.4 t/ha.

The obtained results provide a scientific basis for integrating breeding and agronomic approaches to enhance crop adaptability. The identification of genotypes with high ecological plasticity and stability enables the optimisation of breeding programmes aimed at developing varieties capable of effectively realising their productive potential under variable hydrothermal conditions. At the same time, the decisive role of sowing dates as a key agronomic factor has been established, as it allows the alignment of critical growth and development stages of plants with optimal environmental conditions. This creates favourable conditions for stabilising production by reducing interannual yield fluctuations and improving resource-use efficiency. Further research will focus on studying the effect of sowing and harvesting dates on the storability of root crops in order to extend the consumption period of fresh daikon produce throughout the autumn–spring period. This will contribute to strengthening food security and the development of sustainable agroecosystems capable of adapting to future climate change.

Acknowledgements

None.

Funding

This research was funded by the scientific project "Develop innovative technologies for growing low-spreading vegetable crops" (state registration number: 0122U001637), which was supported by the Ministry of Education and Science of Ukraine.

Conflict of Interest

None.

References

[1] Ali, S., Makanda, T.A., Umair, M., & Ni, J. (2023). MaxEnt model strategies to studying current and future potential land suitability dynamics of wheat, soybean and rice cultivation under climatic change scenarios in East Asia. *PLOS One*, 18(12), article number e0296182. doi: 10.1371/journal.pone.0296182.

[2] Babu, R.R., Baishya, L.K., Reddy, A.G.K., Pongener, A., Raghavendra, H.R., & Naik, N.O. (2024). Climate change effects on sustainable vegetable production in India: A review. *International Journal of Environment and Climate Change*, 14(3), 804-814. doi: 10.9734/IJECC/2024/v14i34089.

[3] Convention on Biological Diversity. (1992, June). Retrieved from https://zakon.rada.gov.ua/laws/show/995_030#Text.

[4] Dang, L.M., Min, K., Nguyen, T.N., Park, H.Y., Lee, O.N., Song, H.-K., & Moon, H. (2023). Vision-based white radish phenotypic trait measurement with smartphone imagery. *Agronomy*, 13(6), article number 1630. doi: 10.3390/agronomy13061630.

[5] Dhand, A., & Garg, N. (2023). Genotype × environment interaction using AMMI and MTSI analysis for growth and yield attributes of radish (*Raphanus sativus* L.) under high temperature stress conditions of North Indian plains. *Scientia Horticulturae*, 313, article number 111880. doi: 10.1016/j.scienta.2023.111880.

[6] Dongarwar, L.N., Borkar, V.H., & Madavi, S.R. (2024). Correlation and path analysis studies among growth and yield contributing parameters of different varieties of radish (*Raphanus sativus* L.). *Advances in Agricultural Technology and Plant Sciences*, 7(20), article number 180135.

[7] Dumitru, E.A., Berevoianu, R.L., Tudor, V.C., Teodorescu, F.-R., Stoica, D., Giucă, A., Ilie, D., & Sterie, C.M. (2023). Climate change impacts on vegetable crops: A systematic review. *Agriculture*, 13(10), article number 1891. doi: 10.3390/agriculture13101891.

[8] Fedosiy, I.O., Bobos, I.M., & Komar, O.O. (2025). Varietal and agrotechnical aspects of quality control of daikon root crops. *Bulletin of Uman National University of Horticulture*, 2, 37-45. doi: 10.32782/2310-0478-2025-2-38-45.

[9] Han, Q., Liu, Y., Jiang, H., Chen, X., & Feng, H. (2023). Evaluation of climate change impacts on the potential distribution of wild radish in East Asia. *Plants*, 12(18), article number 3187. doi: 10.3390/plants12183187.

[10] Hong, H., Lee, J., & Chae, W. (2023). An economic method to identify cultivars and elite lines in radish (*Raphanus sativus* L.) for small seed companies and independent breeders. *Horticulturae*, 9(2), article number 140. doi: 10.3390/horticulturae9020140.

[11] Kamal, N., & Kaur, H. (2023). Effect of different dates of sowing and organic manures on the production potential of radish (*Raphanus sativus* L.). *Progressive Horticulture*, 55(2), 182-185. doi: 10.5958/2249-5258.2023.00028.3.

[12] Kaur, A., & Singh, N. (2022). Effect of sowing time on different radish varieties (*Raphanus sativus* L.). *Journal of Krishi Vigyan*, 11(1), 162-166. doi: 10.5958/2349-4433.2022.00116.7.

[13] Khusanov, N., Boboyev, S., Razzakova, S., Shoira, N., Juliyev, M., & Turabayev, A. (2024). *Raphanus sativus* L. and its determination of planting dates based on seed germination in different ecological environments of Uzbekistan. *E3S Web of Conferences,* 497, article number 03029. doi: 10.1051/e3sconf/202449703029.

[14] Kim, E., Jo, S., Cotrina, D., Magne, J., Yu, Y., & Lee, S.G. (2025). Comparison of productivities of seven different Korean varieties of radish (*Raphanus sativus* L.) at highlands in Bolivia. *Journal of the Korean Society of International Agriculture*, 37(4), 301-310. doi: 10.12719/KSIA.2025.37.4.301.

[15] Klok, S., Kornus, A., Kornus, O., Danylchenko, O., & Skyba, O. (2023). Tropical nights (1976-2019) as an indicator of climate change in Ukraine. *IOP Conference Series: Earth and Environmental Science,* 1126, article number 012023. doi: 10.1088/1755-1315/1126/1/012023.

[16] Luitel, B.P., Bhusal, Y., & Bhandari, B.B. (2024). Evaluation of radish (*Raphanus sativus* L.) varieites in different sowing dates for off-season production at dailekh. *The Journal of Agriculture and Environment*, 25, 117-125.

[17] Manzoor, A., Naveed, M.S., Hussain, T., Ali, I., Akram, M.T., Liaquat, M., Ahmad, R., Anwar, A., Khan, M.A., & Ahmad, I. (2024). Morphological characterization and analysis of genetic variability in radish (*Raphanus sativus*) genotypes for important qualitative and quantitative traits. *Brazilian Archives of Biology and Technology*, 67, article number e24230627. doi: 10.1590/1678-4324-2024230627.

[18] Mari, S.N., Zhang, L., Kaleri, A.A., Jatoi, F.A., & Solangi, M.R.M. (2025). Cultivation of exotic radish varieties in climatic condition of Tando Jam. *Annual Methodological Archive Research Review*, 3(6), 515-525. doi: 10.63075/q38frt70.

[19] Mbambalala, L., Mpanza, T.D.E., Tjelele, T.J., Ncisana, L., Mkhungo, S., Sithole, L., Nzeru, M.S., Rakau, P.N., Rani-Kamwendo, Z.T., & Mkhize, N.R. (2025). Dryland fodder radish genotypes: Planting date effects on nutritive value and in-vitro dry matter degradability in Midlands of KwaZulu-Natal, South Africa. *Grasses*, 4(2), article number 17. doi: 10.3390/grasses4020017.

[20] Nowak, A., Majewska, M., Marzec-Grządziel, A., Ozimek, E., Przybyś, M., Słomka, A., Kutyrieva-Nowak, N., Gałązka, A., & Jaroszuk-Ściseł, J. (2024). Effect of long-term radish (*Raphanus sativus* var. sativus) monoculture practice on physiological variability of microorganisms in cultivated soil. *Journal of Environmental Management*, 367, article number 122007. doi: 10.1016/j.jenvman.2024.122007.

[21] Parajuli, S., & Dhital, P.R. (2023). Effect of plant spacing and sowing dates on the growth and yield of radish (*Raphanus sativus*) in Rupandehi district, Nepal. *Archives of Agriculture and Environmental Science*, 8(4), 579-584. doi: 10.26832/24566632.2023.0804018.

[22] Paul, A., & Machavaram, R. (2026). Climate change impacts on vegetable production: A comprehensive global and Indian review. *International Journal of Vegetable Science*, 1-34. doi: 10.1080/19315260.2026.2630185.

[23] Shilpa, Sharma, M., Kaur, M., Kumar Sharma, A., Sharma, P., & Chauhan, M. (2023). Soil fertility, growth, yield and root quality of radish (*Raphanus sativus* L.) as influenced by integrated nutrient management practices. *Communications in Soil Science and Plant Analysis*, 54(10), 1316-1333. doi: 10.1080/00103624.2022.2142237.

[24] Tyshchenko, A., Tyshchenko, O., Konovalova, V., Fundirat, K., & Piliarska, O. (2023). Methods of determining theadaptability and ecological stability of plants. *Scientific Collection "InterConf+"*, 33(155), 324-342. doi: 10.51582/interconf.19-20.05.2023.029.

[25] Vyshnevskyi, V. (2025). Climate change in Ukraine and its consequences. *Journal of Landscape Ecology,* 18(4), 150-174. doi: 10.2478/jlecol-2025-0032.

[26] Wang, X., Xing, M., Li, J., & Li, B. (2025). The impacts of global climate change and environmental security on fruits and vegetables – a policy-technology nexus perspective. *Foods*, 14(23), article number 4016. doi: 10.3390/foods14234016.

Адаптивний потенціал та селекційна цінність сортів дайкону (*Raphanus sativus* L. *convar. acanthiformis* Sazon.) за різних термінів сівби в умовах Лісостепу України

Іван Федосій
Кандидат сільськогосподарських наук, доцент
Національний університет біоресурсів і природокористування України
03041, вул. Героїв Оборони, 15, м. Київ, Україна
https://orcid.org/0000-0002-5044-9960
Олександр Комар
Кандидат сільськогосподарських наук
Національний університет біоресурсів і природокористування України
03041, вул. Героїв Оборони, 15, м. Київ, Україна
https://orcid.org/0000-0001-7511-4190
Ірина Бобось
Кандидат сільськогосподарських наук, доцент
Національний університет біоресурсів і природокористування України
03041, вул. Героїв Оборони, 15, м. Київ, Україна
https://orcid.org/0000-0001-5193-7192
Олена Сєдова
Асистент
Національний університет біоресурсів і природокористування України
03041, вул. Героїв Оборони, 15, м. Київ, Україна
https://orcid.org/0000-0003-4869-1560
Михайло Ретьман
Кандидат сільськогосподарських наук, старший дослідник
Інститут водних проблем і меліорації Національної академії аграрних наук України
03022, вул. Васильківська, 37, м. Київ, Україна
https://orcid.org/0000-0002-6972-2410

Анотація. Глобальні кліматичні зміни та зміщення агрокліматичних зон в Україні зумовлюють необхідність перегляду традиційних елементів технології вирощування овочевих культур для забезпечення стабільної продовольчої безпеки. Метою дослідження було оцінити адаптивний потенціал сортів дайкону залежно від термінів сівби для формування сталої врожайності в умовах сучасних агрокліматичних трансформацій. Дисперсійний аналіз (Type III SS) показав, що 92,5 % варіації врожайності зумовлено досліджуваними факторами. Найбільший вплив мав термін сівби (62,6 %, $p < 0{,}001$), що суттєво перевищував вплив сорту (15,4 %, $p < 0{,}001$), тоді як вплив року був незначним (4,1 %, $p < 0{,}001$). Серед взаємодій статистично значущою виявилася лише комбінація «термін сівби × рік» (7,5 %, $p < 0{,}001$). Усі сорти характеризувалися високою відносною стабільністю (Sg_i 6,0-14,4 %). За результатами ANOVA та критерію Тьюкі (HSD) у більшості термінів сівби встановлено достовірні відмінності між сортами ($p < 0{,}05$). Сорт ‘Міновасі’ перевищував ‘Гулівер’ у ІІ декаді липня – І декаді серпня (50,8-58,9 проти 47,4-54,6 т/га). Ранній термін (І декада липня) не забезпечив істотних відмінностей між генотипами. Високою пластичністю характеризувалися всі сорти, за винятком ‘Гулівер’ у ранній термін (b_i = -0,39). Для ‘Міновасі’ у І декаді серпня відмічено знижену пластичність (b_i = 0,89). Найбільшу чутливість до умов середовища зафіксовано для ІІ декади липня (b_i = 1,43-2,20). Найвищі показники селекційної цінності отримано за сівби у I декаді серпня (34,8-40,9), що поєднувалося з високою врожайністю (51,0-56,4 т/га) та стабільністю (2,9-3,1). Отримані результати обґрунтовують доцільність використання сорту ‘Міновасі’ та оптимізації термінів сівби (кінець липня – початок серпня) як ефективного агротехнологічного інструменту підвищення продуктивності й стабільності вирощування дайкону в умовах кліматичних змін

Ключові слова: екологічна пластичність; стабільність генотипу; врожайність коренеплодів; гідротермічний стрес; адаптивна здатність

Received 28.11.2025 Revised 26.02.2026 Accepted 23.04.2026 Published: 30.04.2026

Vol. 22, No. 2
2026

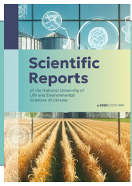

Scientific Reports of the National University of Life and Environmental Sciences of Ukraine

Journal homepage: https://scireports.com.ua/en e-ISSN 2223-1609

UDC 633.15:631.55 DOI: 10.31548/dopovidi/2.2026.51

Justification for the delineation of field productivity zones based on long-term monitoring of maize yield and satellite data

Lesia Harbar
PhD in Agricultural Sciences, Associate Professor
National University of Life and Environmental Sciences of Ukraine
03041, 15 Heroiv Oborony Str., Kyiv, Ukraine
https://orcid.org/0000-0003-4249-0434

Bohdan Vaskivskyi*
Postgraduate Student
National University of Life and Environmental Sciences of Ukraine
03041, 15 Heroiv Oborony Str., Kyiv, Ukraine
https://orcid.org/0009-0003-6852-3844

Abstract. The article presents the results of a long-term analysis of the spatial heterogeneity of maize (*Zea mays* L.) yield in a production field with an area of 448 hectares located in the transition zone between Polissia and the Forest-Steppe of Ukraine. The study was conducted using yield maps from 2019-2020 and 2023-2024 with the aim of assessing the stability of within-field productivity zones and establishing their relationship with satellite data. The spatial structure of productivity was analysed by aggregating yield monitor data into a regular 20 × 20 m grid, followed by classification into three productivity zones. To confirm the agroecological basis of the zones, long-term NDVI composites (Sentinel-2) and maps of soil surface brightness were used. It was found that the spatial boundaries of low, medium, and high productivity zones remained consistent throughout the entire study period, despite interannual fluctuations in the average yield level. The long-term mean values were 6.2 t/ha in the low, 9.5 t/ha in the medium, and 12.3 t/ha in the high productivity zone. The coefficient of variation of zone areas did not exceed 11.6%, indicating their high spatial and temporal stability. Correlation analysis revealed a strong positive relationship between the long-term productivity map and the long-term average NDVI (r = 0.86-0.94), as well as a stable inverse relationship with soil brightness indicators (r = -0.79 to -0.87). High values of the coefficient of determination (R^2 = 0.74-0.88) confirm that the main share of spatial yield variation is driven by persistent soil and landscape factors. The

Suggested Citation:
Harbar, L., & Vaskivskyi, B. (2026). Justification for the delineation of field productivity zones based on long-term monitoring of maize yield and satellite data. *Scientific Reports of the National University of Life and Environmental Sciences of Ukraine*, 22(2), 51-64. doi: 10.31548/dopovidi/2.2026.51.

*Corresponding author

obtained results demonstrate the feasibility of using long-term yield maps in combination with satellite indices for the delineation of stable field productivity zones. This approach provides a scientific basis for the implementation of precision agriculture technologies and spatially differentiated management of agricultural resources

Keywords: *Zea mays* L.; spatial heterogeneity of the field; soil brightness; long-term yield maps; coefficient of determination; precision agriculture; management zones

Introduction

In the current context of intensified farming and increasing spatial heterogeneity of agricultural landscapes, the scientifically informed delineation of productivity zones within a single field is becoming particularly relevant. Intra-field variability in soil properties, micro-relief, water regime and nutrient availability creates persistent spatial differences in crop growth and productivity, which cannot be effectively accounted for when using standardised agronomic solutions. In this context, the role of precision farming approaches is growing, aimed at identifying homogeneous management zones based on spatial data and the subsequent adaptation of technological operations to local field conditions.

The combination of geostatistical approaches with multivariate analysis is effective for identifying intra-field management zones based on a set of soil indicators. Thus, H.M. Salem *et al.* (2024), based on spatial analysis of soil characteristics (in particular pH, organic matter, cation exchange capacity, electrical conductivity, and macro- and microelement content) and subsequent clustering, demonstrated the possibility of forming zones with similar characteristics that differed in terms of crop productivity. This confirms that accounting for intra-field variability is a key factor in improving the accuracy of nutrient management and resource efficiency.

The instrumental capabilities of geoinformation technologies for the formation of agromanagement zones are detailed in the work of M.M. Elsharkawy *et al.* (2022), where it is demonstrated that GIS approaches and spatial multi-criteria procedures enable the integration of heterogeneous data layers (soil, topography, productivity) and can be used as a basis for decision-making regarding the differentiated application of resources in precision farming systems.

A separate line of research is devoted to analysing the causes and consequences of sub-field yield stability/variability over time. S.J. Leuthold *et al.* (2024) demonstrated that zones of yield stability may differ in structure and soil organic matter controls (the ratio and dynamics of the POM and MAOM soil fractions), highlighting the complex nature of the interaction between edaphic factors, productivity and organic matter transformation processes at the sub-field level. This justifies the use of long-term data as a basis for identifying zones aimed at stable management decisions. An important aspect of zoning is the use of Earth remote sensing as a source of timely and spatially continuous indicators of crop condition.

Research by N. Narra *et al.* (2022) showed that open-access satellite data can be used to identify field zones with stable and variable characteristics throughout the growing season based on spectral indicators, creating the conditions for integrating satellite data with yield data in spatial management tasks. In addition to soil-relief and satellite indicators, precision farming approaches are used to validate zones using biologically and technologically significant indicators. M.A. de Oliveira Filho *et al.* (2025) demonstrated that open-access satellite data can be used to identify field zones with stable and variable characteristics during the growing season based on spectral indicators, creating opportunities for integrating satellite-derived metrics with yield data in spatial management applications. In addition to soil, topographic, and satellite indicators, precision agriculture approaches also employ biological and technologically relevant parameters for zone validation. The practical value of the zonal approach becomes apparent when zones form the basis for differentiated technological solutions.

In particular, research by F.A. Baron *et al*. (2025) demonstrated on a heterogeneous field that the optimal maize plant density varies between productivity zones, and that adjusting plant population density to account for these zones can serve as a tool for improving both agronomic and economic performance. At the same time, zoning based on soil electrical conductivity reflects differences in particle size distribution and physical properties and can be useful for justifying sowing adjustments within a field, highlighting the importance of soil environment proxy indicators for technological adaptation. However, the effectiveness of zonal management depends on the combination of spatial decisions with weather conditions and the farming system.

M.M. Mikha *et al*. (2024) demonstrated in their work that a zoned approach to differentiated nitrogen application in a dryland system yields a positive response in years with favourable moisture conditions, whereas during periods of low rainfall, the effectiveness of the technology decreases, indicating the need to account for climatic factors when interpreting the results of zonal management and planning differentiated technologies. Despite a significant body of research in the field of zoning and precision farming, the issue of using long-term yield maps as a basic tool for identifying stable productivity zones within a production field, with subsequent verification by satellite data, remains insufficiently addressed. Of particular relevance is determining the degree of spatio-temporal stability of such zones under production conditions.

In this regard, the aim of the study was to assess the possibility of identifying stable productivity zones within a production field based on long-term maize yield maps and to confirm their agro-ecological determinants using satellite indicators.

Materials and Methods

The study was conducted in accordance with the principles of the Convention on Biological Diversity (1992), in particular the provisions of Article 7, which regulates the monitoring of biodiversity components and the systematisation of relevant spatial data. The application of long-term remote monitoring of yield and satellite indices was consistent with approaches aimed at the sustainable use of agroecosystems and the minimisation of negative anthropogenic impacts on the productive potential of land. The object of the study was a commercial field with an area of 448 ha, located within the territory of LLC Chernihiv Industrial Dairy Company in Chernihiv District, Chernihiv Region, in the transition zone between Polissia and the Forest-Steppe of Ukraine. Throughout the entire study period, the field was planted with the maize hybrid DKS 3939 under the farm's standard uniform production technology. The use of a stable cultivation system made it possible to minimise the influence of agronomic differences on the formation of the spatial yield structure.

The analysis of the spatial structure of productivity was carried out using long-term maize yield maps for 2019-2020 and 2023-2024. Primary yield data were obtained during harvest using a combine harvester equipped with an automatic yield monitoring system and GPS-based satellite positioning. During harvesting, spatially referenced yield records were generated, containing coordinates, yield values, and combine movement parameters. The primary yield data underwent a preprocessing procedure. Anomalous values caused by machinery turning, uneven combine speed, or technical measurement errors were removed from the dataset. Filtering was performed by excluding values outside the statistically acceptable interval determined on the basis of the interquartile range. After cleaning, the data were aggregated into a regular spatial grid. The spatial grid was created using the geographic information system QGIS (version 3.x). The field area was divided into a regular square grid with a cell size of 20 × 20 m. For each cell, the mean yield value was calculated based on all yield monitor points falling within its boundaries. This approach ensured comparability of spatial data across different years of observation.

The long-term productivity map was generated by calculating the mean yield value for each grid cell across all years of the study. The resulting raster was then used for the further delineation of productivity zones. Classification was performed on the basis of relative yield values. For this purpose, yield values were normalised relative to the field mean and divided into three classes: low, medium, and high productivity levels. To ensure correct interannual comparison of spatial patterns, a unified yield gradient scale (from <4.0 to ≥13.0 t/ha) was applied across all study years. For additional assessment of the spatial field structure, satellite indicators were used. In particular, maps of the normalised difference vegetation index (NDVI) derived from Sentinel-2 satellite imagery were analysed. For each study year, composite images representing the period of active crop vegetation were generated. Satellite data processing was performed using QGIS tools and software scripts written in Python.

Within the Python environment (version 3.x), the libraries GDAL, Rasterio, GeoPandas, NumPy, and Pandas were used for spatial data processing. These tools were employed for downloading satellite imagery, calculating NDVI, spatial clipping of data to the boundaries of the study field, and generating long-term rasters. In addition, soil surface brightness maps were used to analyse soil conditions; these were derived from satellite images obtained during periods of minimal vegetation cover. Such imagery made it possible to assess the spatial heterogeneity of surface soil properties. Following the processing of satellite data, all raster indicators (NDVI and soil brightness) were normalised to a relative scale of 0-100 using linear scaling (min-max normalisation). This ensured comparability between different sources of spatial information and enabled their integrated analysis.

The assessment of the spatial and temporal stability of the productivity structure was carried out by comparing the areas of productivity zones between study years. For this purpose, the coefficient of variation (CV) of zone areas was calculated using the formula:

$$CV = SD / Mean \times 100\% , \qquad (1)$$

where SD – the standard deviation of the area of the zone between years, and Mean – the average area of the corresponding zone. Statistical analysis of the relationship between yield maps, NDVI values and soil brightness indices was performed using Pearson's correlation coefficient. The proportion of spatial variation in yield explained by satellite indicators was assessed using the coefficient of determination R^2. Statistical calculations were performed in Python using the SciPy and Statsmodels libraries. Visualisation of spatial data, creation of thematic maps and analysis of productivity structure were carried out in the QGIS environment.

Results

As shown in Figure 1, analysis of yield maps indicates a consistent spatial recurrence of zones with varying levels of productivity throughout the entire observation period. CV of the areas of these zones between years served as a quantitative criterion of spatial stability: for the low-productivity zone it was 7.9%, for the medium-productivity zone 2.9%, and for the high-productivity zone 11.6%, which corresponds to a low level of inter-annual variability in the spatial structure of the field. In all the years studied, areas with consistently low yields (red and yellow tones) are clearly discernible, as are zones of medium and high productivity (light and dark green tones), which retain their spatial position.

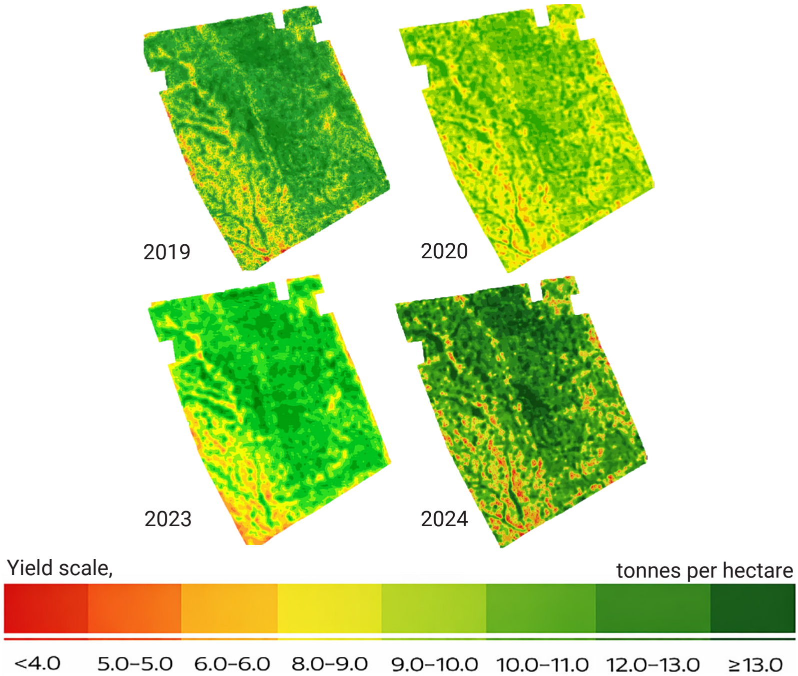

Figure 1. *Spatial heterogeneity of field yield based on long-term data*

Source: authors' own research

At the same time, the intensity of productivity expression varied between years, reflecting the influence of weather conditions and other annual factors. In particular, in 2020 a general decline in yield was observed compared with 2019 and 2024, whereas in 2024 the largest share of high-yielding areas was recorded, namely 33% or 147.8 ha with yields exceeding 11 t/ha. Despite this, the spatial boundaries of low- and high-productivity zones remained stable: the average percentage of spatial overlap between zones in adjacent years was 73.5%, specifically 80.0% for the medium-productivity zone, 69.8% for the low-productivity zone, and 66.5% for the high-productivity zone, indicating the dominant influence of stable soil and topographic factors. The obtained results confirm the feasibility of using long-term yield maps as a reliable basis for delineating field productivity zones, which can be applied for the further differentiation of cultivation practices, in particular seeding rates.

Figure 2 presents a comparison between the soil surface brightness map and the long-term field productivity map constructed from satellite data. Visual analysis indicates consistency in spatial patterns between areas with differing soil brightness and levels of crop productivity. In particular, zones of reduced productivity generally correspond to areas with higher soil surface brightness, indirectly reflecting differences in soil properties and water regime. The obtained results confirm that spatial differences in yield have a stable soil-landscape basis and are consistent with long-term satellite data, which strengthens the justification for using long-term yield maps to delineate field productivity zones. The correlation analysis data (Table 1) indicate a strong relationship between the long-term field productivity map and soil brightness indicators. The values of the correlation coefficient between productivity estimated using the NDVI and the productivity map ranged from 0.86 to 0.94, indicating a very high degree of spatial agreement between satellite-derived indicators and the actual yield structure of the field. Such correlation values suggest that the NDVI reliably reflects differences in crop condition and productivity levels within the studied area.

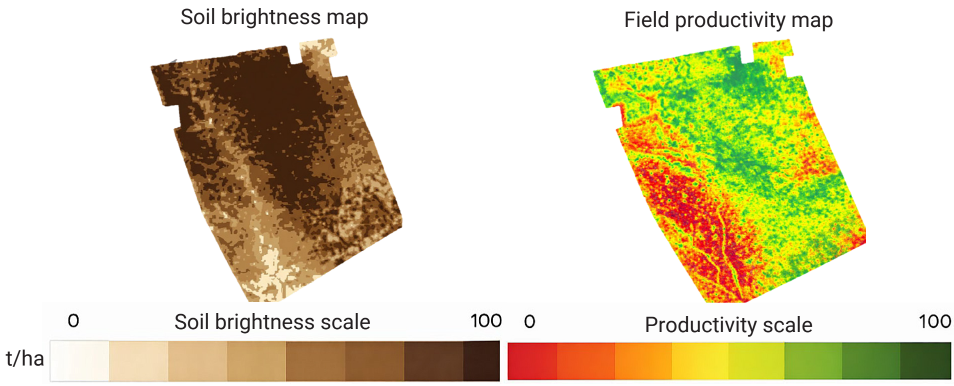

Figure 2. *Spatial heterogeneity of maps showing long-term field productivity and soil brightness*
Source: author's own research

Table 1. *Correlation relationships between long-term field productivity (NDVI) and soil brightness indicators*

Year/ Indicator	Correlation coefficient with the productivity map (long-term average NDVI), r	Correlation coefficient with the soil brightness map, r	Coefficient of determination (R^2)	Moran's I of residuals
2019	0.92	-0.84	0.85	0.18
2020	0.86	-0.79	0.74	0.28
2023	0.91	-0.82	0.83	0.15
2024	0.94	-0.87	0.88	0.12
Mean	0.91	-0.83	0.82	0.18

Source: authors' own research

High correlation coefficients were observed in all years of the study, confirming the stability of the identified patterns. The highest value (r = 0.94) was recorded in 2024, whereas in 2020 the correlation was slightly lower (r = 0.86), which may be associated with less favourable weather conditions during that season and an overall reduction in yield levels. Nevertheless, even under such conditions, the strength of the relationship remained high, confirming the suitability of satellite indices for analysing the spatial structure of crop productivity.

The mean value of the correlation coefficient between NDVI and the productivity map was 0.91, indicating a very strong relationship between vegetation indices and actual yield indicators. This suggests that satellite data can be effectively used to identify field productivity zones and to analyse within-field heterogeneity of agroecosystems. At the same time, a stable inverse relationship was identified between the productivity map and soil brightness (r = -0.79 to -0.87), indicating a decrease in productivity in areas with higher soil surface brightness. This relationship may be explained by the fact that lighter-coloured soils often have lower organic matter content, reduced water-holding capacity, or a coarser texture, which limits plant development and reduces yield formation potential. Accordingly, darker soil areas generally possess more favourable agrophysical and agrochemical properties, creating better conditions for the growth and development of maize plants.

Analysis of the obtained coefficients shows that the strength of the inverse relationship between soil brightness and productivity was stable across all years of the study. The highest absolute correlation coefficient (r = -0.87) was observed in 2024, indicating a particularly clear manifestation of soil factors influencing yield formation under favourable growing conditions. In 2020, this value was slightly lower (r = -0.79), which may be associated with an increased influence of weather factors on yield formation. High values of the coefficient of determination (R^2 = 0.74-0.88) confirm that a substantial proportion of the spatial variation in field productivity is explained by the analysed factors. In particular, from 74% to 88% of yield variability in different years can be attributed to spatial field characteristics reflected in NDVI values and soil surface brightness. The mean value of the coefficient of determination was 0.82, indicating a high explanatory power of the model and confirming the significant role of soil characteristics in shaping the spatial structure of productivity.

To verify the reliability of the correlation analysis, Moran's I index was calculated for the regression residuals, that is, for the difference between the actual yield values and those predicted by the model based on NDVI for the respective year. If the residuals are spatially random (Moran's I ≈ 0), this indicates that the model adequately describes the spatial structure of the field and that autocorrelation does not distort Pearson correlation coefficients. A substantial decrease in the index from the initial level of 0.70 (for yield) to an average value of 0.18 (for regression residuals) confirms that the NDVI of the respective year adequately captures the main spatial structure of field yield. The weak level of residual autocorrelation indicates the absence of significant bias in the model parameter estimates and confirms the statistical reliability of the obtained correlations. Thus, the results of the correlation analysis confirm a close relationship between satellite-derived indicators of crop condition, soil surface characteristics, and actual maize yield. The identified patterns indicate that spatial differences in productivity have a stable soil-landscape basis and can be effectively identified using remote sensing methods. This provides a scientific foundation for the use of satellite data and long-term yield maps in precision agriculture for the delineation of productivity zones and optimisation of agronomic practices within the field. The data presented in Table 2 indicate a clearly expressed spatial heterogeneity of maize yield within the studied field and its stability over multiple years.

Table 2. *Characteristics of field productivity zones based on long-term yield data*

Year	Zone	Number of cells, units	Yield, t/ha	SD, t/ha	Coefficient of variation (CV), %	Zone area	
						ha	%
2019	Low	2,912	6.2	0.84	13.5	116.5	26
	Medium	4,928	9.4	0.71	7.6	197.1	44
	High	3,360	12.6	1.12	8.9	134.4	30
2020	Low	3,248	5.0	0.92	18.4	129.9	29
	Medium	5,152	8.2	0.78	9.5	206.1	46
	High	2,800	10.5	1.05	10.0	112.0	25
2023	Low	3,024	6.5	0.79	12.2	121.0	27
	Medium	5,040	9.8	0.65	6.6	201.6	45
	High	3,136	12.4	0.98	7.9	125.4	28
2024	Low	2,688	7.0	0.81	11.6	107.5	24
	Medium	4,816	10.5	0.69	6.6	192.6	43
	High	3,696	13.8	1.21	8.8	147.8	33

Table 2. *Continued*

Year	Zone	Number of cells, units	Yield, t/ha	SD, t/ha	Coefficient of variation (CV), %	Zone area	
						ha	%
Mean	Low	2,968	**6.2 ± 0.83***	0.84	13.9	121.0	27
	Medium	4,984	**9.5 ± 0.94***	0.71	7.6	201.6	45
	High	3,248	**12.3 ± 1.34***	1.09	8.9	129.9	29
CV for zone areas (%): 7.9 for the low zone; 2.9 for the medium zone; 11.6 for the high zone.							

Note: * – 95% confidence interval; differences between all pairs of zones are statistically significant (Welch's test, $p < 0.01$)
Source: authors' own research

The results showed that throughout all years of observation, the high-productivity zone was characterised by the highest yield levels, ranging from 10.5 to 13.8 t/ha, whereas in the medium-productivity zone yields ranged from 8.2 to 10.5 t/ha, and in the low-productivity zone from 5.0 to 7.0 t/ha. The mean values over the study period were 6.2, 9.5, and 12.3 t/ha for the low-, medium-, and high-productivity zones, respectively, confirming a consistent differentiation in productivity between the identified zones and indicating substantial differences in the yield potential of different parts of the field.

The difference between the long-term average yields of the high- and low-productivity zones was 6.1 t/ha, which corresponds to 65% of the mean field yield. Statistical analysis (Welch's test) confirmed the high significance of differences between all pairs of zones in all years of the study ($p < 0.01$). The long-term mean yields were 6.2 ± 0.83 t/ha (95% CI) for the low-productivity zone, 9.5 ± 0.94 t/ha for the medium-productivity zone, and 12.3 ± 1.34 t/ha for the high-productivity zone (Table 2). Such a gap in productivity indicates the presence of substantial differences in soil and agroecological conditions across different parts of the field, which determine the capacity of plants to form yield. Within a uniform agronomic management system, this implies that different areas of the field have unequal resource-use potential, creating a basis for the implementation of differentiated crop management practices.

Despite interannual fluctuations in the overall yield level of the field, the relationship between productivity zones remained relatively stable. In all years, a clear gradient in yield between low-, medium-, and high-productivity zones was maintained, indicating the stability of spatial differences in productivity. For example, even in 2020, which had the lowest average field yield (8.0 t/ha), the relative differences between zones persisted, and high-productivity areas continued to demonstrate significantly better performance compared with other parts of the field. Under more favourable conditions in 2024, this difference became even more pronounced, indicating the ability of high-productivity zones to more effectively realise their potential under optimal growing conditions.

Analysis of the area of productivity zones showed that the medium-productivity zone occupied the largest share of the field, averaging 45%. This zone forms the main body of the crop and is characterised by relatively stable yields close to the field average. The high-productivity zone accounted for an average of 29% of the field area, indicating a substantial proportion of land with elevated yield potential. At the same time, the low-productivity zone covered approximately 27% of the field and consistently exhibited lower yield levels.

A comparison of zone areas between years shows that their proportions varied only slightly. The share of the low-productivity zone ranged from 24% to 29%, the medium zone from 43% to

46%, and the high zone from 25% to 33%. Such stability in spatial distribution indicates that productivity boundaries are primarily determined by persistent environmental factors, such as soil properties, topography, and water regime, rather than random interannual weather variability. Additional evidence of spatial stability is provided by the low values of the CV of zone areas. The lowest variability was observed in the medium-productivity zone, with a CV of only 2.9%, indicating that its area remained nearly unchanged throughout the study period. For the low-productivity zone, this value was 7.9%, and for the high-productivity zone 11.6%, which also reflects a relatively stable spatial distribution within the field. Even for the most variable high-productivity zone, changes in area remained moderate and did not exceed a few per cent of the total field area.

Thus, the analysis of long-term yield data demonstrates a high degree of spatial stability in the productivity structure of the studied field. The identified zones are characterised not only by substantial differences in yield levels but also by relatively stable boundaries and areas across years. This confirms the suitability of using long-term yield maps for field zoning and provides a foundation for the application of differentiated agronomic practices within precision agriculture systems.

Discussion

The obtained results indicate the presence of a clearly expressed spatial structure of productivity within the studied field, manifested in the stable recurrence of zones with different yield levels over several years. Over four years of observations (2019, 2020, 2023, 2024), three productivity zones were consistently identified within the field, characterised by distinctly different mean yield levels (6.2, 9.5, and 12.3 t/ha for the low-, medium-, and high-productivity zones, respectively) and similar area proportions: on average 27% for the low-, 45% for the medium-, and 29% for the high-productivity zone. Low coefficients of variation in zone area between years (2.9-11.6%) indicate a high degree of spatial stability in the field's productivity structure, despite changes in overall yield levels between years. Similar patterns are confirmed by numerous recent studies on within-field yield variability in precision agriculture systems.

In particular, a large-scale study by B. Maestrini & B. Basso (2021) analysed more than 5,500 yield maps for various crops in the United States. The authors found that zones of consistently high and low productivity persist over many years, even under substantial interannual weather variability. The results of current study are consistent with these findings: the proportion of area belonging to individual productivity zones changed only slightly, and the difference between the average yield levels of the zones remained within the range of 5-7 t/ha throughout the study period. Similar results were reported by Adhikari *et al.* (2023), who identified stable and unstable productivity zones across nine fields based on four-year maize yield datasets. In this case, the share of the low-productivity zone also remained relatively constant (around 27%), which aligns with the concept of "fixed" low-performing areas determined by soil-landscape factors. Comparable conclusions were obtained in the study by F. Castaldi *et al.* (2021), which examined the relationship between long-term yield maps and weather conditions. The authors found that within-field spatial yield patterns persist even under significant variation in precipitation between years, while weather primarily affects the intensity of yield rather than the spatial configuration of productivity zones. A similar pattern was observed in the studied field: 2020 was characterised by a reduced mean yield (8.0 t/ha compared with 9.5-10.5 t/ha in other years), yet the boundaries of low-, medium-, and high-productivity zones remained close to their long-term configuration.

The role of soil properties in shaping spatial productivity heterogeneity is also supported by modelling results presented by I.M. Hernández-Ochoa *et al.* (2025). Based on a thirty-year simulation of crop yields, the authors showed that spatial variability driven by soil characteristics often exceeds interannual variability associated with weather conditions. In this study, this is further confirmed by the stable inverse relationship between productivity and soil surface brightness (r = -0.79 to -0.87), which indirectly reflects the influence of soil texture, organic matter content, and water-holding capacity on yield formation. The importance of integrating multiple sources of spatial information for productivity zoning is highlighted in the work of L.G.G. Sterle & J.P. Molin (2025). The authors demonstrated that combining historical yield maps with soil electrical conductivity data and topographic attributes improves the accuracy of management zone delineation. Similarly, the comparison of the long-term productivity map with the soil brightness map revealed a high degree of spatial agreement between these layers (|r| ≈ 0.8-0.87, R^2 up to 0.88), indicating a stable soil-landscape control over the spatial structure of yield.

The high correlation values between NDVI indicators and the productivity map obtained in the study are consistent with the findings of A. Tamás *et al.* (2023). In this case, the long-term average NDVI showed a correlation with the productivity map in the range of r = 0.86-0.94 (mean 0.91), with a coefficient of determination R^2 between 0.74 and 0.88, indicating that a substantial proportion of spatial yield variability is explained by remote sensing vegetation indices. In the study by A. Tamás *et al.* (2023), NDVI derived from unmanned aerial vehicles demonstrated a strong positive relationship with maize yield (r ≈ 0.80-0.84) during the late vegetative and early reproductive growth stages. Taken together, these findings indicate that NDVI can be effectively used as an indicator of the spatial structure of field-level productivity. Similar results were obtained in the study by D. Radočaj *et al.* (2025), which showed that Sentinel-2 vegetation indices can be used to assess the spatial variability of maize yield. The authors emphasised that the use of red-edge indices and phenological metrics improves the accuracy of correlations with actual yield maps. This is consistent with the observation that the integration of multi-year NDVI indicators, rather than single-date imagery, provides the best agreement with the field productivity structure.

At the same time, P. Killeen *et al.* (2024) highlighted the importance of accounting for spatial data structure when analysing relationships between satellite indicators and yield. The authors demonstrated that standard cross-validation approaches may lead to overestimation of model accuracy, whereas spatially explicit validation provides more realistic results. This underscores the need for caution when interpreting correlations between remote sensing indices and yield, particularly when correlation coefficients are high but not tested for spatial generalisability. Further evidence supporting the effectiveness of satellite indices for yield assessment is provided by B. Zhu *et al.* (2021), who showed that combining NDVI with meteorological data enables the development of more accurate maize yield prediction models at the regional scale. This approach integrates both the biophysical condition of crops and the influence of weather factors, significantly improving model explanatory power. Field-scale results align with this concept: NDVI provides the spatial framework of productivity, while interannual yield differences are largely explained by climatic variability.

Additional improvements in yield prediction accuracy are demonstrated in the study by S. Sarkar *et al.* (2025), which employed machine learning and multispectral data from unmanned platforms. The authors found that integrating satellite indicators with soil and topographic characteristics significantly enhances model performance. This confirms the importance of a comprehensive approach to analysing spatial variability in productivity. A similar principle is evident in this case, where the combination of long-term yield maps with satellite indicators and soil brightness maps enabled more reliable identification of stable productivity zones. Comparable findings were reported by S. Chen *et al.* (2022), who applied machine learning techniques to spatially disaggregate statistical maize yield data.

Their results showed that the use of multi-source datasets, including vegetation indices, climatic variables, and soil properties, allows accurate reconstruction of spatial yield patterns over large areas. Likewise, L. Miao *et al.* (2024) demonstrated the high effectiveness of multi-source data integration for maize yield prediction, showing that combining climatic, satellite, and soil indicators in machine learning models leads to high coefficients of determination. The authors emphasised that climatic factors define general spatial productivity trends, while remote sensing indices reflect the current physiological state of crops.

Thus, the obtained results support current scientific understanding of the formation of spatial productivity patterns in agricultural crops. It has been established that within-field yield variability is primarily driven by stable soil-landscape factors, whereas weather conditions mainly determine the intensity of productivity expression in individual years. High correlations between the long-term productivity map and NDVI ($r \approx 0.9$, $R^2 \approx 0.8$), together with a consistent inverse relationship with soil brightness, confirm that long-term yield maps combined with remote sensing vegetation indices represent an effective tool for delineating field productivity zones and optimising crop management practices in precision agriculture systems.

Conclusions

An analysis of long-term maize yield maps for the 2019-2020 and 2023-2024 periods showed that spatial variations in productivity within the study field are distinct and stable. Despite inter-annual variability in weather conditions and overall yield levels, the spatial distribution of low-, medium- and high-productivity zones remained consistent, indicating the dominant influence of soil and topographical factors in determining maize crop productivity. It was established that the high-productivity zone was characterised by the highest average yield values throughout the entire study period, whilst the medium-productivity zone occupied the largest share of the field area, and the low-productivity zone consistently exhibited the lowest yield levels. The interannual variation in the areas of the zones was insignificant, as confirmed by low values of the CV, and indicates a high spatial and temporal stability of the field's productivity structure.

A comparison of long-term yield maps with a soil surface brightness map and a long-term productivity map derived from average NDVI values revealed a high degree of consistency in spatial patterns. Areas of reduced productivity predominantly corresponded to plots with increased soil brightness and lower NDVI values, whereas highly productive plots were characterised by lower soil surface brightness and consistently high satellite productivity indices. This confirms the agroecological determinants of the identified zones and their relationship with soil properties and water regime. Correlation analysis revealed a close direct relationship between the map of long-term field productivity and the long-term average NDVI, as well as a consistent inverse relationship between productivity and soil brightness. High values of the coefficient of determination indicate that a significant proportion of the spatial variation in field productivity is explained by soil differences that are stable over time. The results obtained confirm the validity of using long-term yield maps as a reliable and informative basis for identifying field productivity zones. Combining yield monitoring data with satellite productivity indicators and soil surface characteristics allows for a more robust spatial analysis and minimises the influence of random inter-annual factors.

The practical implementation of identified productivity zones as a basis for differentiated crop management is a promising direction for further applied research. In particular, it is advisable to develop and field-test zonally differentiated sowing rates for maize seeds, application rates for mineral fertilisers, as well as the differentiated application of plant protection products, the incorporation of additional spatial data layers, and the testing of the approach in fields with other crops and under various soil and climatic conditions.

Acknowledgements

None.

Funding

None.

Conflict of Interest

None.

References

[1] Adhikari, K., Smith, D.R., Hajda, C., & Kharel, T.P. (2023). Within-field yield stability and gross margin variations across corn fields and implications for precision conservation. *Precision Agriculture*, 24, 1401-1416. doi: 10.1007/s11119-023-09995-7.

[2] Baron, F.A., Carvalho, I.R., Adorian Bandeira, W.J., Amado, T.J.C., Corassa, G.M., Fioresi, D., & Martini, R.T. (2025). Optimization of the maize hybrid plant population in a heterogeneous agricultural field. *Colloquium Agrariae*, 21(1), article number e255066. doi: 10.5747/ca.2025.v21.a540.

[3] Castaldi, F., Whalley, R.C.L., Sylvester-Bradley, R., & Rees, R.M. (2021). Spatio-temporal analysis of yield and weather data for defining site-specific crop management zones. *Precision Agriculture*, 22, 1952-1972. doi: 10.1007/s11119-021-09820-z.

[4] Chen, S., Liu, W., Feng, P., Ye, T., Ma, Y., & Zhang, Z. (2022). Improving spatial disaggregation of crop yield by incorporating machine learning with multisource data. *Remote Sensing*, 14(10), article number 2340. doi: 10.3390/rs14102340.

[5] Convention on Biological Diversity. (1992, June). Retrieved from https://www.cbd.int/convention/text/.

[6] de Oliveira Filho, M.A., Santos, A.L.C., Domingues, R.F., Melazzo, G.M., Pontes, B.S., da Silva, R.J., Hurtado, S.M.C., & Catão, H.C.R.M. (2025). Validation of management zones, variability, and spatial distribution of the physiological quality of soybean seeds. *Plants*, 14(12), article number 1856. doi: 10.3390/plants14121856.

[7] Elsharkawy, M.M., Sheta, A., D'Antonio, P., Abd-Elwahed, M.S., & Scopa, A. (2022). Tool for the establishment of agro-management zones using GIS techniques for precision farming in Egypt. *Sustainability*, 14(9), article number 5437. doi: 10.3390/su14095437.

[8] Hernández-Ochoa, I.M., Gaiser, T., Grahmann, K., Engels, A.M., & Ewert, F. (2025). Within-Field temporal and spatial variability in crop productivity for diverse crops – a 30-year model-based assessment. *Agronomy*, 15(3), article number 661. doi: 10.3390/agronomy15030661.

[9] Killeen, P., Kiringa, I., Yeap, T., & Branco, P. (2024). Corn grain yield prediction using UAV-based high spatiotemporal resolution imagery, machine learning, and spatial cross-validation. *Remote Sensing*, 16(4), article number 683. doi: 10.3390/rs16040683.

[10] Leuthold, S.J., Lavallee, J., Basso, B., Brinton, W., & Cotrufo, M.F. (2024). Shifts in controls and abundance of particulate and mineral-associated organic matter fractions among subfield yield stability zones. *SOIL*, 10, 307-319. doi: 10.5194/soil-10-307-2024.

[11] Maestrini, B., & Basso, B. (2021). Subfield crop yields and temporal stability in thousands of US Midwest fields. *Precision Agriculture*, 22, 1749-1767. doi: 10.1007/s11119-021-09810-1.

[12] Miao, L., Zou, Y., Cui, X., Kattel, G.R., Shang, Y., & Zhu, J. (2024). Predicting China's maize yield using multi-source datasets and machine learning algorithms. *Remote Sensing*, 16(13), article number 2417. doi: 10.3390/rs16132417.

[13] Mikha, M.M., Mankin, K.R., Khan, S.B., & Barnard, D.M. (2024). Precision management influences productivity and nutrients availability in dryland cropping system. *Agronomy Journal*, 116(6), 3325-3343. doi: 10.1002/agj2.21686.

[14] Narra, N., Linna, P., & Lipping, T. (2022). Calculating productivity zones of crop fields using open satellite data. In *IGARSS 2022 – 2022 IEEE international geoscience and remote sensing symposium* (pp. 6073-6076). Kuala Lumpur: IEEE. doi: 10.1109/IGARSS46834.2022.9883146.

[15] Radočaj, D., Plaščak, I., & Jurišić, M. (2025). Fusion of Sentinel-2 phenology metrics and saturation-resistant vegetation indices for improved correlation with maize yield maps. *Agronomy*, 15(6), article number 1329. doi: 10.3390/agronomy15061329.

[16] Salem, H.M., Schott, L.R., Piaskowski, J., Chapagain, A., Yost, J.L., Brooks, E., Kahl, K., & Johnson-Maynard, J. (2024). Evaluating intra-field spatial variability for nutrient management zone delineation through geospatial techniques and multivariate analysis. *Sustainability*, 16(2), article number 645. doi: 10.3390/su16020645.

[17] Sarkar, S., Osorio Leyton, G.A., Noa-Yarasca, A., Adhikari, K., Hajda, C., & Smith, D.R. (2025). Integrating remote sensing and soil features for enhanced machine learning-based corn yield prediction in the Southern US. *Sensors*, 25(2), article number 543. doi: 10.3390/s25020543.

[18] Sterle, L.G.G., & Molin, J.P. (2025). Management zones for irrigated and rainfed grain crops based on data layer integration. *Agronomy*, 15(8), article number 1864. doi: 10.3390/agronomy15081864.

[19] Tamás, A., Kovács, E., Horváth, É., Juhász, C., Radócz, L., Rátonyi, T., & Ragán, P. (2023). Assessment of NDVI dynamics of maize (*Zea mays* L.) and its relation to grain yield in a polyfactorial experiment based on remote sensing. *Agriculture*, 13(3), article number 689. doi: 10.3390/agriculture13030689.

[20] Zhu, B., Chen, S., Cao, Y., Xu, Z., Yu, Y., & Han, C. (2021). A regional maize yield hierarchical linear model combining landsat 8 vegetative indices and meteorological data. *Remote Sensing*, 13(3), article number 356. doi: 10.3390/rs13030356.

Обґрунтування виділення зон продуктивності поля за даними багаторічного моніторингу урожайності кукурудзи та супутникових показників

Леся Гарбар
Кандидат сільськогосподарських наук, доцент
Національний університет біоресурсів і природокористування України
03041, вул. Героїв Оборони, 15, м. Київ, Україна
https://orcid.org/0000-0003-4249-0434
Богдан Васьківський
Аспірант
Національний університет біоресурсів і природокористування України
03041, вул. Героїв Оборони, 15, м. Київ, Україна
https://orcid.org/0009-0003-6852-3844

Анотація. У статті наведено результати багаторічного аналізу просторової неоднорідності урожайності кукурудзи (*Zea mays* L.) на виробничому полі площею 448 га в зоні переходу між Поліссям і Лісостепом України. Дослідження проведено на основі карт урожайності за 2019-2020 та 2023-2024 роки з метою оцінки стійкості внутрішньопольових зон продуктивності та встановлення їх зв'язку із супутниковими показниками. Просторову структуру продуктивності аналізували шляхом агрегування даних yield monitor до регулярної сітки 20 × 20 м з подальшою класифікацією на три зони продуктивності. Для підтвердження агроекологічної обумовленості зон використовували багаторічні композити NDVI (Sentinel-2) та карти яскравості ґрунтової поверхні. Встановлено, що просторові межі зон низької, середньої та високої продуктивності зберігалися упродовж усього періоду досліджень, незважаючи на міжрічні коливання середнього рівня урожайності. Середні багаторічні значення становили 6,2 т/га у низькій, 9,5 т/га у середній та 12,3 т/га у високій зоні продуктивності. Коефіцієнт варіації площ зон не перевищував 11,6 %, що свідчить про їх високу просторово-часову стабільність. Кореляційний аналіз показав тісний прямий зв’язок між багаторічною картою продуктивності та середньобагаторічним NDVI (r = 0,86-0,94), а також стабільний обернений зв’язок із показниками яскравості ґрунту (r = -0,79…-0,87). Високі значення коефіцієнта детермінації (R^2 = 0,74-0,88) підтверджують, що основна частка просторової варіації урожайності зумовлена сталими ґрунтово-ландшафтними чинниками. Отримані результати доводять доцільність використання багаторічних карт урожайності у поєднанні із супутниковими індексами для виділення стабільних зон продуктивності поля. Такий підхід створює наукове підґрунтя для впровадження технологій точного землеробства та просторово диференційованого управління агроресурсами

Ключові слова: *Zea mays* L.; просторова неоднорідність поля; яскравість ґрунту; багаторічні карти урожайності; коефіцієнт детермінації; точне землеробство; management zones

Received 02.01.2026 Revised 01.04.2026 Accepted 23.04.2026 Published: 30.04.2026

Vol. 22, No. 2
2026

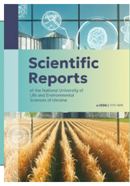

Scientific Reports of the National University of Life and Environmental Sciences of Ukraine

Journal homepage: https://scireports.com.ua/en e-ISSN 2223-1609

UDC 631.4:504.06 DOI: 10.31548/dopovidi/2.2026.65

Conceptual model of post-war restoration of agricultural land with integration of bioenergy technologies

Tetiana Chaika*
PhD in Economics
Separated Structural Unit "Agrarian-Economic Professional College of Poltava State Agrarian University"
36003, 18 Hryhorii Skovoroda Str., Poltava, Ukraine
https://orcid.org/0000-0002-5980-7517

Mykola Shevnikov
Doctor of Agricultural Sciences, Professor
Poltava State Agrarian University
36003, 1/3 Hryhorii Skovoroda Str., Poltava, Ukraine
https://orcid.org/0000-0003-0810-523X

Arsenii Stetsenko
Student
Separated Structural Unit "Agrarian-Economic Professional College of Poltava State Agrarian University"
36003, 18 Hryhorii Skovoroda Str., Poltava, Ukraine
https://orcid.org/0009-0003-6711-0247

Viktor Liashenko
PhD in Agricultural Sciences, Associate Professor
Poltava State Agrarian University
36003, 1/3 Hryhorii Skovoroda Str., Poltava, Ukraine
https://orcid.org/0000-0003-0177-6209

Abstract. Russia's full-scale military actions against Ukraine led to large-scale degradation of agricultural land, which was accompanied by mechanical destruction of soil cover, chemical pollution, and loss of productive potential. The lack of an integrated system of post-war reconstruction led to the need to form a comprehensive model of reclamation, combining environmental and economic tools within a single management approach. The purpose of the study was to develop a conceptual model of post-war restoration of agricultural land based on the integration of engineering, chemical, biotechnological, and economic approaches within the circular land use system. Analytical, comparative, and system structural methods, and conceptual modelling were used. As a result of the study, the

Suggested Citation:
Chaika, T., Shevnikov, M., Stetsenko, A., & Liashenko, V. (2026). Conceptual model of post-war restoration of agricultural land with integration of bioenergy technologies. *Scientific Reports of the National University of Life and Environmental Sciences of Ukraine*, 22(2), 65-89. doi: 10.31548/dopovidi/2.2026.65.

*Corresponding author

scale of physical degradation of soil cover on de-occupied agricultural land was determined and a conceptual model of their agrobiological restoration using phytoremediation crops was proposed. A multi-level recovery model was formed, which included stages of humanitarian demining, technical preparation of the territory, pollution assessment, mechanical reclamation, chemical detoxification, biotechnological regeneration, and long-term phytoremediation with the integration of bioenergy technologies. The expediency of a 15-year phytoremediation cycle in the structure of reclamation with a gradual transition to an economically viable land use system was substantiated. A circular model of biomass processing was proposed, which provides for energy valorisation of phytomass and the return of stabilised products to the soil, ensuring partial or complete self-sufficiency of the recovery process. The practical viability of the model was demonstrated using the example of damaged agricultural land in the Snihurivka urban territorial community of Mykolaiv Oblast, where the bioenergy component was shown to generate a stable cash flow for partial compensation of engineering reclamation costs. The proposed model can be adapted to various types of belligerent agricultural landscapes and creates prerequisites for the development of financially stable reclamation mechanisms. It has the potential for practical application in Ukraine and other countries affected by military operations, and can become the basis for the development of national policies in the field of land restoration and sustainable development of the agricultural sector

Keywords: agrolandscapes; bioenergy crops; circular economy; ecological stabilisation; soil reclamation; phytoremediation; land detoxification

Introduction

Russia's full-scale invasion of Ukraine in 2022 caused a large-scale degradation of land resources. The fighting caused systemic damage to the ground cover: physical destruction as a result of explosions and compaction by equipment was combined with chemical contamination by ammunition detonation products, fuel and lubricants, and remnants of weapons. The high resistance of toxicants in soils has created risks of long-term withdrawal of land from agricultural circulation and has created long-term environmental and socio-economic consequences. Analysis of scientific sources showed that the war led to mechanical damage and prolonged chemical contamination of the soil, which, according to M. Gulich *et al.* (2024), may have a significant impact on ecosystem functions and food system security. T. Chaika & I. Korotkova (2023) noted that without systemic reproduction measures, degraded lands can lose their productive potential for a long period of time. This made it necessary to develop an integrated algorithm for post-war restoration of belligerent landscapes, which combined technical, chemical, and biotechnological tools.

The initial stage of post-war reconstruction provided for a comprehensive identification of the scale and spatial structure of soil cover damage. O. Bonchkovskyi *et al.* (2025) noted that the use of remote sensing data on the Earth's surface helped to quickly identify areas of mechanical disturbance and potential pollution, but stressed the need for further geochemical analysis to assess the risks of toxicant migration in the soil profile. Developing this approach, O. Drebot & O. Korol (2025) noted that the restoration of affected landscapes should be based on the integration of satellite monitoring with an assessment of the state of hydrological systems and biodiversity. The next logical step was to develop decontamination and remediation strategies. V. Samokhvalova (2024) proposed an algorithm that covered consecutive stages – from previous studies and environmental risk assessment to the implementation of measures to reduce pollutant concentrations. O. Mudrak *et al.* (2025) proved that the restoration of belligerently transformed landscapes required the harmonisation of ecosystem system management tools with reclamation and bioremediation measures. Effective implementation of the proposed recovery strategies requires a strong resource base. N. Didenko (2024) suggested that the implementation of comprehensive recovery strategies is impossible without long-term planning, the introduction of advanced technologies, and the attraction of significant financial resources. In turn, V. Naumchuk (2024) noted that the success of phytoremediation and other methods of soil restoration depended on a harmonious combination of environmental, social and economic aspects, in particular through the creation of public-private partnerships that could ensure stable financing of such projects. Special attention should be paid to the transition to adaptive management, which has become necessary for continuous monitoring and correction of recovery strategies. M. Melnykovych *et al.* (2026) identified several strategic ways of post-war reconstruction, among which the key was the use of digital tools to ensure the climate sustainability of landscapes, and the support of ecosystem services, which will contribute to the long-term restoration of land functions.

The final phases of soil restoration should combine environmental feasibility with economic efficiency. As noted by N. Martynova & T. Kolombar (2025), one of the promising areas was the use of phytoextraction involving fast-growing crops, which helped to simultaneously detoxify land and obtain biomass for renewable energy production. The analysis of scientific sources showed that, despite the presence of thorough research of individual technological and managerial decisions, there is no integrated conceptual model in the scientific discourse that would systematically combine the stages of primary damage diagnostics, engineering and chemical reclamation, biotechnological restoration, and the development of bioenergy clusters into a single logically completed system of post-war agricultural land reclamation. The purpose of the study was to substantiate the scientific and methodological foundations of post-war restoration of agricultural land damaged as a result of military operations, and to develop a conceptual model that would ensure ecological stabilisation of the soil cover and the development of an economically viable land use system. To achieve this goal, the following research objectives were defined: 1) to analyse contemporary scientific approaches and practices for restoring soils that have been exposed to military influence; 2) to develop an integrated model that combines engineering, chemical, and biotechnological reclamation measures; 3) to substantiate the economic feasibility of the model and assess its potential for self-financing through the integration of the bioenergy component. The scientific originality of the study was the development of an integrated approach to the post-war restoration of agricultural land, combining phytoremediation, bioenergy use of contaminated biomass, and the principles of circular economics to ensure economically sustainable reclamation of belligerent soils.

Materials and Methods

The study was conducted in 2025 using a systematic and interdisciplinary approach to the development of a conceptual model of post-war restoration of agricultural land damaged by military operations. Geographical coverage provided for the generalisation of international experience in the reclamation of territories affected by military influence (Bosnia and Herzegovina, Lebanon), and the analysis of contemporary practices of phytoremediation and environmental restoration in the EU countries based on scientific publications of C. Lievens *et al.* (2008), J. Vangronsveld *et al.* (2009) and N. Witters *et al.* (2012). The research drew on data from V. Samokhvalova (2024), who developed algorithms for selecting soil reclamation methods, determining the dosage of soil improvers and monitoring soil degradation under military and anthropogenic influences, and

O. Bonchkovskyi *et al.* (2025), which characterised physical disturbances and contamination of the soil cover in north-eastern Ukraine as a result of military operations and laid the basis for morphometric and geochemical assessment of belligerent agricultural landscapes. In addition, official documents of international organisations and other authors on the post-war restoration of agricultural territories were investigated. In particular, W. Verheye *et al.* (2007) discussed algorithms for surveying damaged land and spatial planning for restoration, whilst UNDP (2011) described practices relating to humanitarian demining and the return of agricultural land to productive use in the context of post-conflict recovery. The FAO report (2025) provided an assessment of the scale of degradation of agricultural landscapes and recommendations for the transition from operational mine clearance to integrated environmental reproduction strategies. These documents became an important methodological basis for substantiating the sequence of stages of the conceptual model and consideration of international experience in the development of approaches to the post-war restoration of agricultural land. In addition, analytical, comparative, and system structural methods were used to generalise international experience in land restoration, compare technological solutions for reclamation, and determine their relationships within an integrated model. The conceptual modelling method was used to develop a scheme for combining technical reclamation, chemical detoxification, phytoremediation, and bioenergy processing of biomass. The study considered the provisions of International Mine Action Standards (IMAS 01.10, 2003), UNMAS (n.d.) recommendations. Data from the NATO standards STANAG 2143 and STANAG 2449 presented in EOD publications – overview (n.d.), which regulated the requirements for the safety of cleaning up territories and assessing environmental risks in contaminated areas.

The conceptual model was developed as a consistent system of interrelated stages of land restoration, which included humanitarian demining, technical reclamation, chemical soil stabilisation, phytoremediation, and the use of biomass in bioenergy technologies in accordance with the principles of the circular economy (“Soil-to-Energy”). To substantiate the economic feasibility of the recovery model proposed in the study, a set of economic methods and approaches was applied. The cost calculation was used to determine the amount of financial resources required for the implementation of each technological stage of reclamation – from humanitarian demining to agrochemical land reclamation. The revenue approach was used to assess the economic potential of the bioenergy component of the model by determining the projected revenues from the sale of biofuels and by-products of its processing. Profit and profitability were calculated based on a comparison of gross income with operating expenses for growing crops and processing biomass, which allowed estimating net cash flow and the payback period for capital investments. These approaches provided verification of the financial stability of the conceptual model and its ability to gradually self-sufficiency. Morphometric analysis of explosive craters was performed using Google Earth data for a 122-hectare field in the Snihurivka urban territorial community (UTC) of the Mykolaiv Oblast. Identification of zones of mechanical disturbance of the soil cover was carried out by visual interpretation of images, measurement of morphometric parameters of craters – using the ImageJ programme (USA). The approximate depth of craters was estimated from the empirical ratio between the diameter and depth of explosive craters ($H \approx 0.4 D$) proposed in the study by J.P. Hupy & R.J. Schaetzl (2006). Based on the obtained parameters, the area of the mechanically disturbed surface and the approximate volume of displaced soil were determined. Statistical processing and visualisation of the results were performed in Python.

Results and Discussion

The developed conceptual model of post-war restoration of agricultural land was verified based on initial data of territories that were subjected to intense mechanical and anthropogenic impacts as a result of military operations in the south of Ukraine. The analysis of real conditions of soil cover destruction allowed structuring the reclamation process in the form of a consistent multi-level system that integrated engineering, chemical, biotechnological, and economic recovery tools. The proposed architecture of the model (Table 1) reflects the logic of the transition from primary stabilisation of the territory to long-term phytoremediation and the development of a bioenergy component, which ensured partial economic self-sufficiency of recovery measures.

Table 1. *Stages of implementation of the conceptual model of post-war restoration of agricultural soils*

Stage	Main activities	Goal and expected results
Initial stabilisation of the territory	Humanitarian demining; clearing the territory of man-made residues; levelling the surface	Ensuring the safe condition of the territory and preparing the soil cover for reclamation works
Environmental diagnostics of soils	Soil sampling; laboratory determination of heavy metals, radionuclides, and anthropogenic pollutants	Determining pollution levels and spatial structure
Mechanical reclamation	Filling craters with soil; surface planning; deep loosening of compacted areas	Restoration of topography and agrophysical properties of the soil
Chemical detoxification	Liming; application of sorbents (zeolites, activated carbon); introduction of phosphate meliorants	Immobilisation of toxicants and reduction of their bioavailability
Biological recovery	Application of organic meliorants; microbial inoculation; restoration of the soil microbiome	Increasing biological activity and soil fertility
Phytoremediation and bioenergy use of biomass	Cultivation of remediant plants and bioenergy crops; processing of biomass on the principle of "Soil-to-Energy"	Soil purification and development of economic self-sufficiency of reclamation

Source: based on P. Soudek *et al*. (2014), T. Steliga & D. Kluk (2021), N. Didenko (2024), O. Bonchkovskyi *et al.* (2025)

The initial and most critical stage of restoration was ensuring the safety of the territory and eliminating the consequences of direct mechanical destruction of the soil cover. At this stage, a set of measures for humanitarian demining and technical preparation of the territory was implemented. Humanitarian demining was carried out using advanced technologies for remote detection of explosive objects. The use of sapper drones equipped with magnetometers for detecting metal objects and thermal imagers for detecting thermal anomalies in the ground has allowed increasing the safety and efficiency of mine clearance compared to conventional methods. All mine clearance operations were carried out exclusively by certified operators in accordance with the International Mine Action Standards (IMAS 01.10, 2003) and UNMAS recommendations (n.d.), and national security protocols (Law of Ukraine No. 2642-VIII, 2018). When planning and executing the work, the technical requirements of NATO standards STANAG 2143 (AJP-3.15) and 2449 (AEODP-10) (EOD publications – overview, n.d.). A prerequisite for the transition to the next stages of reclamation was obtaining an official certification on the safety of the territory, which confirmed the absence of explosive objects and allowed further agricultural work.

Technical preparation of the territory and elimination of the remains of fortifications included several consecutive operations. The first step was a diagnostic scan of the territory with multispectral drones, which allowed detecting hidden remnants of military structures, metal accumulations, and other objects that are not noticeable during visual inspection of the surface. Multispectral scanning provided comprehensive information about the state of the surface and subsurface layer of the soil, which became important for planning further reclamation activities

(Qiu *et al*., 2023). Mechanised cleaning of large remnants of machinery, concrete fragments, and metal structures was carried out using specialised stone harvesting machines and heavy equipment (US Army Corps of Engineers, 2015). This operation helped to clear the territory of massive objects that could not be removed manually, and which prevented further agrotechnical operations, created a long-term environmental risk. Special attention was paid to the removal of concrete residues of fortifications, since they not only created physical obstacles, but could also be a source of secondary contamination of the soil with alkaline compounds. Magnetic separation of the upper soil layer was carried out using specialised trawls to extract small metal fragments and shrapnel. The method was based on the physical separation of metal-containing particles in a magnetic field. Its effectiveness in cleaning contaminated soils has been demonstrated in experimental studies by B. Caballero-Mejía *et al*. (2025). As noted by S.D. Young (2012), small metal fragments remaining in the soil were gradually oxidised in the soil solution, which could lead to the release of mobile forms of heavy metals. Such processes created prerequisites for long-term secondary soil contamination. In addition, the presence of a significant proportion of large solid fragments in the arable layer changed the physical properties of the soil and could affect the efficiency of its cultivation.

The final operation of the first stage of reclamation was the dismantling and planning alignment of lines of trenches, dugouts, and other military engineering structures. The development of defensive fortifications was accompanied by significant mechanical disturbances of the soil cover and transformation of the microrelief, which changed the natural structure of surface runoff, reduced the infiltration capacity of the soil, and disrupted the local water balance. The deformation of microtopography caused spatial unevenness of hydrological processes, which could manifest itself in the form of local waterlogging, stagnation of water or, conversely, excessive drainage of individual areas, which was confirmed in the study by D. Caviedes-Voullième *et al*. (2021) on the role of microrelief in surface runoff generation and moisture redistribution. Restoration of natural or agronomically optimised terrain by surface planning has become a necessary prerequisite for stabilising the hydrological regime, ensuring uniform distribution of moisture and nutrients, and forming homogeneous conditions for further agricultural use of the territory.

The second stage of soil cover reclamation was devoted to a comprehensive diagnosis of its condition and quantitative determination of the levels of contamination with various toxicants formed as a result of explosive and man-made impacts in the war zone. The study by M. Solokha *et al*. (2024) reported that military operations were accompanied by the accumulation of heavy metals, explosive components, detonation products, and fuel and lubricants in the soil, which made it necessary to systematically monitor and assess their spatial distribution. In addition, the authors noted that high concentrations of pollutants were observed in the epicentres of explosive impacts, where due to the localised accumulation of toxic components, their levels could exceed the background values. At this stage, systematic soil sampling was carried out, considering typical classification zones of pollution (crater zones and adjacent massifs). The use of standardised sampling methods guaranteed the representativeness of the sample for further laboratory analysis. Similar approaches have also been used in practical soil sampling protocols proposed by the US Army Corps of Engineers (2015). The density of sampling points varied depending on the size of the damaged area and the nature of pollution, but at least one sample per 100 m^2 within crater zones and one sample per 500 m^2 in buffer zones were recommended for a representative assessment of spatial heterogeneity, which provided a reasonable basis for quantifying pollution and subsequent reclamation measures.

According to the approach of S.D.Young (2012), laboratory analysis of the collected samples involved determining the concentrations of heavy metals, including lead (Pb), cadmium (Cd), zinc (Zn), copper (Cu), chromium (Cr), nickel (Ni), and mercury (Hg), which are typical components of anthropogenic loading on soils under conditions of wartime impact. The assessment was carried out both by the gross content of metals and by their mobile (bioavailable) forms, since it was the latter that determined the level of environmental danger and the potential ability of plants to accumulate. X. Cao *et al.* (2003) found that mobile forms of Pb, Cd, Zn, and other metals were characterised by higher phytotoxicity compared to their stabilised compounds, which made it necessary to control them in agroecosystems. The determination of mobile forms was carried out by extraction with an acetate-ammonium buffer solution with a pH of 4.8, which allowed assessing the potential availability of metals for the root system of plants and the real level of soil toxicity.

The radiological survey of the territory included measuring the exposure dose rate of gamma radiation using field dosimeters-radiometers and laboratory determination of the specific activity of radionuclides in the soil, in particular Caesium-137 (^{137}Cs) and Strontium-90 (^{90}Sr). According to M. Solokha *et al.* (2024), the need for radiological monitoring was conditioned by the possibility of radioactive contamination due to the use of certain types of ammunition or conducting combat operations in territories with a previous anthropogenic load. Radionuclides ^{137}Cs and ^{90}Sr are characterised by the ability to be fixed in the soil profile and potentially included in biogeochemical cycles, which created a risk of their entry into plant products. P. Broomandi *et al.* (2020) noted that comprehensive radiological monitoring helped to identify areas of increased radiation danger in a timely manner and determine the feasibility of restrictions on further agricultural use of land. The analysis of chemical contaminants included the determination of residues of explosive compounds (TNT, RDX, HMX), their detonation products (nitrates, nitrites), and components of fuels and lubricants, in particular polycyclic aromatic hydrocarbons and petroleum products. These compounds became characteristic of areas of active military operations and were characterised by high toxicity to the soil microbiota, invertebrates, and plants. Their accumulation significantly slowed down the processes of natural self-regulation and biological restoration of soils. The accumulation of nitro compounds and petroleum products in the topsoil can lead to disruptions in microbial activity, changes in redox conditions, and alterations in the nutrient cycle (Gulich *et al.*, 2024). The results of analytical studies served as a scientific basis for developing targeted recommendations for choosing optimal methods of reclamation of a particular site, including phytoremediation, agrochemical, or engineering measures. Simultaneously, the detailed documented state of pollution of territories was of important legal importance, since it formed the evidence base for assessing environmental damage and justifying compensation claims in accordance with the principles of international environmental law and compensation for environmental damage.

The third stage was aimed at restoring the physical structure and spatial configuration of the soil cover, disturbed as a result of explosive impacts and the movement of heavy military equipment. Detonation of ammunition and mechanical loading caused the destruction of the aggregate structure, compaction, mixing of horizons and the development of crater forms of microrelief, which significantly changed the physical properties of soils. T.L. Chow *et al.* (2007) found that the choice of mechanical reclamation methods and the intensity of their application were determined by the mechanical composition of the soil and the degree of its compaction, since the ratio of sandy, dusty and clay fractions directly affected the restoration of water permeability and structural state. The return of ejected soil to craters has become a major mechanical reclamation operation. During the explosion, significant amounts of soil mass were removed from the epicentre of the detonation and formed peripheral mounds, while less fertile deep horizons were exposed at the bottom of the crater. The discarded top layer retained most of the organic matter and nutrients compared to the exposed subsurface layers, which substantiated the feasibility of its return to the place of its original occurrence. Surface planning and restoration of the microrelief created prerequisites for the development of a productive arable layer and stabilisation of the water regime. As noted by T.L. Chow *et al.* (2007), a mandatory element of this process was the preliminary cleaning of the soil mass from large debris, metal fragments, and foreign inclusions that affected the agrophysical properties of the soil and could complicate the further use of land.

The import of fertile chernozem from ecologically safe territories became a necessary measure in areas of greatest destruction, where the volume losses of soil mass could not be compensated only by the return of discarded material. The development of a clean starting layer with a thickness of 20-30 cm provided conditions for primary rooting of plants and reduced the risk of contact of the root system with increased concentrations of pollutants in crater zones. Imported soil must meet the agrochemical characteristics of zonal soil types, have an optimal content of humus and nutrients and do not contain quarantine weeds, pathogens or pests, which corresponded to the principles of environmentally safe reclamation. For areas that were significantly compacted due to the movement of heavy military equipment, deep loosening of 35-50 cm was applied using diesel units or heavy cultivators. The military load led to the destruction of the soil structure, an increase in volume mass, a decrease in porosity and water permeability, which negatively affected aeration and the availability of nutrients for plants. Violation of the physical parameters of the soil was directly associated with a decrease in the productivity of agrocoenoses, which was confirmed in the studies by T.L. Chow *et al.* (2007) on the impact of compaction on the water regime and crop development. Restoration of the optimal density and structure of arable and sub-arable layers has become a necessary prerequisite for effective phytoremediation and stabilisation of agrophysical properties of the soil at subsequent stages of recovery.

The fourth stage of recovery was crucial for reducing the toxicity of contaminated soils and minimising the risk of toxicants entering plant products. Unlike mechanical removal of pollutants, chemical reclamation was aimed at changing their chemical state and converting them to sedentary or bound forms by regulating the physical and chemical parameters of the soil environment. Liming using calcium carbonate ($CaCO_3$) has become the basic operation of chemical reclamation of acidic and slightly acidic soils that have been acidified under the influence of detonation products. According to M. Solokha *et al.* (2024), nitrogen and sulphur oxides were formed during the explosion, which formed nitric and sulphuric acids under moist conditions, causing a decrease in the pH of the soil solution. According to V. Samokhvalova (2024), the application of lime in doses of 3-8 t/ha, depending on the degree of acidification, provided neutralisation of acidity and created favourable conditions for the development of plants and soil biota. Increasing the pH also significantly affected the behaviour of heavy metals, contributing to their transition to poorly soluble hydroxide and carbonate compounds. As shown by S.D. Young (2012), the motility of Pb, Cd, and Zn was sharply reduced under conditions of neutral and slightly alkaline reaction of the medium, which minimised their bioavailability to plants.

Sorption soil purification was carried out by introducing highly porous materials with a developed specific surface area that can immobilise organic and inorganic toxicants. As noted by P. Broomandi *et al.* (2020), the use of activated carbon at doses of 5-10 t/ha provided effective adsorption of fuel and lubricants and detonation products, in particular polycyclic aromatic hydrocarbons and nitroaromatic compounds, which have become typical for combat areas. The sorption mechanism included physical retention of molecules in micropores and chemical interaction with functional groups on the surface of the sorbent, which reduced the concentration of organic toxicants in the soil solution and limited their migration to plants. The use of activated carbon has significantly reduced the bioavailability of organic pollutants already in the first growing season. Natural zeolites (clinoptilolite, mordenite) were used in doses of 10-15 t/ha to bind mobile forms of heavy metals and stabilise the physical and chemical properties of the soil. The framework structure of zeolites with a developed channel system provided a high capacity of cation exchange, which caused selective absorption of cations Pb^{2+}, Cd^{2+}, Zn^{2+} and other metals from the soil solution and their fixation in the mineral lattice. In addition to the detoxification effect, zeolites improved the water and physical characteristics of the soil, increasing its moisture capacity and buffering, which became an important factor in stabilising agroecosystems at the initial stages of recovery.

The introduction of phosphorite flour in doses of 3-5 t/ha provided chemical immobilisation of heavy metals, primarily lead and cadmium, by converting them into hard-to-dissolve phosphate compounds. X. Cao *et al.* (2003) noted that the stabilisation mechanism is associated with the development of poorly soluble minerals such as pyromorphite ($Pb_5(PO_4)_3Cl$) and other lead phosphates with extremely low solubility, which dramatically reduced the migration capacity of the metal in the soil solution. This approach, according to P. Broomandi *et al.* (2020), has become particularly effective for soils with a high Pb content, characteristic of areas of intense shelling. An additional advantage of phosphorite flour was the improvement of the phosphorous regime of the soil and the restoration of elemental balance in areas that have not been used in agricultural production for a long time. The use of bentonite clays as a natural sorbent with a high cationic exchange capacity contributed to the fixation of heavy metal cations and reduced their bioavailability. The layered structure of bentonites with an expandable interpackage space provided effective absorption of Pb^{2+}, Cd^{2+}, and Zn^{2+} cations and their retention in the mineral structure. Increasing the sorption capacity of the soil helped to stabilise its buffer properties and reduce the toxic load on plants, which corresponded to approaches to chemical reclamation of land disturbed as a result of military operations. In addition to the detoxification effect, bentonite materials improved the water retention capacity and structural condition of the soil, increasing its resistance to fluctuations in acidity and pollutant concentrations.

The fifth stage of the conceptual model was aimed at restoring the biological activity of the soil by regenerating its microbiome and improving its agrophysical properties. Biological degradation of soils in war zones was manifested by a decrease in microbial biomass, a violation of enzymatic activity, and a decrease in the content of organic matter. Therefore, a differentiated approach was applied, in which the composition of land reclamation plants was adapted to the soil and climatic conditions of a particular territory. To stabilise the water regime and activate biological processes in degraded soils at the initial stages of recovery, it was advisable to use a set of materials and biological measures aimed at increasing the water retention capacity, improving the structural state and forming a stable microbial environment. Depending on the hydrothermal conditions and physical properties of the soil, synthetic hydrogels, organo-mineral sorbents, porous natural minerals and microbiological inoculants can be used, the main characteristics of which are given in Table 2.

Table 2. *Technological measures to stabilise the water and biological state of belligerent soils*

Material/technological reception	Terms of use	Application dose	Functional role
Potassium polyacrylates and polyacrylamides	Arid regions, light soils	20-40 kg/ha	High water retention capacity; development of a hydrogel structure with gradual release of moisture

***Table 2.** Continued*

Material/technological reception	Terms of use	Application dose	Functional role
Biochar	Arid regions, light soils; areas with sufficient moisture	10-20 t/ha(dry conditions); 15-25 t/ha (sufficient moisture)	Improvement of soil structure; increase of water retention capacity; development of microenvironments for soil microorganisms; deposition of stable organic carbon
Basalt tuff	Arid regions, light soils	5-20 t/ha	Improvement of the structural state of the soil; development of a microporous environment for microflora; source of trace elements; improvement of buffer properties of the soil system
Microbiological inoculation (plant growth promoting rhizobacteria, PGPR)	Areas with sufficient moisture	1-2 l/ha, titre $\geq 10^8$-10^9 CFU/ml	Activation of mineralisation of organic residues; improvement of nitrogen and phosphorus nutrition; development of a stable soil microbiome

Source: based on W.J. Rawls *et al*. (2003), J.K. Vessey (2003), J. Lehmann & S. Joseph (2015), L. Reczek *et al*. (2020)

The presented complex of materials and biological measures provided simultaneous stabilisation of the water regime, improvement of the structural state and activation of microbiological processes in the soil, which created prerequisites for further stages of phytoremediation and agroecological restoration of degraded territories. The sixth stage of the conceptual model provided for the implementation of a long-term strategy for cleaning the soil from residual concentrations of heavy metals with the parallel development of an economically feasible land use model. The use of phytoremediation in combination with bioenergy production helped to integrate environmental and economic goals of restoration of territories, transforming the reclamation process into a self-supporting bioenergy project. A 15-year crop rotation cycle using specially selected crops was recommended, aimed at gradually reducing the concentration of pollutants in the soil and simultaneously obtaining biomass for energy or technical needs (Martynova & Kolombar, 2025). The choice of such a planning horizon has become scientifically based and is conditioned by the need to go through three consecutive phases of reclamation: stabilisation (1-5 years) – for intensive phytoremediation and neutralisation of toxicants; regeneration (6-10 years) – for restoring the soil structure and accumulation of organic matter due to perennial grasses; adaptation (11-15 years) – for the transition to productive crop rotation and achieving full payback of costs. M.-C. Leewis *et al.* (2024) noted that this duration correlates with the international practice of restoring belligerent landscapes, where the period of complete soil rehabilitation after massive impact was at least 10-12 years.

The selection of phytoremediation crops was carried out according to the functional principle, considering the natural and climatic zone, the mechanical composition of the soil, the nature and intensity of pollution. Field crops with different biological and morphofunctional characteristics could perform the functions of phytoextraction, phytostabilisation, or structural and reclamation restoration of the soil. The efficiency of using industrial and energy crops on metal-contaminated lands was demonstrated in the studies by T. Vamerali *et al.* (2010) and M. Flajšman *et al.* (2023). Within the framework of the conceptual model, three main functional groups of crops were identified, which were used sequentially or in combination, depending on the degree of site degradation. Plant crops used in phytoremediation systems could perform the functions of both phytoextraction and phytostabilisation and structural restoration of the soil. The choice of crops was determined by their morphofunctional characteristics, their ability to accumulate metals or form significant biomass, and their adaptability to degraded soil conditions. The main crops used in such schemes are shown in Table 3.

Table 3. *Phytoremediation crops for the restoration of belligerent soils*

Crop	Main function	Biological features	Practical significance
Cannabis sativa L.	Phytoextraction	High biomass, developed root system, ability to accumulate Cd, Pb, Zn	Extraction of metals from the soil; use of fibre for technical needs
Helianthus annuus L.	Phytoextraction	Significant aboveground biomass, ability to accumulate Pb and Cd	Use in phytoextraction schemes; technical or energy use of oil
Brassica juncea L.	Phytoextraction	Fast growth, short growing season, high metal accumulation capacity	Use as an intermediate crop in phytoremediation crop rotations
Melilotus albus, *M. officinalis*	Phytostabilisation/ sideration	Nitrogen fixation (80-150 kg N/ha), powerful root system	Improving soil structure and increasing microbiological activity
Carthamus tinctorius L.	Structure development	Drought resistance, deep root system (up to 2-3 m)	Cultivation on degraded soils of the steppe zone
Sorghum bicolor L.	Phytostabilisation/ biomass	C4-photosynthesis, high productivity, drought tolerance	Obtaining biomass for bioenergy

Source: based on T. Vamerali *et al.* (2010), P. Soudek *et al*. (2014), T. Steliga & D. Kluk (2021), M. Flajšman *et al.* (2023)

In addition to the ecological function of soil purification and stabilisation, the use of plant crops in phytoremediation systems can provide biomass for energy or technical needs, which formed the economic basis of the reclamation process (Table 4). This integration of environmental and economic functions has become important for ensuring the financial sustainability of long-term reclamation projects, as conventional land reclamation programmes require significant external investment without guaranteed returns. The cultivation of bioenergy crops on contaminated land helped to obtain marketable products even at a time when the use of the territory for the production of food or fodder crops became unacceptable for environmental reasons. The combination of phytoremediation with the production of biomass for renewable energy can significantly increase the economic attractiveness of such projects and reduce their payback period. Thus, the bioenergy component acted not only as a source of income, but also as a mechanism that motivated land users to long-term compliance with phytoremediation crop rotation.

Table 4. *Bioenergy crops for economic support of reclamation*

Crop	Type of bioenergy products	Performance	Usage features
Brassica napus L.	Biodiesel	2.5-4.0 t/ha of seeds	Oil is used for the production of biodiesel; metals mainly accumulate in the vegetative organs
Miscanthus × ×*giganteus*	Solid biofuels	15-25 t/ha of dry biomass	Perennial crop with a plantation life of 15-20 years
Panicum virgatum L.	Biofuels/bioenergy biomass	10-20 t/ha of dry biomass	Tolerance to degraded soils and high efficiency of moisture use

Source: based on G. Knothe (2010), P. Soudek *et al.* (2014), N. Martynova & T. Kolombar (2025)

Thus, the cultivation of phytoremediation and bioenergy crops created a resource basis for further processing of biomass, which allowed integrating the ecological and energy functions of restoring territories. On this basis, a circular model of the use of biomass from reclaimed land ("Soil-to-Energy") can be implemented. The model will be based on the principles of a closed cycle, according to which all products and secondary processing flows were returned to the system or transformed into marketable products, which corresponded to the concept of a circular economy by M. Geissdoerfer *et al.* (2017). The biomass of remediant plants was collected in optimal terms, which ensured maximum accumulation of pollutants and the highest yield of target products. For oilseeds (*Brassica napus*, *Helianthus annuus*, *Carthamus tinctorius*), seeds were collected in the full ripeness phase, while the remaining plant mass could be used for mulching or energy processing. For green extractors (*Cannabis sativa*, *Brassica juncea*), all aboveground biomass was removed. Perennial energy crops (*Miscanthus* × *giganteus*, *Panicum virgatum*) were mowed after the complete drying of the aboveground part and the migration of nutrients to the rhizomes (late autumn – early spring), which reduced the nitrogen content of biomass and improved its fuel characteristics.

The production of biodiesel from oilseeds can be carried out using compact modular plants of small and medium capacity, which allowed organising processing directly at the level of farms or regional centres. G. Knothe (2010) pointed out that the process scheme was based on the transesterification reaction of vegetable oil triglycerides with methanol in the presence of an alkaline catalyst (NaOH or KOH) to form fatty acid methyl esters and glycerol as a byproduct. The yield of biodiesel under optimal conditions was about 96-98% by weight of oil, which corresponded to about 950-980 kg of fuel per 1 tonne of oil. The resulting fuel can be used to meet the farm's own energy needs or sold in accordance with the requirements of the EN standard 14214:2012+A2:2019 (2019). Raw glycerine after purification can be used in the chemical industry or other technical areas. Thermal processing of contaminated biomass (oilseed straw, extractor stalks, meal) was advisable by pyrolysis – thermal decomposition of organic matter without oxygen access at temperatures of 400-600°C (Bridgwater, 2012). As a result, a gaseous fraction (CO, H_2, CH_4), a liquid phase (bioolium), and a solid residue (biochar) were formed. The typical yield of biochar was 20-35% by weight of dry raw materials, depending on the temperature regime. The return of resources to the soil was carried out by introducing biochar obtained from relatively pure biomass (in particular, rhizomes of perennial grasses, characterised by limited transportation of heavy metals to the aboveground part). J. Lehmann & S. Joseph (2015) noted that periodic application of biochar in moderate doses (5-10 t/ha) contributed to the gradual restoration of fertility and stabilisation of the ecological state of reclaimed land. Detoxification and final removal of pollutants from the biological cycle was achieved through controlled disposal of the ash residue formed during pyrolysis of contaminated biomass. A.V. Bridgwater (2012) showed that during pyrolysis, inorganic components, including heavy metals, were concentrated in the solid residue. Such ash is not suitable for agricultural use, but it can be used in solid building materials technologies. B. Chen *et al.* (2024) noted that the fixation of heavy metals in a cement or alkali-activated matrix provided a significant reduction in their mobility and leaching risk, which is confirmed for ash products in the production of foam concrete and other cement-concrete mixtures. An alternative route was to stabilise highly polluted ash, followed by controlled disposal in accordance with hazardous waste management requirements.

The economic efficiency of implementing the proposed conceptual model was formed due to diversified sources of income and synergy between the ecological and production functions of land. Revenues were generated through the production of biodiesel from oilseeds and solid biofuels from perennial energy grasses, and through potential involvement in potential carbon incentive mechanisms. Economic verification of the bioenergy component of the model was carried out based on the V. Mesel-Veseliak (2015) approach, according to which winter rapeseed became the most productive link in crop rotation. Calculations were made using the method of cost balance of products of its deep processing, updated in accordance with market prices at the beginning of 2026. This scenario approach helped to assess the marginal economic potential of the system. With an average seed yield of 3.0 t/ha and a technological yield of methyl esters of

400 kg/t, about 1,364 litres of biofuel were obtained from one hectare of reclaimed land. At the current market price of 46 UAH/l, revenue from the sale of the main energy product amounted to 62.7 thousand UAH/ha. However, the key factor in the economic sustainability of the model was the valorisation of by-products. Obtaining 1,650 kg/ha of high-protein cake (market value ~20 UAH/kg) and 204 kg/ha of technical glycerol (market value ~60 UAH/kg) generated additional income in the amount of 45.2 thousand UAH/ha. Thus, the total gross income from 1 ha reached UAH 108.0 thousand. Even with high operating costs for cultivation and processing (which were estimated at approximately 45-50 thousand UAH/ha), the model generated an estimated net profit of 58.0 thousand UAH/ha. This confirmed the conclusions that deep processing of raw materials has become an alternative to improving the efficiency of agricultural production. Production of solid biofuels (pellets) from perennial energy crops (*Miscanthus × giganteus*, *Panicum virgatum*) was estimated using the energy equivalents method, which involved comparing the calorific value of biomass with the cost of substituted natural gas. With a dry biomass yield of 15-25 t/ha, the gross solid fuel yield provided the replacement of 7-12 thousand m^3 of natural gas per hectare (Gutsalenko & Fabiyanska, 2013). In monetary terms, with the average market price of fuel pellets of 6,500-8,000 UAH/t, this formed a gross income of 97.5-187.5 thousand UAH/ha annually. Even excluding the costs of harvesting, logistics and pelletising (which accounted for up to 40-50% of the cost of the final product), the net economic effect exceeded the indicators of conventional grain production on degraded land, ensuring stable profitability for 15-20 years of operation of the plantation without the need for annual tillage.

An additional economic effect could be associated with the deposition of stable organic carbon in the soil in the form of biochar and the replacement of fossil fuels, potentially allowing participation in voluntary carbon markets. A key feature of the proposed model was its ability to gradually self-finance: revenues from the sale of bioenergy products could compensate for operating costs for growing crops, processing biomass and measures to restore soil fertility. The payback period for initial capital investments was determined by the scale of production, logistics costs, and local market conditions and required a separate feasibility study. Thus, the proposed conceptual model provided for the transformation of the ecological burden caused by military soil damage into a long-term bioenergy project with a combination of restoring ecosystem functions and creating a stable source of income for land users and territorial communities. To illustrate the practical application of individual elements of the proposed conceptual model, a model scenario was formed for a belligerent agricultural landscape (experimental field) with an area of 122 hectares in the Mykolaiv Oblast (Snihurivka UTC). Since the full implementation of the model provided for a multi-year cycle of soil restoration and phased implementation of technological solutions, only key elements of the system were practically tested within the framework of this study, which concerned the initial assessment of the state of the territory, the choice of phytoremediation crops and the economic substantiation of the bioenergy component. Morphometric analysis of satellite images helped to identify 98 explosive craters with a total area of 2.81 hectares and an estimated volume of displaced soil of 73.1 thousand m^3 (Fig. 1). Figure 1 shows the field under study, which is located within agricultural land with a characteristic land use structure for the steppe zone. Visual analysis of the image revealed numerous dark spots of rounded shape, which is a typical sign of explosive craters against the background of a uniform surface of an arable field. The spatial distribution of damage was uneven: areas of increased concentration of craters alternated with relatively undamaged areas, which indicated the chaotic nature of artillery and aviation impacts. To accurately identify the boundaries of craters and measure their morphometric parameters, a detailed analysis of fragments of the image with an increased scale was performed (Fig. 2).

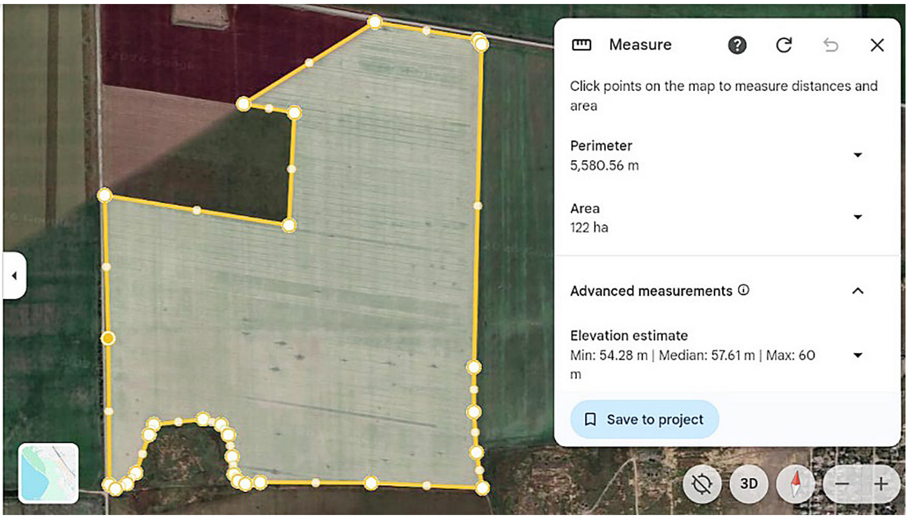

Figure 1. *Satellite image of a 122-hectare experimental field in Snihurivka UTC, Mykolaiv Oblast*

Note: image date – 03.06.2022, plot centre coordinates: 47°05'27"N, 32°46'18"E

Source: Google Earth (2022)

Figure 2. *Fragment of a satellite image of a research field with visually identified explosive craters*

Source: Google Earth (2022)

Analysis of the distribution of craters by diameter showed significant heterogeneity of explosive damage (Fig. 3). Small craters with a diameter of 1.5-3.5 m corresponded mainly to mortar ammunition, while medium-sized craters (3.5-7.0 m) were typical for artillery shells. The vast majority of damage is represented by large-scale craters with a diameter of more than 7 m, which were formed as a result of the use of aviation ammunition or multiple launch rocket systems. The dominance of large craters indicated a high level of mechanical transformation of the soil cover and significant volumes of soil mass movement.

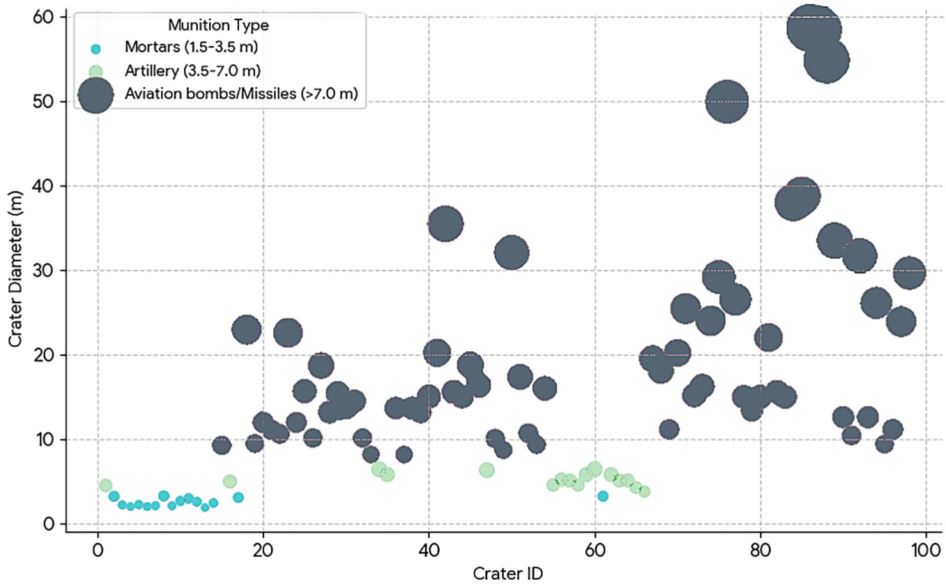

***Figure 3.** Morphometric distribution of explosive craters in the experimental field (n = 98)*

Source: compiled by the authors

Based on the results of morphometric analysis of explosive damage to the experimental field, the key parameters of mechanical transformation of the soil cover necessary for the development of a model scenario for the restoration of agricultural land were determined (Table 5). These parameters included the area of direct crater damage, the volume of displaced soil, and the spatial scale of secondary degradation associated with soil mass spread, surface layer compaction, and the development of geochemical areas of pollution. Generalisation of these indicators determined the initial parameters used for calculating the volume of reclamation works and further modelling the scenario of restoring the belligerent agricultural landscape.

***Table 5.** Initial parameters for forming a model scenario for restoring the belligerent agricultural landscape in Snihurivka UTC*

Indicator	Value
Area of the experimental field, ha	122
Number of explosive craters	98.0
Direct damage percentage, %	2.3
Total area of craters, ha	2.81
Volume of displaced soil, thousand m³	73.1
Estimated number of metal fragments in the degradation zone, thousand units	262.4
Coefficient of spatial expansion of degradation	5.0
Potential reclamation area, ha	14.1

Source: compiled by the authors

The total volume of displaced soil for 98 explosive craters was calculated from their morphometric parameters, considering the empirical ratio H ≈ 0.4D (Hupy & Schaetzl, 2006). Small craters (diameter 1.5-3.5 m, n = 15) had an average area of 5.04 m² and an average depth of 1 m, which corresponded to the volume of one crater of 1.68 m^3 and a total volume of 25.2 m^3. Medium-sized craters (diameter 3.5-7.0 m, n = 16) were characterised by an average area of 21.61 m^2 and a depth of 2.1 m; the volume of one crater was 15.13 m^3, and the total – 242.0 m^3. Large craters (diameter over 7.0 m, n = 67) had an average area of 412.95 m^2 and a depth of 7.9 m, which formed the volume of one crater of 1,087.44 m^3 and the dominant total volume of 72,858.5 m^3. The coefficient of spatial expansion of degradation was assumed to be 5, which corresponded to the upper limit of the theoretically estimated range of contamination propagation beyond the immediate blast zone. This choice is conditioned by the significant dominance of craters formed by large-calibre ammunition (more than 60% of the total number). According to research by G. Certini *et al.* (2013), the area of secondary pollution can exceed the area of direct crater damage by 3-5 times.

The number of metal fragments in Table 5 was estimated based on empirical data on the fragmentation of ammunition according to their typical tactical and technical characteristics, considering GICHD (2014): mortar shells (~1,600 fragments), artillery shells (~2,400) and large-calibre ammunition (~3,000) per hit. According to calculations, the total number of fragments (~262.4 thousand) corresponded to the average density of approximately 18.6 thousand metal fragments per 1 ha within the degradation zone of 14.1 hectares. To assess the practical implementation of restoration measures, an approximate calculation of the cost of reclamation of damaged areas of the agricultural landscape was performed. The cost structure included the main technological operations necessary to restore the productivity of the soil cover. Considering the possible local acidification of the soil environment due to explosive processes and accumulation of detonation products, liming was included in the list of recovery measures as one of the basic methods of chemical land reclamation. The introduction of limestone materials is aimed at stabilising the reaction of the soil solution and reducing the potential mobility of toxic elements in the zone of explosive damage. The approximate cost structure for the implementation of a set of recovery measures is shown in Table 6.

Table 6. *Economic assessment of the implementation of measures to restore the belligerent agricultural landscape in Snihurivka UTC*

Recovery stage	Expenses, thousand UAH
Humanitarian demining	159.6
Laboratory analysis of soil contamination	59.0
Mechanical reclamation	5,960.0
Replacing the top layer of chernozem	47,530.0
Liming	331.4
Total	54,040.0

Source: compiled by the authors

The total cost of implementing a set of restoration measures for the experimental field amounted to UAH 54.04 million, and the largest share of costs (~88%) was formed by the replacement of the upper soil layer, which is conditioned by a significant amount of displaced and degraded soil mass. In terms of unit area, this amounts to an average of 443.0 thousand UAH/ha for the entire experimental field area, which is more than 11 times higher than the average market value of agricultural land in the region. In order to restore the fertility of the belligerent agricultural landscape, a model of phytoremediation was developed for 15 years with crop rotation, in which crops with different functional properties alternated. This structure made it possible to maintain continuous phytoremediation pressure on contaminated soil and at the same time avoid allelopathic fatigue of the soil environment. Crop rotation combines three main functional groups of crops: phytostabilisation (safflower), biological reclamation (sweet clover) and phytoextraction (sorghum). The biomass of all crops was used exclusively for energy purposes through the production of solid biofuels. Considering the proposed structure of phytoremediation crop rotation and the planned bioenergy use of biomass, a generalised estimated calculation of technical and economic parameters of the project is given to illustrate the economic feasibility of implementing the model (Table 7).

Table 7. *Calculated parameters of the phytoremediation project and economic indicators of its implementation*

Indicator	Value
Project duration, years	15
Restoration area, ha	122.0
Average biomass productivity, t/ha per year	7.4
Total biomass production, t/ha	111.0
Annual volume of biomass for processing, t	900
Calorific value of biomass, MJ/kg	16.5-17.2
Briquetting line capacity, kg/h	350-500
Capital investment in equipment, thousand UAH: ➤ briquetting press; ➤ chopper/drying complex; ➤ installation and electrical work	1,558.8 779.4 623.5 155.9
Biomass processing costs, UAH/t	2,703
Wholesale price of fuel briquettes, UAH/t	6,700
Net cash flow from 1 ha, thousand UAH	262.1
Total profit, thousand UAH, including from: ➤ safflower; ➤ sweet clover (productive years); ➤ sorghum	31,974.4 7,739.9 8,790.8 15,443.7
Average annual profit, thousand UAH	2,131.6
Payback period of the briquetting line, years	0.8
Estimated period of compensation for reclamation costs, years	28

Note: calculations are indicative in nature and are given to illustrate the economic feasibility of the proposed recovery model

Source: compiled by the authors

The generalised results of calculations showed that the use of phytoremediation crop rotation with subsequent energy utilisation of biomass allows not only to ensuring ecological detoxification of the soil, but also forming a stable financial flow that partially compensates for the cost of restoring the damaged agricultural landscape. Scientific approaches to assessing the consequences of military influence on the soil cover of Ukraine, presented in the papers by S. Baliuk *et al.* (2024), focused mainly on quantitative fixation of degradation processes, determination of the scale of losses, and normative monetary assessment of damage. Such studies formed the necessary legal and analytical basis for compensation mechanisms and strategic planning, but they were mainly aimed at fixing and classifying damage and to a lesser extent covered issues of long-term restoration of agricultural landscapes and economic reclamation mechanisms. In this regard, it was appropriate to refer to the international experience of restoring territories affected by armed conflicts. International experience in restoring land damaged as a result of armed conflicts has shown that security, engineering and humanitarian approaches have dominated in most cases. As noted by G. Certini *et al.* (2013), military operations led to complex degradation of the soil cover, which included mechanical disruption of the profile, accumulation of metal fragments, and chemical contamination by detonation products. As noted by W. Verheye *et al.* (2007), in Bosnia and Herzegovina after the war, priority was focused on land inventory, mine-contaminated sites, spatial planning, and the gradual return of land to economic use. Similar approaches were implemented in modern humanitarian demining programmes, where the main focus was on the security of territories and restoring the possibility of their use (Osmolovska & Bilyk, 2024). Simultaneously, ecological remediation of soils and mechanisms of economic self-sufficiency in most such programmes were not a central element.

A similar logic could be traced in Lebanon, where post-war reconstruction developed through mine action systems: clearing areas of explosive remnants of war, marking dangerous zones, informing the population about risks, and supporting a return to safe land use. According to UNDP (2011), this approach had a distinct humanitarian and socio-economic impact, particularly for agricultural areas in southern Lebanon, but it also focused primarily on territory security rather than multi-year integrated soil reclamation. The FAO report (2025) confirmed the fact that the current escalation of the conflict in Lebanon has led to systemic degradation of agricultural landscapes due to the mass destruction of perennial plantings and woodlands, which required a transition from operational mine clearance to integrated environmental reproduction strategies. In addition, biological approaches to the restoration of polluted land have been actively developed in the scientific literature. Research by J. Vangronsveld *et al.* (2009) showed that phytoremediation can be an effective tool for stabilising and removing heavy metals from soils, especially in cases of artificial pollution. Simultaneously, the EU and the UK have accumulated considerable experience in using energy crops in phytoremediation systems. As shown by N. Witters *et al.* (2012), based on field studies in Belgium and the Netherlands, combining phytoremediation with energy production or other forms of biomass use may increase the economic viability of such projects. Research by C. Lievens *et al.* (2008), conducted on materials from metal-contaminated areas of Belgium, also confirmed the possibility of using biomass from remediation crops for energy or technical needs. Most of these approaches were implemented as local technological solutions for metal-contaminated or industrially disturbed territories and did not form a comprehensive system of post-war restoration of agricultural landscapes. This led to the need for integrated models that combined security, environmental and economic tools for land reclamation within a single management approach.

The presented analysis showed that most of the international programmes were focused on safe cleaning of territories or local technological rehabilitation. The economic component, as a rule, was not integrated into the system of long-term land restoration. The proposed model was distinguished by a combination of engineering, agrochemical, biotechnological, and energy tools within a single circular land use system, which allowed combining ecological reclamation with the development of an economically viable mechanism for restoring agricultural landscapes. International phytoremediation studies have focused on the effectiveness of individual biotechnological tools. In particular, G.M. Gadd (2004) showed that microorganisms can bind and transform heavy metals through biosorption, biomineralisation, and complexation processes, which contributed to a decrease in their bioavailability in the soil environment. The researcher found that the cell walls of microorganisms rich in functional groups can adsorb metal ions, while the synthesis of exopolysaccharides and siderophores contributed to their binding and conversion to less mobile forms. M. Rajkumar *et al*. (2012) demonstrated that metal-tolerant rhizospheric bacteria, in particular representatives of genera *Bacillus* and *Pseudomonas* (*Bacillus subtilis* and *Pseudomonas fluorescens*), were characterised by high resistance to Pb, Cd, and Zn and could be used as effective phytoremediation agents. Such PGPRs can simultaneously stimulate plant growth and increase the efficiency of soil purification through the synthesis of phytohormones, siderophores and exopolysaccharides, which activated the development of the root system of remediant plants and increased their stress resistance in toxic conditions. Given the suppression of native microflora even at moderate concentrations of heavy metals, inoculation with adapted strains was considered as an appropriate element of restorative measures. A separate area of research was related to the use of sorption materials of organic origin. The combination of phytoremediation followed by thermal processing of biomass was considered as a promising way to safely remove pollutants from the biogeochemical cycle. However, the study mainly considered individual technological or biochemical solutions focused on locally contaminated sites, industrial areas, or waste landfills. They lack a systematic approach to the restoration of large agricultural landscapes that have undergone complex mechanical, chemical and radiological effects as a result of military operations.

Consequently, the conceptual model proposed in the study was distinguished by transformational logic. It combined engineering reclamation, chemical reclamation, biotechnological detoxification, and bioenergy integration into a single 15-year recovery cycle. Mine clearance and physical restoration of the soil profile were considered not as a final stage, but as a starting condition for launching a long-term system of ecological and economic land reintegration. A special difference between the model was the integration of phytoremediation with the bioenergetic component. Unlike classical rehabilitation programmes, which required constant external funding, the proposed approach provided for partial self-financing through the production of biodiesel and solid biofuels. Such a circular "Soil-to-Energy" model ensured the closure of material flows, reducing the environmental burden and creating economic motivation for long-term management of reclaimed land. The results of the practical case demonstrated a structural asymmetry between the scale of primary engineering costs and the potential for further economic returns. The dominance of physical reclamation in the cost structure was confirmed by the conclusions of S. Baliuk *et al*. (2024) on the depth of degradation changes in the soil profile under military influence. This showed that even with efficient bioenergy integration, full reimbursement of engineering costs required a long period of time and a combination of financial mechanisms. Thus, the proposed model in the study did not challenge the previous approaches of other researchers, but expanded them by integrating detoxification, fertility restoration, and economic reintegration technologies into a single long-term system. The transition from the "harm assessment" model to the "ecological and economic transformation" model was a key conceptual contribution of the study.

Conclusions

Thus, the conceptual model of post-war restoration of agricultural land provided a step-by-step process of reclamation, which integrated engineering, chemical, biotechnological, and economic approaches for the restoration of territories after military operations. The use of phytoremediation and bioenergy crops has allowed integrating environmental and economic recovery goals, contributing to sustainable development and reducing the payback period of projects. The study of the de-occupied agricultural landscape in the Snihurivka UTC of the Mykolaiv Oblast revealed a significant level of physical degradation of the soil cover caused by military operations. 98 explosive craters were identified in the 122-hectare research field. The total volume of displaced soil was more than 73.1 thousand m^3, and craters with a diameter of more than 7.0 m, which accounted for 68% of the total number, formed more than 99% of the volume losses. Considering secondary fragmentation and the spread of metal contamination, the zone of functional degradation of the soil cover was estimated at 14.1 hectares, which was approximately five times the area of direct morphological damage. Economic calculations showed that the full range of technical reclamation and agrochemical reclamation required aproximately UAH 54.0 million, which corresponded to the average cost of 443.0 thousand UAH/ha for the entire area of the experimental field. These costs were more than 11 times higher than the average market value of agricultural land in the region, which created a high risk of long-term withdrawal of such territories from agricultural production in the absence of alternative approaches to recovery.

To overcome this imbalance, a conceptual model of agrobiological recovery was proposed, implemented through a 15-year phytoremediation crop rotation using sorghum (*Sorghum bicolor*), safflower (*Carthamus tinctorius*) and sweet clover (*Melilotus* spp.). The combination of phytoextraction of heavy metals, rhizospheric bioaugmentation of microorganisms capable of degradation of organic pollutants, and structural stabilisation of the soil helped to gradually restore the functional suitability of agricultural landscapes in conditions of limited resources. The use of the resulting biomass for the production of solid biofuels has provided potential economic self-sufficiency of phytoremediation measures. The proposed model has become important for planning the restoration of belligerent agricultural landscapes in the steppe regions of Ukraine. The results showed that the integration of biological methods of reclamation with bioenergy use of phytomass can act as an economically justified alternative to traditional high-cost technologies of soil restoration in post-war conditions. The prospect of further research is field verification of the proposed conceptual model on de-occupied agricultural land in various natural and climatic zones of Ukraine.

Acknowledgements

None.

Funding

None.

Conflict of Interest

None.

References

[1] Bonchkovskyi, O., Ostapenko, P., Bonchkovskyi, A., & Shvaiko, V. (2025). War-induced soil disturbances in north-eastern Ukraine (Kharkiv region): Physical disturbances, soil contamination and land use change. *Science of the Total Environment*, 964, article number 178594. doi: 10.1016/j.scitotenv.2025.178594.

[2] Bridgwater, A.V. (2012). Review of fast pyrolysis of biomass and product upgrading. *Biomass and Bioenergy*, 38, 68-94. doi: 10.1016/j.biombioe.2011.01.048.

[3] Broomandi, P., Guney, M., Kim, J.R., & Karaca, F. (2020). Soil contamination in areas impacted by military activities: A critical review. *Sustainability*, 12(21), article number 9002. doi: 10.3390/su12219002.

[4] Caballero-Mejía, B., Moliner, A., Escolástico, C., Hontoria, C., Mariscal-Sancho, I., & Pérez-Esteban, J. (2025). Use of magnetite nanoparticles and magnetic separation for the removal of metal(loid)s from contaminated mine soils. *Journal of Hazardous Materials*, 486, article number 137081. doi: 10.1016/j.jhazmat.2024.137081.

[5] Cao, X., Ma, L.Q., Chen, M., Hardison, D.W., & Harris, W.G. (2003). Lead transformation and distribution in the soils of shooting ranges in Florida, USA. *Science of the Total Environment*, 307(1-3), 179-189. doi: 10.1016/S0048-9697(02)00543-0.

[6] Caviedes-Voullième, D., Ahmadinia, E., & Hinz, C. (2021). Interactions of microtopography, slope and infiltration cause complex rainfall-runoff behavior at the hillslope scale for single rainfall events. *Water Resources Research*, 57(7), article number e2020WR028127. doi: 10.1029/2020WR028127.

[7] Certini, G., Scalenghe, R., & Woods, W.I. (2013). The impact of warfare on the soil environment. *Earth-Science Reviews*, 127, 1-15. doi: 10.1016/j.earscirev.2013.08.009.

[8] Chaika, T., & Korotkova, I. (2023). Directions and reproduction soil fertility technologies in the post-war period in Ukraine. *Agrobiology*, 1, 142-156. doi: 10.33245/2310-9270-2023-179-1-142-156.

[9] Chen, B., Liu, B., Yang, L., Zaland, S., & Ye, H. (2024). Solidification of heavy metal in municipal solid waste incineration fly ash and performance evolution of alkali-activated foam concrete. *Process Safety and Environmental Protection*, 190, 850-862. doi: 10.1016/j.psep.2024.07.065.

[10] Chow, T.L., Rees, H.W., Monteith, J.O., Toner, P., & Lavoie, J. (2007). Effects of coarse fragment content on soil physical properties, soil erosion and potato production. *Canadian Journal of Soil Science*, 87(5), 565-577. doi: 10.4141/CJSS07006.

[11] Didenko, N. (2024). Soil damage and recovery in Ukraine: Lessons from global post-war experiences. *Land Reclamation and Water Management*, 2, 79-86. doi: 10.31073/mivg202402-391.

[12] Drebot, O., & Korol, O. (2025). Transformation of landscapes in conditions of military conflicts. *Agroecological Journal*, 3, 6-12. doi: 10.33730/2077-4893.3.2025.340773.

[13] EN 14214:2012+A2:2019. (2019). *Liquid petroleum products – fatty acid methyl esters (FAME) for use in diesel engines and heating applications – requirements and test methods*. Retrieved from https://standards.iteh.ai/catalog/standards/cen/0a2c5899-c226-479c-b277-5322cc71395d/en-14214-2012a2-2019.

[14] EOD publications – overview. (n.d.). Retrieved from https://surl.li/uypmaf.

[15] FAO. (2025). *Lebanon: Agricultural damage and loss assessment on the impact of conflict. DIEM-impact report, October 2023-November 2024*. Rome: FAO. doi: 10.4060/cd5013en.

[16] Flajšman, M., Košmelj, K., Grčman, H., Kocjan Ačko, D., & Zupan, M. (2023). Industrial hemp (*Cannabis sativa* L.) – a valuable alternative crop for growing in agricultural soils contaminated with heavy metals. *Environmental Science and Pollution Research*, 30, 115414-115429. doi: 10.1007/s11356-023-30474-z.

[17] Gadd, G.M. (2004). Microbial influence on metal mobility and application for bioremediation. *Geoderma*, 122(2-4), 109-119. doi: 10.1016/j.geoderma.2004.01.002.

[18] Geissdoerfer, M., Savaget, P., Bocken, N.M.P., & Hultink, E.J. (2017). The circular economy – a new sustainability paradigm? *Journal of Cleaner Production*, 143, 757-768. doi: 10.1016/j.jclepro.2016.12.048.

[19] GICHD. (2014). *A guide to mine action* (5th ed.). Geneva: Geneva International Centre for Humanitarian Demining.

[20] Google Earth. (2022). Retrieved from https://surl.li/cuwdoc.

[21] Gulich, M., Kharchenko, O., Yemchenko, N., Olshevska, O., & Lyubarska, L. (2024). War in Ukraine: Agricultural soil degradation and pollution and its consequences. *Hygiene of Populated Places*, 74, 49-56. doi: 10.32402/hygiene2024.74.049.

[22] Gutsalenko, L., & Fabiyanska, V. (2013). Condition and main factors of development production of biofuels in Ukraine and the world. *Scientific Papers of Institute of Bioenergy Crops and Sugar Beet*, 19, 168-174.

[23] Hupy, J.P., & Schaetzl, R.J. (2006). Introducing "bombturbation", a singular type of soil disturbance and mixing. *Soil Science*, 171(11), 823-836. doi: 10.1097/01.ss.0000228053.08087.19.

[24] IMAS 01.10. (2003). *Guide for the application and development of International Mine Action Standards (IMAS)* (2nd ed.). New York: United Nations Mine Action Service (UNMAS).

[25] Knothe, G. (2010). Biodiesel and renewable diesel: A comparison. *Progress in Energy and Combustion Science*, 36(3), 364-373. doi: 10.1016/j.pecs.2009.11.004.

[26] Law of Ukraine No. 2642-VIII "On Mine Action in Ukraine". (2018, December). Retrieved from https://zakon.rada.gov.ua/laws/show/2642-19/ed20201210?lang=en#Text.

[27] Leewis, M.-C., Kasanke, C., Uhlik, O., & Leigh, M.B. (2024). Long-term legacy of phytoremediation on plant succession and soil microbial communities in petroleum-contaminated sub-Arctic soils. *SOIL*, 10, 551-566. doi: 10.5194/soil-10-551-2024.

[28] Lehmann, J., & Joseph, S. (Eds.). (2015). *Biochar for environmental management. Science, technology and implementation* (2nd ed.). New York: Routledge.

[29] Lievens, C., Yperman, J., Vangronsveld, J., & Carleer, R. (2008). Study of the potential valorisation of heavy metal contaminated biomass via phytoremediation by fast pyrolysis: Part I. Influence of temperature, biomass species and solid heat carrier on the behaviour of heavy metals. *Fuel*, 87(10-11), 1894-1905. doi: 10.1016/j.fuel.2007.10.021.

[30] Martynova, N., & Kolombar, T. (2025). Phytoremediation technologies promising for the restoration of agricultural lands damaged by military actions. *Regulatory Mechanisms in Biosystems*, 16(3), article number e25155. doi: 10.15421/0225155.

[31] Melnykovych, M., *et al.* (2026). Pathways for Ukraine's post-war nature recovery: Focus on forest socio-ecological systems. *Ambio*, 55, 817-843. doi: 10.1007/s13280-025-02263-0.

[32] Mesel-Veseliak, V. (2015). Production of alternative types of energy resources as a factor of increasing efficiency of agricultural enterprises. *Ekonomika APK*, 22(2), 18-27.

[33] Mudrak, O., Lavrov, V., Kharchenko, S., & Mudrak, H. (2025). Environmental consequences of military actions for land resources of the Snihurivka community of the Mykolaiv region. *Balanced Nature Using*, 3, 67-77. doi: 10.33730/2310-4678.3.2025.342529.

[34] Naumchuk, V. (2024). Strategies for land restoration and reclamation after armed conflicts. *Actual Problems of Economics*, 7, 239-248. doi: 10.32752/1993-6788-2024-1-277-239-248.

[35] Osmolovska, Iu., & Bilyk, N. (2024). *Cleaning the Augean stables: Humanitarian demining in Ukraine*. Prague: GLOBSEC.

[36] Qiu, Z., Guo, H., Hu, J., Jiang, H., & Luo, C. (2023). Joint fusion and detection via deep learning in UAV-borne multispectral sensing of scatterable landmine. *Sensors*, 23(12), article number 5693. doi: 10.3390/s23125693.

[37] Rajkumar, M., Sandhya, S., Prasad, M.N.V., & Freitas, H. (2012). Perspectives of plant-associated microbes in heavy metal phytoremediation. *Biotechnology Advances*, 30(6), 1562-1574. doi: 10.1016/j.biotechadv.2012.04.011.

[38] Rawls, W.J., Pachepsky, Y.A., Ritchie, J.C., Sobecki, T.M., & Bloodworth, H. (2003). Effect of soil organic carbon on soil water retention. *Geoderma*, 116(1-2), 61-76. doi: 10.1016/S0016-7061(03)00094-6.

[39] Reczek, L., Michel, M.M., Trach, Y., Siwiec, T., & Tytkowska-Owerko, M. (2020). The kinetics of manganese sorption on Ukrainian tuff and basalt-order and diffusion models analysis. *Minerals*, 10(12), article number 1065. doi: 10.3390/min10121065.

[40] Samokhvalova, V. (2024). Restoration and use of chemically contaminated soils of land plots under military-technogenic influences: Conceptual provisions and new methods of degradation control. In S. Baliuk, A. Kucher & M. Romashchenko (Eds.), *Soil cover of Ukraine in the conditions of hostilities: State, challenges, activities for soil restoration* (pp. 189-238). Kyiv: Agrarna nauka.

[41] Solokha, M., Demyanyuk, O., Symochko, L., Mazur, S., Vynokurova, N., Sementsova, K., & Mariychuk, R. (2024). Soil degradation and contamination due to armed conflict in Ukraine. *Land*, 13(10), article number 1614. doi: 10.3390/land13101614.

[42] Soudek, P., Petrová, Š., Vaňková, R., Song, J., & Vaněk, T. (2014). Accumulation of heavy metals using *Sorghum* sp. *Chemosphere*, 104, 15-24. doi: 10.1016/j.chemosphere.2013.09.079.

[43] Steliga, T., & Kluk, D. (2021). Assessment of the suitability of *Melilotus officinalis* for phytoremediation of soil contaminated with petroleum hydrocarbons (TPH and PAH), Zn, Pb and Cd based on toxicological tests. *Toxics*, 9(7), article number 148. doi: 10.3390/toxics9070148.

[44] UNDP. (2011). *Mine action in Lebanon: A review of the Lebanon National Mine Action Programme and UNDP support to mine action in Lebanon, final report*. New York: United Nations Development Programme (UNDP).

[45] UNMAS. (n.d.). *UNMAS annual report 2024*. New York: United Nations Mine Action Service (UNMAS).

[46] US Army Corps of Engineers. (2015). *Technical Guidance for Military Munitions Response Actions No. 200-1-15*. Retrieved from https://www.publications.usace.army.mil/Portals/76/Publications/EngineerManuals/EM_200-1-15.pdf.

[47] Vamerali, T., Bandiera, M., & Mosca, G. (2010). Field crops for phytoremediation of metal-contaminated land. A review. *Environmental Chemistry Letters*, 8, 1-17. doi: 10.1007/s10311-009-0268-0.

[48] Vangronsveld, J., *et al.* (2009). Phytoremediation of contaminated soils and groundwater: Lessons from the field. *Environmental Science and Pollution Research*, 16, 765-794. doi: 10.1007/s11356-009-0213-6.

[49] Verheye, W., Boban, T., & Sicignano, A. (2007). *Inventory of post-war situation of land resources in Bosnia and Herzegovina (GCP/BIH/002/ITA). Final tripartite evaluation mission report*. Rome: FAO.

[50] Vessey, J.K. (2003). Plant growth promoting rhizobacteria as biofertilizers. *Plant and Soil*, 255, 571-586. doi: 10.1023/A:1026037216893.

[51] Witters, N., Mendelsohn, R., Van Passel, S., Van Slycken, S., Weyens, N., Schreurs, E., Meers, E., Tack, F., Vanheusden, B., & Vangronsveld, J. (2012). Phytoremediation, a sustainable remediation technology? II: Economic assessment of CO_2 abatement through the use of phytoremediation crops for renewable energy production. *Biomass and Bioenergy*, 39, 470-477. doi: 10.1016/j.biombioe.2011.11.017.

[52] Young, S.D. (2012). Chemistry of heavy metals and metalloids in soils. In B.J. Alloway (Ed.), *Heavy metals in soils* (Vol. 22, pp. 51-95). Dordrecht: Springer. doi: 10.1007/978-94-007-4470-7_3.

Концептуальна модель повоєнного відновлення сільськогосподарських земель з інтеграцією біоенергетичних технологій

Тетяна Чайка
Кандидат економічних наук
Відокремлений структурний підрозділ
«Аграрно-економічний фаховий коледж Полтавського державного аграрного університету»
36003, вул. Григорія Сковороди, 18, м. Полтава, Україна
https://orcid.org/0000-0002-5980-7517

Микола Шевніков
Доктор сільськогосподарських наук, професор
Полтавський державний аграрний університет
36003, вул. Григорія Сковороди, 1/3, м. Полтава, Україна
https://orcid.org/0000-0003-0810-523X

Арсеній Стеценко
Студент
Відокремлений структурний підрозділ
«Аграрно-економічний фаховий коледж Полтавського державного аграрного університету»
36003, вул. Григорія Сковороди, 18, м. Полтава, Україна
https://orcid.org/0009-0003-6711-0247

Віктор Ляшенко
Кандидат сільськогосподарських наук, доцент
Полтавський державний аграрний університет
36003, вул. Григорія Сковороди, 1/3, м. Полтава, Україна
https://orcid.org/0000-0003-0177-6209

Анотація. Повномасштабні воєнні дії росії проти України спричинили масштабну деградацію сільськогосподарських земель, що супроводжувалося механічним руйнуванням ґрунтового покриву, хімічним забрудненням і втратою продуктивного потенціалу. Відсутність інтегрованої системи повоєнного відновлення обумовило потребу у формуванні комплексної моделі рекультивації, що поєднувала екологічні й економічні інструменти в межах єдиного управлінського підходу. Метою роботи стала розробка концептуальної моделі повоєнного відновлення сільськогосподарських земель на засадах інтеграції інженерних, хімічних, біотехнологічних та економічних підходів у межах циркулярної системи землекористування. Було використано аналітичний, порівняльний і системно-структурний методи, а також концептуальне моделювання. У результаті дослідження було визначено масштаби фізичної деградації ґрунтового покриву на деокупованих сільськогосподарських угіддях і запропоновано концептуальну модель їх агробіологічного відновлення з використанням фіторемедіаційних культур. Сформовано багаторівневу модель відновлення, що включала етапи гуманітарного розмінування, технічної підготовки території, оцінки забруднення, механічної рекультивації, хімічної детоксикації, біотехнологічної регенерації та довгострокової фіторемедіації з інтеграцією біоенергетичних технологій. Обґрунтовано доцільність 15-річного циклу фіторемедіації в структурі рекультивації з поетапним переходом до економічно життєздатної системи землекористування. Запропоновано циркулярну модель переробки біомаси, що передбачала енергетичну валоризацію фітомаси та повернення стабілізованих продуктів у ґрунт, забезпечуючи часткову або повну самоокупність процесу відновлення. Практичну життєздатність моделі підтверджено на прикладі пошкоджених сільськогосподарських земель у Снігурівській міській територіальні громаді Миколаївської області, де доведено здатність біоенергетичного компоненту генерувати стабільний грошовий потік для часткової компенсації витрат на інженерну рекультивацію. Запропонована модель може бути адаптована до різних типів белігеративних агроландшафтів і створює передумови для формування фінансово стійких механізмів рекультивації. Вона має потенціал для практичного застосування в Україні й інших країнах, що зазнали військових дій, і може стати основою для формування національних політик у сфері відновлення земель і сталого розвитку аграрного сектору

Ключові слова: агроландшафти; біоенергетичні культури; циркулярна економіка; екологічна стабілізація; рекультивація ґрунтів; фіторемедіація; детоксикація земель

Received 22.12.2025 Revised 19.03.2026 Accepted 23.04.2026 Published: 30.04.2026

Vol. 22, No. 2
2026

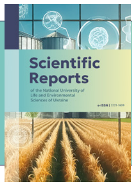

Scientific Reports of the National University of Life and Environmental Sciences of Ukraine

Journal homepage: https://scireports.com.ua/en e-ISSN 2223-1609

UDC 574.5:582.26:556.55 DOI: 10.31548/dopovidi/2.2026.90

Microalgae of lentic water bodies as drivers of ecosystem service provision

Liudmyla Sova*
Postgraduate Student
National University of Kyiv-Mohyla Academy
04655, 2 Hryhorii Skovoroda Str., Kyiv, Ukraine
https://orcid.org/0000-0002-3197-9616

Viktor Karamushka
PhD in Biological Sciences, Associate Professor
National University of Kyiv-Mohyla Academy
04655, 2 Hryhorii Skovoroda Str., Kyiv, Ukraine
https://orcid.org/0000-0002-3327-2243

Abstract. Due to their significant species diversity and sensitivity to environmental changes, microalgae are important indicators of the ecological state of water bodies and, together with other hydrobionts, contribute to the provision of ecosystem services in aquatic systems. Since their contribution to ecosystem service provision in stagnant water bodies remains insufficiently studied and requires further substantiation to assess the ecological value of such systems, this study aimed to examine the relationships between the species composition of microalgae and the formation of relevant ecosystem services in stagnant water bodies, using the example of the Korostyshiv Quarry (Zhytomyr Region, Ukraine). To determine the species composition and distribution of microalgae, standard methods were used (sampling and preservation of water samples, isolation, identification, and quantitative analysis of microalgae using microscopy). The results revealed a relatively balanced phytoplankton community structure with low species diversity: five microalgal species belonging to four different divisions (*Chlorophyta*, *Bacillariophyta*, *Chrysophyta*, and *Dinophyta*). The biomass concentration was relatively low, reaching up to 2 g/L. The species composition of phytoplankton and the results of water chemistry analysis indicate a good ecological state of the water body. Relationships between the functional characteristics of microalgae and ecosystem services were identified. It was found that the species composition of microalgae is a key factor in the formation of ecosystem services, determining primary production, nutrient cycling, and the condition of the aquatic environment. Within the framework of the

Suggested Citation:
Sova, L., & Karamushka, V. (2026). Microalgae of lentic water bodies as drivers of ecosystem service provision. *Scientific Reports of the National University of Life and Environmental Sciences of Ukraine*, 22(2), 90-104. doi: 10.31548/dopovidi/2.2026.90.

**Corresponding author*

CICES classification, it was demonstrated that microalgae in the studied quarry water body contribute to the formation of nearly all types of ecosystem services (3 provisioning, 9 regulating and supporting, and 4 cultural services), albeit with varying intensity. The dominant contribution of microalgae in the quarry ecosystem was associated with regulating and supporting ecosystem services. The results obtained can be used for the development of a national framework for assessing ecosystem services in freshwater lentic ecosystems

Keywords: phytoplankton; quarry ecosystems; biotopes; indicator species; biogeochemical cycling

Introduction

In the context of significant anthropogenic pressure and its destructive impact on the environment, there is an increasing need for detailed investigation of the role of microalgae in lentic water bodies as key factors in the formation of ecosystem services and as indicators of the ecological status of aquatic ecosystems. Microalgae, owing to their high species diversity and sensitivity to environmental changes, can serve as effective indicators of water quality and the ecological status of lakes and other water bodies, as evidenced by recent international studies on this topic. For instance, the study by C.M. Dobrescu *et al.* (2023) elucidated the response patterns of algae to chemical changes in aquatic environments (including variations in temperature, pH, and dissolved substances), thereby confirming their role as bioindicators of water quality. Irish researchers E. O'Neill & N. Rowan (2022) focused on the use of microalgae as natural ecological bioindicators for real-time, simplified monitoring of aquaculture wastewater quality, while also examining their potential for assessing the impacts of extreme climate change, including responses to stress factors. The study by E. Delgado-Fernández *et al.* (2025) demonstrated that microalgae, due to their high species diversity and sensitivity to environmental changes, can serve as effective indicators of water quality and the ecological status of lakes and other water bodies. Based on an assessment of microalgal diversity in the Kimsacocha lake system in Azuay (Ecuador), the authors found that phytoplankton plays a crucial role as a primary producer in lakes, providing valuable information on environmental conditions and water quality.

Particular attention was also given to the comprehensive review by S. Jahan & A. Singh (2023), which examined the role of phytoplankton in the environment and human life as primary producers and as the foundation of trophic chains in aquatic ecosystems. In this context, other international studies have confirmed that monitoring phytoplankton dynamics can serve as a valuable bioindicator for assessing aquatic environments. For example, A. Mondal *et al.* (2020) focused on three categories of phytoplankton species – non-toxic, toxic, and those interacting with zooplankton – and the dynamics of their interactions within an open marine system. Furthermore, P. Chandel *et al.* (2024) expanded upon previous research by highlighting the ability of plankton to adapt to specific ranges of chemical, physical, and biological conditions as an important bioindicator for environmental quality assessment.

International studies have demonstrated that freshwater hydrobionts play a key role in the formation of ecosystem services in aquatic ecosystems. In particular, a close relationship has been identified between the species composition and distribution of microalgae in water bodies and the ecosystem services they provide. For example, L. Naselli-Flores & J. Padisák (2023) argued that the services provided by phytoplankton account for nearly half of global primary production and oxygen generation. In addition, phytoplankton significantly accelerates biogeochemical cycles and nutrient cycling not only in aquatic but also in terrestrial ecosystems, makes a substantial contribution to climate regulation (a regulating service), provides food, fuel, bioactive compounds, pharmaceuticals, and genetic resources (provisioning services), and delivers important cultural services.

The study by D. Updhai *et al*. (2025) emphasised that the value of phytoplankton ecosystem services, beyond their contribution to approximately half of global oxygen production through photosynthesis, also lies in their potential for carbon sequestration. This capacity contributes to mitigating climate change through the biological capture and storage of atmospheric carbon dioxide. Furthermore, phytoplankton plays an important role in water purification, as certain species are capable of removing pollutants from aquatic ecosystems through processes of bioaccumulation or biotransformation. The study by S.M. Thomaz (2023) complements existing knowledge on the formation of ecosystem services by microalgae through investigations of macrophytes. Specifically, the study examines macrophytes as providers of 26 types of ecosystem services, among which supporting and regulating services are identified as the most significant.

In Ukraine, hydrobionts of natural water bodies have been studied in considerable depth. In particular, the morphology, physiology, and ecology of microscopic algae and benthic assemblages have long been a focus of researchers at the Institute of Hydrobiology of the National Academy of Sciences of Ukraine. The habitat preferences of algae within the water column of different types of freshwater ecosystems were investigated by V.I. Shcherbak *et al*. (2025). Their analysis of algal habitat preferences demonstrated that the floristic composition and the ratio of life forms of algae vary significantly depending on environmental conditions and are determined by a combination of abiotic and biotic factors. The proportion of planktonic, benthic, and planktonic-benthic forms differs among lotic, lentic, and transitional ecosystems, forming characteristic spectra for each type of water body and reflecting their adaptive capacities. Despite this variability, algae remain informative indicators.

The reviewed literature highlights the growing significance of microalgae as bioindicators of water quality and ecological health in aquatic ecosystems. International research emphasises the crucial role of microalgae in supporting ecosystem services, including primary production, nutrient cycling, and climate regulation, while also noting their sensitivity to environmental changes. The studies underline the potential of microalgae to provide valuable insights into the ecological state of water bodies, offering a foundation for future environmental monitoring and management efforts. At the same time, the scope and magnitude of ecosystem services associated with microalgae in non-flowing artificial water bodies, such as quarry lakes, require further investigation to enable their assessment and sustainable management. Therefore, this article aimed to examine the species composition and distribution of microalgae in non-flowing water bodies, as well as the formation of their ecosystem services, using the Korostyshiv Quarry as a case study.

Materials and Methods

The object of the study was the Korostyshiv Quarry, which belongs to non-flowing freshwater bodies of a lacustrine type formed after the cessation of quarry exploitation. It represents a complex, multifunctional ecosystem that provides a wide range of ecosystem services essential for maintaining ecological balance and environmental stability. This quarry was chosen because successional processes in such ecosystems occur on a mineral substrate and are essentially primary in nature: water rising from underground horizons creates an environment in which hydrobionts gradually emerge and develop over time. The Korostyshiv Quarry is located on the eastern outskirts of the town of Korostyshiv, Zhytomyr Region (Fig. 1). Its coordinates are 50º19'24.72"N, 29º04'44.53"E. Granite was extracted from the quarry for many years; however, in the early 1990s, it was decommissioned, after which it became naturally filled with water. The surface area of the lake is approximately 48,803 m², with a length of 500 m, a width of 150 m, and a depth of up to 40 m (Ulyhanets & Shynkarenko, 2023). A map showing the location and water sampling sites of the Korostyshiv Quarry is presented in Figure 2. The sampling site was chosen randomly, taking into account accessibility of the water – the selected location lacked rocky cliffs and dense aquatic vegetation (in particular, reeds and cattails).

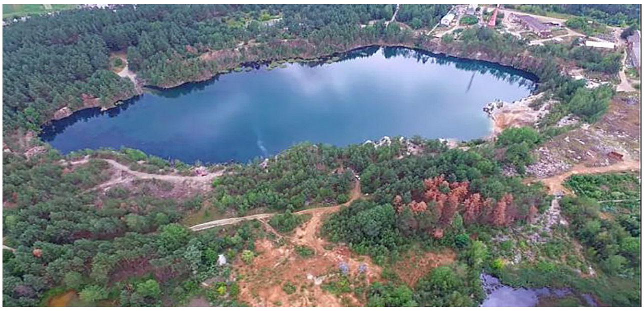

Figure 1. *General view of the Korostyshiv Quarry*

Source: Google Maps (n.d.)

Figure 2. *Map showing the location and water sampling sites in the Korostyshiv Quarry*

Source: Google Maps (n.d.)

Water samples for phytoplankton assessment were collected from the surface layer of the water (15-20 cm) using a Ruttner bathometer. The surface water layer is more strongly heated by sunlight, more oxygenated, and richer in organic substances entering the water body from the air, which is important for microalgal development. Samples of 0.5 dm³ were fixed with a 40% formaldehyde solution at a ratio of 1:100 and concentrated by sedimentation for at least 10 days. Sampling was conducted in September 2025, when the summer heat had subsided, and the autumn rains had not yet begun, which could otherwise have significantly affected the state of phytoplankton and its distribution within the water body. Algal abundance was determined by direct counting in a Najott chamber (0.02 cm³), and biomass was measured using the stereometric method. Algal abundance is reported in thousands of cells per dm³ and biomass in mg/dm³. Species contributing ⩾10% of the total phytoplankton biomass in a sample were classified as dominants. The species composition of algae was determined using standard methods

(Shcherbak, 2006; Arsan *et al.,* 2006). For this purpose, MBB-1A and Axio Imager microscopes (Carl Zeiss, Germany) were used at magnifications of x20, x40, and x100. To determine species, identification keys for freshwater algae were used (Topachevsky *et al.*, 1984; Vasser *et al.,* 1989).

The Pantle-Buck saprobic index (S), in the Sládeček modification, was calculated according to R.A.E. Knoben *et al.* (2006). This index helps to assess the ecological status of the water body by determining the presence of specific algal species, which serve as indicators of water quality. Chemical analyses of water samples were performed at the certified laboratory AKVO (n.d.). Water samples were analysed for physicochemical, organoleptic, and chemical indicators that characterise the quality of the water body and indicate the conditions under which aquatic organisms exhibit an appropriate level of vital activity, thereby supporting the formation of ecosystem services. The ecosystem services provided by microalgae were assessed according to CICES version 5.2 (n.d.). The study complied with the ethical standards set out in the Convention on Biological Diversity (1992). The collected data and applied methods allow for a comprehensive assessment of the ecological status of the water body and the determination of the role of microalgae in ecosystem service formation.

Results and Discussion

Based on its main characteristics, the Korostyshiv Quarry corresponds to the parameters of oligotrophic water bodies with macrophyte vegetation (B1.1.1), according to the classification presented in the National Habitat Catalogue (Kuzemko *et al.*, 2018). According to the habitat classification by EUNIS (n.d.), the quarry can be assigned to class C1.1 (permanent oligotrophic lakes, ponds, and water bodies). The water body was formed by the flooding of the decommissioned quarry with groundwater, followed by the development of successional processes that led to the emergence of typical aquatic vegetation. In the littoral zone, slight overgrowth is observed, with dominant species such as common reed (*Phragmites australis*), riparian sedge (*Carex riparia*), and narrow-leaved cattail (*Typha angustifolia*), among others. It is evident that meltwater and rainwater also contributed to the replenishment of the water body, introducing substances from the atmosphere and the surrounding land surface. These waters also carried microorganisms, algae, and protists that inhabited the mineral surfaces and soils of the catchment area into the quarry. At the same time, the results of chemical analyses indicate high water quality in the quarry. According to all tested parameters, the water quality of the quarry meets high standards (Table 1).

Table 1. *Results of chemical analysis of water samples from the Korostyshiv Quarry*

	Parameter	EU Standard limit	Ukrainian Sanitary Standard (DSanPiN) limit	Result
1	Colour, points	≤1	≤2	2
2	Odour, points	≤1	≤2	2
3	Temperature, °C	25	25	25
4	Total mineral content, mg/dm³	≤1,000	≤1,000	238
5	pH (hydrogen index)	6.5-8.5	6.5-8.5	7.2
6	Total hardness, mg-eq/dm³	≤1.5	≤7	4.48
7	Carbonate hardness, mg-eq/dm³	≤1.5	Not regulated	2.7
8	Calcium (Ca), mg/dm³	≤100	≤130	70.5
9	Total iron, mg/dm³	≤0.2	≤0.2	0.01
10	Manganese, mg/dm³	≤0.05	≤0.05	0.01
11	Total alkalinity, mmol/dm³	≤6.5	≤6.5	0.74
12	Permanganate oxidisability, mg O_2/dm³	≤5	≤5	0.9
13	Polyphosphates (PO_4)	≤1	≤3.5	0.1
14	Residual chlorine, mg/dm³	≤0.05	≤0.05	0.01

Table 1. *Continued*

	Parameter	EU Standard limit	Ukrainian Sanitary Standard (DSanPiN) limit	Result
15	Nitrates (NO_3), mg/dm³	≤10	≤50	0.01
16	Nitrites (NO_2), mg/dm³	≤0.1	≤0.1	0.01
17	Ammonium salts, mg/dm³	≤0.2	≤0.5	0.1
18	Ammonia, mg/dm³	≤0.2	≤0.5	0.01
19	Oxidation-reduction potential (ORP), mV	Not regulated	Not regulated	+183
20	Magnesium, mg/dm³	≤10	≤80	10.5

Source: developed by the authors based on data AKVO (n.d.)

The data presented in Table 1 indicate that the values of almost all physicochemical water parameters are significantly lower than the limits established by EU standards and Ukrainian sanitary regulations. An exceedance was recorded only for carbonate hardness. Overall, the analysis results confirm the high quality of the water and, by implication, the absence of significant pollution sources in this water body. Accordingly, the high quality of water indicators identified through chemical analysis indicate the effective provision of regulating ecosystem services, particularly the biological purification of water by algae. Adequate water quality is a key prerequisite for the functioning of hydrobionts, ensuring supporting ecosystem services and the conservation of biodiversity. In addition, the qualitative characteristics of water determine the potential for recreational use of the water body, thereby contributing to the formation of cultural ecosystem services. The results of the analysis of the water samples used to determine the species composition of microalgae from the Korostyshiv Quarry are presented in Tables 2 and 3.

Table 2. *Species of microalgae identified in the water of the Korostyshiv Quarry*

Algal species	Number of cells in sample	Abundance, thousand cells/L	Biomass, mg/L
Dinobryon divergens	62	186	0.670
Ankistrodemus fusiformis	36	108	0.011
Peridiniopsis quadridens	4	12	0.227
Crucigenia quadrata	32	96	0.009
Nitzschia vermicularis	2	6	0.006

Source: developed by the authors

Table 3. *Quantitative characteristics of microalgal divisions identified in the water of the Korostyshiv Quarry*

Division		Abundance, thousand cells/L	Biomass, mg/L
2	*Chlorophyta* – Green algae	204	0.019
1	*Bacillariophyta* – Diatoms	6	0.006
1	*Chrysophyta* – Golden algae	186	0.670
1	*Dinophyta* – Dinoflagellates	12	0.227
$\sum = 5$		408	0.922

Source: developed by the authors

The phytoplankton results indicate low species diversity, with only five algal species belonging to four different divisions identified in the sample. Such a community structure may suggest good water quality and that the ecosystem is at an early stage of development. The highest abundance among the species was observed for *Dinobryon divergens* (186 × 10^3 cells/L), which belongs to the division *Chrysophyta*, indicating the dominant role of golden algae in this biotope. The significant development of *Dinobryon* is typical of oligo- and mesotrophic water bodies with relatively clean water and normal transparency. The second most abundant group consisted of green algae (*Chlorophyta*) – 204 thousand cells/L, indicating good light conditions and a moderate trophic status of the water body. Representatives of this division (*Ankistrodesmus fusiformis*, *Crucigenia quadrata*) have low biomass but consistently form part of the community, providing its structural foundation. Diatoms in the sample are represented only by *Nitzschia vermicularis* at low abundance, yet their presence confirms a normal oxygen regime and a typical level of mineralisation. *Dinophyta* algae in this sample are present in very low abundance (12 thousand cells/L). The species *Peridiniopsis quadridens* does not dominate in this sample, indicating the absence of local 'blooms' or excessive organic enrichment.

The total abundance of phytoplankton in the sample is 408 thousand cells/L, and the biomass is 0.922 mg/L, which is typical for water bodies with a moderate trophic level. The predominance of *Dinobryon* in the biomass (0.670 mg/L) indicates the dominant role of mixotrophic nutrition in the community structure, as golden algae are capable of combining photosynthesis with heterotrophic mechanisms. The value of the saprobic index (S = 1.85) indicates β-mesosaprobic conditions, i.e., a moderate level of organic pollution, which overall reflects the good ecological status of the water in the Korostyshiv Quarry.

The biomass concentration is relatively low – up to 2 g/L. Based on approximate calculations, in the 1-meter-thick surface layer of the quarry water, algal biomass reaches 90 kg. It is evident that in the deeper horizons of the water body, this value would be significantly lower, because the surface layers have more favourable conditions for the development of microalgae (in particular, greater availability of organic matter, better illumination, and higher temperature). Such algal biomass plays a role in oxygen production, the purification of the aquatic ecosystem from pollutants, and the cycling of elements.

Overall, the analysed water sample demonstrated a heterogeneous phytoplankton community without clear dominance of toxic or eutrophic groups. The phytoplankton structure also indicated a stable, moderately trophic, and ecologically favourable condition of the Korostyshiv Quarry water body, with a predominance of golden and green algae. Determining the composition of microalgae as producers of ecosystem services in the quarry water environment enabled the identification and systematisation of potential relationships between the functional traits of microalgae and their associated ecosystem services (Table 4).

Table 4. *Linkages between the functional characteristics of microalgae in water bodies and their ecosystem services*

No.	Functional characteristics of microalgae	Influence of functional characteristics on the formation of ecosystem services
1	Provision of primary production of organic matter supporting biocenoses	Microalgae (phytoplankton, diatoms, etc.) represent the first trophic level in aquatic ecosystems and provide primary production of organic matter that supports biocenoses (e.g. fish and zooplankton). They play a key role in maintaining trophic networks and biodiversity, forming the basis of numerous provisioning ecosystem services
2	Oxygen production and regulation of gas composition	The photosynthetic activity of microalgae leads to oxygen production and the regulation of dissolved gases in water. This is an important supporting ecosystem function and part of regulating services associated with maintaining the physicochemical environment
3	Nutrient cycling	Microalgae participate in the cycling of nitrogen, phosphorus, and other biogenic elements in water bodies. They accumulate these substances and, after cell death, return them to the aquatic environment, thereby influencing nutrient cycling processes

***Table 4.** Continued*

No.	Functional characteristics of microalgae	Influence of functional characteristics on the formation of ecosystem services
4	Self-purification and filtration	Certain algal species (e.g. *Chlorella*) contribute to the removal of excess nutrients (nitrogen, phosphorus) from water bodies, thus supporting waste neutralisation and water purification – an important ecosystem service
5	Indicators of environmental condition	Due to their high sensitivity to environmental changes, the species composition of microalgae is widely used as a bioindicator of water quality. This enables the assessment of the ecological status of water bodies and changes in ecosystem services over time
6	Regulation of water conditions	Various characteristics of water bodies (trophic status, nutrient availability, pH) determine the composition and dominance of certain microalgal species. Changes in algal communities reflect shifts in ecological processes that ensure the stability of the aquatic environment
7	Negative effects under imbalance	Certain species (e.g., *Microcystis aeruginosa*, a cyanobacterium) can form toxic blooms that reduce water quality and negatively affect biodiversity and human health. This illustrates how shifts in microalgal species composition may disrupt ecosystem services

Source: developed by the authors based on E. O'Neill & N. Rowan (2022), V. B-Béres *et al*. (2023), C.M. Dobrescu *et al*. (2023), E. Delgado-Fernández *et al*. (2025)

Thus, the species diversity of microalgae directly determines the scope and quality of ecosystem service provision in aquatic ecosystems. In particular, diatoms and green algae are actively involved in biological water purification processes, absorbing nutrients and contributing to the delivery of regulating services. Representatives of green and diatom algae also form the basis of primary production and serve as a food source for zooplankton, ensuring supporting ecosystem services through trophic interactions. At the same time, excessive development of cyanobacteria may deteriorate water quality and limit regulating and cultural services due to toxicity and algal blooms. Therefore, a balanced structure of microalgal communities is a key factor in maintaining ecosystem functional stability and their capacity to deliver a wide range of ecosystem services.

The identified relationships between the functional traits of microalgae in water bodies and ecosystem services indicate the following:

- the species composition of microalgae is an important factor in the formation of ecosystem services, directly influencing primary production in water bodies, the cycling of biogenic elements, and their incorporation into trophic chains;
- the species composition of microalgae reflects the ecological status of water, as well as regulating and supporting processes, including self-purification;
- changes in the species composition of microalgae can either improve (through selfregulation and purification) or disrupt (through toxic blooms) water quality and, consequently, the quality of ecosystem services.

Considering the structure of ecosystem services provided by freshwater and marine algae according to the Millennium Ecosystem Assessment (MEA) classification, and taking into account the findings of V. B-Béres *et al*. (2023), the relationships between microalgae, ecosystem services, and their impacts on humans and biodiversity are presented in Figure 3. It is shown that the species composition of microalgae determines supporting, regulating, provisioning, and cultural services, including photosynthesis, water purification, and the formation of food resources. Microalgae also serve as indicators of water quality and play a key role in ecosystem self-purification processes. At the same time, changes in their composition can either improve environmental conditions or cause negative phenomena, such as toxic algal blooms.

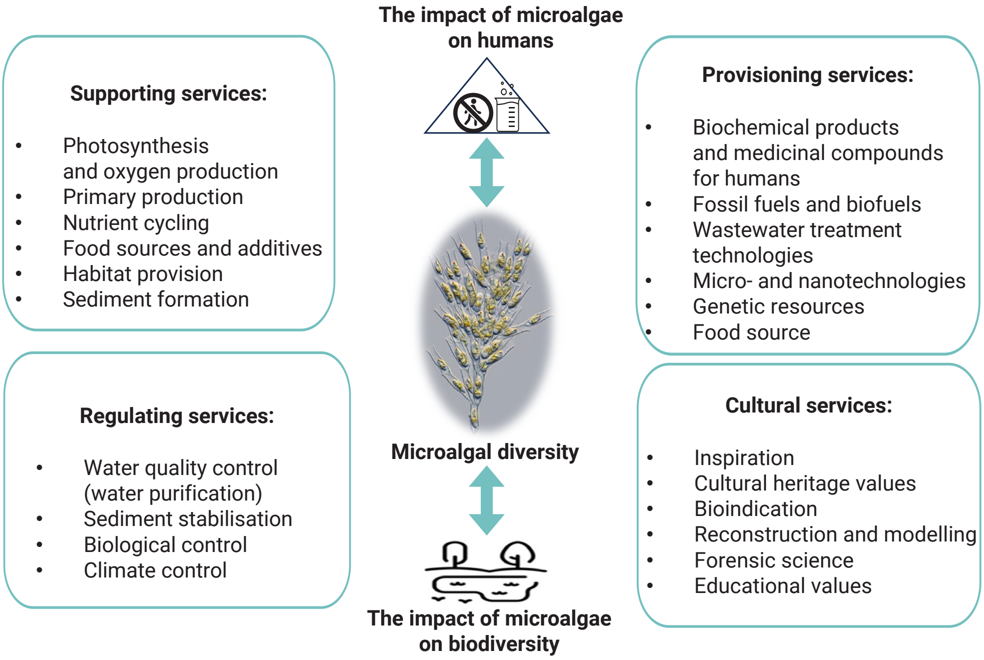

Figure 3. *The impact of microalgae on humans and biodiversity as mediated through ecosystem services*

Source: interpreted by the authors based on V. B-Béres *et al.* (2023)

Given that the species diversity of microalgae is a factor in the formation of ecosystem services, their potential was analysed in the context of ecosystem service provision by lentic freshwater bodies (flooded quarries), which are associated with three service categories according to the CICES classification (CICES Version 5.2, n.d.). The proposed refinements to this classification may be useful in applied studies of microalgal ecosystem services, as they are based on the expansion and detailing of codes following the logic: 'Class' → 'Subclass'. The ecosystem services of microalgae in lentic freshwater bodies, specifically the Korostyshiv Quarry, are presented in Table 5.

Table 5. *Ecosystem services formed by microalgae in lentic freshwater bodies (quarries)*

ES codes	Ecosystem services
1.1.4.1	***Provisioning (biotic)*** Primary production of microalgal biomass as the foundation of trophic chains (formation of the food base for zooplankton, benthos, and fish)
1.1.6.1	Microalgal biomass as a potential raw material for feed, bioactive substances, biofuels, and pharmaceutical products
1.1.6.2	Genetic resources of microalgae (a source of biochemical and biotechnological materials)
2.2.1.1	***Regulating and maintenance services*** Biological filtration, sequestration, and accumulation of nutrients (nitrogen, phosphorus) during photosynthesis
2.2.1.2	Reduction of eutrophication processes through the regulation of nutrient levels in water
2.2.2.1	Maintenance of primary productivity and energy balance of aquatic ecosystems

Table 5. *Continued*

ES Codes	Ecosystem services
2.2.2.3	Formation and maintenance of habitats for aquatic organisms (oxygen provision, creation of micro-niches)
2.2.3.1	Biological control of pathogenic microorganisms and potentially harmful algae
2.2.4.2	Participation in organic matter decomposition and biogeochemical cycles
2.2.5.1	Regulation of the chemical composition of freshwater systems (pH, dissolved oxygen content, nutrient concentrations)
2.2.6.1	Regulation of atmospheric gas composition through photosynthetic oxygen production
2.2.6.2	Biological carbon uptake and sequestration (participation in the carbon cycle)
3.1.1.2	***Cultural services*** Aesthetic and educational value (influence on water transparency and colour; observation of natural processes)
3.1.2.1	Scientific research and monitoring of aquatic ecosystem condition (microalgae as bioindicators of water quality)
3.2.2.2	Heritage (existence) value – conservation of biodiversity and unique microalgal taxa
6.1.1.1	Indirect contribution to recreational services (maintenance of the ecological status of water bodies suitable for recreation)

Source: interpreted by the authors based on CICES Version 5.2 (n.d.)

As shown in the table, the ecosystem services of microalgae in lentic quarry water bodies constitute a factor influencing the formation of virtually all ecosystem services. The magnitude of these services primarily depends on biomass production. This aspect is crucial for provisioning, regulating, and supporting services. The analysis of species composition and biomass of microalgae in the Korostyshiv Quarry aquatic ecosystem (Tables 1 and 2) indicates limited species diversity and relatively low productivity, which may be associated with seasonal factors and the relative youth of the ecosystem. For example, such responses of algae to chemical changes in water bodies, such as variations in temperature, pH, and dissolved substances, confirm their role as bioindicators of water quality (Dobrescu *et al.*, 2023), which, in turn, influences the formation of the majority of ecosystem services. Consequently, the ecosystem services of microalgae in lentic quarry water bodies are predominantly of a regulating and supporting nature, while simultaneously providing an important ecological foundation for the realisation of provisioning and cultural services throughout the aquatic ecosystem.

Newly created quarry reservoirs have their own characteristics that distinguish them from the ecosystems of previously formed water bodies. There are many mechanisms by which aquatic plants and animals can colonise new habitats that were not previously present. Several actual and potential pathways can be identified through which living organisms may populate a newly established aquatic system. Firstly, although there may be a considerable distance between the surface of a quarry and that of the nearest water body, they can be connected through groundwater. In such cases, invertebrates or algae may reach the quarry via aquatic pathways. Storm runoff and meltwater represent another potential mechanism for the migration of organisms from inundated land surfaces and other water bodies into the quarry water body.

Some organisms lay eggs that adhere to plants or even to the feet of birds migrating from other water bodies to quarries (Hirsch *et al.*, 2018). In this way, not only representatives of ichthyofauna but also other organisms, including freshwater jellyfish, can disperse. At the polyp stage, they inhabit aquatic plants. When these plants are transported to other water bodies – via underwater dispersal, by birds or other animals, or by humans – the jellyfish can enter their freeswimming or medusa stage. Humans moving from one water body to another may also inadvertently carry aquatic organisms on their equipment, such as fishing or diving gear. Through such mechanisms, the distribution range of freshwater jellyfish of the genus *Craspedacusta*, originally from China, has extended to freshwater bodies in Europe, North and South America, Africa, and Australia (Lüskow *et al.*, 2024). These water bodies include isolated lakes and quarry water bodies.

The presence of unicellular algae in quarry waters can be explained more simply: algae are widespread in soils, on rock surfaces, and in other moist biogeocoenoses surrounding the quarry water body, and they migrate via water and air currents. Young quarry ecosystems are characterised by clean water, minimal levels of pollutants, and a corresponding microbial community. During the development of these systems, higher aquatic plants appear and spread, and the diversity of hydrobiont species, including fish, increases. Ecosystem services in young quarry ecosystems differ in scale from those of well-established, long-term quarry water bodies, yet they encompass provisioning, regulating, supporting, and cultural services. The manifestation and availability of these services are closely linked to the condition of the aquatic environment and its biotic components. Hydrobionts play a particularly important role in the formation of ecosystem services (Naselli-Flores & Padisák, 2023; Thomaz, 2023).

A comparison of the results of the phytoplankton study conducted in the Korostyshiv Quarry with other similar studies makes it possible to identify both common patterns and certain differences determined by the stage of ecosystem development and local environmental conditions. First and foremost, the results obtained from the phytoplankton investigation in the Korostyshiv Quarry are consistent with general approaches to the formation of hydrobiota in natural water bodies, as outlined in the studies of V.I. Shcherbak (2006) and O.P. Bilous *et al*. (2018). Furthermore, the findings correlate with the general understanding of the functioning of young quarry ecosystems. In this study, a limited species diversity of phytoplankton was identified (five species representing four divisions), which corresponds to the characteristic features of the initial stages of aquatic biocoenosis formation in quarry water bodies, as demonstrated in previous studies by P. Hirsch *et al*. (2018) and F. Lüskow *et al*. (2024).

The study emphasised that the water quality indicators of the Korostyshiv Quarry comply with European standards, while the phytoplankton biomass level is moderate. Accordingly, the results obtained further confirm the relationship between high water quality and the characteristics of the biota, which is consistent with findings reported in other studies. In particular, C.M. Dobrescu *et al*. (2023) examined the response of algae to chemical changes in aquatic environments (including variations in temperature, pH, and dissolved substances), thereby confirming their role as bioindicators of water quality. E. Delgado-Fernández *et al*. (2025) emphasised the capacity of microalgae to serve as effective indicators of water quality and the ecological status of lakes and other water bodies, as certain species exhibit high sensitivity to environmental changes.

Another important aspect of the consistency between the results obtained and contemporary scientific approaches to assessing the role of microalgae in the functioning of aquatic ecosystems is the determination of their contribution to the formation of ecosystem services. In this study, it is substantiated that phytoplankton predominantly provides regulating and supporting services, as well as, to some extent, cultural and provisioning services, particularly through its influence on water quality and the recreational potential of the water body. Similar conclusions have been presented in studies by E. Acevedo-Trejos *et al*. (2018) and J.F. Tweddle *et al*. (2018), which emphasise that microalgae play a key role in regulating the chemical composition of water and biogeochemical cycles, and also act as sensitive indicators of the ecological status of aquatic ecosystems. At the same time, certain differences can be observed between the results obtained and the generalisations presented in other studies. These differences are primarily related to the stage of ecosystem development. In the present study, a relatively low species diversity of phytoplankton was recorded under conditions of structural balance, indicating a stable yet not fully developed biocoenosis. In contrast, studies by P. Hirsch *et al.* (2018) and F. Lüskow *et al.* (2024) highlighted that, during further succession, quarry water bodies undergo increasing biotic complexity: algal diversity rises, higher aquatic plants emerge, and the composition of hydrobiota expands, including the development of ichthyofauna.

Differences are also evident in the approaches to assessing ecosystem services. In this study, the CICES classification was applied to substantiate the contribution of phytoplankton to the provision of provisioning, regulating, supporting, and cultural ecosystem services, with an emphasis on their quantitative and functional assessment. At the same time, studies by V. BBéres *et al.* (2023) and L. Naselli-Flores & J. Padisák (2023) predominantly adopted a more generalised approach, in which ecosystem services are considered as a derivative of the overall state of biota and hydroecological conditions, without detailed differentiation of the roles of individual taxonomic groups.

The results of the present study are generally consistent with the established principles regarding the patterns of biota formation and ecosystem service development in quarry water bodies reported in other studies. The identified combination of relatively low species diversity and favourable hydrochemical conditions indicates an early or intermediate stage of ecological succession in the studied Korostyshiv Quarry water body. This confirms that the formation of biotic structure and ecosystem functions occurs gradually and depends on a complex interplay of natural and anthropogenic factors. At the same time, the presented results highlight the important role of phytoplankton as an indicator of ecological status and as a key component in the provision of regulating and supporting ecosystem services.

Conclusions

In summary, the data obtained allow for the formulation of key conclusions that reflect the main results of the study, demonstrating the importance of identifying relationships between the species composition of microalgae and the formation of corresponding ecosystem services. It was established that the phytoplankton of the studied water body of the Korostyshiv Quarry is characterised by a relatively balanced community structure under conditions of limited species diversity: five microalgal species belonging to four divisions (*Chlorophyta*, *Bacillariophyta*, *Chrysophyta*, and *Dinophyta*) were identified, which generally indicates a favourable ecological status of the aquatic environment. The biomass level remained moderate and does not exceed 2 g/L, which is consistent with the results of chemical analysis confirming that water quality indicators comply with European regulatory requirements and Ukrainian standards.

The study also revealed functional relationships between the taxonomic structure of microalgae and the processes of ecosystem service formation. It was shown that the species composition of phytoplankton determines the intensity of primary production, the characteristics of nutrient cycling, and the overall state of the aquatic ecosystem. Taking into account the CICES classification, it was substantiated that microalgae act as an important factor in the formation of a wide range of ecosystem services (provisioning, regulating, supporting, and cultural), with their contribution varying across different service groups. The study further indicates that the high quality of water indicators of the quarry, as established by chemical analysis, reflects the effectiveness of the regulating ecosystem services provided by algae. Good water quality is a key determinant for the development of hydrobionts (supporting ecosystem services) and for the recreational use of the water body by the population.

Further research will make it possible to address the questions arising at this stage of the analysis of non-flowing aquatic ecosystems. Additional attention should be paid to determining the species composition and quantitative characteristics of epiphyton in quarry water bodies. This approach may contribute to the development of a national framework for assessing ecosystem services of freshwater lentic ecosystems.

Acknowledgements

The authors express their gratitude to Prof. P. Klochenko for assistance in the algological research.

Funding

Field studies and algological research were supported by a grant from the UFLP programme of the International Education Institute, USA, and a grant from the Simons Foundation International [SFI-PD-Ukraine-00014577, O.G.].

Conflict of Interest

None.

References

[1] Acevedo-Trejos, E., Marañon, E., & Merico, A. (2018). Phytoplankton size diversity and ecosystem function relationships across oceanic regions. *Proceedings of the Royal Society B: Biological Sciences,* 285(1879), article number 20180621. doi: 10.1098/rspb.2018.0621.

[2] AKVO. (n.d.). Retrieved from https://akvo.com.ua/ua/.

[3] Arsan, O.M., Davydov, O.A., Diachenko, T.M., & Yevtushenko M.Y., & Zhukinskiy, V.M. (2006). *Methods of hydroecological research of surface waters*. Kyiv: Logos.

[4] B-Béres, V., Stenger-Kovács, C., Buczkó, K., Padisák, J., Selmeczy, G.B., Lengyel, E., & Tapolczai, K. (2023). Ecosystem services provided by freshwater and marine diatoms. *Hydrobiologia*, 850, 2707-2733. doi: 10.1007/s10750-022-04984-9.

[5] Bilous, O.P., Nezbritska, I.M., Klochenko, P.D., & Kirpenko, N.I. (2018). *Collection of microalgae cultures HPDP.* Kyiv: HPDP.

[6] Chandel, P., Mahajan, D., Thakur, K., Kumar, R., Kumar, S., Brar, B., Sharma, D., & Sharma, A.K. (2024). A review on plankton as a bioindicator: A promising tool for monitoring water quality. *World Water Policy*, 10(1), 213-232. doi: 10.1002/wwp2.12137.

[7] CICES Version 5.2. (n.d.). Retrieved from https://cices.eu/.

[8] Convention on Biological Diversity. (1992). Retrieved from https://www.cbd.int/convention.

[9] Delgado-Fernández, E., Cruz, D., Ayavaca, R., Benítez, Á., & Hernández, B. (2025). Microalgal diversity as bioindicators for assessing and sustaining water quality in the high mountain lakes of Quimsacocha, Azuay, Ecuador. *Sustainability*, 17(4), article number 1620. doi: 10.3390/su17041620.

[10] Dobrescu, C.M., Turtureanu, A., & Dorobat, L.M. (2023). Algae as biological indicators of water pollution. *Journal of Danubian Studies and Research*, 13(1), 32-38.

[11] EUNIS. (n.d.). *European Nature Information System*. Retrieved from https://eunis.eea.europa.eu/index.jsp.

[12] Google Maps. (n.d.). *Korostyshiv Quarry*. Retrieved from https://surl.li/kbswzx.

[13] Hirsch, P., Nguyen, A., Müller, R., Adrian-Kalchhauser, I., & Burkhardt-Holm, P. (2018). Colonizing islands of water on dry land – on the passive dispersal of fish eggs by birds. *Fish and Fisheries*, 19(3), 502-510. doi: 10.1111/faf.12270.

[14] Jahan, S., & Singh, A. (2023). The role of phytoplanktons in the environment and in human life, a review. *Basrah Journal of Science,* 41(2), 392-411. doi: 10.29072/basjs.20230212.

[15] Knoben, R.A.E., Roos, C., & van Oirschot, M.C.M. (2006). *Biological assessment methods for watercourses (UNECE task force on monitoring and assessment report)*. Lelystad: United Nations Economic Commission for Europe.

[16] Kuzemko, A.A., Didukh, Ya.P., Onyshchenko, V.A., & Sheffer, Ya. (Eds.). (2018). *National catalogue of biotopes of Ukraine*. Kyiv: IE Yu.Ya. Klymenko.

[17] Lüskow, F., *et al*. (2024). Hidden gems: Scattered knowledge hampered freshwater jellyfish research over the past one-and-a-half centuries. *Ecology and Evolution*, 14, article number e70350. doi:10.1002/ece3.70350.
[18] Mondal, A., Pal, A.K., & Samanta, G.P. (2020). Rich dynamics of non-toxic phytoplankton, toxic phytoplankton and zooplankton system with multiple gestation delays. *International Journal of Dynamics and Control*, 8, 112-131. doi: 10.1007/s40435-018-0501-4.
[19] Naselli-Flores, L., & Padisák, J. (2023). Ecosystem services provided by marine and freshwater phytoplankton. *Hydrobiologia*, 850, 2691-2706. doi: 10.1007/s10750-022-04795-y.
[20] O'Neill, E., & Rowan, N. (2022). Microalgae as a natural ecological bioindicator for the simple real-time monitoring of aquaculture wastewater quality including provision for assessing impact of extremes in climate variance – a comparative case study from the Republic of Ireland. *Science of The Total Environment,* 802, article number 149800. doi: 10.1016/j.scitotenv.2021.149800.
[21] Shcherbak, V.I. (2006). Phytoplankton. In *Methods of hydroecological research of surface waters* (pp. 8-32). Kyiv: Lohos.
[22] Shcherbak, V.I., Semenyuk, N.E., Davydov, O.A., & Koziychuk E.Sh. (2025). Peculiarities of the biotopic location of algae in the water column of freshwater hydroecosystems of various types. *Algology,* 35 (2), 104-127. doi: 10.15407/alg35.02.104.
[23] Thomaz, S.M. (2023). Ecosystem services provided by freshwater macrophytes. *Hydrobiologia,* 850, 2757-2777. doi: 10.1007/s10750-021-04739-y.
[24] Topachevsky, A.V., Masyuk, N.P. & Makarevich, M.F. (Eds.). (1984). *Freshwater algae of the Ukrainian SSR*. Kyiv: Higher School.
[25] Tweddle, J.F., Gubbins, M., & Scott, B.E. (2018). Should phytoplankton be a key consideration for marine management? *Marine Policy*, 97, 1-9. doi: 10.1016/j.marpol.2018.08.026.
[26] Ulyhanets, S., & Shynkarenko, U. (2023). Geotourism: Development based on geoheritage (case of Korostyshiv Quarry). In *Selected papers from the V international conference on European dimensions of sustainable development (1-2 June, Kyiv)* (pp. 274-281). Kyiv: National University of Food Technologies. doi: 10.24263/EDSD-2023-5-29.
[27] Updhai, D., Shukla, K., Mishra, A., & Shukla, S. (2025). Freshwater phytoplankton: A significant provider of ecosystem services in aquatic environments. In J. Gupta & A. Verma (Eds.), *Green equilibrium* (pp. 179-196). Singapore: Springer. doi: 10.1007/978-981-96-3993-9_9.
[28] Vasser, S.P., Kondratyeva, N.V., & Masyuk, N.P. (Eds.). (1989). *Algae: Handbook.* Kyiv: Naukova Dumka.

Мікроводорості непроточних водойм як фактори формування екосистемних послуг

Людмила Сова
Аспірант
Національний університет «Києво-Могилянська академія»
04655, вул. Григорія Сковороди, 2, м. Київ, Україна
https://orcid.org/0000-0002-3197-9616
Віктор Карамушка
Кандидат біологічних наук, доцент
Національний університет «Києво-Могилянська академія»
04655, вул. Григорія Сковороди, 2, м. Київ, Україна
https://orcid.org/0000-0002-3327-2243

Анотація. Завдяки значному видовому різноманіттю та чутливості до змін середовища мікроводорості є важливими індикаторами екологічного стану водойм та у складі інших гідробіонтів формують екосистемні послуги гідросистем. Оскільки їх внесок у забезпечення екосистемних послуг непроточних водойм досліджений обмежено й потребує подальшого обґрунтування для визначення екологічної цінності водойм, мета роботи полягала у дослідженні взаємозв'язків між видовим складом мікроводоростей та формуванням відповідних екосистемних послуг непроточних водойм на прикладі Коростишівського кар'єра (Житомирська область, Україна). Для визначення видового складу та розподілу мікроводоростей застосовували стандартні методики (відбір та консервація проб води, виділення, ідентифікація та кількісні характеристики мікроводоростей за допомогою мікроскопії). Виявлено відносно збалансовану структуру фітопланктонного угруповання водойми кар'єру з невисоким видовим різноманіттям: п'ять видів мікроводоростей, що належать до чотирьох різних відділів (*Chlorophyta*, *Bacillariophyta*, *Chrysophyta* та *Dinophyta*). Концентрація біомаси була відносно невисокою – до 2 г/л. Видовий склад фітопланктону та результати хімічного аналізу проб води вказують на добрий екологічний стан водойми. Визначені взаємозв'язки між функціональними характеристиками мікроводоростей та екосистемними послугами. Показано, що видовий склад мікроводоростей є ключовим чинником формування екосистемних послуг, визначає первинну продукцію, кругообіг біогенних елементів і стан водного середовища. З урахуванням класифікації екосистемних послуг CICES показано, що мікроводорості досліджуваної водойми кар'єру є фактором, що впливає на формування практично усіх типів екосистемних послуг (3 – забезпечувальних, 9 – регулювальних та підтримувальних, 4 – культурних), але з різною інтенсивністю. Показано, що домінуючим в умовах екосистеми кар'єру був внесок мікроводоростей у формування регулювальних та підтримувальних екосистемних послуг. Результати можуть бути використані для розроблення механізму оцінювання екосистемних послуг прісноводних лентичних водойм

Ключові слова: фітопланктон; екосистеми кар'єрів; біотопи; індикаторні види; кругообіг біогенних елементів

Received 06.01.2026 Revised 03.04.2026 Accepted 23.04.2026 Published: 30.04.2026

Vol. 22, No. 2
2026

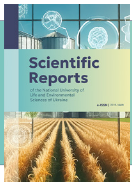

Scientific Reports of the National University of Life and Environmental Sciences of Ukraine

Journal homepage: https://scireports.com.ua/en e-ISSN 2223-1609

UDC 633.11:631.559:551.5 DOI: 10.31548/dopovidi/2.2026.105

Growing season duration and productivity of soft winter wheat under different weather conditions

Valerii Prydatko
Postgraduate Student
National University of Life and Environmental Sciences of Ukraine
03041, 15 Heroiv Oborony Str., Kyiv, Ukraine
https://orcid.org/0009-0005-8997-9765

Hanna Kovalyshyna*
Doctor of Agricultural Sciences, Professor
National University of Life and Environmental Sciences of Ukraine
03041, 15 Heroiv Oborony Str., Kyiv, Ukraine
https://orcid.org/0000-0002-2715-7679

Abstract. In the conditions of variability of weather factors in the Northern Forest-Steppe zone of Ukraine, it is important to assess the impact of hydrothermal conditions on the development of winter wheat productivity. The purpose of the study was to establish the influence of temperature and moisture supply in certain periods of vegetation on the weight of 1,000 grains of winter wheat. The study was conducted in the field during 2023-2025 using generally accepted methods for evaluating elements of the crop structure. It was found that the weight of 1,000 grains varied significantly depending on hydrothermal conditions during the grain filling period. In 2024, due to a lack of precipitation in April-May and elevated temperatures in June-July (up to 30-35°C), there was a reduction in the duration of the grain filling period, which led to the development of less full grain and a decrease in the weight of 1,000 grains. But in 2025, with a more uniform distribution of precipitation in May-June (up to 47.9-68.0 mm) and a moderate temperature regime, better water supply to plants was provided, which contributed to an increase in the intensity of photosynthesis and the accumulation of dry matter in the grain. As a result, the weight index of 1,000 grains increased from 46.8 to 47.4 g. It was revealed that the critical period for the development of this indicator were phases earing – grain filling, during which the combination of high temperatures and moisture deficiency limited plant productivity. A close relationship has been established between weather conditions and the level of implementation

Suggested Citation:
Prydatko, V., & Kovalyshyna, H. (2026). Growing season duration and productivity of soft winter wheat under different weather conditions. *Scientific Reports of the National University of Life and Environmental Sciences of Ukraine*, 22(2), 105-119. doi: 10.31548/dopovidi/2.2026.105.

**Corresponding author*

of the productive potential of varieties. The practical significance of the results obtained lies in the possibility of optimising the sowing time and selection of varieties considering their response to hydrothermal conditions, and in adjusting the fertiliser and moisture supply system to reduce the negative impact of dry periods on the development of grain weight. The results obtained can be used by agronomists and breeders to increase the stability of winter wheat yield in the context of climate change

Keywords: hydrothermal regime; phenological phases of development; weight of 1,000 grains; elements of ear productivity; correlations of traits; plant moisture supply

Introduction

Soft winter wheat (*Triticum aestivum* L.) is one of the leading grain crops that ensures food security in many countries of the world, in particular in Ukraine, where it occupies a significant area in the structure of crops (Lyfenko *et al.,* 2021). The implementation of its productive potential largely depends on the growing conditions, among which the temperature regime and moisture supply during the growing season play a decisive role. In the conditions of climate variability, the assessment of the influence of hydrothermal factors on the growth and development of the winter wheat crop is particularly relevant. Recent studies show that temperature fluctuations and uneven precipitation distribution can significantly change the duration of phenological phases of plant development, which directly affects the development of elements of the crop structure. E.E. Rezaei *et al.* (2023) showed that an increase in air temperature combined with a lack of moisture can significantly reduce wheat yield even in conditions of increased CO_2 concentrations in the air, whereas R. Kopecká *et al.* (2023) highlighted the role of physiological and biochemical mechanisms of plant adaptation to abiotic stresses.

Critical for the development of productivity are the phases of tubing, earing, and grain filling, during which the main elements of yield are established. Research by M.M. Hassona *et al.* (2024) proved that sufficient water supply during these periods contributes to an increase in the intensity of photosynthesis, the accumulation of assimilants, and the development of a fuller grain. But the lack of moisture, combined with high temperatures, limits the duration of the grain filling period and reduces its weight. Recent experimental studies indicate a complex and ambiguous nature of the influence of the temperature factor on the productivity of winter wheat. In particular, X. Du *et al.* (2022) found that an increase in temperature in the early spring period accelerates the passage of the main phenological phases of plant development. It can extend the effective growth period due to changes in the temperature regime in subsequent phases, which has a positive effect on photosynthetic activity and grain development.

Special attention in contemporary research is paid to the influence of moisture deficiency during grain filling on the development of its morphometric and productive indicators. A. Zamani *et al.* (2024) found that terminal water stress leads to a decrease in the weight of 1,000 grains by 14.6-24.6% and a significant deterioration in the morphometric characteristics of the grain, while a close positive relationship was found between the grain weight and its linear dimensions. An important feature of yield development is the interaction of genotype and environmental conditions. The response of winter wheat varieties to hydrothermal conditions differs significantly depending on their genetic characteristics, which determines the level of their adaptability to climate change. The research by T. Stella *et al.* (2023) and A. Menzir *et al.* (2025) showed that the selection of varieties with high adaptive potential is one of the key elements of yield stabilisation in a changing environment. In this context, the assessment of varieties of different origins in specific soil and climatic conditions has become particularly important.

An important factor in the development of productivity is the interaction of genotype and environmental conditions. R. Mohammadi *et al.* (2025) showed that environmental conditions determine up to 94.2% of wheat yield variability, while the contribution of genotype is much smaller, and the interaction of genotype and environment is formed under the influence of temperature and precipitation. This indicates the dominant role of hydrothermal factors in the development of productivity and the need to consider them when evaluating varieties. Climate variability is one of the main factors determining the level of variability in grain yields. The study by B. Monteleone *et al.* (2023) showed that climate factors can explain a significant proportion of yield fluctuations, especially in extreme weather conditions. In turn, P.A.J. Van Oort *et al.* (2023) proved that droughts and excessive moisture are the main causes of yield anomalies.

Thus, the development of the weight of 1,000 grains is the result of a complex interaction of temperature, water supply, and genotypic characteristics of the variety. Simultaneously, despite a significant number of studies, the complex influence of hydrothermal conditions on the duration of individual growing seasons and the development of productivity elements in specific agroclimatic conditions remains insufficiently investigated. This is especially true in the conditions of the Northern Forest-Steppe of Ukraine, where the combination of elevated temperatures in summer and uneven precipitation distribution creates specific conditions for the growth and development of winter wheat plants. In this regard, it is relevant to investigate the characteristics of the reaction of varieties of different origins to hydrothermal conditions in this zone. Thus, the purpose of the study was to establish the influence of hydrothermal conditions on the duration of vegetation periods and the development of the weight of 1,000 grains in 8 varieties of soft winter wheat of various origins in the conditions of the Northern Forest-Steppe of Ukraine during 2023-2025.

Materials and Methods

The study was conducted during the 2023-2024 and 2024-2025 growing years in the field conditions of the Northern Forest-Steppe of Ukraine (Chernihiv Oblast, Pryluky Raion). The object of the study was 8 varieties of soft winter wheat of various origins: ‘MIP Vyshyvanka’, ‘Vezha Myronivska’, ‘MIP Valensiya’ (V.M. Remeslo Myronivka Institute of Wheat, Ukraine), ‘Nosivochka’ (Nosivka breeding and experimental station, Ukraine), ‘Emerik’ (KWS, Germany), ‘Meskal’ (Limagrain, France), ‘Julia’ (Selgen, Czech Republic), and ‘Tobak’ (Saaten Union, Germany).

Field experiments were conducted on production crops in compliance with the generally accepted technology for growing winter wheat for this zone. Placement of varieties was carried out on the principle of continuous plots, while each variety was grown on a separate accounting plot of 1 ha. The predecessors were in 2024 – sunflower, in 2025 – soybean. The upper arable soil horizon was characterised by an average degree of humus content – approximately 4.6%. The availability of mobile forms of phosphorus determined by the Machigin method was in the range of 3.3-3.4 mg per 100 g of soil, while the concentration of exchange potassium was 9.8-10.3 mg per 100 g of soil (Zubko & Ivaniuk, 2023).

Sowing was carried out at the optimal time for the zone in late September (29.09.2024) – early October (01.10.2023), depending on the weather conditions of the year. Phenological observations were carried out during the entire growing season with the fixation of the main phases of plant development: germination, tillering, tubing, earing, and ripening. The duration of interphase periods was determined by the calendar dates of the onset of the corresponding phases. To characterise the hydrothermal conditions, data from the Meteoblue meteorological service (n.d.) were used, which were verified by comparing them with open-access data from regional weather stations. The average daily air temperature, the amount of precipitation, and their distribution over decades and months of the growing season were analysed.

The condition of crops after overwintering was assessed during the recovery phase of spring vegetation on a visual scale, considering the uniformity of seedlings, the degree of damage to plants, and their viability. Elements of the crop structure were evaluated on a sample of plants selected by random (randomised) sampling from each accounting site during the full ripeness phase. At least 25 typical plants of each variety were selected for analysis. The length of the ear, the number of spikelets in the ear, the number of grains in the ear, and the weight of grain from one ear were determined. The weight of 1,000 grains was determined according to the generally accepted method by weighing a pre-selected and purified grain sample with conversion to standard humidity.

Statistical processing of the obtained data was carried out using descriptive statistics. The average value (M) was determined for each indicator. Correlation analysis with calculation of the Pearson correlation coefficient (r) was used to evaluate the relationships between indicators. Calculations were performed using Microsoft Excel software suite. The difference between the indicators was interpreted as significant at $p < 0.05$. The study was conducted in compliance with ethical principles defined by international documents, in particular the Convention on Biological Diversity (1992). In the course of the study, the requirement to preserve biodiversity and prevent negative impact on the studied species was considered.

Results and Discussion

During the growing season, winter wheat plants go through successive phases of development associated with the development and differentiation of organs. According to generalised data, the growing season is conventionally divided into two main stages: from germination to earing, and from earing to full ripening. Simultaneously, the main role in the development of future productivity is played by the period of germination – earing, during which most stages of plant organogenesis are implemented, which determines the potential for crop development, as indicated by B.V. Blyzniuk *et al.* (2019). The passage of these phases and the intensity of growth processes are largely determined by environmental conditions and the level of supply of plants with the main factors of life. According to T. Adamenko (2017), the variability of weather conditions during the growing year has a significant impact on the growth and development of winter wheat plants, which depends on the frequency and amount of precipitation and air temperature indicators. Plants develop best with optimal provision of the necessary factors during the period of growth and development.

Monitoring of crops during the growing season of soft winter wheat plants in 2023-2024 in the Northern Forest-Steppe zone of Ukraine indicated a significant influence of weather conditions on the duration of their growth and development periods. In terms of hydrothermal parameters, the study years were contrasting in both autumn and spring (Fig. 1, 2). Accordingly, this affected both the timing of sowing and germination, and the quality of the resulting grain. Analysis of air temperature indicators in the autumn period of 2023 (Fig. 1) indicates that before sowing in September, the average ten-day temperatures fluctuated in the range of 24.0-25.0°C, and precipitation was observed in the first and second ten-day periods – 2.0 and 5.0 mm. Sowing was carried out on October 1, and shoots appeared on October 16. Temperatures in October by decade were: 16.7°C, 14.0°C, 14.2°C, and ten-day precipitation was as follows: 4.0 mm, 24.0 mm, and 32.0 mm. Such hydrothermal conditions contributed to the appearance of friendly shoots and their further development. In November, there was a decrease in air temperature, and the amount of precipitation for the month exceeded 89 mm. The winter period was characterised by unstable weather, periodic thaws were noted. In March 2024, the average ten-day temperature was 5.6°C, 6.7°C, and 11.8°C, respectively, precipitation was observed in the second and third ten day periods of the month – 12.2 and 14.5 mm. A small amount of precipitation in April and May caused a lack of moisture during the period of plant tubing and earing. In June and July 2024, air temperatures were high – 20-35°C, precipitation was recorded in June. The lack of precipitation and high air temperatures in July led to rapid ripening of grain. The developed grain had a small size and low grain weight indicators.

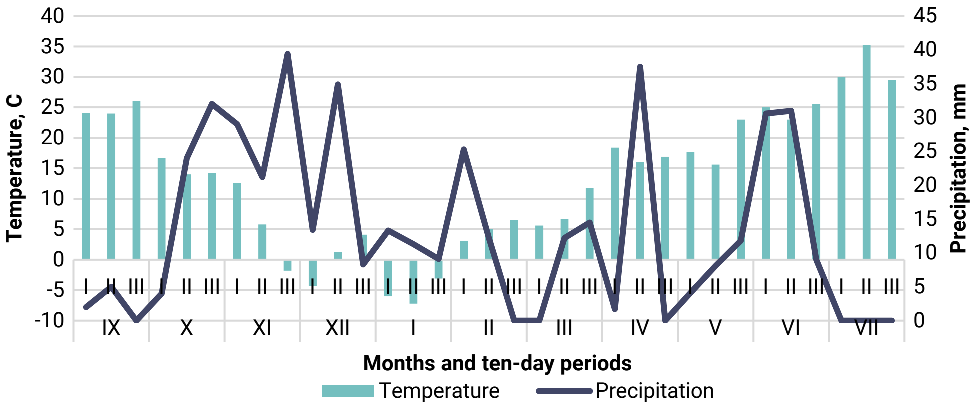

Figure 1. *Hydrothermal indicators of the growing season of winter wheat, 2023/2024*

Source: developed by the authors based on own research

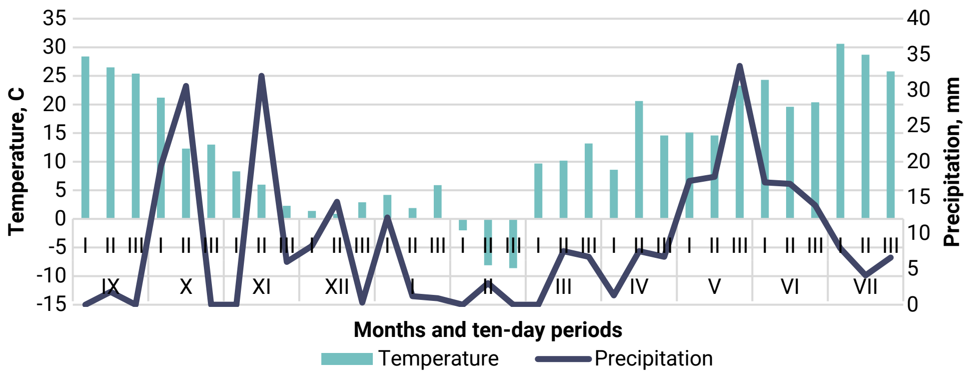

Figure 2. *Hydrothermal indicators of the growing season of winter wheat, 2024/2025*

Source: developed by the authors based on own research

Pre-sowing period 2024 (Fig. 2) in all three ten-day periods of September, the month was characterised by increased air temperature indicators – 28.4°C, 26.5°C, 25.4°C, respectively, and a slight amount of precipitation (1.8 mm) only in the second ten days of the month. Sowing was carried out on September 28, and seedlings were received on October 10. The appearance of shoots was promoted by a sufficient amount of moisture (up to 50 mm) and warm weather, especially in the first ten days of October (21.2°C). Weather conditions in winter contributed to the normal overwintering of winter wheat plants. In the spring period of 2025 (March-April), air temperatures ranged from 9.7°C to 20.6°C, but precipitation was insignificant. The month of May was characterised by increased air temperatures, and over 68 mm of precipitation fell during the month, especially in the third ten-day period (33.4 mm). In June-July, high air temperatures were recorded, especially in July (up to 30.6°C) and sufficient precipitation. In June, 47.9 mm fell during the month, which contributed to good filling and grain development.

According to data from the Myronivka Institute of Wheat named after V.M. Remeslo of NAAS of Ukraine (2025), during 2020-2025 in the Forest-Steppe zone of Ukraine, the end of the autumn vegetation of winter crops mainly occurs in November, as evidenced by the shift of the seasonal boundaries of the growing season and leads to a later termination of the autumn vegetation. The results obtained regarding the duration of the "sowing – germination" period and the features of the autumn growing season are consistent with the data of other studies. In particular, it was found that the emergence of seedlings is significantly affected not only by the moisture supply of the soil, but also by the sum of effective temperatures and sowing times, which was confirmed in M studies by M. Korkhova (2019). At a later time of sowing, the temperature regime played a decisive role, which can limit the duration of the autumn vegetation of plants.

Summarising the phenophases of ontogenesis of the studied winter wheat varieties by years of research, calendar dates were determined in the process of plant growth and development of grain (Table 1). Setting the time frame for passing the main phases of ontogenesis allows assessing the response of plants to hydrothermal conditions of the year and identify critical periods of development that are sensitive to stress factors. In addition, comparing the duration of interphase periods allowed assessing the adaptability of varieties and the features of crop development depending on weather conditions.

Table 1. *Phenological observations of plant development, 2023-2025*

Phases of plant development	2023-2024	2024-2025
sowing	October 1, 2023	September 29, 2024
germination	October 16	October 10
end of the autumn growing season (EAGS)	December 1-3	December 25-28
time of resumption of spring growth (TRSG)	March 5-10, 2024	March 14-15, 2025
tillering	March 25-30	March 21-25
tubing	April 15-20	April 15-20
earing	May 6-9	April 27-30
flowering	May 18-23	May 6-11
milk ripeness	June 22-27	June 18-22
waxy ripeness	July 5-6	July 2-4
full ripeness	July 10-11	July 12-14
harvest	July 12	July 22

Source: developed by the authors based on own research

The table data indicate a certain shift in the timing of individual phases of plant development between the years of research, in particular, the earlier beginning of the spring vegetation and the earing and flowering phases in 2024-2025. The late end of the autumn growing season in the second year indicates the influence of warmer weather conditions in the winter period. In general, the variation in the calendar dates of the ontogenesis phases reflects the dependence of the rate of plant development on the hydrothermal regime of the year. Analysis of the duration of interphase periods of development of soft winter wheat varieties showed a significant variability in their passage depending on the conditions of the growing season. It was found that in 2024-2025, compared to 2023-2024, there was a reduction in the "sowing – germination" period by 3-5 days, which is due to more favourable temperature conditions and sufficient moisture supply in the post-sowing period (Table 2).

Table 2. *Duration of interphase periods of development of soft winter wheat varieties depending on the growing conditions of 2023-2025*

Variety	sowing-germination	germination-EAGS	EAGS-TRSG	TRSG-tillering	tillering-tubing	tubing-earing	earing-flowering	flowering-milk ripeness	milk ripeness-waxy ripeness	waxy ripeness-full ripeness	full ripeness-harvest	Active growing season time
'Nosivochka'	14/10	47/77	95/79	20/7	21/25	21/12	12/9	35/43	13/14	5/10	2/10	190/217
'MIP Vyshyvanka'	15/11	47/77	97/79	20/9	21/25	20/11	12/11	34/42	13/12	4/10	2/9	188/217
'Vezha Myronivska'	15/11	48/78	97/78	20/9	20/26	20/11	13/10	33/42	13/13	4/10	2/8	188/218
'MIP Valensiya'	14/10	48/78	95/78	21/9	21/25	20/11	12/10	34/43	13/13	5/10	2/9	190/218
'Emerik'	15/11	47/77	95/78	20/8	21/26	21/11	12/11	35/42	13/13	4/10	2/9	190/218
'Meskal'	15/11	48/79	97/77	21/10	20/26	19/10	13/11	33/41	13/13	4/10	2/8	188/219
'Julia'	15/10	46/77	95/79	21/8	21/26	20/10	12/11	35/43	13/13	5/9	2/10	190/217
'Tobak'	15/11	48/79	98/77	20/10	21/26	19/10	14/11	31/42	13/12	4/10	2/8	187/219

Note: the numerator contains data for the growing season 2023-2024, and the denominator contains data for 2024-2025

Source: developed by the authors based on own research

According to the results obtained, the greatest differences between years were noted for the periods "germination – EAGS" and "EAGS – TRSG". In particular, in 2024-2025, the duration of the autumn growing season increased by an average of 30-32 days, while the duration of the winter period decreased by 15-20 days, which indicates the influence of an increased temperature background in the autumn-winter period. In the spring and summer period, there were also differences in the duration of individual phases of development. In particular, in 2024-2025, the period of "tubing-earing" was reduced to 10-12 days, compared to 19-21 days in the previous year, which indicates an acceleration of plant development under the influence of elevated temperatures. Simultaneously, the period of "flowering – milk ripeness" was longer in 2024-2025 (41-43 days), which created favourable conditions for grain filling.

The total duration of active vegetation in 2024-2025 was longer and amounted to 217-219 days, while in 2023-2024 it ranged from 187-190 days. The greatest duration of the growing season was characterised by the varieties 'Meskal' and 'Tobak', which indicates their relatively late-maturing type of development, while a shorter period was observed in the variety 'Vezha Myronivska'. The dependence of the duration of the autumn vegetation on the hydrothermal regime was noted: in 2023/2024, the duration of the autumn vegetation was 48 days, and in 2024/2025 – 78.5 days (Table 3). The state of winter wheat crops after overwintering was determined by the duration of the winter dormancy period and the timing of the resumption of spring vegetation. The lengthening of the dormant period of plants affected the intensity of their further growth, development, and productivity. Later, the resumption of spring vegetation in 2024/2025 indicated a longer period of winter dormancy, which could lead to a certain suppression of the physiological state of plants and delay the initial stages of spring development. Simultaneously, the early resumption of vegetation in 2023/2024 contributed to a more active start of growth processes, but in the conditions of further moisture deficiency, it did not ensure the full implementation of the productive potential of plants. Thus, the combination of the duration of the winter period and the conditions of the spring-summer vegetation determined the further growth and development of winter wheat yield.

Table 3. *Duration of growing seasons of winter wheat varieties depending on the hydrothermal conditions of the studied years in the zone of Northern Ukraine*

Development phases	Calendar dates	Duration, days
2023/2024		
sowing-germination	01.10-16.10	16
germination-EAGS	16.10-01-03.12	48
EAGS-TRSG	01-03.12-05-10.03	97.5
TRSG-earing	05-10.03-06-09.05	62
earing-full ripeness	06-09.05-10-11.07	65
2024/2025		
sowing-germination	28.09-10.10	12
germination-EAGS	10.10-25-28.12	78.5
EAGS-TRSG	25-28.12-14-15.03	79
TRSG-earing	14-15.03-27-30.04	46
earing-full ripeness	27-30.04-12-14.07	76.5

Source: developed by the authors based on own research

The duration of the period of restoration of spring vegetation to earing in the years under study significantly differed and amounted to 62 days in 2023/2024, while in 2024/2025 – only 46 days (Table 3). The reduction of this period in 2024/2025 indicates an acceleration in the rate of plant development, which was conditioned by the increased temperature background in the early spring period. Simultaneously, a longer period in 2023/2024 contributed to the gradual passage of development phases, which could positively affect the development of generative organs. Thus, the duration of the period of "TRSG – earing" is an important indicator of the response of plants to hydrothermal conditions of the year and determines the features of the development of winter wheat productivity. Starting from the second ten days of May and in the summer, the period of earing – full ripeness of winter wheat began. It is at this time that dry and hot weather, lack of moisture in the soil was noted, which led to a violation of the processes of development of generative organs. A large number of sterile and underdeveloped flowers were laid in the ear, the grain was weak, which leads to a shortage of crops.

Overwintering of winter wheat plants was estimated after the resumption of spring vegetation, which in 2023/2024 occurred in early March, while in 2024/2025 – in mid-March. It was found that higher overwintering rates in 2025 were statistically significant for individual varieties, in particular 'Nossvochka', 'MIP Vyshyvanka', and 'Vezha Myronivska', which indicates their increased resistance to overwintering conditions. This indicates genetically determined differences in the ability of varieties to maintain plant viability in winter (Table 4).

Table 4. *Grain yield of winter wheat varieties depending on TRSG, 2024-2025*

Variety	Overwintering, %		Average	TRSG		Yield, t/ha		Average
	2024	2025		2024	2025	2024	2025	
'Nosivochka'	**95**	**95**	**95.0**	05.03	14.03	3.86	5.64	4.75
'MIP Vyshyvanka'	90	**95**	92.5	08.03	15.03	3.87	5.36	4.62

***Table 4.** Continued*

Variety	Overwintering, %		Average	TRSG		Yield, t/ha		Average
	2024	2025		2024	2025	2024	2025	
'Vezha Myronivska'	90	**95**	92.5	09.03	15.03	3.94	6.24	5.09
'MIP Valensiya'	90	90	90.0	06.03	14.03	**5.56**	7.13	**6.35**
'Emerik'	85	90	87.5	06.03	14.03	4.67	6.94	5.81
'Meskal'	85	85	85.0	09.03	15.03	5.07	7.24	6.16
'Julia'	90	90	90.0	05.03	14.03	4.59	7.31	5.95
'Tobak'	85	90	87.5	10.03	15.03	**5.28**	**7.68**	**6.48**
Average	88.75	91.25	90.0	-	-	4.61	6.69	5.65

Note: values that differ significantly from the mean at the 5% significance level are highlighted in bold
Source: developed by the authors based on own research

The results showed that the later resumption of spring vegetation in 2025 was associated with a longer winter dormancy period, which contributed to better plant preservation and reduced the level of their physiological depletion. This ensured a more uniform restoration of growth processes in the spring and the development of a productive stem. Yield analysis showed that in 2025 there was a significant increase in yield compared to 2024, and for individual varieties ('MIP Valensiya', 'Tobak'), these differences were statistically significant. This showed that the combination of more favourable overwintering conditions and optimal recovery time for spring vegetation created prerequisites for effective productivity development. Even with a high level of overwintering, the yield level was also determined by further hydrothermal conditions of the spring-summer vegetation period. Thus, the level of overwintering of plants and the time of restoration of spring vegetation are interrelated factors that determine the start of spring development and the further implementation of the productive potential of winter wheat varieties.

Yield is a complex quantitative feature that is formed under the influence of a set of productivity elements, in particular the length of the ear, the number of spikelets and grains in the ear, the weight of grain from the ear, and the weight of 1,000 grains. The results showed that the manifestation of these traits is largely determined by both varietal characteristics and hydrothermal conditions of years of research. It was found that higher indicators of ear length, which were statistically significant relative to the average value, were formed in the varieties 'Meskal', 'Emerik' and 'Julia' in 2024, and in the varieties 'Julia', 'Mescal', and 'Vezha Myronivska' in 2025, which indicates their genetically determined potential for the development of a more developed ear (Table 5).

***Table 5.** Elements of productivity of an ear of soft winter wheat, depending on the variety, 2024-2025*

Varieties	Ear length, cm	Number of spikelets per ear, units/ear	Number of grains per ear, units	Grain weight per ear, g	Weight of 1,000 grains, g
2024					
'Nosivochka'	7.2	17.7	40.3	1.97	**48.9**
'MIP Vyshyvanka'	8.0	18.3	42.6	2.20	**50.5**
'Vezha Myronivska'	8.6	17.8	43.3	2.01	46.5
'MIP Valensiya'	7.7	17.7	43.6	2.08	47.7
'Emerik'	**9.3**	**19.7**	47.0	2.06	43.8
'Meskal'	**9.5**	**19.7**	**51.0**	**2.35**	46.1
'Julia'	**9.2**	**20.3**	**48.3**	**2.25**	46.6

Table 5. *Continued*

Varieties	Ear length, cm	Number of spikelets per ear, units/ear	Number of grains per ear, units	Grain weight per ear, g	Weight of 1,000 grains, g
2024					
'Tobak'	7.2	17.7	41.3	1.83	44.4
Average	8.3	18.6	44.7	2.09	46.8
2025					
'Nosivochka'	8.3	19.7	42.3	2.14	**50.6**
'MIP Vyshyvanka'	9.7	21.0	52.0	**2.67**	**51.7**
'Vezha Myronivska'	10.3	20.3	49.7	2.34	47.1
'MIP Valensiya'	9.3	18.3	**55.0**	**2.68**	48.8
'Emerik'	9.7	21.0	47.7	2.12	44.6
'Meskal'	**10.7**	**22.3**	52.7	2.51	47.7
'Julia'	**10.8**	21.0	**54.0**	**2.62**	48.5
'Tobak'	8.3	18.3	42.7	1.93	45.3
Average	9.6	20.2	49.5	2.37	48.0
Average for two years	8.95	19.4	47.1	2.23	47.4

Note: values that differ significantly from the mean at the 5% significance level are highlighted in bold
Source: developed by the authors based on own research

Simultaneously, the increase in ear length was conditioned by an increase in the number of spikelets and grains in the ear, which is confirmed by the presence of statistically significant values of these indicators in the varieties 'Meskal' and 'Julia'. This indicates a more intensive development of generative organs and a higher potential for grain productivity of these varieties. However, it was found that an increase in the number of grains in the ear was not always confirmed by an increase in their weight, which indicates the manifestation of compensatory processes between the elements of productivity. In particular, in 2024, statistically significant higher mass indicators of 1,000 grains were observed in the varieties 'Nosivochka' and 'MIP Vyshyvanka', which indicates the development of a more complete grain with a smaller number of grains in the ear. A similar trend continued in 2025, where these varieties were also characterised by high values of this indicator. Simultaneously, varieties with high grain counts ('Meskal', 'Julia') had a lower weight of 1,000 grains, which confirms the presence of feedback between these traits.

One of the main phases of winter wheat development is the period of development of the number of spikelets in the ear, which significantly affects the future productivity of plants. Laying of spikelets occurs at the IV stage of organogenesis, which falls at the end of the tillering phase and the beginning of the tubing. The number of developed spikelets is a genetically determined trait and varies depending on the variety, which determines its potential for yield. In addition, a statistically significant increase in grain weight from the ear in 2025 was observed in the varieties 'MIP Vyshyvanka', 'MIP Valensiya' and 'Julia', which indicates a more effective use of assimilants during grain filling under favourable weather conditions. Thus, the development of elements of ear productivity is the result of a complex interaction of varietal characteristics and growing conditions, while the most productive varieties were those that achieved an optimal balance between the number of grains and their weight.

A close positive relationship was established between the length of the ear and the number of spikelets in the ear ($r = 0.87$), and between the length of the ear and the number of grains in the ear ($R = 0.86$) (Table 6). This confirms that the linear size of the ear increases with increasing spike size. The number of grains in the ear has a direct relationship with the weight of grain from the ear ($r = 0.86$).

Table 6. *Interdependence of elements of the ear productivity structure*

Elements of the ear productivity structure	Ear length, cm	Number of spikelets per ear, units/ear	Number of grains per ear, units	Grain weight per ear, g	Weight of 1,000 grains, g
Ear length, cm	1.00				
Number of spikelets per ear, units/ear	**0.87**	1.00			
Number of grains per ear, units	**0.86**	0.67	1.00		
Grain weight per ear, g	0.63	0.52	**0.86**	1.00	
Weight of 1,000 grains, g	-0.20	-0.09	0.00	0.51	1.00

Note: values that differ significantly from the average for 5% of the significance level are highlighted in bold
Source: developed by the authors based on own research

The weight of grain from the ear also has a moderate positive relationship with the length of the ear and the number of spikelets, which confirms the complex nature of the development of this indicator. Simultaneously, the weight of 1,000 grains has an inverse weak relationship with the length of the ear (r = -0.20) and the number of spikelets (r = -0.09), and no interdependence was observed with the number of grains in the ear during the study years (r = 0.00). Instead, a moderate positive relationship was established between the weight of 1,000 grains and the weight of 1 grain from the ear (r = 0.51). The obtained results showed that the development of productivity of soft winter wheat in the conditions of the Northern Forest-Steppe of Ukraine is determined by the complex interaction of hydrothermal conditions and genotypic features of varieties. The established differences between the years of research confirmed the determining role of weather factors in the implementation of the productive potential of culture, which is consistent with the conclusions of L. Qiao *et al.* (2022), which estimated the impact of weather conditions on the development of grain yields at the level of 32-39%.

Of particular importance in the development of productivity is the period of overwintering and restoration of spring vegetation. In the presented study, higher indicators of overwintering and yield were noted in 2025, which is associated with more favourable conditions for the winter period and a later restoration of plant vegetation. This is partially consistent with data by B.V. Blyzniuk *et al.* (2019), who noted that excessive lengthening of the winter dormancy period can lead to a decrease in plant viability. Simultaneously, the results confirmed that in the absence of extreme stresses, a longer winter period can contribute to better plant preservation and a more uniform restoration of spring growth. An important element of the yield structure is the number of spikelets in the ear, which determines the potential for grain development. As noted by V.V. Bazalii *et al.* (2024), to achieve a high level of yield, it is necessary to form 21-23 spikelets per ear. In the current study, the maximum values of this indicator were close to the specified level in a more favourable weather conditions in 2025, which indicates a significant impact of hydrothermal conditions during the period tillering – tubing on the development of generative organs. The results also confirmed that the weight of 1,000 grains is a sensitive indicator of growing conditions, especially during the grain filling period. Similar patterns were established by N. Zamlila *et al.* (2025), which showed that the variability of this indicator is largely determined by the conditions of the year and their interaction with the genotype. In the current study, higher weight values of 1,000 grains in 2025 were conditioned by more uniform moisture and moderate temperatures, while in 2024, lack of moisture and high temperatures led to the development of weak grains.

The results obtained are consistent with the data by I.V. Havryliuk & H.M. Kovalyshyna (2024), who also established a significant variability of elements of the structure of the crop of soft winter wheat depending on the genotype, environmental conditions, and their interaction. Their study confirmed statistically significant differences between varieties in terms of ear length, number of spikelets, grain weight per ear, and weight of 1,000 grains, which helped to identify genotypes with high stability of these traits. Similar patterns were found in the current study, where the level of manifestation of productivity elements varied significantly depending on the weather conditions of the year. This confirmed that the structural yield indicators are not only genotypic predestination, but also largely determined by hydrothermal growing conditions, which should be considered when selecting adaptive varieties for specific soil and climatic zones.

The obtained patterns are consistent with the results of L. Prysiazhniuk *et al.* (2022), who proved that the conditions of the growing area are one of the key factors of variability in grain yield and quality. This confirms that the effectiveness of implementing the potential of varieties largely depends on the compliance of their biological characteristics with specific soil and climatic conditions. In the context of current climate change, the results obtained are particularly relevant. According to A.M. Polyovyi *et al.* (2022), in the Forest-Steppe zone of Ukraine, there is a tendency to increase air temperature and decrease precipitation, which increases the risk of arid phenomena. M. Shtakal *et al.* (2022) noted that contemporary varieties are capable of generating a high level of productivity, but their stability depends on the weather conditions of the year. Thus, the results of the study confirm that the development of productivity of soft winter wheat is determined by the interaction of genotype and hydrothermal conditions, while the main periods are the development of generative organs and grain filling. The obtained data emphasise the need to select adaptive varieties and optimise technological elements of cultivation based on climate risks.

Conclusions

The study examined the influence of hydrothermal conditions on the duration of interphase periods of soft winter wheat development and the development of its productivity. It was found that the duration of ontogenesis phases significantly depends on weather conditions. In particular, in 2024/2025, compared to 2023/2024, the "sowing – germination" period was shorter by 3-5 days, the autumn vegetation lasted longer by 30-32 days, the winter rest time decreased by 15-20 days, and the "restoration of spring vegetation – earing" period was reduced from 62 to 46 days. This showed that a higher temperature background in autumn and spring accelerated the passage of plant development phases. The study found that with uniform moisture in May-June and moderate temperature conditions in 2025, plants formed a longer and more productive period of grain filling. Under these conditions, the average yield of varieties was 6.69 t/ha, which was 2.08 t/ha higher than in 2024, the average values of the ear length, the number of spikelets and grains in the ear, the weight of grain from the ear, and the weight of 1,000 grains were also higher. Critical for the development of the weight of 1,000 grains and overall productivity was the "earing – filling period of grain": lack of moisture and high temperatures at this time reduced the fullness of grain, while sufficient water supply contributed to its better filling.

The average weight of 1,000 grains for two years was 47.4 g, and the highest indicators of this feature were formed by the variety 'MIP Vyshyvanka', which indicates its ability to provide better grain fulfilment under different growing conditions. Correlation analysis showed a close positive relationship between the length of the ear and the number of spikelets ($r = 0.87$), the length of the ear and the number of grains ($r = 0.86$), and between the number of grains in the ear and the weight of one grain from the ear (r = 0.86). This confirms that the increase in the ear's linear dimensions was due to an increase in its grain density and grain weight. According to the aggregate indicators of productivity and yield, the varieties 'Tobak', 'MIP Valensiya' and 'Meskal' performed best, which formed the highest average yield over the years of research – 6.48, 6.35 and 6.16 t/ha, respectively. The variety 'MIP Vyshyvanka' was distinguished by the highest weight indicators of 1,000 grains, and the varieties 'Meskal' and 'Julia' – by the highest indicators of grain density content. This gives grounds to recommend 'Tobak', 'MIP Valensiya' and 'Meskal' as promising for growing in the conditions of the Northern Forest-Steppe of Ukraine, and the 'MIP Vyshyvanka' variety – as a valuable source material for selecting forms with high grain content. A promising area of further research is a comprehensive assessment of the interaction of genotype and hydrothermal conditions in long-term experiments. This is necessary to clarify the regularities of the development of winter wheat productivity in conditions of climate variability. It is expected that the results obtained will contribute to the identification of adaptive genotypes and optimisation of technological measures of cultivation.

Acknowledgements

None.

Funding

None.

Conflict of Interest

None.

References

[1] Adamenko, T. (2017). Agrometeorological features of the spring-summer period and their influence on agricultural crops. *Agronomist*, 3, 14-15.

[2] Bazalii, V.V., Lavrynenko, Y.O., Domaratskyi, E.O., & Panfilova, A.V. (2024). Problems and effectiveness of breeding of winter wheat varieties with increased environmental stability. *Factors in Experimental Evolution of Organisms,* 35, 13-17. doi: 10.7124/FEEO.v35.1651.

[3] Blyzniuk, B.V., Los, R.M., Demydov, O.A., Kyrylenko, V.V., Humeniuk, O.V., & Daniuk, T.A. (2019). The influence of weather conditions on the duration of particular vegetation periods and the yield of bread winter wheat in the Forest-Steppe and Polissia. *Myronivka Bulletin,* 8, 73-90.

[4] Convention on Biological Diversity. (1992, June). Retrieved from https://zakon.rada.gov.ua/laws/show/995_030#Text.

[5] Du, X., Gao, Z., Sun, X., Bian, D., Ren, J., Yan, P., & Cui, Y. (2022). Increasing temperature during early spring increases winter wheat grain yield by advancing phenology and mitigating leaf senescence. *Science of the Total Environment*, 812, article number 152557. doi: 10.1016/j.scitotenv.2021.152557.

[6] Hassona, M.M., Abd El-Aal, H.A., Morsy, N.M., & Hussein, A.M. (2024). Abiotic and biotic factors affecting crop growth and productivity: Unique Buckwheat production in Egypt. *Agriculture,* 14(8), article number 1280. doi: 10.3390/agriculture14081280.

[7] Havryliuk, I.V., & Kovalyshyna, H.M. (2024). Characteristics of soft winter wheat varieties by crop structure and grain quality indicators. *Ukrainian Black Sea Region Agrarian Science,* 28(4), 68-84. doi: 10.56407/bs.agrarian/4.2024.68.

[8] Kopecká, R., Kameniarová, M., Černý, M., Brzobohatý, B., & Novák, J. (2023). Abiotic stress in crop production. *International Journal of Molecular Sciences*, 24(7), article number 6603. doi: 10.3390/ijms24076603.

[9] Korkhova, M.M. (2019). Influence of sowing time and duration of winter rest on growth, development and yield of winter wheat plants. *Taurida Scientific Herald*, 110(1), 95-102. doi: 10.32851/2226-0099.2019.110-1.13.

[10] Lyfenko, S., Nakonechnyy, M., & Nargan, T. (2021). Peculiarities of the selection of soft winter steppe ecotype wheat varieties in connection with climate change in the conditions of Southern Ukraine. *Bulletin of Agricultural Science*, 99(3), 53-62. doi: 10.31073/agrovisnyk202103-07.

[11] Menzir, A., Firew, Y., Kassaye, M., & Mequanint, G. (2025). Yield performance and stability of durum wheat varieties in northwestern Ethiopia. *BMC Plant Biology,* 25(1), article number 1710. doi: 10.1186/s12870-025-07581-9.

[12] Meteoblue. (n.d.). Retrieved from https://lnk.ua/FOQvH4PRP.

[13] Mohammadi, R., Roostaei, M., Armion, M., Abdipour, M., Rahmati, M., & Shahbazi, K. (2025). Deciphering genotype× environment interaction for grain yield in durum wheat: An integration of analytical and empirical approaches for increased yield stability and adaptability. *European Journal of Agronomy,* 168, article number 127656. doi: 10.1016/j.eja.2025.127656.

[14] Monteleone, B., Borzí, I., Bonaccorso, B., & Martina, M. (2023). Quantifying crop vulnerability to weather-related extreme events and climate change through vulnerability curves. *Natural Hazards*, 116(3), 2761-2796. doi: 10.1007/s11069-022-05791-0.

[15] Myronivka Institute of Wheat named after V.M. Remeslo of NAAS of Ukraine. (2025). *Information on weather conditions and crop status of the Myronivka Wheat Institute named after V.M. Remesl of the NAAS of Ukraine on January 17, 2025*. Retrieved from https://mip.com.ua/novini/986-informatsiia-pohodnykh-umov-ta-stanu-posiviv-myronivskoho-instytutu-pshenytsi-imeni-v-m-remesla-naan-ukrainy-na-17-sichnia-2025-roku.

[16] Polyovyi, A.M., Bozhko, L.Yu., Barsukova, O.A., & Kostyukevych, T.K. (2022). The impact of climate warming on the productivity of eggplant and sweet pepper in the steppe zone of Ukraine. *Scientific Progress & Innovations,* 1, 29-37. doi: 10.31210/visnyk2022.01.03.

[17] Prysiazhniuk, L., Khomenko, T., Liashenko, S., & Melnyk, S. (2022). Productivity indicators of new winter soft wheat (*Triticum aestivum* L.) varieties depending on cultivation factors. *Plant Varieties Studying and Protection*, 18(4), 273-282. doi: 10.21498/2518-1017.18.4.2022.273989.

[18] Qiao, L., *et al.* (2022). Soil quality both increases crop production and improves resilience to climate change. *Nature Climate Change,* 12(6), 574-580. doi: 10.1038/s41558-022-01376-8.

[19] Rezaei, E.E., Webber, H., Asseng, S., Boote, K., Durand, J.L., Ewert, F., Martre, P., & MacCarthy, D.S. (2023). Climate change impacts on crop yields. *Nature Reviews Earth & Environment*, 4(12), 831-846. doi: 10.1038/s43017-023-00491-0.

[20] Shtakal, M., Holyk, L., Levchenko, O., Shpakovych, I., & Ivashchenko, S. (2022). Evaluation of winter wheat varieties and lines for stable yield and adaptability under climate change in the Forest-Steppe zone. *Bulletin of Agricultural Science*, 100(3), 62-69. doi: 10.31073/agrovisnyk202203-08.

[21] Stella, T., *et al.* (2023). Wheat crop traits conferring high yield potential may also improve yield stability under climate change. *In Silico Plants*, 5(2), article number diad013. doi: 10.1093/insilicoplants/diad013.

[22] Van Oort, P.A.J., Timmermans, B.G.H., Schils, R.L.M., & Van Eekeren, N. (2023). Recent weather extremes and their impact on crop yields of the Netherlands. *European Journal of Agronomy*, 142, article number 126662. doi: 10.1016/j.eja.2022.126662.

[23] Zamani, A., Emam, Y., & Edalat, M. (2024). Response of bread wheat cultivars to terminal water stress and cytokinin application from a grain phenotyping perspective. *Agronomy*, 14(1), article number 182. doi: 10.3390/agronomy14010182.

[24] Zamlila, N., Klymenko, O., Volohdina, H., & Zaika, Y. (2025). Variability and adaptability of winter soft wheat lines according to thousand-grain weight. *Scientific Horizons,* 28(11), 36-46. doi: 10.48077/scihor11.2025.36.

[25] Zubko, O.O., & Ivaniuk, M.F. (2023). *Efficiency of primary tillage systems for winter wheat after peas under the conditions of the Agronomic Research Station of NULES of Ukraine*. (Master's thesis, National University of Life and Environmental Sciences of Ukraine, Kyiv, Ukraine).

Тривалість вегетації та продуктивність пшениці м'якої озимої за різних погодних умов

Валерій Придатко
Аспірант
Національний університет біоресурсів і природокористування України
03041, вул. Героїв Оборони, 15, м. Київ, Україна
https://orcid.org/0009-0005-8997-9765
Ганна Ковалишина
Доктор сільськогосподарських наук, професор
Національний університет біоресурсів і природокористування України
03041, вул. Героїв Оборони, 15, м. Київ, Україна
https://orcid.org/0000-0002-2715-7679

Анотація. В умовах мінливості погодних факторів у зоні північного Лісостепу України актуальним є оцінювання впливу гідротермічних умов на формування продуктивності пшениці озимої. Метою дослідження було встановити вплив температурного режиму та вологозабезпечення в окремі періоди вегетації на формування маси 1000 зерен пшениці озимої. Дослідження проведено в польових умовах упродовж 2023-2025 рр. із використанням загальноприйнятих методик оцінювання елементів структури врожаю. Встановлено, що маса 1000 зерен істотно варіювала залежно від гідротермічних умов у період наливу зерна. У 2024 р. за дефіциту опадів у квітні-травні та підвищених температур у червні-липні (до 30-35 °C) спостерігалося скорочення тривалості періоду наливу зерна, що призвело до формування менш виповненого зерна та зниження маси 1000 зерен. Натомість у 2025 р. за більш рівномірного розподілу опадів у травні-червні (до 47,9-68,0 мм) і помірного температурного режиму забезпечувалося краще водопостачання рослин, що сприяло підвищенню інтенсивності фотосинтезу та накопиченню сухої речовини в зернівці. У результаті показник маси 1000 зерен підвищився з 46,8 до 47,4 г. Виявлено, що критичним періодом для формування цього показника є фаза колосіння – наливу зерна, під час якої поєднання високих температур і дефіциту вологи обмежує продуктивність рослин. Встановлено тісний зв'язок між погодними умовами та рівнем реалізації продуктивного потенціалу сортів. Практичне значення отриманих результатів полягає у можливості оптимізації строків сівби та підбору сортів із урахуванням їх реакції на гідротермічні умови, а також у коригуванні системи удобрення та вологозабезпечення з метою зменшення негативного впливу посушливих періодів на формування маси зерна. Отримані результати можуть бути використані агрономами та селекціонерами для підвищення стабільності врожайності пшениці озимої в умовах кліматичних змін

Ключові слова: гідротермічний режим, фенологічні фази розвитку, маса 1000 зерен, елементи продуктивності колоса, кореляційні зв'язки ознак, вологозабезпечення рослин

Received 19.12.2025 Revised 16.03.2026 Accepted 23.04.2026 Published: 30.04.2026

Vol. 22, No. 2
2026

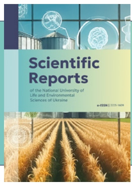

Scientific Reports of the National University of Life and Environmental Sciences of Ukraine

Journal homepage: https://scireports.com.ua/en e-ISSN 2223-1609

UDC 504.05:621.311.21:519.237 DOI: 10.31548/dopovidi/2.2026.120

Structuring of the scientific field of hydropower potential based on keyword analysis and hierarchical clustering

Yaroslav Adamenko*
Doctor of Technical Sciences, Professor
Ivano-Frankivsk National Technical University of Oil and Gas
76019, 15 Karpatska Str., Ivano-Frankivsk, Ukraine
https://orcid.org/0000-0001-5665-7958

Volodymyr Maikovych
Postgraduate Student
Ivano-Frankivsk National Technical University of Oil and Gas
76019, 15 Karpatska Str., Ivano-Frankivsk, Ukraine
https://orcid.org/0009-0007-6373-270X

Abstract. The relevance of this study stems from the need to systematise contemporary scientific approaches to assessing the environmentally safe utilisation of the hydropower potential of rivers. The environmental assessment of the implementation of renewable energy sources on water bodies lies at the intersection of hydrological, ecological, hydropower, technical and economic aspects. The aim of the study was to structure the scientific field of the environmentally safe use of hydropower potential based on keyword analysis, hierarchical clustering and the identification of interrelationships between the main thematic areas of research. Using the STATISTICA software, a statistical analysis of keyword clusters was conducted. For an in-depth analysis, a histogram, a dendrogram constructed using Ward's method, and a heat map of correlation links were applied. The information base consisted of 100 scientific publications from the last 20 years from 22 countries worldwide. During the study, a database of 454 keywords was compiled, followed by their preliminary normalisation, frequency analysis, and clustering. Twelve thematic clusters were identified, among which "hydropower systems and resources", "economics of natural resource use and energy", "hydrological characteristics and data", and "methodology and research tools" were dominant. It was established that the modern scientific field has a multi-level hierarchical structure and is characterised by close interaction between ecological, energy, hydrological, and economic domains. The results obtained confirmed the interdisciplinary nature of the research and demonstrated the appropriateness of applying a comprehensive approach to assessing the hydropower potential of

Suggested Citation:
Adamenko, Ya., & Maikovych, V. (2026). Structuring of the scientific field of hydropower potential based on keyword analysis and hierarchical clustering. *Scientific Reports of the National University of Life and Environmental Sciences of Ukraine*, 22(2), 120-134. doi: 10.31548/dopovidi/2.2026.120.

**Corresponding author*

rivers, taking into account natural, technical, environmental, and economic factors. The practical significance of the study lies in identifying shortcomings and unresolved aspects in scientific approaches to assessing the environmentally safe use of hydropower potential

Keywords: river systems; small hydropower; environmental safety; water resources; interdisciplinary research

Introduction

In the context of the rapid development of modern science, there has been a significant increase in the number of scientific publications, particularly in the fields of hydropower, ecology, and water resource management. Research is becoming distinctly interdisciplinary, combining hydrological, ecological, technical, economic, and climatic aspects. As a result, a complex and multidimensional scientific field is being formed, in which information is largely fragmented, and the connections between individual research areas are not always obvious. Under such conditions, bibliometric analysis methods, particularly keyword analysis and clustering, are gaining increasing relevance, as they make it possible to reveal the structure of scientific knowledge, identify the main thematic areas, and establish relationships between them.

Contemporary research in the fields of hydropower, water resources and ecology is characterised by an increasingly interdisciplinary approach, combining energy, hydrological, ecosystem, management and analytical aspects. In the latest scientific literature, hydropower is viewed not only as a source of renewable energy, but as a factor in the comprehensive transformation of river systems, influencing the hydrological regime, channel processes, biodiversity and water use. In particular, A. Kuriqi *et al*. (2021) demonstrated that even diversion and run-of-river small hydropower plants can significantly alter natural flow, disrupt ecological water flows and affect the trophic levels of river ecosystems.

Further development of this issue is presented in the work by A. Iho *et al*. (2023), where the sustainability of hydropower is analysed as the result of a balance between energy benefits, environmental constraints, legal norms and public acceptability. The authors demonstrated that the assessment of hydropower project prospects should not be narrowly technical but interdisciplinary, taking into account the conflict between energy production and the conservation of river ecosystems. In the same vein, F. He *et al*. (2024) synthesised global data on the impact of hydropower on river biodiversity and demonstrated that the main consequences are river fragmentation, barrier effects on species migration, and habitat alteration.

The current focus of research has shifted even further towards finding a compromise between energy efficiency and environmental safety. Ukrainian scientists have made a significant contribution to the development of this field. In the works of Ya. Adamenko & V. Maikovych (2025), L. Arkhypova *et al*. (2025) and V. Arkhypova *et al*. (2025), hydropower is considered as a component of the natural and technogenic safety of hydroecosystems. They also justified the need for an environmental assessment of the use of renewable energy sources, taking into account a basin-based approach.

At the same time, contemporary research into water resources is increasingly being integrated with energy and environmental issues. X. Yang *et al*. (2022), analysing water resources as hydropower potential, found that the leading themes are water scarcity, pressure on river basin systems, regional sustainability and multi-criteria assessment methods. They demonstrated that the scientific field is shifting from simple resource accounting to a comprehensive assessment of the limits of sustainable water use. A similar integrative logic was identified by Y. Lv *et al.* (2023), who, within the framework of the water-energy-food nexus concept, demonstrated that water, energy and food form an interdependent cycle, and research in this field is rapidly expanding thanks to cross-sectoral models and scenario analysis.

The methodological foundation for analysing such interdisciplinary fields in contemporary research is bibliometrics. N. Donthu *et al.* (2021) substantiated bibliometric analysis as a tool for identifying the intellectual structure of a scientific domain, its thematic clusters, the evolution of concepts, and scientific linkages. W.M. Lim *et al.* (2024) further clarified that the reliability of bibliometric conclusions largely depends on the integration of multiple databases, data cleaning, and the normalisation of author names, keywords, and sources. This perspective was deepened by M. Nowakowska (2025), who demonstrated that data preprocessing is not merely a technical detail but a critical stage that determines the accuracy of network maps, clustering, and the interpretation of results. The importance of the bibliometric approach for environmental issues was also confirmed in the work of R. Shu *et al.* (2024), which, based on studies of environmental safety network formation, showed that bibliometric analysis enables the identification of stages in the evolution of a scientific field, the core of key themes, emerging trends, and inter-thematic connections.

Thus, contemporary publications indicate that research in hydropower, water resources, and ecology is developing towards the integration of the ecosystem approach, basin management, and modern methods of scientific mapping. For this reason, the use of bibliometric analysis is appropriate for systematising the scientific field, identifying leading thematic clusters, and determining current trends in hydropower research and related environmental domains. Despite the active development of research and the availability of powerful analytical tools, the problem of the lack of a comprehensive structuring of the scientific field remains, particularly for Ukrainian-language publications. This necessitates the application of approaches that combine keyword normalisation with subsequent clustering to obtain a more reliable and generalised picture of the development of scientific research. Thus, the aim of the study was to systematise and structure the contemporary scientific field in the areas of hydropower, water resources, and ecology based on bibliometric analysis, using scientific mapping methods, in particular keyword normalisation and clustering, in order to identify the main thematic areas, relationships, and development trends in research.

Materials and Methods

Bibliometric analysis of scientific publications is one of the most important tools for studying the structure of contemporary scientific knowledge. Its application makes it possible to identify the main trends in the development of scientific research, determine leading thematic areas, and establish relationships between key concepts used in scholarly works. The methodology of the present study was based on a step-by-step bibliometric analysis of keywords from scientific publications, followed by their normalisation, quantitative processing, and clustering in order to structure the scientific field. The study comprised five stages.

The first stage involved the formation of a sample of scientific publications. For this purpose, a search for scientific sources was conducted in international scientometric databases, including Scopus, Web of Science, and Google Scholar. The search was carried out using the following keywords: "hydropower", "small hydropower", "hydropower potential", "water resources", "environmental safety", "environmental impact assessment", "monitoring", "environmental impact assessment", and others. The unit of analysis was a scientific article. For each publication, the following variables were recorded: author(s), year of publication, title, and keywords. The criteria for including articles in the sample were: scientific articles in peer-reviewed journals; relevance to the fields of hydropower, water resources, or environmental assessment;

and the presence of keywords. During the selection process, 58 Ukrainian and 42 scientific publications by authors from 22 countries were analysed, covering the period 2005-2025 and addressing issues of environmental safety in hydropower. As a result, a sample of 100 scientific publications was formed, from which 454 keywords were identified (Adamenko & Maikovych, 2026).

The second stage involved the normalisation of keywords. The aim of this stage was to identify and eliminate duplication of words and their synonymous fragmentation. Normalisation included: merging synonyms (for example: "small hydropower" = "mini hydropower plants"); reducing different grammatical forms to a base form (for example: "river", "rivers", "riverine" = "river"); and unifying variations in wording (for example: "Prut River basin", "Middle Dnipro", "rivers of Ukraine" = "river basins"). The processing was carried out through a combined approach involving manual expert normalisation using an agreed glossary of terms (thesaurus). This stage made it possible to form a unified list of keywords suitable for further statistical analysis. The collected data were systematised in tabular form using Microsoft Excel. In the resulting table, each scientific source corresponds to a set of keywords reflecting the main aspects of the study, including the hydropower potential of rivers, the development of small hydropower, environmental constraints on the use of water resources, as well as the application of geoinformation technologies in water system research.

The third stage – constructing the data matrix. Based on the normalised keywords, a species trait matrix was formed:

$$X = \{x_{i,j}\}, i = 1, \dots, n; j = 1, \dots, m, \quad (1)$$

where n – number of publications; m – number of keywords; $x_{ij} \in \{0.1\}$ – a binary indicator of the presence of keyword j in publication i. The matrix values are binary (0/1). A value of 1 indicates that the keyword is present in the publication; a value of 0 indicates that the keyword is absent. The structure of the binary matrix enabled the formalisation of textual information and subsequent statistical processing of the data, the determination of the frequency of use of key terms, and the performance of a cluster analysis of research themes. This stage allowed for the creation of a structured database, which facilitated the effective subsequent analysis and visualisation of scientific trends.

The fourth stage of the research involved frequency analysis of keywords. The unit of measurement was the keyword, and the indicator was the number of publications in which it appeared, calculated using the formula:

$$f_j = \sum_{i=1}^{n} x_{ij}, \quad (2)$$

where f_j – the number of publications containing the keyword j. No threshold filtering was applied – all keywords were included in the analysis, which allowed the structure of the field under study to be preserved in its entirety. Frequency analysis was used to identify the most frequently used terms, to outline the structure of the research, and to prepare the data for subsequent clustering. It also made it possible to assess the importance of each term, track changes in research interests over time, and identify the most relevant research areas for further analysis.

The fifth stage – cluster analysis – aimed to group keywords into thematic clusters, identify the structure of the research field, and establish interrelationships between research areas. To analyse the structure of the scientific field, hierarchical agglomerative cluster analysis was applied, based on the use of Euclidean distance as a measure of similarity and Ward's method as the criterion for cluster merging. Euclidean distance was calculated using the formula:

$$d(x, y) = \sqrt{\sum_{k=1}^{m}(x_k - y_k)^2}, \quad (3)$$

where x and y – feature vectors (keywords or clusters).

Clustering was performed using Ward's method, which minimises the increase in intra-cluster variance according to the formula:

$$\Delta E = \frac{n_A \times n_B}{n_A + n_B} \times \|\bar{x}_A - \bar{x}_B\|^2, \qquad 4)$$

where n_A, n_B – cluster sizes, $\bar{x}_A$ $\bar{x}_B$ – cluster centres; || × || – Euclidean norm.

Variables were standardised prior to clustering. Ward's method ensured the formation of compact and homogeneous clusters and helped to avoid the "chain clustering" effect. This approach enabled a clear structuring of the scientific field of hydropower and environmental safety, identifying the main thematic groups that interact most closely with one another. To interpret and visualise the research results, a histogram was used to display the frequency distribution of keywords and clusters; a dendrogram to display the hierarchical structure of the clusters; and a heatmap to display the correlation matrix between clusters. The data were visualised using STATISTICA (for constructing the dendrogram) and Python (for constructing the heatmap). The bibliometric analysis methods applied, including keyword normalisation, frequency analysis and clustering, ensured the reliability of the classification, allowing for an accurate interpretation of the main trends and directions in research on hydropower potential and the environmental safety of water resources.

Results and Discussion

The analysis of keyword frequency showed that the most commonly used terms in scientific publications are "hydropower", "capacity", "ecology", "electricity", "small hydropower", and "hydropower potential". This indicates that researchers primarily focus on assessing the energy characteristics of water resources and determining their potential use within renewable energy systems. Based on the conducted frequency analysis of keywords, twelve thematic clusters were identified, reflecting the main directions of scientific research in the field of small hydropower and environmental safety. Each cluster represents specific aspects of the studied topics and includes keywords derived from scientific publications. This makes it possible to assess the structure of the scientific field and determine which research aspects are the most significant.

Cluster 1. Hydrological characteristics and data. This cluster covers research into the quantitative and qualitative parameters of water bodies, including hydrological regime, discharge, water levels and seasonal dynamics. It forms the basis for all research into water systems, as it provides the primary information framework. This cluster includes the following keywords: river discharge, river flow, water level, hydrological regime, water consumption, floods, low water, hydrological data, etc.

Cluster 2. Geographic scope. This cluster reflects the spatial context of the research and includes an analysis of territorial characteristics, regional differences and the geographical conditions shaping natural processes. This cluster includes the following keywords: Carpathian region, Ukraine, Dniester basin, Carpathian Foothills, regional characteristics, etc.

Cluster 3. River basins. This cluster covers research into river basins as integrated natural and territorial systems. It encompasses water resource management, the basin approach and ecosystem interactions. This cluster includes the following keywords: river basin, basin management, catchment, river system, Danube basin, Prut basin, etc.

Cluster 4. Hydropower systems and resources. This cluster covers research into hydropower potential, the operation of hydropower plants and the assessment of hydropower resources. It is of key importance for the development of renewable energy. Characteristic keywords: hydropower potential, hydropower plants, small hydropower plants, energy resources, hydropower, hydropower systems, etc.

Cluster 5. Environmental monitoring and control – includes systems for monitoring the state of the environment, the collection and analysis of environmental data, and the monitoring of pollution levels. This cluster includes the following keywords: environmental monitoring, water quality control, observation, pollution, automated stations, environmental indicators.

Cluster 6. Environmental protection and safety – covers research aimed at reducing negative environmental impacts and ensuring environmental safety. Examples of keywords: environmental safety, nature conservation, environmental protection, anthropogenic impact, environmental risks, etc.

Cluster 7. Engineering and technical aspects of systems. This cluster includes technical solutions, engineering structures and technologies related to water and energy systems. Examples of keywords: engineering systems, hydraulic structures, technical solutions, design, system optimisation, infrastructure, etc.

Cluster 8. Environmental assessment and impact – these are procedures for assessing the impact of activities on the environment, analysing environmental consequences and forecasting changes. This cluster includes the following keywords: environmental impact assessment, environmental assessment, impact on ecosystems, impact analysis, environmental criteria.

Cluster 9. Climatic processes and climate change. This cluster includes research into climate change and its impact on water resources and ecosystems. Examples of keywords: climate change, climatic factors, temperature, precipitation, climate models, global warming, etc.

Cluster 10. Renewable energy – this cluster covers research into alternative energy sources, including hydro, solar and wind energy. This cluster includes the following keywords: renewable energy sources, green energy, solar energy, wind energy, small hydropower.

Cluster 11. Economics of natural resource use and energy. This cluster reflects the economic aspects of natural resource use and energy development. Examples of keywords: economic efficiency, natural resource use, energy market, investment, economic assessment, tariff policy, etc.

Cluster 12. Methodology and research tools – includes methods, models and data analysis tools used in research. This cluster includes the following keywords: mathematical modelling, statistical analysis, GIS technologies, remote sensing, machine learning, research methods, etc.

Individual clusters of keywords reflect thematic areas of research, in particular: hydropower systems and resources, the economics of natural resource use and energy, hydrological characteristics and data, methodology and research tools, engineering and technical aspects of systems, environmental protection and ecological safety, river basins, renewable energy, environmental assessment and impact, environmental monitoring and control, geographical territory, climatic processes and climate change. A histogram was constructed based on the identified clusters, reflecting the quantitative distribution of thematic clusters of keywords within the studied corpus of scientific publications; it serves as an important tool for assessing the structure of contemporary scientific research in the fields of ecology, hydrology and energy (Fig. 1). It allows not only the identification of dominant areas, but also the assessment of the balance between different thematic blocks that form the overall picture of research activity. The analysis of the histogram shows that the most represented cluster is "Hydropower systems and resources", which has the highest value among all clusters. This indicates the high relevance of research in the field of hydropower potential utilisation, optimisation of hydropower plant operation, and assessment of the resource base. The dominance of this cluster may be associated with the active development of renewable energy and the need to transition to more environmentally safe energy sources. The second position is occupied by the cluster "Economics of natural resource use and energy", highlighting the importance of economic aspects in research. This points to the integration of economic analysis into natural science and technical studies, which is a characteristic feature of the modern scientific approach to sustainable development. A significant share is also occupied by the clusters "Hydrological characteristics and data" and "Methodology and research tools".Their high representation indicates considerable attention to data collection, analysis, and interpretation, as well as to the development of new research methods. This forms the foundation for ensuring the reliability and validity of scientific results. The cluster "Engineering and technical aspects of systems" reflects the practical orientation of research, encompassing issues of design, optimisation, and operation of technical systems related to water resources and energy.

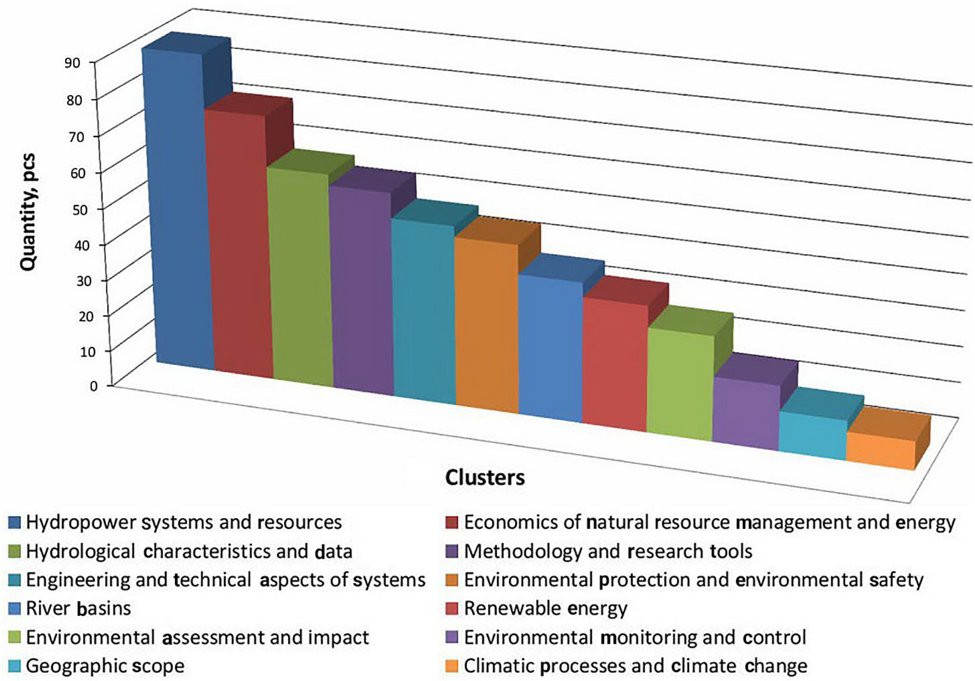

Figure 1. *Histogram of the cluster distribution*

Source: compiled by the authors

The cluster "Environmental protection and ecological safety" demonstrates a moderate level of representation, indicating a steady interest in environmental issues. This area is an integral component of most studies and is often integrated with other clusters. The clusters "River basins" and "Renewable energy" show somewhat lower values but remain important research directions, reflecting both natural science aspects and current energy trends. Less represented are the clusters "Environmental assessment and impact" and "Environmental monitoring and control", which may indicate their integration into other research areas or their relatively narrow specialisation. The lowest frequency is observed for "Geographic scope" and "Climatic processes and climate change". This may be because these areas often serve as supporting or contextual elements in studies rather than primary focuses. Overall, the histogram demonstrates an uneven distribution of clusters, with both dominant and peripheral research areas. This makes it possible to conclude that energy and hydrological studies are prioritised, alongside the importance of integrating economic and environmental aspects. The obtained results confirm the interdisciplinary nature of modern research, combining natural, technical, and socio-economic components. Such a structure is characteristic of comprehensive studies aimed at addressing global environmental and energy challenges.

Analysing the structure of the scientific field using hierarchical agglomerative cluster analysis resulted in a dendrogram (Fig. 2). It reflects the hierarchical structure of similarity between thematic clusters, allowing a visual assessment of how different research areas are interconnected. The dendrogram makes it possible not only to identify groups of terms with the greatest similarity but also to distinguish key thematic blocks at different levels of the hierarchy. Its analysis enabled a detailed characterisation of the structure of the studied domain, contributing to a deeper understanding of the relationships between various aspects of hydropower and environmental safety at different stages of research.

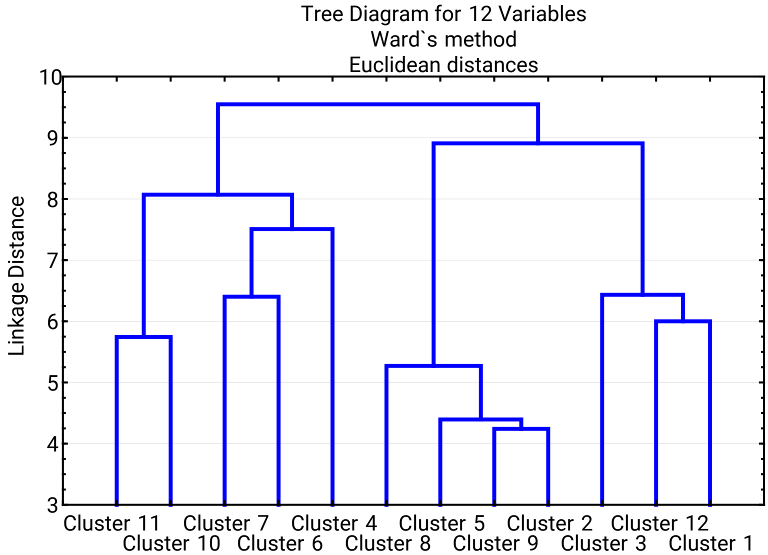

Figure 2. *Dendrogram of keyword clusters (using Ward's method)*

Note: Cluster 1 – Hydrological characteristics and data; Cluster 2 – Geographic scope; Cluster 3 – River basins; Cluster 4 – Hydropower systems and resources; Cluster 5 – Environmental monitoring and control; Cluster 6 – Environmental protection and ecological safety; Cluster 7 – Engineering and technical aspects of systems; Cluster 8 – Environmental assessment and impact; Cluster 9 – Climatic processes and climate change; Cluster 10 – Renewable energy; Cluster 11 – Economics of natural resource use and energy; Cluster 12 – Methodology and research tools

Source: compiled by the authors

At the lowest level of clustering (distance 3-5), the most homogeneous groups are formed. In particular, a close relationship is observed between "Climatic processes and climate change" and "Geographic scope". This is explained by the fact that climatic phenomena are directly linked to spatial characteristics, and their study is traditionally conducted within a geographical context. Another example is the merging of "Environmental monitoring and control" with "Environmental assessment and impact". Such interaction is logical, as monitoring serves as a tool for data collection, whilst assessment is the result of their analysis. This indicates the methodological unity of these fields.

At the next level (5-7), cluster aggregation occurs. An ecological-climatic block is formed, combining environmental assessment, monitoring, and climatic and geographical aspects. This block reflects the modern approach to studying natural systems as complex and interconnected. In parallel, a hydrological-methodological cluster is formed, including "Hydrological characteristics and data", "River basins", and "Methodology and research tools". This highlights the fundamental role of hydrology as a core science providing the empirical and methodological basis for research. A separate energy-economic block is also distinguished, combining "Renewable energy" and "Economics of natural resource use". This combination reflects contemporary trends in integrating economic mechanisms into the fields of energy and resource management. It emphasises the importance of linking energy and economic aspects to ensure sustainable development, facilitating the efficient use of renewable energy sources and the optimisation of natural resource consumption.

At a higher level of clustering (7-9), a technical-ecological block is formed, including "Hydropower systems and resources", "Engineering and technical aspects of systems", and "Environmental protection and ecological safety". This indicates the applied nature of research aimed at developing technological solutions while considering environmental constraints. At the highest level of the hierarchy (above 9), all clusters are integrated into a single system, confirming the integrity of the studied field and its interdisciplinary nature. It was established that none of the areas exists in isolation; rather, they all form an interconnected scientific system. Thus, the conducted cluster analysis made it possible to identify a clear hierarchical structure of research, determine key thematic blocks, and establish relationships between them. At the lower level of clustering, homogeneous pairs of thematic areas were formed; at the intermediate level, integrated ecological-climatic, hydrological-methodological, and energy-economic blocks emerged; and at the higher level, a generalised technical-ecological block was identified. Overall, all clusters are united into a single interdisciplinary scientific system. The obtained results may be used for further planning of scientific research, the development of interdisciplinary approaches, and the optimisation of the structure of scientific studies.

As a result of constructing the heatmap (Fig. 3), relationships between thematic clusters of scientific research were visualised. The heatmap illustrates correlation relationships between the main directions, where positive values indicate the co-occurrence of clusters within publications, while negative values indicate their mutual independence or opposition. In this case, the variables are the thematic clusters of keywords that characterise scientific directions. The values in the matrix reflect the degree of correlation between clusters: positive values indicate joint representation in studies, whereas negative values indicate independence or contrast between them. As can be seen in the figure, the colour scale ranges from low, including negative values (dark purple and blue shades), indicating inverse or weak relationships, to high positive values (yellow shades), which characterise stronger interactions between clusters. Maximum values (close to 1) are observed along the main diagonal, which is expected, as each cluster is perfectly correlated with itself. The analysis of off-diagonal elements revealed a complex and uneven network of inter-cluster relationships. Among the identified dependencies, moderate positive correlations can be observed between the clusters "Environmental assessment and impact" and "Environmental monitoring and control". This is explained by the fact that environmental impact assessment largely relies on monitoring data, while monitoring results are used to refine and verify impact assessments. It is also important to note the presence of relationships between the clusters "Renewable energy", "Hydropower systems and resources", and "Economics of natural resource use and energy", indicating the integration of technical, resource, and economic aspects in contemporary research, in line with the concept of sustainable development. A noticeable relationship is also observed between the clusters "Climatic processes and climate change" and "Hydrological characteristics and data", although the strength of this connection is moderate or relatively low; however, this does not diminish their conceptual interdependence. At the same time, some clusters demonstrate weak or negative relationships. In particular, "River basins" show a low level of correlation with economic and energy clusters, which may indicate their predominantly descriptive or geographical nature. Similarly, engineering and technical aspects are partially isolated from environmental studies, pointing to a certain degree of disciplinary fragmentation.

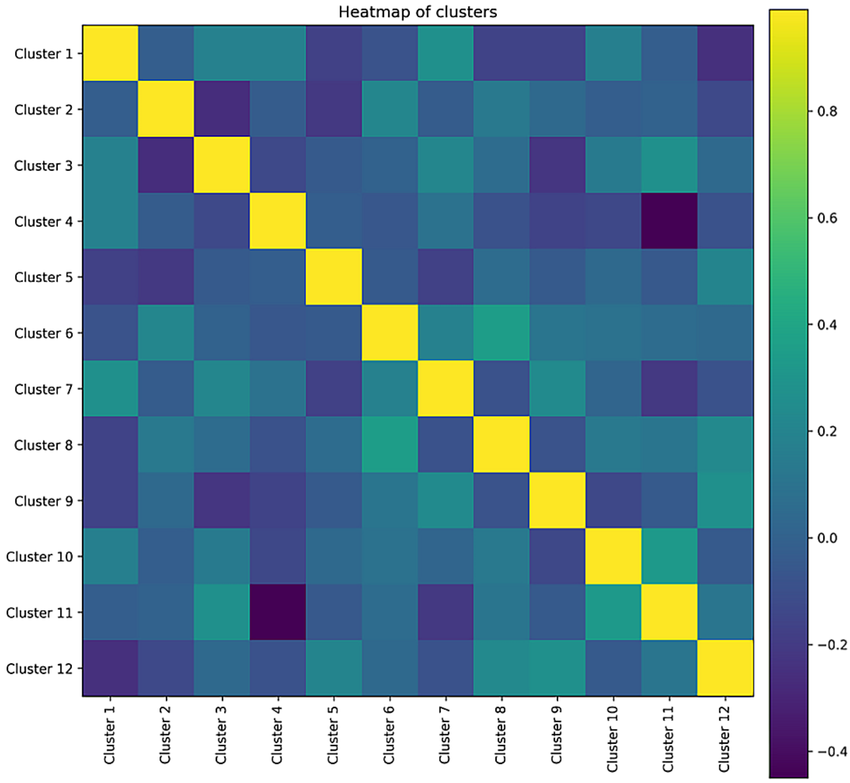

***Figure 3.** Heatmap of keyword clusters*

Note: Cluster 1 – Hydrological characteristics and data; Cluster 2 – Geographic scope; Cluster 3 – River basins; Cluster 4 – Hydropower systems and resources; Cluster 5 – Environmental monitoring and control; Cluster 6 – Environmental protection and ecological safety; Cluster 7 – Engineering and technical aspects of systems; Cluster 8 – Environmental assessment and impact; Cluster 9 – Climatic processes and climate change; Cluster 10 – Renewable energy; Cluster 11 – Economics of natural resource use and energy; Cluster 12 – Methodology and research tools
Source: compiled by the authors

Based on the structure of the heatmap, several functional blocks can be identified:

1) a natural–hydrological block, including "River basins", "Geographic scope", and "Hydrological characteristics";

2) an energy–economic block, combining "Renewable energy", "Hydropower", and "Economics of natural resource use";

3) an environmental block, consisting of "Environmental assessment", "Monitoring", and "Environmental protection";

4) a methodological block, which performs an integrative function and ensures interconnections between different thematic areas. The cluster "Methodology and research tools" plays an important role, as it is linked to a number

of other clusters, confirming the universality of modern research methods applied across various scientific domains.

The resulting heatmap can be used as a tool for the strategic planning of scientific research, as it makes it possible to identify the most integrated areas (in particular, "environmental assessment – monitoring", "energy – economics"), which should be developed as interdisciplinary research; to detect weakly connected or relatively isolated clusters that represent potential research gaps; to justify priority research directions by focusing efforts on key interconnections; and to define the role of the methodological cluster as an integrating foundation for comprehensive studies.

The obtained results of the bibliometric analysis confirm that the modern scientific field in hydropower, water resources, and ecology is formed as a complex interdisciplinary system. Similar conclusions are presented in the work of M. Aria & C. Cuccurullo (2017), which demonstrated that the application of scientific mapping tools makes it possible to identify the structure of research and key thematic clusters. In the present study, a similar approach was applied, but it was extended through keyword normalisation, which improved the accuracy of clustering. A comparison with the study by A. Duran-Sanchez *et al.* (2018) indicates that contemporary research is dominated by themes of sustainable development, resource management, and environmental safety. In the presented cluster model, these areas are reflected in the corresponding thematic blocks ("River basins", "Environmental safety", "Environmental monitoring"), confirming the consistency of the obtained results with international trends.

A significant development of bibliometric methods is presented in the work of N. Donthu *et al.* (2021), which emphasises the importance of combining different approaches, including keyword co-occurrence analysis, citation analysis, and clustering, for a comprehensive study of scientific fields. A similar integrated approach was implemented in the present study. This made it possible not only to identify thematic clusters but also to establish relationships between them, in line with contemporary methodological approaches in bibliometrics. Hierarchical clustering methods are widely applied in modern research on energy and ecology. In particular, N. J. van Eck & L. Waltman (2017) demonstrated that cluster analysis based on relationships between publications (especially citation links) allows for effective structuring of scientific domains and the identification of thematic research groups. In the present study, the use of Ward's method, which minimises within-cluster variance, ensured the formation of clear and logically interpretable clusters, consistent with modern approaches to the analysis of bibliometric data.

Among the key directions of contemporary research are water resource management, assessment of water capacity of territories, environmental monitoring, and the pursuit of sustainable development. This was clearly demonstrated in the bibliometric study by X. Yang *et al.* (2022), which focused on key indicators of water ecosystem development in terms of their capacity to meet human needs. In the present work, these directions are represented by corresponding thematic clusters, confirming the validity and relevance of the obtained structure of the scientific field. An important aspect of contemporary scientific research in the field of hydropower is its interdisciplinary nature. In particular, L. Leydesdorff *et al.* (2019) showed that most research areas emerge at the intersection of ecology, energy, and economics. This conclusion is also confirmed in the present study through the formation of integrated clusters such as "Renewable energy", "Economics of natural resource use", and "Hydropower". The obtained results are also consistent with modern research in the field of renewable energy, particularly the work of P. Kut & K. Pietrucha-Urbanik (2023), which demonstrates that the development of renewable energy is closely linked to environmental constraints, issues of sustainable development, and resource efficiency. In the current cluster structure, this is reflected in the close relationships between thematic blocks related to renewable energy, environmental safety, and the economics of natural resource use, confirming the interdisciplinary nature of the research problem.

Studies by Ukrainian scholars D.V. Stefanyshyn & Y.S. Vlasiuk (2019), as well as Y.S. Vlasiuk & D.V. Stefanyshyn (2019), emphasised the need to improve environmental impact assessment procedures, particularly by accounting for cumulative effects and improving the quality of input data. In the present study, this is reflected in the formation of the clusters "Environmental assessment" and "Environmental monitoring", further confirming the relevance of the obtained results. At the same time, the works of D.A. Szatten *et al.* (2025) focus on the basin approach and hydrological characteristics of river systems. In this study, these approaches are represented in the clusters "Hydrological characteristics" and "River basins".

In summary, the obtained results reflect contemporary trends in the development of scientific research in the field under study and confirm its interdisciplinary nature. The identified relationships between thematic clusters indicate the systemic nature of scientific knowledge and its orientation towards addressing complex environmental and energy challenges. The resulting structure of the scientific field demonstrates coherence between individual research areas and confirms their complementary nature. This indicates the gradual formation of an integrated approach to studying issues related to water resource use and the development of energy systems, taking into account environmental constraints.

Conclusions

As a result of the study, a comprehensive structuring of the scientific field in the areas of hydropower, ecology, and natural resource use was carried out based on bibliometric keyword analysis using normalisation, frequency analysis, hierarchical clustering, and visualisation. The bibliometric analysis confirmed the pronounced interdisciplinary nature of contemporary research, which is formed at the intersection of hydrology, ecology, energy, and economics. The keyword normalisation stage revealed an important pattern: without the unification of terminology, particularly in Ukrainian-language sources, fragmentation of the scientific field occurs. Normalisation made it possible to develop a consistent semantic structure and to increase the reliability of further analysis. Frequency analysis showed the dominance of studies related to hydropower, energy potential, and environmental aspects of water resource use. This indicates the orientation of modern science towards issues of energy efficiency and environmental safety.

Hierarchical cluster analysis revealed a multi-level structure of the scientific field. At the lowest level, homogeneous thematic pairs emerged (monitoring – assessment, climate – geography, hydrology – basins), reflecting the natural interrelationships between research areas. At the intermediate level, these were grouped into functional blocks: ecological-climatic, hydrological-methodological, and energy-economic. At the highest level, an integrated technical-ecological block emerged, indicating a combination of applied and ecological aspects of research. The study also confirmed the role of methodological approaches as an integrating element that influences the degree of proximity between research areas. Correlational patterns were also identified: strong links between environmental assessment and monitoring, the integration of energy and economic research, and the dependence of hydrological processes on climatic factors. At the same time, weakly related research areas were identified, indicating the presence of fragmentation and potential research gaps in the field under study.

The limitations of the study relate to the sample size (100 publications), the possible subjective influence during keyword normalisation, and the use of a binary matrix that does not account for the weight of terms. Furthermore, the absence of a temporal analysis limited the assessment of the dynamics of research areas' development. This may affect the granularity of the results, but does not alter the general patterns identified. Prospects for further research lie in expanding the sample, integrating bibliometrics with network analysis and machine learning methods, applying dynamic analysis and weighting coefficients, and developing automated approaches to terminology normalisation. It is expected that these steps will allow for a more detailed study of the evolution of scientific fields, as well as the identification of new links between hydropower and environmental aspects. Particularly promising are interdisciplinary studies at the intersection of hydropower, ecology, economics and climate change, which may contribute to the development of more effective strategies for the sustainable use of water resources and the reduction of negative environmental impacts.

Acknowledgements

None.

Funding

None.

Conflict of Interest

None.

References

[1] Adamenko, Ya., & Maikovych, V. (2025). Analysis of scientific and practical studies on hydropower risks associated with the construction of small hydropower plants in the tourist and recreational regions of the Ukrainian Carpathians. *Visnyk of Lviv State University of Life Safety*, 32, 7-19. doi: 10.32447/20784643.32.2025.01.

[2] Adamenko, Ya., & Maikovych, V. (2026). *100 articles* [XLSX]. Retrieved from https://docs.google.com/spreadsheets/d/1dW62OUbitK0x5rpqw_fmCfCo9sLdo_GX/edit?gid=807718291#gid=807718291.

[3] Aria, M., & Cuccurullo, C. (2017). Bibliometrix: An R-tool for comprehensive science mapping analysis. *Journal of Informetrics*, 11(4), 959-975. doi: 10.1016/j.joi.2017.08.007.

[4] Arkhypova, L., Korchemlyuk, M., Rashevska, H., Vynnychenko, I., & Tyshchuk, I. (2025). Practical aspects of environmental assessment of water bodies transformation. *Scientific Horizons*, 28(5), 65-78. doi: 10.48077/scihor5.2025.65.

[5] Arkhypova, V., Volkova, V., & Hruzdieva, O. (2025). Problems of natural waters in Ukraine and ways to address them. *SWorldJournal*, 2(33-02), 280-293. doi: 10.30888/2663-5712.2025-33-02-039.

[6] Donthu, N., Kumar, S., Mukherjee, D., Pandey, N., & Lim, W.M. (2021). How to conduct a bibliometric analysis: An overview and guidelines. *Journal of Business Research*, 133, 285-296. doi: 10.1016/j.jbusres.2021.04.070.

[7] Duran-Sanchez, A., Alvarez-Garcia, J., & del Río-Rama, M.D.I.C. (2018). Sustainable water resources management: A bibliometric overview. *Water*, 10(9), article number 1191. doi: 10.3390/w10091191.

[8] He, F., Zarfl, C., Tockner, K., Olden, J.D., Campos, Z., Muniz, F., Svenning, J.-C., & Jähnig, S.C. (2024). Hydropower impacts on riverine biodiversity. *Nature Reviews Earth & Environment*, 5, 755-772. doi: 10.1038/s43017-024-00596-0.

[9] Iho, A., Soininen, N., Vehviläinen, I., Koljonen, S., Artell, J., & Belinskij, A. (2023). Rivers under pressure: Interdisciplinary feasibility analysis of sustainable hydropower. *Environmental Policy and Governance*, 33(2), 191-205. doi: 10.1002/eet.2013.

[10] Kuriqi, A., Pinheiro, A.N., Sordo-Ward, A., Bejarano, M.D., & Garrote, L. (2021). Ecological impacts of run-of-river hydropower plants – current status and future prospects on the brink of energy transition. *Renewable and Sustainable Energy Reviews*, 142, article number 110833. doi: 10.1016/j.rser.2021.110833.

[11] Kut, P., & Pietrucha-Urbanik, K. (2024). Bibliometric analysis of renewable energy research on the example of the two European countries: Insights, challenges, and future prospects. *Energies*, 17(1), article number 176. doi: 10.3390/en17010176.

[12] Leydesdorff, L., Wagner, C.S., & Bornmann, L. (2019). Interdisciplinarity as diversity in citation patterns among journals: Rao-Stirling diversity, relative variety, and the Gini coefficient. *Journal of Informetrics*, 13(1), 255-269. doi: 10.1016/j.joi.2018.12.006.
[13] Lim, W.M., Kumar, S., & Donthu, N. (2024). How to combine and clean bibliometric data and use bibliometric tools synergistically: Guidelines using metaverse research. *Journal of Business Research*, 182, article number 114760. doi: 10.1016/j.jbusres.2024.114760.
[14] Lv, Y., Yuan, M., Zhou, X., Wang, Y., & Qu, X. (2023). The water-energy-food nexus: A systematic bibliometric analysis. *Environmental Science and Pollution Research*, 30, 121354-121369. doi: 10.1007/s11356-023-29863-1.
[15] Nowakowska, M. (2025). A comprehensive approach to preprocessing data for bibliometric analysis. *Scientometrics*, 130(9), 5191-5225. doi: 10.1007/s11192-025-05415-x.
[16] Shu, R., Ma, G., Zou, Y., Guo, N., Su, H., & Zhang, G. (2024). Bibliometric analysis of ecological security pattern construction: Current status, evolution, and development trends. *Ecological Indicators*, 169, article number 112754. doi: 10.1016/j.ecolind.2024.112754.
[17] Stefanyshyn, D.V., & Vlasiuk, Y.S. (2019). Some critical comments on the quality of environmental impact assessment reports for small hydropower plants in Ukraine. *Environmental Safety and Natural Resources*, 32(4), 43-59. doi: 10.32347/2411-4049.2019.4.43-59.
[18] Szatten, D.A., Obodovskyi, O., & Brzezinska, M. (2025). Erosive stability channel factor for Brda River (Poland): A key assessment of the human impact of the catchment changes. *International Journal of Sediment Research*, 40(1), 146-157. doi: 10.1016/j.ijsrc.2024.11.002.
[19] van Eck, N.J., & Waltman, L. (2017). Citation-based clustering of publications using CitNetExplorer and VOSviewer. *Scientometrics*, 111(2), 1053-1070. doi: 10.1007/s11192-017-2300-7.
[20] Vlasiuk, Y.S., & Stefanyshyn, D.V. (2019). On some problems of environmental impact assessment of small hydropower plants in Ukraine. *Environmental Safety and Natural Resources*, 31(3), 79-92. doi: 10.32347/2411-4049.2019.3.79-92.
[21] Yang, X., Sun, B., Lei, S., Li, F., & Qu, Y. (2022). A bibliometric analysis and review of water resources carrying capacity using René Descartes's discourse theory. *Frontiers in Earth Science*, 10. doi: 10.3389/feart.2022.970582.

Структуризація наукового поля гідроенергетичного потенціалу на основі аналізу ключових слів та ієрархічної кластеризації

Ярослав Адаменко
Доктор технічних наук, професор
Івано-Франківський національний технічний університет нафти і газу
76019, вул. Карпатська, 15, м. Івано-Франківськ, Україна
https://orcid.org/0000-0001-5665-7958
Володимир Майкович
Аспірант
Івано-Франківський національний технічний університет нафти і газу
76019, вул. Карпатська, 15, м. Івано-Франківськ, Україна
https://orcid.org/0009-0007-6373-270X

Анотація. Актуальність дослідження зумовлена необхідністю систематизації сучасних наукових підходів до оцінювання екологічно безпечного використання гідроенергетичного потенціалу річок. Екологічне оцінювання впровадження відновлюваних джерел енергії на водних об'єктах перебуває в полі міждисциплінарного поєднання гідрологічних, екологічних, гідроенергетичних, технічних та економічних аспектів. Метою роботи стала структуризація наукового поля екологічно безпечного використання гідроенергетичного потенціалу на основі аналізу ключових слів, ієрархічної кластеризації та виявленням взаємозв'язків між основними тематичними напрямами досліджень. Використовуючи програмний продукт STATISTICA був проведений статистичний аналіз кластерів ключових слів. Для поглибленого аналізу застосовано гістограму, дендрограму, побудовану методом Варда, та теплову карту кореляційних зв'язків. Інформаційну базу становили 100 наукових публікацій за останні 20 років із 22 країн світу. У процесі дослідження сформовано базу даних із 454 ключових слів, проведено їх попередню нормалізацію, частотний аналіз і кластеризацію. Виокремлено 12 тематичних кластерів, серед яких домінують «гідроенергетичні системи та ресурси», «економіка природокористування та енергетики», «гідрологічні характеристики та дані», «методологія та інструменти досліджень». Встановлено, що сучасне наукове поле має багаторівневу ієрархічну структуру та характеризується тісною взаємодією між екологічними, енергетичними, гідрологічними й економічними напрямами. Отримані результати підтвердили міждисциплінарний характер досліджень і засвідчили доцільність використання комплексного підходу до оцінювання гідроенергетичного потенціалу річок з урахуванням природних, технічних, екологічних та економічних чинників. Практичне значення дослідження полягає у ідентифікації недоліків та невирішених аспектів у наукових підходах до оцінки екологічно безпечного використання гідроенергетичного потенціалу

Ключові слова: річкові системи; мала гідроенергетика; екологічна безпека; водні ресурси; міждисциплінарні дослідження

Received 05.01.2026 Revised 02.04.2026 Accepted 23.04.2026 Published: 30.04.2026

Vol. 22, No. 2
2026

Scientific Reports of the National University of Life and Environmental Sciences of Ukraine

Journal homepage: https://scireports.com.ua/en e-ISSN 2223-1609

UDC 636.084.4:547.495.9 DOI: 10.31548/dopovidi/2.2026.135

Practical considerations in the selection of creatine forms for calf feeding

Dmytro Nosevych*
PhD in Agricultural Sciences, Associate Professor
National University of Life and Environmental Sciences of Ukraine
03041, 15 Heroiv Oborony Str., Kyiv, Ukraine
https://orcid.org/0000-0003-2495-2084

Tetiana Antoniuk
PhD in Agricultural Sciences, Associate Professor
National University of Life and Environmental Sciences of Ukraine
03041, 15 Heroiv Oborony Str., Kyiv, Ukraine
https://orcid.org/0000-0001-5045-5546

Abstract. The purpose of the study was to evaluate the feasibility of adding different forms of creatine to milk and whole milk replacer. The following creatine sources were examined: creatine hydrochloride, creatine monohydrate, creatine phosphate, and creatine malate. Creatine preparations, at a dosage equivalent to 15 g per 6 L of milk, were assessed for water solubility and subsequently added to milk and milk replacer. Creatine hydrochloride demonstrated excellent water solubility and readily passed through the filter after mixing with milk. Amount of dry matter retained on the filters decreased by 0.2 g/L compared with milk, indicating improved filtration properties. After one hour of standing, the residue in the lower fraction remained 0.1 g/L lower than in the corresponding milk fraction. Creatine monohydrate remained insoluble in water but did not induce milk coagulation. Residue retained on the filters increased by 0.1 g/L compared with milk, while after one hour of standing the residue in the lower fraction increased by 0.5 g/L relative to the control. Creatine phosphate dissolved well in water; however, mixing with milk increased the residue on the filters by 0.1 g/L immediately after mixing, and after one hour of storage the mixture separated, forming protein coagulates. The residue retained on the filters in the lower fraction exceeded the control by 3.5 g/L. Creatine malate showed slower dissolution in water due to the presence of large agglomerates. In prepared mixtures with milk, the residue retained on the filters increased by 0.6 g/L compared with the control, and after one hour of standing the residue in the lower fraction exceeded the control by 5.3 g/L. Protein coagulates formed

Suggested Citation:
Nosevych, D., & Antoniuk, T. (2026). Practical considerations in the selection of creatine forms for calf feeding. *Scientific Reports of the National University of Life and Environmental Sciences of Ukraine*, 22(2), 135-149. doi: 10.31548/dopovidi/2.2026.135.

*Corresponding author

in the upper fraction of the mixture after one hour of standing, making it unsuitable for filtration. In mixtures with whole milk replacer, all forms of creatine slightly accelerated the sedimentation of suspension components; however, this effect was not critical. For calf milk mixtures, the inclusion of creatine hydrochloride was recommended due to its high solubility and lack of rapid milk coagulation

Keywords: milk; milk replacer; cattle; solubility; milk protein coagulation; esophageal groove reflex

Introduction

Creatine was a nitrogen-containing compound involved in energy storage in muscle tissue. Various forms of creatine were widely used in sports nutrition to enhance muscle energy supply and promote muscle growth. B. Wax *et al.* (2021) reported that creatine-containing drugs have been shown to increase intracellular creatine concentration, thereby enhancing adenosine triphosphate resynthesis, improving work performance, increasing maximal strength, and promoting lean muscle mass accretion. Creatine supplementation also accelerated the recovery of muscle strength following intensive exercise. Approximately half of the daily creatine requirement was synthesised endogenously from amino acids, particularly arginine, glycine, and methionine, while the remainder was obtained from dietary sources. According to S.M. Ostojic (2021), low creatine intake was associated with slower growth, reduced muscle mass, higher body fat content, and other functional impairments. In cattle production, the ability of various creatine forms to increase muscle mass may be beneficial as a strategy to enhance meat productivity and carcass quality. The utilisation of nitrogen-containing compounds in cattle was closely associated with rumen digestion. The rumen hosted a complex microbiome, including associations of proteolytic, peptidolytic, and ureolytic bacteria, as reported by P. Tan *et al.* (2021), which degraded available protein to ammonia, followed by its incorporation into microbial protein synthesis. Creatine, like other free amino acids, was utilised by rumen microorganisms; therefore, its direct inclusion in feed as a supplement was ineffective. One of the potential approaches to creatine supplementation was its inclusion in ruminant diets in a bypass form. Another option was the addition of creatine to milk replacers during calf feeding. Feeding creatine mixed with milk may be technologically feasible due to the oesophageal groove reflex, which was active in calves during milk consumption. M. Marszałek *et al.* (2022) reported that the high concentration of cholinergic and nitrergic neurons in the oesophageal groove of calves, which facilitated its closure reflex, liquid feeds and feed additives mixed with milk bypass the rumen and were directly delivered to the abomasum.

Studies by J. de Souza Pinheiro *et al.* (2024) in goat kids demonstrated that regulating milk replacer intake can influence not only animal performance and body development but also metabolism and cellular hypertrophy. Based on this, exploring strategies to influence muscle cell hypertrophy in calves through creatine supplementation in milk feeds was of particular interest. There were various forms of creatine that can theoretically be used in animal feeding. Guanidinoacetic acid, a naturally synthesised precursor of creatine derived from amino acids, was commonly used as a feed additive. A study by K.J. Hazlewood *et al.* (2024) demonstrated that supplementation of milk replacer with guanidinoacetic acid in Holstein calves for 7 weeks, starting from one week of age, affected growth performance. The authors reported that supplementation at 1 or 2 g/day increased plasma creatine concentration, improved average daily gain and body weight at 8 weeks of age, and enhanced starter feed intake, without adverse effects on animal health. However, the EFSA FEEDAP Panel (EFSA Panel on Additives and Products or Substances used in

Animal Feed) *et al.* (2022) concluded that the use of guanidinoacetic acid as a feed additive was acceptable only under specific conditions, including low inclusion levels in feed or water, due to safety considerations and potential adverse effects observed in animal studies. Therefore, it was advisable to evaluate other sources of creatine in animal nutrition, particularly those widely used in human sports nutrition that have demonstrated efficacy and safety. According to C. Fazio *et al.* (2021), creatine monophosphate was considered one of the most bioavailable forms with proven efficacy; however, other forms such as creatine magnesium chelate, creatine citrate, creatine malate, creatine ethyl ester, creatine nitrate, and creatine pyruvate were also widely used. According to R.B. Kreider *et al.* (2022), creatine monohydrate remained the primary source of creatine in sports nutrition, with advantages in bioavailability, efficacy, and safety. The potential use of creatine as a feed additive in animal nutrition remained insufficiently studied. J.R. Stout *et al.* (2025) reported that one of the first attempts to evaluate the effectiveness of creatine monohydrate supplementation in a racehorse mare encountered difficulties due to its low solubility in water, which hindered the preparation of a solution for oral administration. The use of creatine monohydrate as an additive to milk may also be problematic due to low solubility and sediment formation, which could reduce intake by calves. Other creatine forms with higher solubility and better dispersion in milk mixtures may induce coagulation of milk proteins, which must be taken into account. The aim of this study was to evaluate, under laboratory conditions, the technological feasibility of incorporating the most commercially available forms of creatine into milk feeds for calf feeding.

Materials and Methods

The study was conducted in 2025 at the Laboratory of Milk and Dairy Product Quality, Department of Milk and Meat Production Technologies, National University of Life and Environmental Sciences of Ukraine. The study evaluated the solubility of different creatine forms in water and their suitability for incorporation into milk and milk replacers. Four of the most commercially available creatine compounds were used for analysis: creatine hydrochloride, creatine monohydrate, creatine phosphate, and creatine malate. Creatine hydrochloride was a sports nutrition product manufactured by LLC "Sport Nutrition Import", containing added colorant and flavouring. Creatine monohydrate was produced by PE "Powerful Progress Ukraine" and contained flavouring. Creatine phosphate and creatine malate were manufactured in People's Republic of China and supplied by LLC "Himlaborreaktyv". To assess the solubility of creatine preparations in water, three experimental flasks (250 cm^3) were prepared for each creatine compound, each containing 200 cm^3 of water at 38-40°C. Flasks containing water without additives served as controls. A 0.5 g sample of each creatine preparation was added to the experimental flasks and thoroughly mixed. The sample weight was calculated based on an estimated daily creatine intake of 15 g, intended to be dissolved in 6 L of liquid feed, corresponding to the average daily milk allowance per calf. Each samples were visually evaluated for sediment formation, and the presence of undissolved material was determined by filtration followed by weighing of the filters after drying. Filters made of black spunbond (10 × 10 cm) were used for filtration. Filters were weighed before filtration, and the presence of residue was visually assessed after filtration. To determine potential losses of the preparation during filtration that were not visually detectable, the filters were dried in a drying oven for 40 minutes at 105 ± 2°C and reweighed after cooling. Weighing was performed using RADWAG THB-600 (Poland) laboratory scales (d = 0.01 g).

To assess the feasibility of incorporating creatine preparations into milk, samples were prepared analogously to the water-based experiment. The mixtures were thoroughly stirred and visually compared with the control samples. Immediately after mixing, 50 cm^3 samples were taken from each flask. Composite samples (150 cm^3) were prepared from the three experimental replicates and the control and filtered through pre-weighed black spunbond filters. The filters were cooled to room temperature, and reweighed. The remaining milk-creatine mixtures were held for one hour, after which the consistency of the upper and lower layers was assessed. From the upper third of each experimental and control flask, 50 cm³ samples were collected and combined into composite samples (150 cm³), which were filtered through pre-weighed filters. Filtration results were evaluated visually, and the filters were dried, cooled, and reweighed. The lower layer of milk and milk-creatine mixtures (100 cm³ per flask) was filtered in the same manner, and the differences in the mass of dried filters were determined. To evaluate the possibility of adding creatine to milk replacer, a working solution was prepared containing 130 g of milk replacer powder per 1 L of water. The study used milk replacer "Telyatko Ultra Active" (Shencon Corporation, n.d.) intended for calves from 15 days of age, containing up to 70% dairy components. Creatine compounds were added at a rate of 15 g per 6 L of solution. For this purpose, 1.25 g of creatine preparation was added to 65 g of milk replacer powder and dissolved in 0.5 L of water at 50-55°C. The liquid mixtures were visually evaluated immediately after dissolution and after 15 minutes. Subsequently, the mixtures were remixed, and changes were visually assessed after 5, 10, and 15 minutes. To determine potential losses of creatine and milk components during sediment filtration, arithmetic means, standard errors, and significance of differences (p-values) were calculated.

Results and Discussion

Creatine compounds were promising for inclusion in animal diets as a means of stimulating productivity; however, in cattle production their application was limited due to the physiological characteristics of ruminant digestion. There were two most practical approaches for incorporating creatine into cattle diets. The first involved supplementation of adult animals and growing stock in a rumen-protected form that ensured bypass of the rumen. The second approach involved administration to calves via liquid feeding with milk-based feeds, allowing the utilisation of the oesophageal groove reflex. The inclusion of novel feed components for calf nutrition required preliminary evaluation of their compatibility with milk feeds prior to conducting efficacy studies. In particular, when using different forms of creatine as additives to milk feeds, losses of the preparation due to sedimentation may occur, as well as possible alterations in the structure of milk mixtures resulting from interactions with the additives. The investigated feed-grade creatine sources were therefore evaluated for solubility in water and their interaction with milk and milk replacer. Creatine compounds exhibited different solubility characteristics in water (Fig. 1). Creatine hydrochloride dissolved rapidly, resulting in a clear solution with a pink coloration (due to added colorants). No sediment was observed, only a small number of air bubbles were present on the bottom and walls of the flask.

a b c d

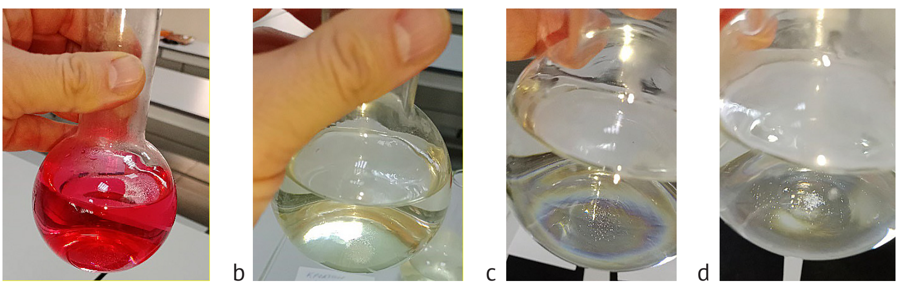

***Figure 1.** Dissolution of creatine compounds in water at 38-40°C*

Note: a – creatine hydrochloride; b – creatine monohydrate; c – creatine phosphate; d – creatine malate

Source: developed by the authors

After dissolution of creatine monohydrate, a clear solution with a slightly yellowish tint (due to the colorant) was obtained. However, sediment remained at the bottom of the flask and did not dissolve even after prolonged and thorough mixing. The undissolved residue appeared as a homogeneous, well-wetted powder. The creatine phosphate solution was a clear, homogeneous liquid with no visible difference in colour compared to the control (water). The compound dissolved rapidly, with only a small number of fine air bubbles remaining at the bottom of the flask. Dissolution of creatine malate in warm water resulted in a clear solution with a slightly yellowish colour. In two out of three flasks, no sediment was observed; in one flask, a small number of crystals of undissolved compound were present, which completely dissolved over time. The control sample and experimental aqueous solutions of creatine preparations were filtered through spunbond filters. Visually, the filters remained clean, and no residue was observed on their surface. Potential retention of creatine compounds on the filter surface or within its structure, not detectable visually, was assessed by weighing before and after drying (Table 1).

Table 1. *Determination of creatine preparation residues on filters (after filtration of aqueous solutions)*

Sample	Mass before filtration (n = 3), g	Mass after filtration (n = 3), g	Difference before and after filtration, g	p-value
Control	0.57 ± 0.015	0.57 ± 0.018	0.01	0.091752
Creatine hydrochloride	0.62 ± 0.011	0.62 ± 0.019	0.00	0.370901
Creatine monohydrate	0.56 ± 0.007	0.56 ± 0.008	0.00	0.211325
Creatine phosphate	0.66 ± 0.023	0.66 ± 0.029	0.00	0.500000
Creatine malate	0.65 ± 0.028	0.66 ± 0.025	0.01	0.091752

Source: developed by the authors

The weights of the dried filters before and after filtration did not differ significantly. The observed differences were within the limits of statistical error, indicating that the preparations were well dissolved in water. In the case of creatine monohydrate, which appeared visually undissolved, its fine particle structure allowed it to pass through the filter pores without noticeable losses. In terms of water solubility, creatine hydrochloride appeared to be the most suitable for practical application. Creatine phosphate and creatine malate required slightly longer dissolution time, whereas creatine monohydrate required specific handling conditions to minimise sedimentation of undissolved particles. Creatine preparations were also mixed with milk. During mixing, no visible changes in the milk were observed, except for coloration caused by preparations containing added colorants (Fig. 2).

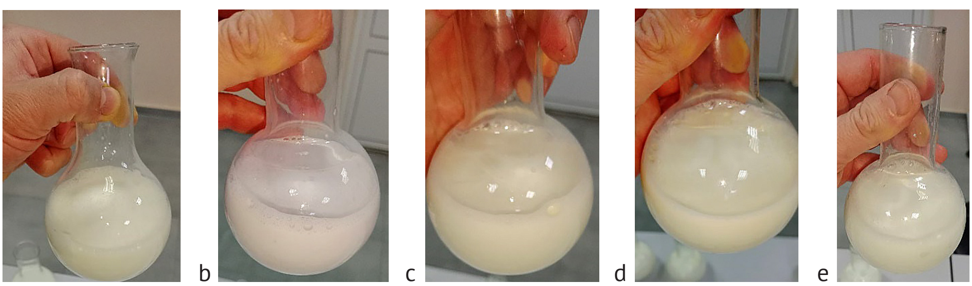

a b c d e

Figure 2. *Dissolution of creatine compounds in milk at 38-40°C*

Note: a – milk (control); b – creatine hydrochloride; c – creatine monohydrate; d – creatine phosphate; e – creatine malate

Source: developed by the authors

Since it was difficult to visually assess solubility in milk, this was evaluated by filtration. Immediately after mixing creatine preparations with milk, composite samples from the experimental flasks were prepared and filtered (Fig. 3). The filters remained relatively clean, and the mixtures passed through them readily, indicating the absence of visible coagulated particles or large insoluble residues. This suggested that, immediately after mixing, the creatine preparations were sufficiently dispersed in milk and did not noticeably interfere with its filtration properties.

a b c

Figure 3. *Filters after filtration of milk mixtures with creatine preparations*

Note: a – immediately after mixing (from left to right, starting from the top row: creatine hydrochloride; creatine monohydrate; creatine phosphate; creatine malate); b – after an hour, upper layer (from left to right, starting from the top row: creatine hydrochloride; creatine monohydrate; creatine phosphate; creatine malate); c – after an hour, lower layer (from left to right, starting from the top row: milk; creatine hydrochloride; creatine monohydrate; creatine phosphate; creatine malate)

Source: developed by the authors

The filters were dried and weighed. It was established that filtration of milk and milk-creatine mixtures resulted in an increase in filter mass (Table 2). Based on the difference in filter weight, the loss of dry matter from milk or milk mixtures was calculated per 1 L of filtered liquid. The mass of the filters increased in all samples, indicating deposition of milk components or milk-creatine mixture constituents on their surface. Immediately after mixing, dry matter losses during filtration in mixtures containing creatine monohydrate and creatine phosphate were similar and slightly higher (by 0.1 g/L) than in the control. The inclusion of creatine hydrochloride improved filtration properties and reduced dry matter losses on the filter by approximately 50%. The highest dry matter loss (1.0 g/L) was observed in the mixture containing creatine malate, with filter deposition exceeding the control by 0.6 g/L (2.4 times higher).

Table 2. *Determination of residues on filters (prepared milk mixtures with creatine preparations)*

Sample	Volume, cm³	Filter mass, g	Filter mass after filtration, g	Dry matter loss per 1 L of milk mixture, g
Milk (control)	150	0.65	0.71	0.4
Creatine hydrochloride	150	0.55	0.58	0.2
Creatine monohydrate	150	0.62	0.69	0.5
Creatine phosphate	150	0.60	0.67	0.5
Creatine malate	150	0.55	0.70	1.0

Source: developed by the authors

Milk feeds and mixtures for calves were not always administered immediately, depending on feeding management practices and herd size. During storage, even short-term (e.g., during transport within the farm and prior to feeding), phase separation and chemical interactions may occur, altering the structure of the mixtures. To simulate the period between preparation of milk mixtures with creatine sources and their actual administration, control samples and experimental mixtures were held for one hour. Since storage of milk led to separation of the fat fraction, the upper third and the lower settled fraction were filtered separately. It was found that the upper layer, characterised by higher fat content, in milk and mixtures containing creatine hydrochloride, monohydrate, and phosphate passed through the filter, leaving only minor coagulated particles on the surface (Fig. 3). In contrast, the mixture containing creatine malate exhibited increased viscosity and did not pass through the filter (Fig. 4a). After filtering, a substantial amount of coagulated material with a syrup-like consistency remained on the filter.

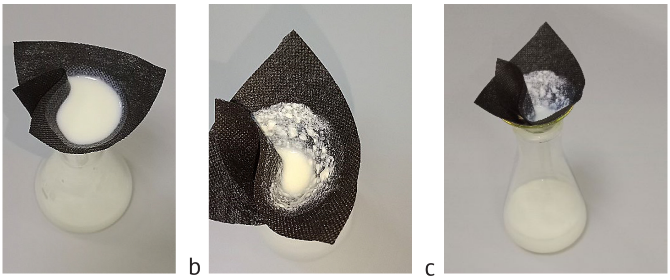

a b c

Figure 4. *Filtration of milk-creatine mixtures after one hour of incubation*

Note: a – mixture with creatine malate, upper layer; b – mixture with creatine malate, lower layer; c – mixture with creatine phosphate, lower layer

Source: developed by the authors

Drying of the filters after filtration of the upper fraction (Table 3) showed that, for milk, the proportion of filtered dry matter remained unchanged compared with the fresh sample (Table 2). In mixtures containing creatine hydrochloride, this parameter increased by 0.3 g/L relative to the corresponding values in Table 2, whereas in mixtures with creatine monohydrate and creatine phosphate it decreased by 0.2 g/L and 0.1 g/L, respectively. Overall, the changes after one hour were minor. The inability to filter the upper layer of the mixture containing creatine malate was likely associated with the acidic properties of oxalic acid present in the compound, leading to casein coagulation and curd formation. The lower layer of milk mixtures, containing less fat, exhibited different filtration behaviour compared to the upper layer. Mixtures containing creatine phosphate and creatine malate filtered slowly and produced a large amount of curd residues (Fig. 4b, 4c). As a result, the volume of filtered mixture had to be reduced. The filters after these mixtures contained substantial amounts of curd deposits, indicating interaction between the creatine preparations and milk components.

Table 3. *Determination of residues on filters*
(milk mixtures with creatine drugs, one hour after mixing, upper layer)

Sample	Volume, cm^3	Filter mass, g	Filter mass after filtration, g	Dry matter loss per 1 L of milk mixture, g
Milk (control)	150	0.58	0.64	0.4
Creatine hydrochloride	150	0.71	0.78	0.5
Creatine monohydrate	150	0.52	0.57	0.3
Creatine phosphate	150	0.61	0.67	0.4
Creatine malate	150	0.63	**not filtered**	

Source: developed by the authors

Drying of filters after filtration of the lower fraction (Table 4) showed that dry matter losses in the control (milk) and in mixtures containing creatine hydrochloride decreased compared to the upper fraction and to filtration immediately after mixing. This suggested that the previously retained material on the filters was mainly associated with the fat fraction. The addition of creatine hydrochloride to milk, at the concentrations specified in the methodology, did not induce coagulation; on the contrary, it reduced milk viscosity. Consequently, dry matter losses during filtration – both immediately after mixing and in the lower fraction after one hour of settling – were lower than in the control. Due to reduced viscosity, fat globules rose more rapidly; therefore, after filtration of the upper layer, an increase in retained dry matter on the filter was observed due to partial absorption of fat by the spunbond material. The addition of creatine phosphate and creatine malate acidified the milk and led to partial casein coagulation, increasing the viscosity of the system. As a result, after one hour of incubation, a substantial amount of curd formed in the lower fraction, and total dry matter losses during filtration increased to 3.7 g/L (creatine phosphate) and 5.5 g/L (creatine malate), which was 7.4 and 5.5 times higher than immediately after mixing, and 18.5 and 27.5 times higher than in the control, respectively. In absolute terms, the amount of dry matter retained on the filters exceeded the control by 3.5 g/L in the mixture containing creatine phosphate and by 5.3 g/L in the mixture containing creatine malate. Creatine monohydrate should be considered separately. Its inclusion led to a slight increase in dry matter losses during filtration compared to milk and caused a minor increase in viscosity, reflected in reduced losses in the upper fraction and increased losses in the lower fraction. Overall, these changes were not critical, and the increase in viscosity may help maintain mixture homogeneity for a longer period and prevent rapid sedimentation of undissolved particles.

Table 4. *Determination of residues on filters*
(milk mixtures with creatine drugs, one hour after mixing, lower layer)

Sample	Volume, cm^3	Filter mass, g	Filter mass after filtration, g	Dry matter loss per 1 L of milk mixture, g
Milk (control)	300	0.57	0.64	0.2
Creatine hydrochloride	300	0.58	0.62	0.1
Creatine monohydrate	300	0.63	0.83	0.7
Creatine phosphate	100	0.68	1.05	3.7
Creatine malate	100	0.56	1.11	5.5

Source: developed by the authors

Creatine can be added not only to whole milk but also to milk replacer. This approach was technologically more convenient, as it allowed preparation of a balanced mixture in advance. Such a mixing strategy was particularly relevant in specialised beef production systems, where calves were raised without access to a lactating herd and were fed exclusively with milk replacer. Creatine preparations were added to artificial milk mixtures, and their dissolution and phase separation during short-term storage were evaluated. According to the manufacturer's instructions for the milk replacer used in the study (Shencon Corporation, n.d.), the recommended time for feeding reconstituted milk replacer was 5 to 15 minutes, due to sedimentation of components and loss of homogeneity. Freshly reconstituted milk replacer was a turbid suspension of light beige colour. After 15 minutes, sedimentation and phase separation occurred, with a visible boundary between the whey fraction and the sediment, the latter occupying approximately the lower quarter of the flask. Mixtures containing creatine preparations also exhibited phase separation after 15 minutes (Fig. 5).

a b c

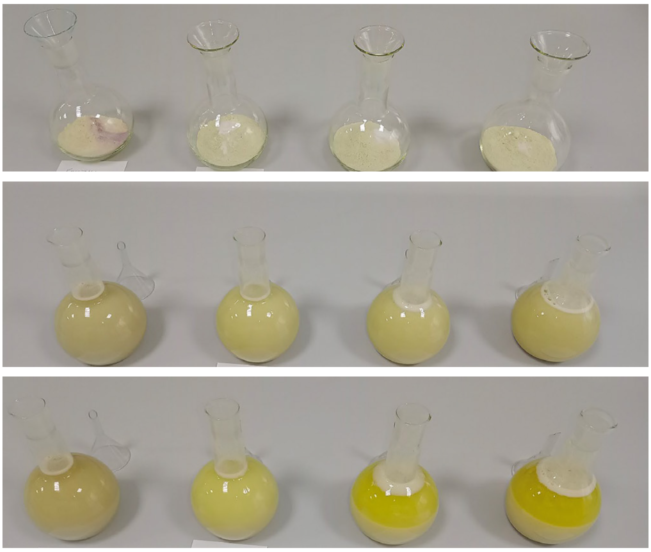

Figure 5. *Addition of creatine compounds to milk replacer*

Note: flasks from left to right: milk replacer + creatine hydrochloride; milk replacer + creatine monohydrate; milk replacer + creatine phosphate; milk replacer + creatine malate; a – dry mixture; b – mixture after dissolution; c – mixture 15 minutes after dissolution

Source: developed by the authors

The addition of creatine affected the coagulation behaviour of the milk replacer. After 15 minutes of settling, separation into whey and sediment phases was observed. In the flask containing creatine hydrochloride, the overall pattern of phase separation was similar to that of the control sample. In the presence of creatine monohydrate, sedimentation of components occurred, but a distinct phase boundary was not clearly visible, indicating improved retention of mixture homogeneity. In contrast, samples containing creatine phosphate and creatine malate exhibited a clearly defined phase boundary, and the whey fraction appeared more yellow and significantly more transparent than in the control and the other experimental samples. This indicated reduced viscosity and pronounced phase separation, which was undesirable for feeding calves with standardised milk replacers. To evaluate the dynamics of phase separation, the mixtures were remixed and sedimentation was monitored at 5-minute intervals. In the control sample (milk replacer without additives), slight clarification of the upper third was observed after 5 minutes. After 10 minutes, clarification extended to a larger portion of the upper layer, accompanied by the formation of a visible sediment occupying approximately the lower quarter of the flask. After 15 minutes, a distinct boundary between whey and sediment was evident. The pattern of phase separation was similar to that observed immediately after preparation, indicating that the functional properties of the milk replacer were preserved. Therefore, additional mixing can restore homogeneity prior to feeding. In mixtures containing creatine preparations, the rate of sedimentation after remixing increased compared to the control (Fig. 6). After 5 minutes, all samples showed clarification of the upper layer and formation of visible sediment. After 10 minutes, a distinct phase boundary had already formed, and after 15 minutes, the transparency of the whey fraction further increased. This indicated that storage beyond the recommended time was associated with loss of homogeneity, which should be considered in feeding management. The most pronounced signs of accelerated component deposition, consistent with the initial mixing, were observed in samples containing creatine phosphate and creatine malate. These effects were likely due to interactions between these compounds and mixtures components, similar to those observed, when added to whole milk.

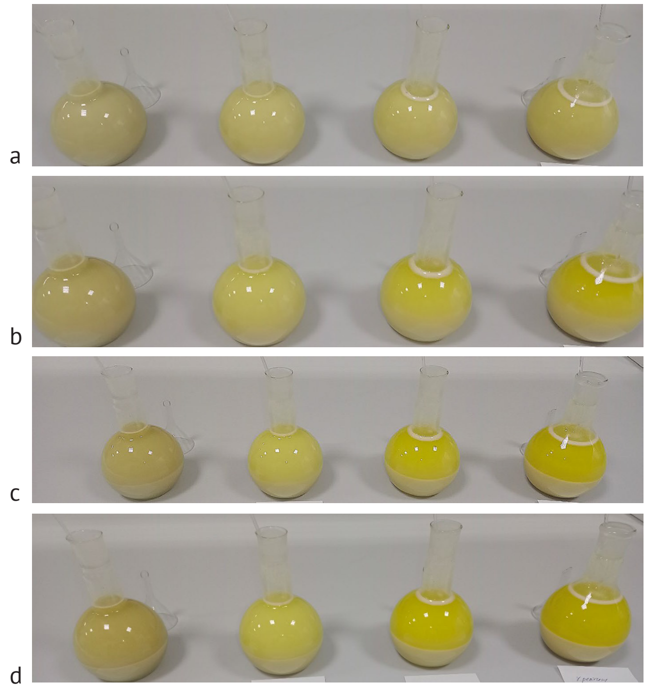

Figure 6. *Changes in the consistency of milk replacer-creatine mixtures over 15 minutes*
Note: flasks from left to right: milk replacer + creatine hydrochloride; milk replacer + creatine monohydrate; milk replacer + creatine phosphate; milk replacer + creatine malate; a – mixture after re-mixing; b – mixture 5 minutes after re-mixing; c – mixture 10 minutes after re-mixing; d – mixture 15 minutes after re-mixing
Source: developed by the authors

The search for strategies to enhance muscle development in calves raised for beef production remains relevant even during the milk-feeding period. In studies by R.E. Carter *et al.* (2025), it was demonstrated that feeding calves milk replacer with increased crude protein and crude fat content prior to weaning promotes higher body weight and greater muscle fibre cross-sectional area. In the present study, various creatine compounds were considered as potential factors influencing muscle growth. Creatine was synthesised endogenously in animals; however, under conditions of increased physiological demand and rapid muscle growth, additional dietary intake was desirable. As creatine was classified as a carninutrient, it was available primarily from animal-derived products, including milk. M.E. Brosnan & J.T. Brosnan (2016) reported that creatine concentrations in blood plasma and muscle tissue declined, when animals were fed plant-based diets, which often occurred, when whole milk feeding was restricted to reduce rearing costs. Creatine sources intended for inclusion in milk-based feeds must possess appropriate technological properties. The present study confirmed that different creatine preparations differed in their solubility in water. Creatine hydrochloride exhibited the highest solubility and can be effectively used in liquid feeding systems. Creatine phosphate also demonstrated high solubility and ease of incorporation into solutions. In contrast, creatine malate required longer dissolution time due to its heterogeneous powder structure, including the presence of larger crystals and aggregates, which should be considered, when incorporating it into liquid feeds. In the case of creatine monohydrate, its low solubility may result in sedimentation and reduced effectiveness, when administered in liquid feeds, as reported by J. Antonio *et al.* (2021). However, in this study, no significant residue was detected on filters, indicating sufficient dispersion within the solution. Therefore, minimising prolonged settling can reduce potential losses due to sedimentation. According to G. Escalante *et al.* (2022), the solubility of creatine monohydrate can be improved in solutions with lower pH; however, this was not feasible in milk due to its buffering capacity and the risk of protein coagulation under acidic conditions. Mixing with carbohydrate or protein powders was recommended to improve suspension stability and reduce sedimentation, which was applicable, when incorporating creatine into milk or milk replacer.

Milk feeds for calves were commonly supplemented with various additives aimed at optimising nutrition, balancing diets, and improving productivity and immune status. J.N. Wilms *et al.* (2024) demonstrated that the fat composition of milk replacer significantly influenced metabolism in dairy calves, indicating that lipid sources can be strategically used to modulate metabolic responses. P. Górka *et al.* (2021) reported that supplementation of milk replacer with probiotics and nucleotides positively affected growth performance and altered the composition of microbiota, suggesting improved gut health and digestive efficiency in calves. M.G. Coelho *et al.* (2023) investigated the inclusion of essential oil blends, including peppermint and eucalyptus, as well as menthol crystals, and found that such additives can enhance calf performance and health status, likely due to their antimicrobial and immunomodulatory properties. Additives may also be introduced directly into whole milk. For instance, S. Guven & T. Cimrin (2023) evaluated the effects of commercial supplements containing organic acids, plant extracts, and prebiotics. Sodium butyrate has been widely studied as a growth-promoting additive and as a factor improving calves' adaptation to weaning. Its supplementation has been shown to enhance growth performance and modulate gut microbiota in preweaning calves, as demonstrated by D. Wu *et al.* (2023). These effects were largely attributed to its role in supporting intestinal function through the nourishment of epithelial cells, as reported by A.B. Amin *et al.* (2022). In addition, sodium butyrate has been proposed as a potential alternative to antibiotic growth promoters due to its positive effects on gut health and its safety profile, which was highlighted in studies by W. Liu *et al.* (2021). Most studies have focused on the effects of additives on calf performance, gut microbiota composition, and disease incidence, while the technological properties of the mixtures have received less attention. In this study, certain creatine forms added to milk altered its physicochemical properties and induced coagulation. This can be explained by the formation of creatine salts through the addition of acidic moieties to the creatine molecule, which lowers the pH of aqueous solutions. While this enhanced creatine solubility, it negatively affected milk stability. Under these conditions, creatine monohydrate appeared to be the most suitable option for inclusion in milk, as it was not exert a pronounced acidifying effect. In present study, creatine hydrochloride did not cause significant coagulation even after one hour of incubation in milk, although Z.-M. Murillo *et al.* (2022) reported its ability to reduce pH.

The inclusion of feed additives in milk and milk replacers may affect not only the structure of the mixture but also its palatability. M. Terré *et al.* (2022) noted that the addition of sensory additives with a bitter taste – characteristic of creatine phosphate and creatine malate – can lead to feed aversion in calves and reduced intake. According to G. Escalante *et al.* (2022), who analysed the chemical properties and bioavailability of various creatine forms, creatine monohydrate remained the only form with strong evidence supporting its high bioavailability, efficacy, and safety. Milk replacers played an important role in calf feeding. Although they do not always reduce the cost of rearing, as reported by K.T. Sharpe & B.J. Heins (2021), they can compensate for milk shortages and were well suited for automated feeding systems. Their composition included dairy components but may be supplemented with more affordable and accessible ingredients, as well as deficient nutrients. However, due to the inclusion of plant-based components aimed at reducing production costs, the content of carninutrients, including creatine, was reduced. In present study, the inclusion of creatine preparations in milk replacer resulted in a slight acceleration of phase separation, particularly with creatine phosphate and creatine malate. However, the overall separation pattern was similar to that observed in the control sample, indicating the feasibility of incorporating creatine into milk replacers.

Conclusions

Among the key parameters influencing the quality of milk mixtures it was determined the solubility of creatine preparations and their potential interactions with milk components, which may alter structural and physicochemical properties. Creatine compounds differed in their degree of solubility in water. Creatine hydrochloride dissolved most rapidly, creatine phosphate demonstrated relatively good solubility. Creatine malate tended to form aggregates and required longer dissolution time. Creatine monohydrate exhibited low solubility and tended to sediment; therefore, its inclusion in calf milk mixtures must take this characteristic into account. The study demonstrated that mixing creatine preparations with milk may lead to changes in its properties and consistency. In prepared mixtures containing creatine hydrochloride, filtration properties improved compared with milk, and the deposition of dry matter on the filters decreased by 0.2 g/L. In mixtures containing creatine monohydrate, creatine phosphate, and creatine malate, the amount of residue retained on the filters increased by 0.1, 0.1, and 0.6 g/L, respectively. After one hour of standing, the filtration properties of the mixtures changed, most notably in the lower fraction. Compared with the lower fraction of milk, the amount of residue retained on the filters decreased by 0.1 g/L in mixtures with creatine hydrochloride, whereas it increased by 0.5, 3.5, and 5.3 g/L in mixtures containing creatine monohydrate, creatine phosphate, and creatine malate, respectively. Creatine monohydrate impaired filtration properties but, during storage, partially reduced the rate of phase separation. Creatine hydrochloride decreased milk viscosity, resulting in altered filtration characteristics of the upper and lower fractions during storage; however, dry matter retention on filters did not exceed that of the control. Creatine malate and creatine phosphate induced coagulation when mixed with milk. So, creatine hydrochloride proved to be the most technologically suitable additive for milk mixtures, due to its high solubility and the absence of significant coagulation effects at a dosage of 15 g per 6 L within one hour, as well as its ability to reduce the viscosity of milk replacer. The use of creatine monohydrate was feasible, provided that its low solubility was taken into account and the suspension was maintained in a homogeneous state prior to feeding. Creatine malate and creatine phosphate altered the structure of milk mixtures; therefore, their inclusion as feed additives may have adverse technological effects. Further research should investigate the effects of creatine preparations on calf growth when administered with milk or milk replacer.

Acknowledgements

None.

Funding

None.

Conflict of Interest

None.

References

[1] Amin, A.B., Trabi, E.B., Zhu, C., & Mao, S. (2022). Role of butyrate as part of milk replacer and starter diet on intestinal development in pre-weaned calves. A systematic review. *Animal Feed Science and Technology*, 292, article number 115423. doi: 10.1016/j.anifeedsci.2022.115423.

[2] Antonio, J., *et al.* (2021). Common questions and misconceptions about creatine supplementation: What does the scientific evidence really show? *Journal of the International Society of Sports Nutrition*, 18(1), article number 13. doi: 10.1186/s12970-021-00412-w.

[3] Brosnan, M.E., & Brosnan, J.T. (2016). The role of dietary creatine. *Amino Acids*, 48, 1785-1791. doi: 10.1007/s00726-016-2188-1.

[4] Carter, R.E., Emenheiser, J.C., Zinn, S.A., Govoni, K.E., Felix, T.L., & Reed, S.A. (2025). Effects of milk replacer composition on growth and development of beef × dairy crossbred calves. *Translational Animal Science*, 9, article number txaf005. doi: 10.1093/tas/txaf005.

[5] Coelho, M.G., da Silva, A.P., de Toledo, A.F., Cezar, A.M., Tomaluski, C.R., Barboza, R.D.F., Virginio Júnior, G.F., Manzano, R.P., & Bittar, C.M.M. (2023). Essential oil blend supplementation in the milk replacer of dairy calves: Performance and health. *Plos One*, 18(10), article number e0291038. doi: 10.1371/journal.pone.0291038.

[6] de Souza Pinheiro, J., Dornelas Silva, P.S., de Andrade, D.R., Veloso Tropia, N., Ramos Oliveira, T.P., Rezende Gesteira, J.M., Navajas Renno, L., Facioni Guimarães, S.E., & Marcondes, M.I. (2024). Can milk replacer allowance affect animal performance, body development, metabolism, and skeletal muscle hypertrophy in preweaning dairy kids? *Journal of Dairy Science*, 107(12), 10708-10723. doi: 10.3168/jds.2024-25230.

[7] EFSA FEEDAP Panel (EFSA Panel on Additives and Products or Substances used in Animal Feed), *et al.* (2022). Safety and efficacy of a feed additive consisting of guanidinoacetic acid for all animal species (Alzchem Trostberg GmbH). *EFSA Journal*, 20(5), article number e07269. doi: 10.2903/j.efsa.2022.7269.

[8] Escalante, G., Gonzalez, A.M., St Mart, D., Torres, M., Echols, J., Islas, M., & Schoenfeld, B.J. (2022). Analysis of the efficacy, safety, and cost of alternative forms of creatine available for purchase on Amazon. com: Are label claims supported by science? *Heliyon*, 8(12), article number e12113. doi: 10.1016/j.heliyon.2022.e12113.

[9] Fazio, C., Elder, C.L., & Harris, M.M. (2022). Efficacy of alternative forms of creatine supplementation on improving performance and body composition in healthy subjects: A systematic review. *The Journal of Strength and Conditioning Research*, 36(9), 2663-2670. doi: 10.1519/JSC.0000000000003873.

[10] Górka, P., Budzińska, K., Budziński, W., Jankowiak, T., Kehoe, S., & Kański, J. (2021). Effect of probiotic and nucleotide supplementation in milk replacer on growth performance and fecal bacteria in calves. *Livestock Science*, 250, article number 104556. doi: 10.1016/j.livsci.2021.104556.

[11] Guven, S., & Cimrin, T. (2023). Effects of adding natural additives to whole milk on performance, faecal, and blood parameters in suckling Holstein calves. *South African Journal of Animal Science*, 53(6), 774-783. doi: 10.4314/sajas.v53i6.01.

[12] Hazlewood, K.J., Zumbaugh, C.A., Jones, C.K., Atkinson, E.M., Tingler, H.L., Inhuber, V.K., Brouk, M.J., Antony, R.M., & Titgemeyer, E.C. (2024). Effect of guanidinoacetic acid supplementation on the performance of calves fed milk replacer. *Animals*, 14(19), article number 2757. doi: 10.3390/ani14192757.

[13] Kreider, R.B., Jäger, R., & Purpura, M. (2022). Bioavailability, efficacy, safety, and regulatory status of creatine and related compounds: A critical review. *Nutrients*, 14(5), article number 1035. doi: 10.3390/nu14051035.

[14] Liu, W., La, A.L.T.Z., Evans, A., Gao, S., Yu, Z., Bu, D., & Ma, L. (2021). Supplementation with sodium butyrate improves growth and antioxidant function in dairy calves before weaning. *Journal of Animal Science and Biotechnology*, 12, article number 2. doi: 10.1186/s40104-020-00521-7.

[15] Marszałek, M., Serzysko, T., & Sienkiewicz, W. (2022). Immunohistochemical study on the development of cholinergic and nitrergic nerve structures in the bovine esophageal groove. *Polish Journal of Veterinary Sciences*, 25(1), 165-174. doi: 10.24425/pjvs.2022.140853.

[16] Murillo, Z.-M., Cardona, G.-C., & Acosta, B.-L. (2022). Creatine hydrochloride versus creatine monohydrate. Differences in solubility, ergogenic effects, and body composition. *Perspectivas En Nutrición Humana*, 24(2), 233-246. doi: 10.17533/udea.penh.v24n2a06.

[17] Ostojic, S.M. (2021). Creatine as a food supplement for the general population. *Journal of Functional Foods*, 83, article number 104568. doi: 10.1016/j.jff.2021.104568.

[18] Sharpe, K.T., & Heins, B.J. (2021). Growth, health, and economics of dairy calves fed organic milk replacer or organic whole milk in an automated feeding system. *JDS Communications*, 2(6), 319-323. doi: 10.3168/jdsc.2021-0084.

[19] Shencon Corporation. (n.d.). *Whole milk replacer Teliatko. Ultra active*. Retrieved from https://shencon.com.ua/zameniteli_moloka/zamenitel_celnogo_moloka_telenokultra_aktiv.

[20] Stout, J.R., Kreider, R.B., Candow, D.G., Forbes, S.C., Rawson, E.S., Antonio, B., & Antonio, J. (2025). The birth of modern sports nutrition: Tracing the path from muscle biopsies to creatine supplementation – a narrative review. *Journal of the International Society of Sports Nutrition*, 22(1), article number 2463373. doi: 10.1080/15502783.2025.2463373.

[21] Tan, P., *et al.* (2021). Amino acids metabolism by rumen microorganisms: Nutrition and ecology strategies to reduce nitrogen emissions from the inside to the outside. *Science of the Total Environment*, 800, article number 149596. doi: 10.1016/j.scitotenv.2021.149596.

[22] Terré, M., Tortadès, M., Genís, S., Cresci, R., Frongia, A., Verdú, M., & Blanch, M. (2022). Short communication: A milk replacer aversion model in calves to test flavour-masking effects. *Livestock Science*, 256, article number 104830. doi: 10.1016/j.livsci.2022.104830.

[23] Wax, B., Kerksick, C.M., Jagim, A.R., Mayo, J.J., Lyons, B.C., & Kreider, R.B. (2021). Creatine for exercise and sports performance, with recovery considerations for healthy populations. *Nutrients*, 13(6), article number 1915. doi: 10.3390/nu13061915.

[24] Wilms, J.N., Kleinveld, N., Ghaffari, M.H., Sauerwein, H., Steele, M.A., Martín-Tereso, J., & Leal, L.N. (2024). Fat composition of milk replacer influences postprandial and oxidative metabolisms in dairy calves fed twice daily. *Journal of Dairy Science*, 107(5), 2818-2831. doi: 10.3168/jds.2023-23972.

[25] Wu, D., Zhang, Z., Shao, K., Wang, X., Huang, F., Qi, J., Duan, Y., Jia, Y., & Xu, M. (2023). Effects of sodium butyrate supplementation in milk on the growth performance and intestinal microbiota of preweaning Holstein calves. *Animals*, 13(13), article number 2069. doi: 10.3390/ani13132069.

Практичні аспекти вибору форм креатину для згодовування телятам

Дмитро Носевич
Кандидат сільськогосподарських наук, доцент
Національний університет біоресурсів і природокористування України
03041, вул. Героїв Оборони, 15, м. Київ, Україна
https://orcid.org/0000-0003-2495-2084
Тетяна Антонюк
Кандидат сільськогосподарських наук, доцент
Національний університет біоресурсів і природокористування України
03041, вул. Героїв Оборони, 15, м. Київ, Україна
https://orcid.org/0000-0001-5045-5546

Анотація. Метою дослідження було проаналізувати можливість додавання різних форм креатину в молоко і замінник незбираного молока. Було проаналізовано креатин гідрохлорид, креатин моногідрат, креатин фосфат і креатин малат. Препарати креатину, у дозуванні еквівалентному 15 г на 6 л молока було перевірено на розчинність у воді при додаванні до молока і замінника незбираного молока. Креатин гідрохлорид характеризувався відмінною розчинністю у воді, після додавання до молока суміш добре проходила через фільтр. Кількість сухої речовини, що затримується на фільтрах, зменшилася на 0,2 г/л, порівняно з молоком, що свідчить про покращені фільтраційні властивості. Після однієї години відстоювання залишок у нижній фракції залишався на 0,1 г/л меншим, ніж у відповідній фракції молока. Креатин моногдірат у воді залишався нерозчиненим, після розведення в молоці утворення згустків не викликав. Було визначено, що залишок у сумішах, що затримується на фільтрах, збільшився на 0,1 г/л порівняно з молоком, тоді як після однієї години відстоювання залишок у нижній фракції збільшився на 0,5 г/л відносно контролю. Креатин фосфат добре розчинявся в воді, однак змішування з молоком збільшувало залишок на фільтрах на 0,1 г/л одразу після змішування, а через годину зберігання суміш розділялася, утворюючи білкові коагуляти. Залишок, що затримувався на фільтрах у нижній фракції, перевищував контрольний на 3,5 г/л. Креатин малат мав подовжений час розчинення у воді через наявність великих агломератів. У приготованих сумішах з молоком залишок, що затримувався на фільтрах, збільшувався на 0,6 г/л порівняно з контролем, а через годину відстоювання залишок у нижній фракції перевищував контрольний на 5,3 г/л. Білкові коагуляти у верхній фракції суміші після години відстоювання зробили її непридатною для фільтрації. В суміші із замінником незбираного молока всі форми креатину прискорювали швидкість осідання компонентів суспензії, але цей вплив не був критичним. Було визначено, що в молочні суміші для телят доцільно включати креатин гідрохлорид, який має високу розчинність і не призводить до швидкого згортання молока

Ключові слова: молоко; замінник незбираного молока; велика рогата худоба; розчинність; коагуляція молочного білка; рефлекс стравохідного жолоба

Received 18.11.2025 Revised 13.02.2026 Accepted 23.04.2026 Published: 30.04.2026

Vol. 22, No. 2
2026

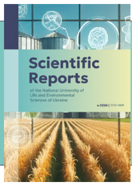

Scientific Reports of the National University of Life and Environmental Sciences of Ukraine

Journal homepage: https://scireports.com.ua/en e-ISSN 2223-1609

UDC 602.3:504.064 DOI: 10.31548/dopovidi/2.2026.150

Mathematical modelling of soil phytoremediation efficiency from Pb, Cu and Ni

Oleksandra Sydorenko*
Master's Student
National Technical University of Ukraine "Igor Sikorsky Kyiv Polytechnic Institute"
03056, 37 Beresteiskyi Ave., Kyiv, Ukraine
https://orcid.org/0009-0004-5890-7630

Nataliia Golub
Doctor of Technical Sciences, Professor
National Technical University of Ukraine "Igor Sikorsky Kyiv Polytechnic Institute"
03056, 37 Beresteiskyi Ave., Kyiv, Ukraine
https://orcid.org/0000-0003-1448-1872

Abstract. The study aimed at a quantitative comparative assessment of lead, copper, and nickel removal dynamics from soil by the "metal-plant" system based on mathematical modelling to predict the cleaning timelines of contaminated areas. Soil contamination with heavy metals (Pb, Cu, Ni) due to intensive anthropogenic activities and large-scale military operations in Ukraine posed a critical threat to environmental safety and public health. Phytoremediation using hyperaccumulator plants, such as *Brassica juncea*, was considered a promising and environmentally friendly method for ecosystem restoration. However, the planning of such measures was complicated by the varying rates of element removal and their toxic effects on biomass, which necessitated the development of accurate predictive models. An exponential model of metal uptake kinetics was used to predict the cleaning timelines of contaminated areas. It was established that the soil cleaning efficiency for one vegetative period (180 days) was 92.9% for copper, 80.6% for nickel, and only 53.5% for lead. The findings revealed that the high remediation efficiency of copper was due to its high mobility and low phytotoxicity. Conversely, lead exhibited the strongest inhibitory effect, significantly limiting its extraction rate. Based on the multi-metal model, an additive toxic effect of pollutant mixtures was demonstrated, leading to a 78% reduction in the overall productivity of phytoremediators compared to monometallic contamination. The obtained results allowed for the optimisation of restoration strategies for anthropogenically

Suggested Citation:
Sydorenko, O., & Golub, N. (2026). Mathematical modelling of soil phytoremediation efficiency from Pb, Cu and Ni. *Scientific Reports of the National University of Life and Environmental Sciences of Ukraine*, 22(2), 150-166. doi: 10.31548/dopovidi/2.2026.150.

*Corresponding author

stressed territories and lands affected by military conflicts. The developed model can be used to assess the economic feasibility of phytoremediation measures

Keywords: heavy metals; phytoextraction; toxic stress; multi-metal model; soil recovery; environmental safety

Introduction

Soil contamination with heavy metals, such as lead (Pb), copper (Cu), and nickel (Ni), remained one of the most critical environmental challenges globally, posing a severe threat to ecological safety and human health. In the context of Ukraine, this issue had acquired unprecedented urgency due to large-scale military operations and intensive industrial activities. Military-related pollution was characterised by high concentrations of metal complexes originating from ammunition fragments and destroyed infrastructure, which required immediate and effective remediation strategies. Among various decontamination methods, phytoremediation – the use of hyperaccumulator plants to extract pollutants – was recognised as a sustainable, cost-effective, and ecologically safe approach. As noted by X. Shen *et al.* (2022), who conducted a critical review on the performance and challenges of heavy metal removal, this method offered significant environmental benefits and minimised secondary ecological impact. G.A. Bortoloti & D. Baron (2022) explored the biochemical and physiological mechanisms of *Brassica* plants, highlighting their inherent potential for the phytoremediation of toxic elements. *Brassica juncea* (Indian mustard) was widely regarded as an ideal biological object for these purposes. For instance, I. Ali *et al.* (2022) screened various *Brassica* species for the phytoremediation of contaminated soils and confirmed that Indian mustard provided the highest extraction rates under complex geochemical conditions. The selection of this plant as a model was justified by its ability to rapidly generate significant above-ground biomass, its robust root system, and its documented tolerance to toxic stress. Supporting this, M. Sut-Lohmann *et al.* (2023) demonstrated that *Brassica juncea* remained a feasible hyperaccumulator of potentially toxic metals even under the extreme environmental conditions typical of anthropogenically disturbed zones. Understanding the dynamics of soil cleaning required an integrated assessment of the physiological response of the plant to toxic stress. S. Maher *et al.* (2025) provided a comparative assessment of *Brassica juncea* for efficient phytoremediation, emphasising that the mobility of metals within the soil matrix was a decisive factor for extraction kinetics.

Elements like copper and nickel often exhibited relatively higher mobility, making them more accessible for plant uptake. In contrast, lead was frequently characterised by low mobility and a strong tendency for fixation within the soil structure. Researcher P. Rani *et al.* (2023) highlighted *Brassica juncea* as a potential crop for the simultaneous phytoremediation of various heavy metals, which was crucial, when dealing with complex multi-vector pollution rather than simple ions. The chemical complexity of soil pollution in areas of active military conflict presented a unique challenge for ecological restoration. The "chemical fingerprint" of war involved a heterogeneous mixture of heavy metal complexes. The transition from monometallic to multi-metal modelling was essential for creating realistic environmental management plans. P. Cârdei *et al.* (2021) developed a mathematical model to simulate the transfer of heavy metals from soil to plant, which had become a fundamental basis for modern predictive systems. Scientists T. Leonavičienė *et al.* (2023) focused on the modelling of environmental processes and management, providing a methodological framework for assessing large-scale decontamination projects. A.M. Kamal & A.F. Alali (2025) applied kinetic modelling of heavy metal uptake and translocation in *Brassica juncea*, proving that such analytical frameworks allowed for accurate forecasting of remediation outcomes before field implementation. Dynamic models based on systems of ordinary differential equations allowed researchers to simulate temporal changes in plant biomass, calculate metal accumulation in tissues, and forecast the reduction of concentrations in the soil solution over a vegetative period (Cârdei *et al*., 2021). Such predictive tools were essential for optimising remediation parameters and assessing the feasibility of decontamination projects before their field implementation. Despite the progress in single-metal modelling, there remained a significant gap in understanding the combined toxic effects of metal mixtures, which were typical for war-affected soils. Most existing frameworks do not fully account for the additive inhibitory pressure that multiple pollutants exert on plant growth. The aim of this research was to provide a quantitative comparative assessment of Pb, Cu, and Ni removal dynamics from contaminated soils using *Brassica juncea* based on a unified nonlinear dynamic model. The scientific novelty of this work lain in the implementation of an extended multi-metal model that quantified the additive toxic effect of pollutant mixtures, specifically adapted to initial concentrations corresponding to the anthropogenic pressure found in military conflict zones in Ukraine.

Materials and Methods

Parameter justification and physical meaning used model

To ensure a rigorous comparative analysis of the phytoremediation efficiency of various heavy metal complexes (rather than simple ions), a unified nonlinear dynamic model of the "metal-plant" system was applied. The system was described by three interrelated state variables: plant biomass (*B*), normalised metal concentration in plant tissues (*Me*), and metal concentration in the soil (*S*). The system of nonlinear ordinary differential equations was formulated as follows:

$$\frac{dPB}{dt} = PB\,(a - b\,PB) - PB\,\frac{d\,Me}{e+Me}; \qquad (1)$$

$$\frac{dMe}{dt} = \alpha\,S\,(1 - Me) - \beta\,Me; \qquad (2)$$

$$\frac{dS}{dt} = -\alpha\,PB\,S + \beta\,PB\,Me + \phi\,(S_0 - S). \qquad (3)$$

The first equation described the dynamics of biomass growth. The term *B(a - bB)* represented standard logistic growth, where *a* – specific growth rate and *b* defined the carrying capacity of the environment. The term *B(d · Me) / (e + Me)* introduced the inhibitory toxic effect caused by the accumulation of heavy metal complexes, where *d* represented the maximum toxicity coefficient and *e* – half-saturation constant for toxicity. The second equation modelled the kinetics of metal uptake by the hyperaccumulator *Brassica juncea*. The absorption was driven by the soil concentration (*S*) and the specific absorption coefficient (α), bounded by a biological saturation effect *(1 - Me)*. The partial excretion or return of metals was governed by the coefficient β. The third equation defined the mass balance in the soil, accounting for the depletion due to plant extraction (-αBS), the return from decaying tissues ($\beta B \cdot Me$), and natural soil recovery processes driven by the coefficient φ towards an equilibrium concentration S_0 (Cârdei *et al*., 2021).

Experimental scenarios, computational setup and software implementation

The numerical simulation was strictly conducted for a vegetative period of 180 days, accurately representing the growth cycle of herbaceous hyperaccumulators in a temperate climate. To determine the base system parameters, it was utilised the mathematical modelling methodology for environmental processes proposed by T. Leonavičienė *et al.* (2023). Based on this methodology, base parameters for the overall system were standardised as follows: $a = 0.10$, $b = 0.01$, $e = 1.0$, $\beta = 0.0005$ day^{-1}, $\varphi = 0.0001$ day^{-1}, and an equilibrium concentration $S_0 = 100$ mg/kg. Differences between the metal complexes were implemented exclusively through the metal-specific absorption coefficients (α) and toxicity constants (d) to ensure a controlled comparative baseline. The values for these specific parameters were adapted based on the phytoextraction assessment methodology presented by J. Suman *et al*. (2018). The established values were: lead (Pb): $\alpha = 0{,}0010$ day^{-1}, d = 0,07; copper (Cu): $\alpha = 0{,}0025$ day^{-1}, d = 0,03; nickel (Ni): $\alpha = 0{,}0018$ day^{-1}, d = 0,05. Unlike base scenarios with a fixed *S0*, this study investigated varied initial soil pollution levels reflecting the anthropogenic impact of military actions in Ukraine: Cu (100, 150, 300 mg/kg), Pb (70, 125, 150 mg/kg), and Ni (50, 100, 150 mg/kg). Furthermore, an advanced multi-metal model was implemented to simulate the simultaneous presence of multiple pollutants. In this model, the total toxic effect (T_{total}) was integrated into the system of differential equations as a linear combination (additive contribution) of individual metal complexes inhibiting biomass growth. Mathematically, this factor was expressed as:

$$T_{total} = \sum_{i=1}^{n}(d_i \cdot C_i), \quad (4)$$

where d_i – toxicity constant of the i-th metal, and C_i – current concentration in plant tissues. The mathematical modelling was executed in the Python programming environment. The NumPy library was utilised for efficient multidimensional array operations and data structuring. The SciPy library, specifically the *odeint* integrator from the *scipy.integrate* module, was employed for the robust numerical resolution of the stiff system of non-linear differential equations. Time-series data visualisations were generated using Matplotlib.

Results and Discussion

Analysis of biomass growth under toxic stress

The simulation of *Brassica juncea* growth over a 180-day period provided a detailed view of how complex compounds of heavy metals influence primary productivity. In the control scenario (Fig. 1), where concentrations remained at background levels, the biomass accumulation followed an ideal sigmoidal trajectory. The absence of significant inhibitory pressure allowed the plant to reach its maximum carrying capacity by approximately the 100th day of vegetation. The graph clearly distinguished an intensive exponential growth phase between days 20 and 60, after which the growth rate gradually slowed down, stabilising at a level of approximately 10.0 kg/m^2. This indicated the optimal functioning of the plant's enzymatic systems in the absence of toxic stress.

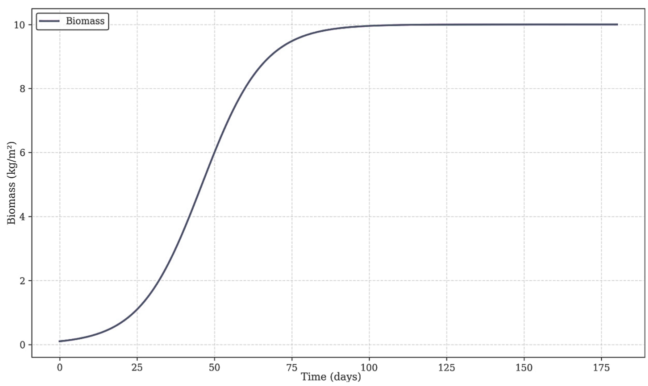

Figure 1. *Dynamics of mustard biomass growth at standard (background) soil metal concentrations*
Note: Cu – 25 mg/kg, Pb – 20 mg/kg, Ni – 20 mg/kg (control)
Source: developed by the authors

However, the introduction of copper complexes (Fig. 2) shifted this equilibrium. Even at the maximum tested concentration of 300 mg/kg, the biomass reduction remained minimal.

This resilience was mathematically represented by the toxicity constant d = 0.03. From a biological perspective, this indicated that, while Cu was a heavy metal, its role as an essential micronutrient allowed the plant to maintain high metabolic activity even under elevated loads. The "zoom-in" area in Figure 2 clearly demonstrated that the difference between 100 mg/kg and 300 mg/kg variants was less than 5%, confirming the low sensitivity of the hyperaccumulator to this specific pollutant. Throughout the entire vegetative cycle, the growth curves for different Cu concentrations nearly duplicated the trajectory of the control, suggesting highly effective internal copper detoxification mechanisms in *B. juncea* tissues.

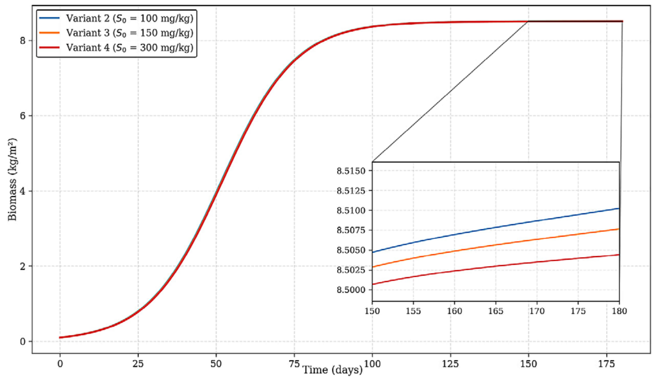

***Figure 2.** Dynamics of Brassica juncea biomass growth at different initial Cu concentrations in the soil*
Source: developed by the authors

In stark contrast, the modelling of lead (Pb) contamination (Fig. 3) revealed a critical suppression of growth. With a toxicity coefficient of d = 0.07, lead complexes exert more than double the inhibitory pressure compared to copper. The biomass curve for the 150 mg/kg variant failed to reach the 7.0 kg/m^2 mark, showing a significant "lag phase" in the middle of the vegetative cycle. This suggested that the energy resources of *B. juncea* were redirected from growth to detoxification and structural sequestration within the root tissues, which aligned with the phytostabilisation strategy. The graph showed that with increasing Pb concentrations, the plateau was reached much earlier but at significantly lower biomass levels, indicating irreversible physiological disruptions upon reaching a critical threshold.

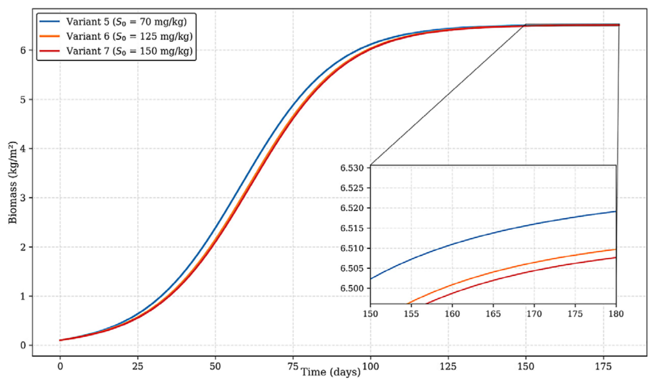

***Figure 3.** Dynamics of Brassica juncea biomass growth at different initial Pb concentrations in the soil*
Source: developed by the authors

Nickel (Ni) represented an intermediate case (Fig. 4). With d = 0.05, the biomass stabilisation occurs around 7.5 kg/m^2 for the highest dose. The transition from the active growth phase to the plateau was smoother than that of lead, indicating a more balanced interaction between the metal complex and the plant's enzymatic systems. Analysis of the charts showed that at a concentration of 50 mg/kg, the effect of nickel was moderate; however, at 150 mg/kg, there was a clear 25% reduction in productivity compared to the control. This confirmed nickel's status as an element with moderate phytotoxicity, where accumulation capacity was limited by the gradual depletion of the plant's adaptive reserves.

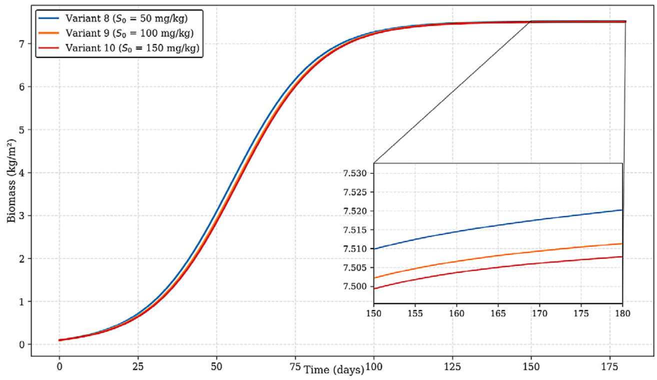

Figure 4. *Dynamics of Brassica juncea biomass growth at different initial Ni concentrations in the soil*

Source: developed by the authors

So, the dynamics of biomass accumulation served as an integrated indicator of the phytoremediation system's stability. A comparative analysis of the modelling results confirmed a toxicity hierarchy of Pb > Ni > Cu. The established mathematical relationships allowed for both the confirmation of growth inhibition and the quantitative prediction of biomass loss, which was crucial for calculating the total efficiency of metal removal from the soil. The results obtained regarding the selective toxicity of heavy metals were consistent with several foundational studies in the field. B.V. Tangahu *et al.* (2011) emphasised that the efficiency of phytoremediation was intrinsically linked to the plant's ability to maintain biomass production under chemical stress, noting that lead consistently exhibited the highest inhibitory potential among common industrial pollutants. Finding of this research that copper acted as a less toxic stressor aligned with the observations of P.C. Nagajyoti *et al.* (2010), who highlighted the dual role of Cu as both a nutrient and a potential toxicant depending on the concentration threshold.

Kinetics features of metal accumulation and soil decontamination

The dynamics of metal uptake showed that the saturation of plant tissues occurred much faster than the depletion of the soil reservoir. In the control scenario (Fig. 5), the accumulation of Cu, Pb, and Ni in plant tissues remained minimal, reflecting standard background levels. The plotted curves demonstrated a near-zero slope throughout the 180-day period, confirming the baseline state of the plant without induced phytoextraction. For copper (Fig. 6), the normalised concentration in the plant reached 90% of its maximum within the first 40 days. The visual trajectory of the graphs demonstrated a sharp exponential rise followed by an early and stable plateau, indicating rapid tissue saturation. This rapid "loading" phase was driven by the high absorption coefficient α = 0.0025. The specific absorption coefficient (α) used in this study represented the combined influence of soil pH, organic matter content, and the plant's genetic potential for uptake. Comparative analysis revealed that the high α for copper allowed for a rapid saturation of plant tissues, creating a "pull effect" that continuously drawn the metal from the soil solution. This was mathematically evidenced by the steep decline in soil concentration (S) during the first half of the vegetative period.

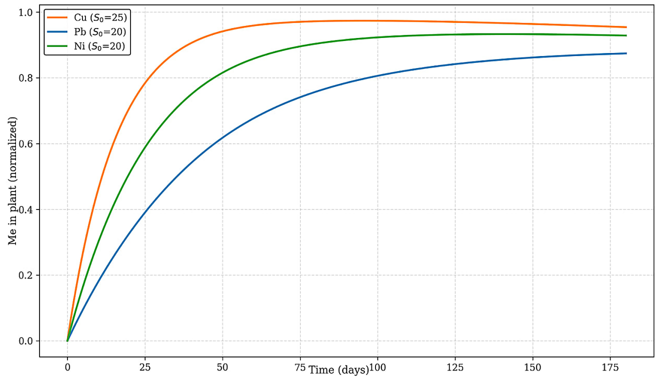

Figure 5. *Dynamics of Cu, Pb, and Ni accumulation in plant tissues (control)*
Source: developed by the authors

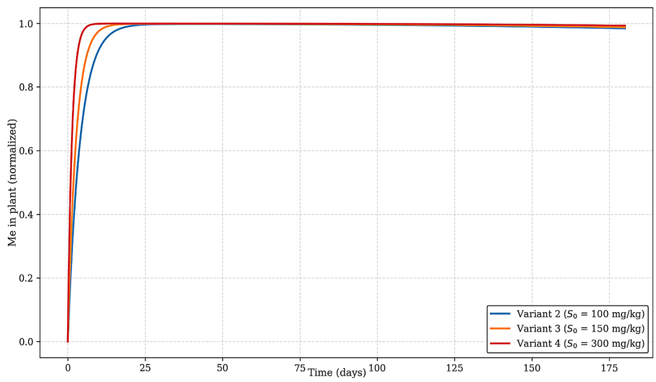

Figure 6. *Dynamics of Cu accumulation in plant tissues at different initial concentrations*
Source: developed by the authors

In contrast, lead (Fig. 7) was characterised by a detrimental combination of low mobility and high toxicity. The corresponding curves exhibited a prolonged, gentle slope without a distinct early peak, reflecting the slow and limited translocation of the metal into the tissues. The low absorption of lead (α = 0.0010) was compounded by its high toxicity constant (d = 0.07). This created a negative synergy: the metal was absorbed slowly, but the small amount that was absorbed causes disproportionately large damage to the metabolic machinery of *B. juncea*. This feedback loop – where the metal inhibits the very biomass needed to remove it – was a central finding of this modelling exercise. This confirmed the thesis that the majority of absorbed Pb was typically retained in the root system rather than translocated to the shoots, confirming the necessity of long-term monitoring for Pb-polluted sites.

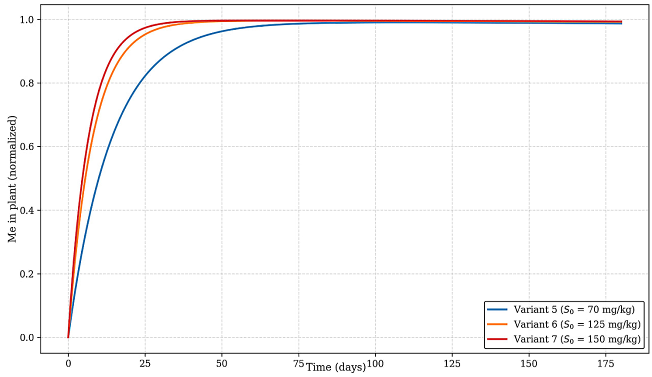

Figure 7. *Dynamics of Pb accumulation in plant tissues at different initial concentrations*
Source: developed by the authors

For nickel (Fig. 8), the model recorded intensive accumulation kinetics, positioned between the rapid uptake of copper and the slow absorption of lead. Visually, the accumulation curves lack the steep initial surge seen with copper but reach higher final concentration levels than lead, achieving dynamic equilibrium closer to the end of the 180-day cycle. The steady increased in normalised concentration confirmed its moderate mobility.

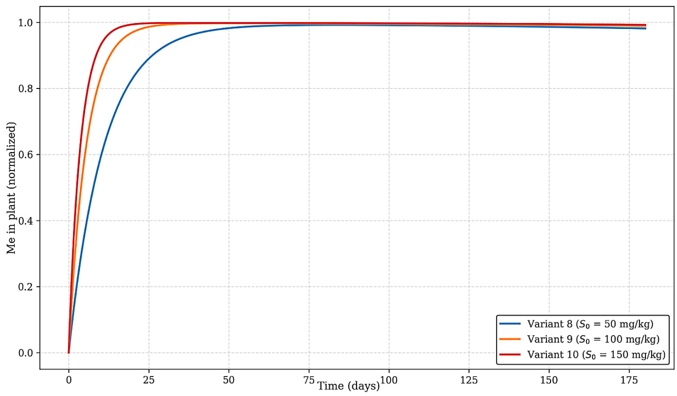

Figure 8. *Dynamics of Ni accumulation in plant tissues at different initial concentrations*
Source: developed by the authors

The model's ability to decouple growth dynamics from uptake kinetics allowed to identify that the primary limitation in remediation was not just the chemistry of the soil, but the physiological vulnerability of the plant's growth mechanisms to metal complexes. Ultimately, the overall efficiency of phytoextraction was determined not solely by the specific absorption coefficient but by the total formed biomass capable of storing these elements.

The additive effect in multi-metal systems

The temporal decrease in heavy metal complex concentrations within the soil matrix occurred significantly more intensively at higher initial baseline values of S_0. This dynamic was physically explained by the larger concentration gradient established between the soil solution and the root surface. A steeper concentration gradient thermodynamically driven more active plant uptake, forcing the physiological transport mechanisms to operate at maximum capacity. Figure 9 illustrated this process under control conditions. The graph showed that at background pollution levels, the reduction in soil metal concentrations was minimal and followed a nearly linear trajectory, as the low concentration gradient does not trigger maximum uptake rates.

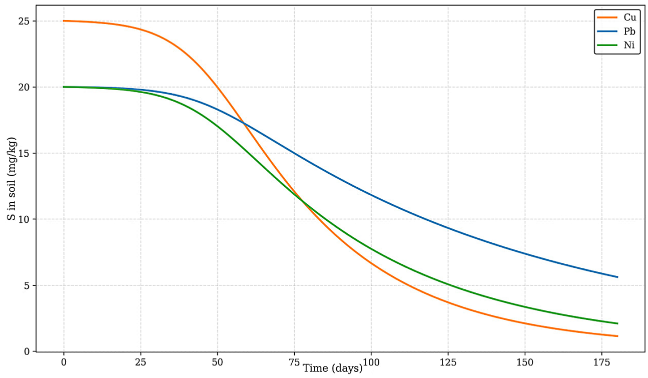

Figure 9. *Changes in Cu, Pb, and Ni concentrations in the soil (control)*
Source: developed by the authors

According to the model's numerical outputs, the most effective soil cleaning over a single vegetative period was recorded for copper, achieving an exceptional decontamination efficiency of 92.9% (Fig. 10). This metric was visually represented by the significant vertical gap between the initial starting point on the Y-axis (S_0 = 300 mg/kg) and the final residual concentration at day 180, which dropped to approximately 21.3 mg/kg. The steep downward slope of the curves in Figure 10 indicated that the most intensive cleaning occurred during the first 60-80 days of growth. This remarkably high metric was directly associated with copper's high bioavailability and the robust biomass growth it permits. The plant was able to generate a massive biological "sink" (maximum root and shoot biomass), which continuously pulled the metal from the soil without succumbing to severe growth inhibition.

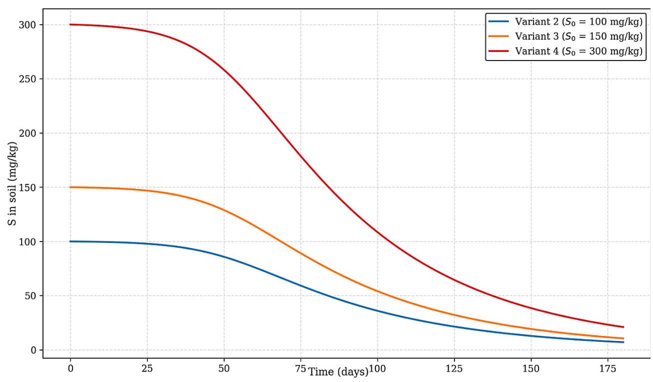

Figure 10. *Decrease in Cu concentration in the soil at different initial pollution levels*
Source: developed by the authors

In contrast, lead demonstrated the lowest removal rate, peaking at only 53.5% efficiency (Fig. 11). On the graph, this limited efficiency was evidenced by the much shallower slope of the curves compared to copper. Even after 180 days, the final concentration for the 150 mg/kg scenario remained high (above 69 mg/kg), which was clearly visible as the curve failed to approach the lower portion of the Y-axis. The severe limitation in Pb extraction was a direct consequence of the smaller "biological sponge" (reduced biomass) available to soak up the pollutant due to its high toxicity. These computational results were in agreement with the empirical conclusions drawn by A. Pruteanu *et al.* (2026), who pointed to the strict dependence of purification intensity on the initial dose of elements in the substrate.

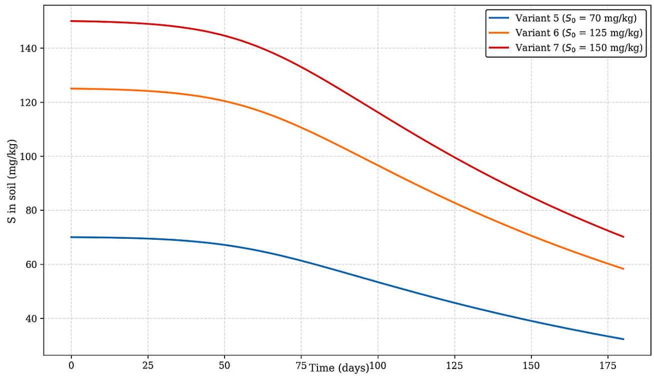

Figure 11. *Decrease in Pb concentration in the soil at different initial pollution levels*
Source: developed by the authors

For nickel, the extraction rate reached a highly effective 80.6% (Fig. 12). This efficiency was indicated on the figure by the final convergence of the concentration curves toward lower values, representing a substantial reduction from the initial levels. The trajectory showed a steady decline throughout the period, meaning the "cleaning" process for Ni was more prolonged and consistent than for Cu. This robust computational result was supported by the experimental findings of K. Selvaraj *et al.* (2021), who emphasised the significant potential of mustard plants for active Ni accumulation.

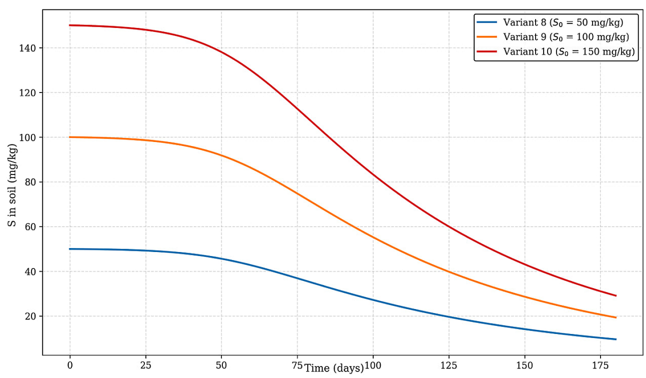

Figure 12. *Decrease in Ni concentration in the soil at different initial pollution levels*
Source: developed by the authors

So, the comparative analysis of soil decontamination dynamics confirmed that the cleaning efficiency was determined by the synergy between metal mobility and the resulting plant biomass.

While the model predicted high success for copper and nickel remediation, the persistent nature of lead concentrations highlighted the limitations of using *B. juncea* as a sole remediator for Pb-heavy sites. These findings emphasised the necessity of accounting for metal-specific toxicity, when planning long-term ecological restoration projects.

Multi-metal contamination and additive toxic stress dynamics. Practical implications and environmental risk assessment

A critical and highly innovative component of this mathematical research was the numerical simulation of simultaneous soil contamination by a "cocktail" of all three heavy metal complexes (Pb, Cu, and Ni). This scenario was not merely a theoretical exercise but a high-fidelity representation of the complex anthropogenic pressure characteristic of industrial zones and territories significantly affected by modern military actions in Ukraine. In such environments, soil was rarely contaminated by a single element; rather, it faced a multi-vector assault from various metal species originating from shell fragments, propellants, and destroyed infrastructure. In the case of a multi-metal mixture, the model established that the combined toxic effect led to a drastically more pronounced and non-linear inhibition of *Brassica juncea* biomass growth compared to any single-element system (Fig. 13). Specifically, while the control variant reached a stable biomass of 10.0 kg/m^2, the multi-metal scenario results in a dramatic stagnation of growth, with the final biomass barely reaching 2.2 kg/m^2 by the end of the 180-day vegetative period. This represented nearly 78% reduction in biological productivity. Mathematically, this was the result of the additive nature of the toxicity constants S. Sharma & B. Singh (2024) recently demonstrated through similar numerical simulations that multi-metal interactions led to a non-linear surge in oxidative stress, which validated the growth stagnation observed in model.

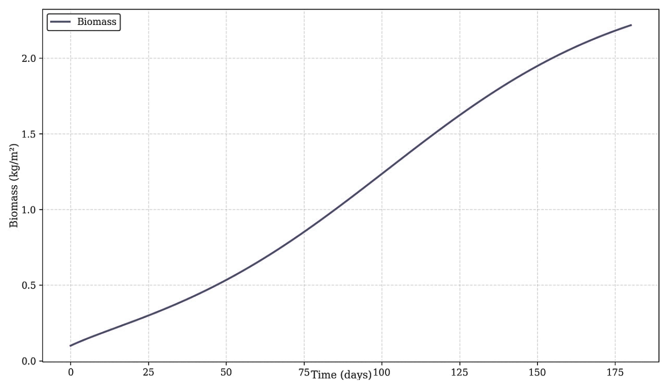

***Figure 13.** Dynamics of mustard biomass growth at elevated concentrations of three metals simultaneously (mixture)*

Source: developed by the authors

This severe suppression of biological productivity directly created a "biomass bottleneck", which significantly impaired the overall efficiency of the remediation process. As shown in Figure 14, while the normalised concentration of each metal within the surviving plant tissues remained relatively high, the total mass of pollutants extracted from the soil was much lower than in monometallic variants. The visual trajectory of the accumulation curves demonstrated a rapid initial spike followed by an early, compressed plateau. This rapid saturation, evident within the first 30 days, was not indicative of efficient extraction; rather, it visually confirmed that the stunted plant cannot safely distribute the toxic load across new growing tissues, leading to premature physiological gridlock.

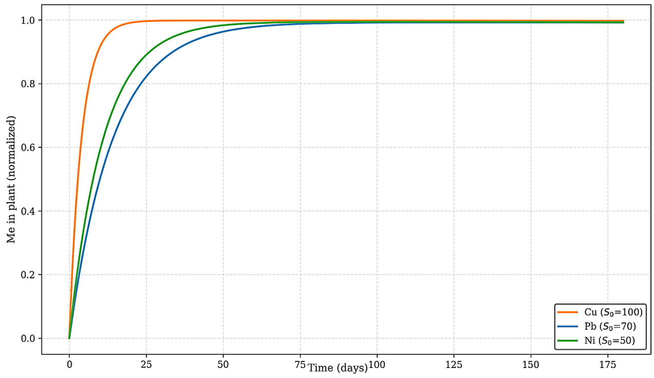

Figure 14. *Dynamics of Cu, Pb, and Ni accumulation in plant tissues at elevated concentrations of three metals simultaneously*

Source: developed by the authors

This occurred because there was simply not enough physical plant tissue (the "biological sponge") available to store the absorbed complexes. Consequently, it was observed a marked deceleration of the overall soil cleaning process (Fig. 15). The soil concentration curves for all three metals in the mixture showed a much flatter trajectory compared to their respective single-metal scenarios, indicating that the time required for complete decontamination would increase by several vegetative cycles. This highlighted the absolute necessity of accounting for the combined influence of metals, when forecasting phytoremediation efficiency for real-world environmental restoration projects.

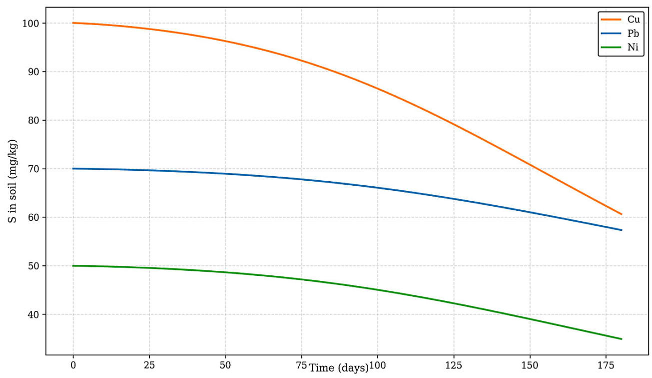

Figure 15. *Changes in Cu, Pb, and Ni concentrations in the soil at elevated concentrations of three metals simultaneously*

Source: developed by the authors

The observed decrease in process intensity during mixed contamination point to complex biological competition between different metal complexes for root absorption mechanisms (ion transporters) and subsequent antagonistic intracellular effects. This phenomenon was thoroughly described in the seminal work of A. Małecka *et al.* (2019). Researchers established that *B. juncea* (v. Malopolska) effectively activated antioxidant enzyme systems, such as SOD and APX, to combat oxidative stress during metal accumulation. The authors' results proved that, while the plant was a robust hyperaccumulator, extreme multi-metal loads can eventually overwhelm these defense mechanisms, redirecting energy from growth to survival. The consistency of our numerical outputs – showing the predictable 92.9% efficiency for Cu and 80.6% for Ni in isolation, but a systemic failure to reach these metrics in the mixture – robustly confirmed the adequacy and predictive power of the developed dynamic model. Findings of this research suggested that for military-polluted sites, remediation strategies must be adjusted to account for this synergistic inhibition, potentially requiring lower planting densities or the introduction of microbial bio-stimulants to support biomass resilience under extreme multi-vector stress. One of the most significant findings was the extreme sensitivity of the remediation timeline to the initial pollutant "cocktail". For lands affected by heavy artillery fire, where Cu and Pb concentrations often exceeded baseline levels by several orders of magnitude, a single vegetative cycle was clearly insufficient for full decontamination. Based on model of this study, the 53.5% efficiency for lead indicated that at least three consecutive 180-day cycles would be required to reach safe thresholds in highly polluted soils. Furthermore, the model highlighted a critical "toxic threshold" identified by the parameter e = 1.0 (half-saturation constant). When plant tissue concentrations exceeded this value, the growth inhibition became non-linear and accelerates rapidly. For practitioners, this meant that phytoremediation efforts must be carefully monitored: if initial biomass growth was severely stunted within the first 30-45 days, the system had likely entered a "toxic spiral", where extraction cannot keep pace with biomass degradation.

The obtained simulation results regarding selective toxicity and accumulation patterns were consistent with several foundational and contemporary studies. Specifically, the critical physiological disruptions and growth inhibition observed under lead stress align with the findings of A. Ado *et al.* (2015). Scientists recorded that high lead concentrations significantly decreased root and shoot length, as well as the total chlorophyll content in *B. juncea*. This corresponded to the research of G. DalCorso *et al.* (2019), who demonstrated that heavy metal stress triggers complex molecular signalling pathways that regulated metal transporters. Researchers' work highlighted that the genetic potential of the plant to sequester metals in vacuoles was the primary driver of tolerance. The efficiency of *Brassica juncea* as a versatile hyperaccumulator in model of this study supported the empirical observations of H. Ali *et al.* (2013). The authors established that phytoextraction was the most commercially viable technique for large-scale soil recovery due to its low cost and environmental compatibility. Scientists' study confirmed that the success of the process was fundamentally dependent on the plant's ability to produce high biomass in the presence of bioavailable metal ions. Furthermore, the synergistic toxic effects in multi-metal mixtures demonstrated in this research correlate with the recent numerical simulations by S. Sharma & B. Singh (2024). The authors proved that the interaction between different heavy metals led to a non-linear increase in phytotoxicity, which cannot be predicted by studying metals in isolation. Scientists' findings emphasised that Pb specifically acted as a strong inhibitor of the translocation of other essential and non-essential elements. This was further supported by the comprehensive remediation frameworks proposed by A. Yan *et al.* (2020), who demonstrated that revegetation with hyperaccumulators not only removed toxins but also restored soil microbial health. L. Liu *et al.* (2018) established that the choice of remediation technique must be strictly aligned with the chemical speciation of metals and the target clean up level. Researchers concluded that phytoextraction remained the most effective strategy for managing low-to-medium pollution in industrial substrates.

Strategy of induced extraction discussed in this research was supported by B. Kos &

D. Leštan (2003). The authors demonstrated that using biodegradable chelating agents can increase lead solubility by several orders of magnitude, thereby significantly enhancing the uptake rate. Researchers' results also showed that the integration of permeable barriers was a necessary safety measure to prevent the leaching of mobilised lead into the groundwater. The necessity of assessing environmental risks in complex zones was further reinforced by O.O. Okedeyi *et al.* (2014). Scientists established that the enrichment of heavy metals in surface soils and local vegetation was directly proportional to the intensity of nearby industrial activities. Study of South Africa confirmed that metals like Cu and Pb showed a high bioaccumulation factor, posing a risk of entering the food chain. The application of non-linear differential equations to track these environmental dynamics followed the predictive concepts established by A. Rein *et al.* (2011). Researchers introduced dynamic plant uptake models that accounted for changes in plant growth and transpiration over time, proving that such models were more accurate than static risk assessments. It also confirmed that accounting for the time-dependency of both soil and plant tissue concentrations was vital for realistic remediation forecasting. Finally, the mathematical rigor of system evaluation conducted in this research was consistent with the methodological approaches of Y. Ouyang (2005). The author proved that principal component analysis and similar multivariate mathematical tools were essential for evaluating the performance of monitoring systems in complex ecological environments. Scientist's findings demonstrated that these models allowed for the identification of the most significant environmental variables that drive the dynamics of pollutant transfer. So, the integration of these diverse scientific findings confirmed that the efficiency of phytoremediation was a product of complex interactions between metal chemistry, plant physiology, and mathematical growth laws. The developed model provided a robust analytical tool for predicting these interactions and optimising soil restoration in anthropogenically stressed regions.

Conclusions

Based on the results of the mathematical modelling of phytoremediation processes for soils contaminated with heavy metals (Pb, Cu, Ni) using Indian mustard (*Brassica juncea*), it was determined that adapted system of nonlinear differential equations adequately described the dynamics of the "metal-plant" system over a 180-day vegetative period. The model incorporated the relationship between biomass accumulation and the inhibitory impact of metal-specific toxicity, enabling the prediction of soil cleaning efficiency without the need for prolonged field experiments A significant differentiation in phytoremediation efficiency was established depending on the pollutant type. The system demonstrated the highest self-cleaning capacity for copper (92.9% efficiency), driven by a combination of a high specific absorption coefficient ($\alpha = 0.0025$ day^{-1}) and low phytotoxicity ($d = 0.03$). For nickel, this metric was 80.6%, whereas lead proved to be the least accessible for extraction (53.5%) due to its critical suppression of biomass growth ($d = 0.07$). Furthermore, the numerical simulation of multi-metal contamination confirmed the presence of an additive toxic effect. The simultaneous presence of lead, copper, and nickel at concentrations typical for war-affected territories led to a cumulative inhibition of *B. juncea* biomass growth (down to 2.2 kg/m^2), which represented a 78% reduction in biological productivity compared to monometallic scenarios. The selection of soil restoration strategies was scientifically substantiated: Indian mustard was a highly effective tool for the complete phytoextraction of Cu and Ni. In the case of lead contamination, phytoremediation should be considered a phytostabilisation method aimed at metal immobilisation. The perspectives for further research include expanding the dynamic model to account for the impact of soil amendments, such as EDTA, and microbial biostimulants to support biomass resilience and optimise recovery timelines for agricultural lands in Ukraine affected by military conflict.

Acknowledgements

The authors express their gratitude to the Department of Bioenergy, Bioinformatics and Ecobiotechnology of the National Technical University of Ukraine "Igor Sikorsky Kyiv Polytechnic Institute" for providing consultative support.

Funding

None.

Conflict of Interest

None.

References

[1] Ado, A., Sale, I.A., Badamasi, M.T., Nazamuddenkhan, N., & Majumdara, R.S. (2015). Effect of heavy metal on *Brassica juncea* growth exposed to different lead treatments. *International Journal of Scientific & Engineering Research*, 6(6), 1088-1095.

[2] Ali, H., Khan, E., & Sajad, M.A. (2013). Phytoremediation of heavy metals – concepts and applications. *Chemosphere*, 91(7), 869-881. doi: 10.1016/j.chemosphere.2013.01.075.

[3] Ali, I., Khan, M.J., Shah, A., Deeba, F., Hussain, H., Yazdan, F., Khan, M.U., & Khan, M.D. (2022). Screening of various *Brassica* species for phytoremediation of heavy metals-contaminated soil of Lakki Marwat, Pakistan. *Environmental Science and Pollution Research*, 29, 37765-37776. doi: 10.1007/s11356-021-18109-7.

[4] Bortoloti, G.A., & Baron, D. (2022). Phytoremediation of toxic heavy metals by *Brassica* plants: A biochemical and physiological approach. *Environmental Advances*, 8, article number 100204. doi: 10.1016/j.envadv.2022.100204.

[5] Cârdei, P., Tudora, C., Vlăduț, V., Pruteanu, M.A., Găgeanu, I., Cujbescu, D., Bordean, D.-M., Ungureanu, N., Ipate, G., & Cristea, O.D. (2021). Mathematical model to simulate the transfer of heavy metals from soil to plant. *Sustainability*, 13(11), article number 6157. doi: 10.3390/su13116157.

[6] DalCorso, G., Fasani, E., Manara, A., Visioli, G., & Furini, A. (2019). Heavy metal pollutions: State of the art and innovation in phytoremediation. *International Journal of Molecular Sciences*, 20(14), article number 3412. doi: 10.3390/ijms20143412.

[7] Kamal, A.M., & Alali, A.F. (2025). Kinetic modeling of heavy metal uptake and translocation in *Brassica juncea* L. for phytoremediation engineering. *Discover Environment*, 3, article number 296. doi: 10.1007/s44274-025-00502-5.

[8] Kos, B., & Leštan, D. (2003). Induced phytoextraction/soil washing of lead using biodegradable chelate and permeable barriers. *Environmental Science & Technology*, 37(3), 624-629. doi: 10.1021/es0200793.

[9] Leonavičienė, T., Kirjackis, J., & Baltrėnaitė-Gedienė, E. (2023). *Modelling of environmental processes and management*. Vilnius: Vilnius Tech. doi: 10.20334/2023-055-S.

[10] Liu, L., Li, W., Song, W., & Guo, M. (2018). Remediation techniques for heavy metal-contaminated soils: Principles and applicability. *Science of the Total Environment*, 633, 206-219. doi: 10.1016/j.scitotenv.2018.03.161.

[11] Maher, S., *et al.* (2025). Comparative assessment of *Spinacia oleracea* and *Brassica juncea* for efficient phytoremediation of heavy metal contaminated soils. *International Journal of Phytoremediation*, 28(5), 874-884. doi: 10.1080/15226514.2025.2586661.

[12] Małecka, A., Konkolewska, A., Hanć, A., Barałkiewicz, D., Ciszewska, L., Ratajczak, E., Staszak, A.M., Kmita, H., & Jarmuszkiewicz, W. (2019). Insight into the phytoremediation capability of *Brassica juncea* (v. *Malopolska*): Metal accumulation and antioxidant enzyme activity. *International Journal of Molecular Sciences*, 20(18), article number 4355. doi: 10.3390/ijms20184355.

[13] Nagajyoti, P.C., Lee, K.D., & Sreekanth, T.V.M. (2010). Heavy metals, occurrence and toxicity for plants: A review. *Environmental Chemistry Letters*, 8, 199-216. doi: 10.1007/s10311-010-0297-8.

[14] Okedeyi, O.O., Dube, S., Awofolu, O.R., & Nindi, M.M. (2014). Assessing the enrichment of heavy metals in surface soil and plant (*Digitaria eriantha*) around coal-fired power plants in South Africa. *Environmental Science and Pollution Research*, 21, 4686-4696. doi: 10.1007/s11356-013-2432-0.

[15] Ouyang, Y. (2005). Evaluation of river water quality monitoring stations by principal component analysis. *Water Research*, 39(12), 2621-2635. doi: 10.1016/j.watres.2005.04.024.

[16] Pruteanu, A., Nițu, M., Vlăduț, V., Matache, M., Voicea, I., Iuliana, G., Vanghele, N., Nenciu, F., Cujbescu, D., & Badea, D.O. (2026). Induced phytoextraction of heavy metals from soils using *Brassica juncea* and EDTA: An efficient approach to the remedy of zinc, copper and lead. *Environments*, 13(1), article number 23. doi: 10.3390/environments13010023.

[17] Rani, P., Rose, P.K., Kidwai, M.K., & Meenakshi. (2023). *Brassica Juncea* L.: A potential crop for phytoremediation of various heavy metals. In R.P. Singh, P. Singh & A. Srivastava (Eds.), *Heavy metal toxicity: Environmental concerns, remediation and opportunities* (pp. 285-311). Singapore: Springer. doi: 10.1007/978-981-99-0397-9_14.

[18] Rein, A., Legind, C.N., & Trapp, S. (2011). New concepts for dynamic plant uptake models. *AR and QSAR in Environmental Research*, 22(1-2), 191-215. doi: 10.1080/1062936X.2010.548829.

[19] Selvaraj, K., Ramasubramanian, V., & Makesh Kumar, B. (2021). Phytoremediation potential of *Brassica juncea* in nickel contaminated soil. *Paripex – Indian Journal of Research*, 10(4), 150-159. doi: 10.36106/paripex.

[20] Shen, X., Dai, M., Yang, J., Sun, L., Tan, X., Peng, C., Ali, I., & Naz, I. (2022). A critical review on the phytoremediation of heavy metals from environment: Performance and challenges. *Chemosphere*, 291, article number 132979. doi: 10.1016/j.chemosphere.2021.132979.

[21] Suman, J., Uhlik, O., Viktorova, J., & Macek, T. (2018). Phytoextraction of heavy metals: A promising tool for clean-up of polluted environment? *Frontiers in Plant Science*, 9, article number 1476. doi: 10.3389/fpls.2018.01476.

[22] Sut-Lohmann, M., Grimm, M., Kästner, F., Raab, T., Heinrich, M., & Fischer, T. (2023). *Brassica juncea* as a feasible hyperaccumulator of chosen potentially toxic metals under extreme environmental conditions. *International Journal of Environmental Research*, 17, article number 38. doi: 10.1007/s41742-023-00528-8.

[23] Tangahu, B.V., Sheikh Abdullah, S.R., Basri, H., Idris, M., Anuar, N., & Mukhlisin, M. (2011). A review on heavy metals (As, Pb, and Hg) uptake by plants through phytoremediation. *International Journal of Chemical Engineering*, 2011, article number 939161. doi: 10.1155/2011/939161.

[24] Yan, A., Wang, Y., Tan, S.N., Yusof, M.L.M., Ghosh, S., & Chen, Z. (2020). Phytoremediation: A promising approach for revegetation of heavy metal-polluted land. *Frontiers in Plant Science*, 11, article number 359. doi: 10.3389/fpls.2020.00359.

Математичне моделювання ефективності фіторемедіації грунтів від Pb, Cu та Ni

Олександра Сидоренко
Магістрант
Національний технічний університет України «Київський політехнічний інститут імені Ігоря Сікорського»
03056, Берестейський просп., 37, м. Київ, Україна
https://orcid.org/0009-0004-5890-7630
Наталія Голуб
Доктор технічних наук, професор
Національний технічний університет України «Київський політехнічний інститут імені Ігоря Сікорського»
03056, Берестейський просп., 37, м. Київ, Україна
https://orcid.org/0000-0003-1448-1872

Анотація. Метою дослідження була кількісна порівняльна оцінка динаміки вилучення свинцю, міді та нікелю з ґрунту системою «метал-рослина» на основі математичного моделювання для прогнозування термінів очищення забруднених територій. Забруднення ґрунтового покриву важкими металами (Pb, Cu, Ni) внаслідок інтенсивної техногенної діяльності та масштабних воєнних дій в Україні становило критичну загрозу екологічній безпеці та здоров'ю населення. Фіторемедіація із використанням рослин-гіперакуляторів, таких як *Brassica juncea*, розглядалася як перспективний та екологічно безпечний метод відновлення екосистем. Проте планування таких заходів ускладнювалося різною швидкістю вилучення елементів та їхнім токсичним впливом на біомасу, що потребувало розробки точних прогностичних моделей. У роботі було використано експоненціальну модель кінетики поглинання металів для прогнозування термінів очищення забруднених територій. Було встановлено, що ефективність очищення ґрунту за один вегетаційний період (180 днів) становила 92,9 % для міді, 80,6 % для нікелю та лише 53,5 % для свинцю. Також, у дослідженні було виявлено, що висока ефективність ремедіації міді зумовлена її високою мобільністю та низькою фітотоксичністю. Натомість свинець виявив найсильніший інгібуючий ефект, що суттєво обмежував швидкість його екстракції. На базі мультиметальної моделі було продемонстровано адитивний токсичний ефект суміші забруднювачів, що призводило до зниження загальної продуктивності фіторемедіантів на 78 % порівняно з монометалевим забрудненням. Отримані результати дозволили прогнозувати залишкову концентрацію токсикантів, оптимізувати стратегії відновлення техногенно навантажених територій та земель, що постраждали від воєнних конфліктів. Розроблена модель може бути використана для оцінки економічної доцільності фіторемедіаційних заходів

Ключові слова: важкі метали; фітоекстракція; токсичний стрес; мультиметальна модель; відновлення ґрунтів; екологічна безпека

Received 01.12.2025 Revised 09.03.2026 Accepted 23.04.2026 Published: 30.04.2026

Vol. 22, No. 2
2026

Scientific Reports of the National University of Life and Environmental Sciences of Ukraine

Journal homepage: https://scireports.com.ua/en e-ISSN 2223-1609

UDC 577.151.6:579.222 DOI: 10.31548/dopovidi/2.2026.167

Effect of Fe^{2+} ions on cultivation of amino acid producers of the aspartic acid family

Iryna Demianenko*

PhD in Technical Sciences, Senior Lecturer
National Technical University of Ukraine "Igor Sikorsky Kyiv Polytechnic Institute"
03056, 37 Beresteiskyi Ave., Kyiv, Ukraine
https://orcid.org/0000-0002-0832-3619

Igor Levtun

PhD in Technical Sciences, Senior Lecturer
National Technical University of Ukraine "Igor Sikorsky Kyiv Polytechnic Institute"
03056, 37 Beresteiskyi Ave., Kyiv, Ukraine
https://orcid.org/0000-0003-2498-035X

Abstract. The study aimed to experimentally assess the effect of Fe^{2+} (in the form of $FeSO_4$) on the viability and growth of microorganisms producing amino acids of the aspartic acid family. The study was conducted under laboratory culture conditions, comparing control and experimental treatments; viability was determined by colony-forming ability using the serial dilution and plating method with cell concentration recalculation, whilst the physical component was assessed by the effective magnetic susceptibility χ, calculated from resonance measurements of the frequency shift of the oscillating circuit. The study determined that $FeSO_4$ (1%) caused a sharp decrease in the concentration of viable cells in all tested strains: for *Corynebacterium glutamicum*, the amount decreased from 15×10^{10} to 9×10^8 cells/cm^3, for *Brevibacterium flavum* – from 2×10^{10} to 4×10^8 cells/cm^3, for *Brevibacterium* sp. 90 – from 3×10^{10} to 8×10^8 cells/cm^3, corresponding to a decrease of approximately 1.6-2.2 log. The dose-dependent analysis for *B. flavum* in meat peptone broth was 7.97×10^{-3}-8.459×10^{-3}, for "cells + meat peptone broth" 8.028×10^{-3}-8.408×10^{-3}, and the differences between the medium and the cell suspensions did not exceed $\pm 0.4 \times 10^{-3}$. The results can be directly applied in industrial biotechnology and research laboratories that cultivate *Corynebacterium*/*Brevibacterium* for the production of amino acids, for the adjustment of the trace

Suggested Citation:
Demianenko, I., & Levtun, I. (2026). Effect of Fe^{2+} ions on cultivation of amino acid producers of the aspartic acid family. *Scientific Reports of the National University of Life and Environmental Sciences of Ukraine*, 22(2), 167-185. doi: 10.31548/dopovidi/2.2026.167.

*Corresponding author

element composition of media, and for the rapid monitoring of culture viability based on colony-forming ability

Keywords: colony-forming ability; magnetic susceptibility; dose-dependent effect; producers; biotechnology

Introduction

The biotechnological cultivation of producers of amino acids from the aspartic acid family remains one of the key areas of modern industrial microbiology, as L-lysine, L-threonine and related metabolites are essential components of feed additives and biosynthetic pathways in the food and pharmaceutical industries. The efficiency of such processes is determined not only by the genetic potential of the strain, but also by the trace element composition of the medium, which influences the availability of cofactors, the intensity of redox reactions and stress resistance. The key players are divalent iron ions (Fe^{2+}), which simultaneously ensure the functioning of iron-containing proteins and can initiate pro-oxidative cascades, affecting the viability and reproductive capacity of cells. In amino acid production, this poses a practical problem: even minor fluctuations in the forms and concentrations of iron can alter biomass yield and, indirectly, productivity indicators, whereas in industrial practice standard formulations are used without optimising the iron supply process according to the strain.

In scientific discourse, the view that iron homeostasis in *Corynebacterium glutamicum* is a multi-level regulatory network rather than a linear "capture-storage" scheme is becoming increasingly established. A. Krüger *et al.* (2025), based on genomic analysis, demonstrated a high degree of interconnection between the regulators diphtheria toxin regulator (DtxR) and haem response regulator (HrrA) and identified numerous new targets that link iron and haem regulation. Such interconnectivity implies that changes in Fe^{2+} availability may indirectly influence not only individual biosynthetic enzymes but also energy metabolism and cell survival through the reallocation of regulatory priorities. A significant body of knowledge is emerging from studies of the response to iron deficiency. A. Küberl *et al.* (2020) found that iron deficiency in *C. glutamicum* is associated with a specific reorganisation of gene expression and is functionally linked to thiamine biosynthesis. This broadens the interpretation of iron as an integrator of metabolic modules and suggests that the "iron optimum" is not merely about avoiding toxicity, but also involves preventing deficiency-induced shifts capable of altering metabolic pathways. Furthermore, F. Müller (2020) demonstrated that the CO_2/HCO_3^- (carbon dioxide/bicarbonate) regime correlates with iron homeostasis in *C. glutamicum*, which is crucial for cultivation on shakers and in fermenters, where gas exchange and buffering capacity can alter redox conditions and, consequently, iron bioavailability.

The practical significance of iron-sensitive pathways has also been confirmed in studies on metabolic engineering. F. Thoma *et al.* (2023) demonstrated that the introduction of iron-responsive biosynthesis of protocatechuic acid (3,4-dihydroxybenzoic acid) improves the growth properties of *C. glutamicum*; that is, iron can be regarded as a tool for controlling culture development due to the possibility of directing iron-dependent metabolic pathways. At the same time, growth characteristics are also modified by non-specific chemical stressors: T. Walter *et al.* (2020) showed that indole elicits a distinct physiological response and alters the state of cells, highlighting the need to separate the effects of iron from concomitant environmental factors during experimental evaluation of Fe^{2+}. Data from studies of other metabolic pathways further confirm the context-dependence of iron's effects and the role of process parameters and substrate composition in shaping the response directed towards product biosynthesis. Thus, Y. Lin *et al.* (2025) demonstrated that a high yield of poly-γ-glutamic acid can be achieved using unrefined sugarcane molasses under non-sterile, repeated-batch fermentation, and that the technological result is ensured by a combination of an optimised medium and repeated cultivation cycles in the fermenter. In the phototrophic model by S. Kovalova *et al.* (2025), a combined effect of Fe^{2+}/Fe^{3+} complexes and light on the metabolism of *Chlorella vulgaris* was established, highlighting the role of associated physical conditions in shaping the system's response. In Corynebacteria, another dimension of variability is associated with chelation: J.T. Raynal *et al.* (2022) demonstrated that iron-chelating agents alter the growth curves of *Corynebacterium pseudotuberculosis* strains, confirming sensitivity specifically to iron bioavailability, rather than merely to its nominal concentration. Iron bioavailability may limit bacterial growth and metabolic activity in various niches. C.C. Murdoch & E.P. Skaar (2022) summarised the concept of "nutritive immunity", whereby the host restricts metals, and microorganisms respond with systems for their uptake and utilisation. In this context, G. Zhao *et al.* (2025) demonstrated that Fe^{2+} can specifically enhance the biosynthesis of L-homoserine, L-threonine and L-isoleucine in *C. glutamicum* via a regulatory mechanism that integrates the cell's iron status with the control of key steps in the aspartate pathway, forming the basis for the technological control of amino acid production through the optimisation of iron conditions during cultivation.

Therefore, the available data confirm two key points: Fe^{2+} can enhance the biosynthetic pathways of amino acids in the aspartate family and alter the regulatory networks of corynebacteria, but iron is simultaneously capable of inducing stress responses, which manifest as impaired growth or altered growth curves upon modification of bioavailability. From an applied perspective, the link between the "metabolic" and "viability" interpretations of iron requires further investigation: in studies describing the regulatory effects of Fe^{2+}, systematic comparisons of the dose-dependent effect of $FeSO_4$ on the reproductive capacity (colony-forming unit (CFU)) in various industrial strains, and the associated physical parameters of the culture system, which could reflect iron binding/redistribution in the medium, are scarcely considered. This gap poses a problem: does the addition of Fe^{2+} in the form of $FeSO_4$ lead to consistent changes in CFU in typical producers, and is this effect accompanied by changes in the integral physical characteristic of culture samples – effective magnetic susceptibility χ – within a concentration range relevant to culture media.

The study aimed to experimentally assess the effect of Fe^{2+} ions (in the form of $FeSO_4$) on the cultivation of amino acid producers of the aspartic acid family, based on indicators of viability and the physical properties of the culture system. The following objectives were set within the scope of the study: to quantitatively compare the effect of $FeSO_4$ (1%) on CFU/cm^3 in *Corynebacterium glutamicum*, *Brevibacterium flavum* and *Brevibacterium* sp. 90; to characterise the dose-dependent toxicity of lower $FeSO_4$ concentrations (0.063-0.5%) on *Brevibacterium flavum* in terms of colony formation; to determine the effective magnetic susceptibility χ for the medium and the *Brevibacterium flavum* cell suspension at different mass fractions of $FeSO_4$ and to compare the physical data with the microbiological viability indicators.

Materials and Methods

The experiment was conducted under laboratory conditions based on aseptic techniques (work in a biological safety cabinet, use of sterile glassware and consumables) and mandatory sterilisation of culture media in an autoclave. The source of the strains was the collection of microorganisms at the Institute of Food Biotechnology and Genomics of the National Academy of Sciences of Ukraine. The subjects of the study were three museum producer strains typical for the biosynthesis of compounds of the aspartate family: *Brevibacterium* sp. 90, *Corynebacterium glutamicum*, and *Brevibacterium flavum*. The selection was conducted based on the following criteria: viability of the overnight culture on standard nutrient media; obtaining typical isolated colonies without signs of contamination; reproducibility of growth in the control without the addition of $FeSO_4$. Exclusion criteria were signs of foreign microflora as determined by microscopy/colony morphology; unstable growth under control conditions; deviation of the medium pH outside the operating range specified by the protocol. For each cultivation condition, three independent biological replicates (n = 3) were performed, using separate inoculants on different days; technical replicates consisted of 2-4 parallel inoculations for each of the last 2-3 dilutions, and the determination of effective magnetic susceptibility was performed as the average of 3 repeated resonance measurements (m = 3) for each sample.

Meat-peptone media and their modifications were used as the basic nutrient components. The following were used: meat-peptone agar (OXOID; official representative in Ukraine – "Unilab"); iron sulphate ($FeSO_4$) (manufacturer "Fidespert"). Two types of media were prepared: meat-peptone broth (MPB): MPB – 100 cm^3, distilled water – up to 1 dm^3, pH 7.2 adjusted using 0.1 N NaOH; enriched meat-peptone agar (MPA enriched): MPB 100 cm^3, glucose – 0.1 g, yeast extract – 0.25 g, agar 30 g. To assess the effect of Fe^{2+} as a function of dose, a $FeSO_4$ solution was added to MPB (working volume 30 cm^3) in the following mass fractions: 0.063%; 0.125%; 0.25%; 0.5%; 1%. The dose determination stage (0.063-0.5% $FeSO_4$) was conducted only for *Brevibacterium flavum* as a model strain, since a sharply inhibitory effect was observed for all three cultures at 1% $FeSO_4$ during the screening stage, and further refinement of the concentration range was conducted on one representative culture to reduce the scope of the experiments and focus on mechanistic interpretation. For *Corynebacterium glutamicum* and *Brevibacterium* sp. 90, this study was limited to assessing the effect of 1% $FeSO_4$ as a test for the presence/severity of a toxic regime, whilst detailed dosing for these strains was not included in the phase plan. The media were sterilised in an autoclave at 1 atm and 120°C for 30 minutes, after which the agar-containing media were melted in a water bath and poured at a temperature of 47-50°C into Petri dishes or onto slants.

The following equipment was used in the study: a microbiological safety cabinet; a BIOSAN ES-20 shaker-incubator (Biosan; Latvia); an autoclave; a steriliser; a water bath; a refrigerator; a thermostat; a KFK-2 spectrophotometer (photoelectric concentration colourimeter) (model KFK-2; the manufacturer was specified in the laboratory instrument's technical data sheet); an I-150 digital pH meter. Laboratory glassware included bacteriological loops, graduated pipettes of 1/2/5/10 cm^3, sterile test tubes, conical flasks, Petri dishes, a spirit lamp, stands and sterile stoppers. For radio-technical resonance determination of magnetic susceptibility, the following were used: C1-93 oscilloscope (mass-produced in the USSR), Ch3-64/1 computing frequency meter (mass-produced in the USSR), VM 560 Tesla Q-factor meter (Tesla), and an LC (inductor-capacitor) circuit comprising a capacitor and a specially manufactured copper solenoid with a sample container. The block diagram of the setup and the design of the solenoid with the container are shown in Figure 1. The overnight culture was prepared on slanted solid medium (MPA medium, 2.5% agar) in test tubes containing 5 cm^3 of medium; incubation was conducted for 24 hours at 30°C in a thermostat. To prepare the inoculum, several colonies of the same type were selected, transferred to a flask containing sterile saline solution and suspended with cell concentration control. The main cultivation was conducted in 250 cm^3 Erlenmeyer flasks containing 30 cm^3 of the appropriate medium (control without $FeSO_4$ or an experiment with a specified mass fraction of $FeSO_4$). Incubation was conducted on a shaker-incubator at 30°C with stirring at 140 rpm in parallel variants for 24 hours.

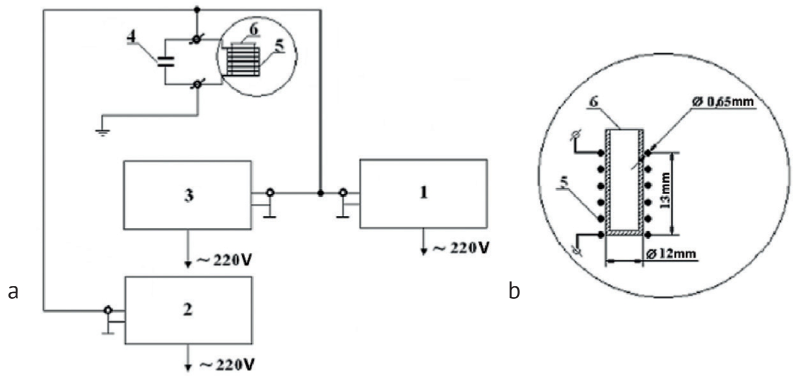

Figure 1. *Block diagram of the setup (a) and design of the solenoid with a sample container (b)*
Note: 1 – high-frequency oscillator; 2 – resonant circuit (LC) (solenoid L and capacitor C); 3 – circuit quality factor meter (Q-meter); 4 – frequency meter (measurement of resonant frequency); 5 – oscilloscope (visual monitoring of signal shape); 6 – solenoid with sample container (unit for introducing the sample into the inductor)
Source: compiled by the authors

The toxicity of Fe^{2+} was assessed by counting viable cells using a series of dilutions and plating on solid medium. After 24 hours of incubation, the suspension was removed from the shaker, and a series of dilutions was prepared in saline (7 tubes, 4.5 cm^3 each; the first tube was filled with 0.5 cm^3 of culture with an expected concentration of approximately 10^9 cells/cm^3; subsequent transfers were then conducted to tube No. 7, using separate sterile pipettes for each step). The last 2-3 dilutions were selected for plating, with 2-4 parallel plates prepared for each dilution. Two seeding formats were used: the deep method (0.5 cm^3 of suspension into the centre of a Petri dish, followed by pouring 10-15 cm^3 of molten agar (47-50°C) and uniform mixing); the surface method (0.1 cm^3 of suspension onto the agar surface, spread with a sterile Drygalski spatula until the surface was completely dry). Quantitative assessment of viability was performed using surface inoculation of 0.1 cm^3 of suspension onto agar, spread with a Drygalski spatula; deep inoculation of 0.5 cm^3 was used as an auxiliary method to obtain isolated colonies under high growth density and was not used for calculations. The plates were incubated upside down at 32°C for 48-72 hours. For quantitative counting, preference was given to plates with 20-150 colonies; under conditions of Fe^{2+} growth inhibition, when lower N values were recorded in all suitable dilutions, plates with $N < 20$ were included in the calculations as an estimate limited by the lower limit of quantification, and the absence of colonies was recorded as a result below the limit of detection for the corresponding dilution and inoculum volume. Quantitative results of the initial count were recorded as the number of colonies per plate for the selected dilutions; CFU/cm^3 values were used for comparison between variants, incorporating dilution and inoculum volume. This approach was reasonably applied to distinguish the effect of Fe^{2+} on cell reproductive capacity from changes in optical density, which may be distorted by aggregation or changes in cell size.

To investigate possible changes in the magnetic properties of culture fluid/cells in the presence of Fe^{2+}, a radio-technical resonance method was employed, the principle of which involved measuring the shift in the resonance frequency of an LC circuit when a sample was introduced into a solenoid. The method was implemented at frequencies of 12-20 MHz with an error not exceeding 0.2%. The setup comprised an LC circuit (capacitor C and solenoid L), a Q-factor meter, an oscilloscope for visual signal monitoring, and a frequency meter for determining the resonance frequency. Measurements were conducted sequentially: 2-hour warm-up of the setup; recording of the baseline value; measurement for the container with air; measurement for the container with the culture. The calculation apparatus included the relationship between the solenoid inductance and the resonant frequency of the LC circuit, and the derivation of the formula for the effective magnetic susceptibility of the sample. The solenoid inductance was described by equation (1):

$$L = k\mu\mu_0 N^2 \frac{S}{l}, \quad (1)$$

where μ_0 – magnetic constant, which is $4\pi \cdot 10^{-7}$ H/m; – magnetic permeability of the medium in the solenoid; N – number of solenoid turns; l – solenoid length; k – coefficient that depends on the ratio of the length to the diameter of the solenoid coil; S – cross-sectional area of the solenoid.

For an empty solenoid and a solenoid with a sample, the inductance was described by equation (2):

$$L_0 = k\mu_0 N^2 \frac{S}{l}. \quad (2)$$

The change in inductance is calculated using equation (3):

$$\Delta L = L - L_0 = k(\mu - 1)\mu_0 N^2 \frac{S}{l} = \chi\mu_0 N^2 \frac{S}{l} k, \quad (3)$$

where χ – magnetic susceptibility of a biological sample.

The resonant frequency of the circuit was determined using equation (4):

$$\omega = \frac{1}{\sqrt{LC}} \text{ or } f = \frac{1}{2\pi\sqrt{LC}}, \quad (4)$$

where ω – cycle frequency.

Resonant frequency of the LC circuit (5):

$$\omega_0 = \frac{1}{\sqrt{L_0 C}}. \quad (5)$$

Resonant frequency of an LC circuit containing a biological sample (6):

$$\omega = \frac{1}{\sqrt{LC}}. \quad (6)$$

Shift in the resonance frequency resulting from a change in the solenoid's inductance upon insertion of a biological sample was calculated using equation (7):

$$|\Delta\omega| = |\omega - \omega_0| = \frac{1}{\sqrt{C}}\left(\frac{1}{\sqrt{L_0 + \Delta L}} - \frac{1}{\sqrt{L}}\right) = \\ = \left|\frac{1}{\sqrt{L_0 C}}\left(1 + \frac{\Delta L}{L_0}\right)^{-\frac{1}{2}} - 1\right|. \quad (7)$$

At $\frac{\Delta L}{L_0} \ll 1$ – formula was applied (8):

$$|\Delta\omega| \approx \left|\omega_0\left(1 - \frac{\Delta L}{2L_0} - 1\right)\right| = \omega_0\left|\frac{\Delta L}{2L_0}\right| = \\ = \omega_0 \frac{\chi\mu_0 N^2 \frac{S}{l} k}{2\mu_0 N^2 \frac{S}{l} k} = \frac{\omega_0 \chi}{2}. \quad (8)$$

From this ratio, the magnetic susceptibility of the biological sample was determined using equation (9):

$$\chi = \frac{2\Delta\omega}{\omega_0} \rightarrow \chi = \frac{2\Delta f}{f_0}. \quad (9)$$

The use of this method was justified to assess whether variations in the mass fraction of $FeSO_4$ are accompanied by changes in the integral paramagnetic/diamagnetic characteristics of the culture system, which could potentially reflect the binding or deposition of iron by cellular components or changes in the composition of the medium. The study did not involve humans or vertebrate animals; the work was conducted with laboratory bacterial cultures in accordance with microbiological safety and aseptic procedures (sterilisation of media, biosafety cabinet, disposal of contaminated materials following internal regulations of the laboratory).

Results

Effect of Fe^{2+} ions on the cultivation of various strains of microorganisms

The key finding of the comparative experiment was the demonstration of a marked inhibitory effect of 1% $FeSO_4$ on the growth of all strains studied. The summarised data are presented in Table 1, which shows the cell counts in the experimental group (MPB medium + 1% $FeSO_4$) and in the control group (MPB medium without the addition of iron salts).

Table 1. *The effect of Fe^{2+} ions ($FeSO_4$, 1%) on the growth of microorganisms (viable cells, cells/cm³)*

Strain name/culture medium	Experiment: MPB solution + $FeSO_4$ (1%)	Control, MPB collection
Corynebacterium glutamicum	$9 \times 10^8 \pm 4.5 \times 10^7$	$15 \times 10^{10} \pm 7.5 \times 10^9$
Brevibacterium flavum	$4 \times 10^8 \pm 2 \times 10^7$	$2 \times 10^{10} \pm 1 \times 10^9$
Brevibacterium sp. 90	$8 \times 10^8 \pm 4 \times 10^7$	$3 \times 10^{10} \pm 1.5 \times 10^9$

Note: sowing method: surface, V = 0.1 cm³
Source: compiled by the authors

Table 1 showed that in the control (without $FeSO_4$), high concentrations of viable cells were formed, characteristic of active growth of the producers under the conditions used. In particular, for *C. glutamicum*, the control value was 15×10^{10} cells/cm³, whereas in the presence of 1% $FeSO_4$ it was only 9×10^8 cells/cm³. Thus, Fe^{2+} at a high mass fraction caused a reduction in CFU of approximately 167-fold (approximately 2.2 logarithmic orders), indicating suppression of the population's reproductive capacity.

For *Brevibacterium flavum*, the control value was 2×10^{10} cells/cm³, whereas in the 1% $FeSO_4$ treatment, 4×10^8 cells/cm³ were obtained, representing a reduction of approximately 50-fold (~1.7 log). For *Brevibacterium* sp. 90, the control reached 3×10^{10} cells/cm³, whereas in the presence of $FeSO_4$ (1%), 8×10^8 cells/cm³ were obtained, corresponding to a reduction of approximately 37.5-fold (~1.6 log). The results confirmed the universality of the inhibitory effect of Fe^{2+} (under conditions of 1% $FeSO_4$ addition) for three taxa of the Actinobacteria/Corynebacteria group, which are typical producers of metabolites of the aspartate family.

Notably, in all cases, a viable fraction of the population was maintained at a level of 10^8 cells/cm³ in the experimental groups; in other words, Fe^{2+} at this concentration did not cause complete elimination of the cultures during a 24-hour incubation. Instead, a sharp decrease in the final CFU count was observed, which is most consistent with a mechanism of inhibition of cell proliferation/division or the induction of sublethal damage, manifested as a reduction in colony-forming ability. The dynamics of CFU reflect the cumulative effect on the reproductive potential of the population, are linked to biomass yield, and correlate indirectly with productivity in terms of target metabolites.

The comparative sensitivity of the strains to 1% $FeSO_4$, assessed by the fold reduction in CFU, varied: the most pronounced decline was observed for *C. glutamicum*, whereas for *Brevibacterium flavum* and *Brevibacterium* sp. 90 it was less pronounced but still significant. This is consistent with the probable species/strain-specific regulation of iron homeostasis, the intensity of antioxidant defence, and the ability to bind/sequester excess iron. In practical terms, this means that even for closely related producers, an identical concentration of Fe^{2+} in the medium may present varying degrees of technological risk in terms of growth stability. Overall, the results of this stage indicated that $FeSO_4$ at a mass fraction of 1% is the concentration at which the toxic effects of Fe^{2+} become apparent for the tested producers, which justified the need to investigate lower concentrations to establish a range within which a controlled effect of iron is possible without significant growth inhibition.

Analysis of the toxic effects of low concentrations of iron ions on a culture of *Brevibacterium flavum*

Following the establishment of the inhibitory effect of 1% $FeSO_4$ on the growth of producer strains, a dose-dependent comparison was conducted for *Brevibacterium flavum* in the presence of $FeSO_4$ at mass fractions of 0.063%, 0.125%, 0.25% and 0.5%, and in a control without iron salts. Quantitative indicators of viability under these conditions are presented in Table 2, which demonstrates a decrease in colony formation with increasing $FeSO_4$ concentration.

Table 2. *Number of Brevibacterium flavum colonies on a Petri dish at different concentrations of $FeSO_4$ (N, colonies/dish)*

N, colonies per plate	Percentage content of iron salts				
	Control	0.063%	0.125%	0.25%	0.5%
10^{-7} (culturing)	31 ± 1.55	12 ± 0.6	1 ± 0.05	0	3 ± 0.15
10^{-8} (culturing)	6 ± 0.3	3 ± 0.15	2 ± 0.1	1 ± 0.05	0

Note: values are provided as M ± SD; 0 – no colonies detected; culture method: surface, V = 0.1 cm^3
Source: compiled by the authors

Even the lowest concentration of $FeSO_4$ tested (0.063%) was associated with a reduction in colony formation compared with the control. In Table 2, for the concentration level marked as $×10^7$, the control value was 31 colonies, whereas at 0.063% it was 12 colonies; the reduction was 19 colonies, i.e., approximately a 61% relative decrease compared to the control. For the $×10^8$ level, the control was 6 colonies, and at 0.063%, 3 colonies, corresponding to a 50% reduction. This consistent trend across the two concentration levels ($×10^7$ and $×10^8$) confirmed that even 0.063% $FeSO_4$ is not a "neutral" concentration for *Brevibacterium flavum*, but exerts an inhibitory effect on colony-forming activity. An increase in $FeSO_4$ to 0.125% was accompanied by a further reduction in the number of colonies. At the $×10^7$ level, the value decreased from 31 (control) to 1, corresponding to approximately a 96.8% reduction relative to the control; at the $×10^8$ level, the control 6 colonies decreased to 2 (a 66.7% reduction). Thus, 0.125% $FeSO_4$ was characterised as the concentration at which a marked decline in colony-forming ability occurred, i.e., suppression of the population's generative activity. For 0.25% $FeSO_4$ in Table 2, at a level of $×10^7$, the absence of colonies was recorded (marked "-"), which was interpreted as a drop in colony formation below the detection limit for the corresponding dilution/inoculum volume. At a concentration of $×10^8$, 1 colony was recorded compared to 6 in the control (a decrease of 83.3%). The combination of a "zero" result at one level of representation and a minimal result at another was consistent with a situation where a viable fraction of the population is maintained, yet approaches critically low levels; under such conditions, the discreteness of CFU (the stochasticity of colony formation at low numbers) increases significantly, which is typical for concentrations close to toxicity thresholds.

At 0.5% $FeSO_4$ in Table 2, 3 colonies were recorded at a dilution of $×10^7$, whereas at a dilution of $×10^8$, no colonies were detected ("0"). At first glance, this may appear to be an imperfect monotonicity of the effect compared to 0.25%; however, such a pattern is to be expected when the number of viable cells is low, as small fluctuations in cell distribution within the droplet/inoculum volume and random survival can alter the number of colonies by a few units. The overall fact remains significant: compared to the control (31 for $×10^7$ and 6 for $×10^8$), the figures at 0.5% remained sharply reduced (a 90.3% drop for the $×10^7$ level and a complete absence of colonies at the $×10^8$ level). This confirmed the persistence of a pronounced toxic effect of Fe^{2+} at 0.5% $FeSO_4$.

The set of numerical values in Table 2 revealed a general trend: as the mass fraction of $FeSO_4$ increased from 0% to 0.5%, there was a systematic decrease in colony formation. The visual representation was consistent with the tabulated data and reproduced the decreasing nature of the growth response of *Brevibacterium flavum* to an increase in Fe^{2+} concentration. Aggregated mean growth rates (×10^7) were used to construct Figure 2.

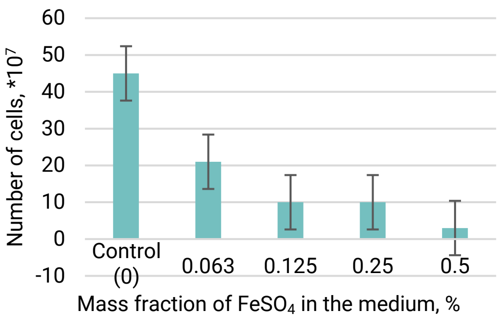

***Figure 2.** The dependence of microbial growth on the concentration of Fe^{2+} ions*

Source: compiled by the authors

To verify the accuracy of the growth interpretation, the cell count in the initial inoculum suspension was determined in parallel. When plating from dilutions of 10^{-6} and 10^{-7}, 11 and 5 colonies were recorded respectively; on this basis, the average number of cells in the initial suspension was recorded as 30×10^6, and when converted to 1 cm^3, 6×10^4. Subsequently, an increase in cell count was observed after 24-hour cultivation on a shaker by approximately three orders of magnitude compared to the inoculum, which quantitatively corresponded to a transition from 10^4 to 10^7-10^8 under conditions of active growth. This trend confirmed that the control cultivation regime ensured intensive population growth, whereas the presence of $FeSO_4$ at concentrations of 0.063-0.5% reduced the rate of this growth, limiting the ability to form colonies as the Fe^{2+} content increased.

No "growth stimulation window" was identified within the tested range: each concentration of $FeSO_4$ (0.063-0.5%) was associated with a reduction in colony formation compared with the control. This indicated that, under the cultivation conditions applied, Fe^{2+} acted primarily as a stressor that limited the reproductive capacity of the cells, rather than as an inducer of biomass accumulation. The consistent decrease in CFU with increasing $FeSO_4$ concentration confirmed the dose-dependent toxicity of Fe^{2+} for *Brevibacterium flavum* and provided an experimental basis for further optimisation of the trace element composition of media in biotechnologies for producers of amino acids of the aspartic acid family. The final pattern was formulated as an inversely proportional increase in generative capacity with a decrease in the mass fraction of iron salts, but without reaching the control level, even at the lowest concentration studied.

A study of the magnetic susceptibility of the *Brevibacterium flavum* culture

The next step was to determine the effective magnetic susceptibility of the *Brevibacterium flavum* culture fluid in the presence of iron salts at various concentrations, as well as to compare the parameters of the "cell-free" and "cell-containing" media. The results of the initial resonance measurements and the subsequent calculation of the effective magnetic susceptibility χ are summarised in Table 3.

***Table 3.** Data recorded by a magnetic susceptibility meter*

Mass fraction of iron salts in the medium, %	Culture medium, MPB	Cells of *Brevibacterium flavum* from the MPB
0	$8.459 \times 10^{-3} \pm 0.4 \times 10^{-3}$	$8.305 \times 10^{-3} \pm 0.4 \times 10^{-3}$
0.063	$8.373 \times 10^{-3} \pm 0.4 \times 10^{-3}$	$8.27 \times 10^{-3} \pm 0.4 \times 10^{-3}$
0.125	$7.97 \times 10^{-3} \pm 0.4 \times 10^{-3}$	$8.408 \times 10^{-3} \pm 0.4 \times 10^{-3}$
0.25	$8.282 \times 10^{-3} \pm 0.4 \times 10^{-3}$	$8.307 \times 10^{-3} \pm 0.4 \times 10^{-3}$
0.5	$8.304 \times 10^{-3} \pm 0.4 \times 10^{-3}$	$8.028 \times 10^{-3} \pm 0.4 \times 10^{-3}$

Source: compiled by the authors

In all experimental setups, both for the control MPB and for the "*Brevibacterium flavum* cells + MPB" system, χ values of the order of 10^{-3} were recorded, which corresponded to a paramagnetic type of magnetic response from the system within the scope of the experiment. The key finding was that the χ values for the medium and for the samples containing cells coincided within the margin of error for every tested mass fraction of $FeSO_4$ (0-0.5%), i.e., the contribution of the cellular component to the total magnetic response did not manifest as a statistically distinguishable effect at the given sensitivity of the method.

Quantitatively, this pattern was observed at all points in the series. In the control variant (0% $FeSO_4$), χ for MPB was $8.459 \times 10^{-3} \pm 0.4 \times 10^{-3}$, whereas for the "*Brevibacterium flavum* cells + MPB" sample it was $8.305 \times 10^{-3} \pm 0.4 \times 10^{-3}$. The difference between these values was 0.154×10^{-3} and did not exceed the stated error ($\pm 0.4 \times 10^{-3}$), indicating the absence of a significant difference between the medium and the cell suspension under control conditions. A similar pattern was observed at 0.063% $FeSO_4$: χ for the MPB was $8.373 \times 10^{-3} \pm 0.4 \times 10^{-3}$, and for the sample with cells – $8.27 \times 10^{-3} \pm 0.4 \times 10^{-3}$; the difference was 0.103×10^{-3} and was also within the margin of error.

At 0.125% $FeSO_4$, values of χ $7.97 \times 10^{-3} \pm 0.4 \times 10^{-3}$ were recorded for the MPB and $8.408 \times 10^{-3} \pm 0.4 \times 10^{-3}$ for the cell suspension. This pair is the most contrasting in the series; the difference was 0.438×10^{-3} and lay at the limit of the stated uncertainty. Given the measurement uncertainty ($\pm 0.4 \times 10^{-3}$) and the absence of similar shifts in neighbouring concentrations, this deviation was interpreted as a measurement/sample fluctuation rather than as an indication of a monotonic concentration trend, a conclusion supported by subsequent data points: at 0.25% $FeSO_4$, χ was $8.282 \times 10^{-3} \pm 0.4 \times 10^{-3}$ (MPB) and $8.307 \times 10^{-3} \pm 0.4 \times 10^{-3}$ (cells + MPB), i.e. the difference was only 0.025×10^{-3}; at 0.5% $FeSO_4$, χ was $8.304 \times 10^{-3} \pm 0.4 \times 10^{-3}$ (MPB) and $8.028 \times 10^{-3} \pm 0.4 \times 10^{-3}$ (cells + MPB), with a difference of 0.276×10^{-3}, which also did not exceed the error margin.

A comparison of all points in the series revealed two substantial properties of the results obtained. Firstly, the absence of a stable monotonic trend in χ with respect to the $FeSO_4$ concentration within the range of 0-0.5%. The values of χ for the MPB fluctuated within the range of approximately $(7.97\text{-}8.459) \times 10^{-3}$, and for the "cell + MPB" system – within the range of $(8.028\text{-}8.408) \times 10^{-3}$. These fluctuations did not form a unidirectional relationship of the type "increase in Fe^{2+} → increase in χ" or "increase in Fe^{2+} → decrease in χ". In the context of the resonance method, this meant that the resonance frequency shift (Δf), on which χ depends via equation (10), did not demonstrate systematic circuit tuning during the transition between $FeSO_4$ concentrations, and consequently, the change in the solenoid's inductance (L) upon sample introduction remained similar in all cases.

Secondly, there was no systematic difference between "MPB" and "cells + MPB". At each concentration point, the difference between the χ of the medium and the χ of the cell suspension was less than or comparable to $\pm 0.4 \times 10^{-3}$. Under these conditions, there were no grounds for concluding that biomass made a significant additional contribution to the system's magnetic response. In practical terms, this meant that, within the framework of the sample preparation and method sensitivity used, the dominant factor in the magnetic response remained the "background" contribution of the medium (including dissolved components and salts), whilst the contribution of the cellular component was either small or masked by the background.

The physical results obtained were of fundamental interpretative significance when compared with the microbiological data. In the biological section, a marked inhibition of *Brevibacterium flavum* growth was observed with increasing $FeSO_4$ concentration, and a sharp inhibition of growth at 1% $FeSO_4$; that is, Fe^{2+} acted as a potent regulator of the culture's viability and reproductive activity. In contrast, the χ parameter, which reflects the total magnetic response of the "environment/culture" system in the LC circuit, remained relatively stable within the range of 0-0.5% $FeSO_4$ and did not reflect the same contrasting concentration effect. This indicated a distinction: the toxic (biological) effect of Fe^{2+} manifested at the level of cellular physiology and reproductive capacity but was not accompanied by a marked shift in the integral magnetic susceptibility of the samples within the accuracy limits of the applied resonance technique and the selected concentrations.

The overall results showed that the mass fraction of iron salts in the culture medium is a critical factor for the viability and reproductive capacity of the studied producers: a 1% concentration of $FeSO_4$ had a toxic effect and reduced the number of viable cells to 10^8/cm^3, compared with control values of 10^{10}-10^{11}/cm^3. For *Brevibacterium flavum*, within the range of 0.063-0.5%, the inhibitory effect of Fe^{2+} was established, with a decreasing growth trend as the concentration increased, as confirmed by tabular and graphical data. Physical measurements demonstrated paramagnetic properties in both the medium and the suspension containing *Brevibacterium flavum* cells at all concentrations studied, with the magnetic susceptibility values of the medium and the samples containing cells coinciding within the margin of error, indicating no significant "cellular" contribution to χ in the experimental setup employed.

Discussion

The results obtained showed that increased bioavailability of Fe^{2+} in the culture medium was associated with a reduction in the colony-forming ability of industrially relevant actinobacteria. Upon the addition of $FeSO_4$ at a mass fraction of 1% to all three tested cultures (*Corynebacterium glutamicum*, *Brevibacterium flavum*, *Brevibacterium* sp. 90), a sharp decrease in the concentration of viable cells to approximately 10^8 cells/cm^3 was observed, compared to control levels of 10^{10}-10^{11} cells/cm^3. Such a consistent response at high Fe^{2+} levels is consistent with the concept of iron as a bifunctional factor: an essential cofactor, but in excess, a catalyst for oxidation reactions that reduce reproductive capacity and colony formation. Notably, the experiment maintained a viable fraction at 10^8/cm^3, meaning that rather than an immediate lethal effect, there was primarily a profound inhibition of proliferation/colony-forming ability, which is critical precisely for the technological phase of biomass accumulation and the subsequent yield of target metabolites. The mechanistically identified phenotype is consistent with oxidative stress as the probable "final pathway" of metal-ion toxicity in heterotrophic cultures. S. Yu *et al.* (2025) demonstrated that *C. glutamicum* develops a time-regulated adaptation programme to H_2O_2-induced oxidative stress, involving the remodelling of antioxidant defence and redox balance systems, which determines the population's ability to resume growth following damage. In the context of Fe^{2+} addition, this has direct implications: in the presence of excess Fe^{2+}, even moderate peroxide flows can shift to a more damaging mode due to the catalysis of radical transformations; consequently, the reduction in CFU at 1% $FeSO_4$ may reflect a situation where the adaptive capacity of redox regulation becomes insufficient to maintain normal reproduction. Accordingly, the observed decline in colony formation is logically consistent with the model of sublethal damage, where the cell retains viability but loses the ability to form colonies on a solid medium.

A dose-dependent test for *Brevibacterium flavum* (0.063-0.5% $FeSO_4$) clarified the nature of Fe^{2+} toxicity and demonstrated the absence of a stimulatory window within this specific concentration range: a decrease in colony formation relative to the control was already observed at 0.063%, whilst at 0.125-0.5% the inhibition became markedly pronounced, including the absence of colonies in some dilutions. This pattern corresponds to the threshold (non-linear) effects of metals, where crossing a critical level of bioavailability causes a disproportionate deterioration in reproductive parameters. The results of D. Li *et al.* (2024), who demonstrated that Cu^{2+}, Mn^{2+} and Fe^{3+} differentially influence the biotransformation of Cr(VI) in the *Shewanella oneidensis*/*Bacillus subtilis* biosystem under bimetallic conditions; that is, the effect of an ion is determined not only by its nature but also by the ionic background and interactions within the system. When applied to the cultivation of amino acid producers, this highlights that the toxicity of Fe^{2+} can be modified by other trace elements and environmental components, necessitating further multifactorial optimisation.

Results from bioleaching and geomicrobiological models confirm that the biological effect of Fe^{2+} depends to a large extent on its form and microenvironment. W. Zeng *et al.* (2023) performed in situ detection of Cu^{2+}, Fe^{3+} and Fe^{2+} at the microbe-mineral interface during the bioligation of chalcopyrite and demonstrated dynamic changes in iron forms at the microinterface, where local concentrations and Fe^{2+}/Fe^{3+} ratios may differ from the system averages. This is also relevant for liquid culture media: under aeration and changes in pH/redox status, the Fe^{2+}/Fe^{3+} ratio is potentially unstable, which may explain varying degrees of toxicity at similar nominal concentrations. In iron-oxidising bacteria, Fe^{2+} acts as an energy substrate, and therefore, its effect on growth may be opposite. A.C. Khachatryan (2019) demonstrated that Fe^{2+}/Fe^{3+} alters the growth of *Leptospirillum ferriphilum* and the rate of Fe^{2+} oxidation, i.e., iron is an integral element of the energetics and adaptation of these cultures. A similar conclusion was supported by A. Khachatryan *et al.* (2021), establishing that metal ions can modify both biomass growth and the rate of ferrous oxidation in *L. ferriphilum* CC. A comparison with such systems highlights a fundamental difference: for producers of amino acids of the aspartate family, an excess of Fe^{2+} predominantly leads to a state of stress and inhibition, whereas in chemolithotrophs, Fe^{2+} can support growth processes.

At the level of microbial consortia, iron can alter not only individual growth but also the functioning of the entire system. J.R. González-Paz *et al.* (2022) demonstrated that Fe^{2+} and Fe^{3+} influence the productivity of microbial fuel cells and alter the composition of the microbial community; that is, metal ions act as selection factors and may drive the redistribution of functional groups within the system. When applied to pure cultures, this can be interpreted as a potential manifestation of population restructuring (an increase in the proportion of cells with reduced reproduction or persistent forms) under the pressure of metal-induced stress. The study found no stable changes in the effective magnetic susceptibility χ in the range of 0-0.5% $FeSO_4$ for both the MPB and the "cell + MPB" suspension: the values of χ remained of the order of 10^{-3} and coincided within the margin of error. This result indicates that the integral physical parameters of the medium in the present setup are relatively "inert" to changes in population viability and can be determined primarily by the contribution of dissolved components and salts. Consequently, magnetic susceptibility, given the sensitivity of the method used, cannot be regarded as a sensitive surrogate marker of Fe^{2+} toxicity for *Brevibacterium flavum* within the concentrations studied; instead, CFU remains a direct and technologically relevant criterion for assessing reproductive capacity. The observed variability in the sensitivity of strains to 1% $FeSO_4$ (with the greatest decrease observed in *C. glutamicum*) is consistent with a probable difference in the mechanisms of metal tolerance. At the genus *Brevibacterium* level, the existence of metal-tolerant strains has been confirmed by genomic data. S. Manzoor *et al.* (2024) described *Brevibacterium metallidurans* sp. nov. and demonstrated the presence of functional genomic features associated with heavy metal tolerance, confirming a potential difference in metal-adaptation potential within the genus. The applied potential of such tolerance is also reflected in bioremediation studies: S. Sher *et al.* (2023) demonstrated the ability of *Brevibacterium* sp. strain CS2 to interact effectively with arsenic and considered the strain as a candidate for the treatment of industrial effluents, whilst S. Sher *et al.* (2024) demonstrated that the interaction of arsenic with *Brevibacterium* sp. CS2 is accompanied by changes in the protein profile, i.e., the activation of stress response systems. Although arsenic and iron differ in their biochemical effects, the very fact that stress proteomic responses are engaged supports the interpretation that metal-induced stress may reduce reproduction and colony formation through the reallocation of cellular resources to defence programmes.

Biotechnological practice shows that metal-ion inhibition is often mitigated by optimising the medium composition and controlling the process phase. W. Raza *et al.* (2010) demonstrated that response surface methodology (RSM) can be used for the quantitative assessment of the influence of metal ions and the identification of optimal combinations to maximise the production of bioactive compounds; that is, metal ions can act as both inhibitors and controllable optimisation factors, depending on their dosage. A similar approach was adopted by R. Zhang *et al.* (2025), who, by optimising medium components via RSM, increased the production of menaquinone-7 in *Bacillus subtilis*, confirming the effectiveness of a multifactorial approach for medium formulation. The concept of separating growth phase dependence and metal-ion inhibition is reinforced by the work of G. Yang *et al.* (2025), which proposes a two-stage engineering strategy that can be used for the reduction of metal-induced production limitations without compromising growth characteristics in *Escherichia coli*. In the context of the results obtained, this implies that the observed toxic effect of Fe^{2+} at high concentrations does not preclude the existence of lower controllable concentrations; however, identifying these requires formalised experimental design, incorporating the interactions of Fe^{2+} with other trace elements and cultivation parameters.

An additional aspect of interpretation relates to the bioavailability and binding of iron. Although the cited source has a medical-biochemical context, T. Mazur *et al.* (2024) demonstrated that chelating compounds can alter the pools of Cu^{2+}, Fe^{2+}/Fe^{3+} and Zn^{2+} in biological systems, thereby affecting the availability of metals. When applied to culture media, this implies that the nominal mass fraction of $FeSO_4$ does not equate to the effective concentration of free Fe^{2+}, and toxicity may be determined by the proportion of labile forms of iron. N. Niessen & J. Soppa (2020) demonstrated, using archaea as an example, that siderophore production can be regulated and used as a tool to adjust the cell's iron supply. Consequently, the absence of changes in χ whilst CFU changes may be consistent with the physical signal being determined predominantly by dissolved components of the medium, whilst the biological effect is realised through intracellular damage and regulatory responses sensitive to free Fe^{2+}.

The results obtained regarding the inhibition of producer growth at elevated $FeSO_4$ concentrations (a reduction in CFU to approximately 10^8 cells/cm^3 compared with the control value of 10^{10}-10^{11} cells/cm^3) should also be interpreted within the broader context of the interaction of microorganisms with mineral/ionic components of the environment and external inducers of systemic stability, which may alter metabolic fluxes without necessarily leading to a parallel increase in biomass. D. Xia *et al.* (2025) demonstrated that synergistic catalysis between coal and various minerals during biogas synthesis alters the mechanisms of the process, through the influence of mineral phases on electron transfer, the rate of hydrolysis/acidogenesis, and the availability of reaction centres. Although their model concerns anaerobic consortia, the conclusion is fundamental: a mineral component can act as a catalytic modifier of the bioprocess, shifting its efficiency through physicochemical interactions, and not merely through classical biological factors. In this study, Fe^{2+} at high concentrations acted in the opposite direction – not as a mineral catalyst for the process, but as a factor that exacerbates stress and limits reproductive capacity; however, the very idea of "mineral-mediated process control" confirms the need to monitor the salt composition of media in amino acid technologies.

Further evidence of the ecological and functional plasticity of the genus *Brevibacterium* is provided by studies on industrially contaminated environments, where high metal ion concentrations are common. A.N. Putri *et al.* (2021) demonstrated that a mixed culture of *Pseudomonas aeruginosa* and *Brevibacterium* sp. can be effective for the removal of components of acidic mine drainage; that is, *Brevibacterium* can function under conditions of high ionic strength, low pH and the presence of metals, ensuring the ecologically significant transformation of pollutants. In light of the data obtained, this highlights that both relatively metal-tolerant and metal-sensitive strains may exist within the genus; therefore, the inhibition of CFU in the tested *Brevibacterium flavum* by $FeSO_4$ does not contradict the general metal tolerance of the genus, but rather indicates strain specificity and a distinction between survival in stressful niches and effective growth under biotechnological conditions. The functional diversity of *Brevibacterium* is also confirmed in the study by S. Pei *et al.* (2021), which describes three new species (*B. limosum*, *B. pigmenatum*, *B. atlanticum*) capable of decolourising dyes; their isolation from marine sediments highlights the breadth of the genus's metabolic strategies. This is relevant for the interpretation of the results for two reasons. Firstly, the ability to transform complex organic compounds is often accompanied by well-developed detoxification systems and redox enzymes, which may potentially overlap with responses to metal-induced stress. Secondly, the presence of different ecotypes of *Brevibacterium* indirectly supports the conclusion that the optimal "windows" of trace elements for growth/production are not universal across the genus, but must be determined separately for each strain; which is why the established absence of a stimulatory effect of Fe^{2+} in the range of 0.063-0.5% for *Brevibacterium flavum* is technologically significant, but should not be mechanically extrapolated to other *Brevibacterium* species.

A transcriptomic approach, as presented by H.J. Kim *et al.* (2023). The study demonstrated that the antimicrobial activity of prodigiosin against *Cutibacterium acnes* was accompanied by specific transcriptomic shifts; that is, the cellular response to a stressor is reflected as a reorganisation of gene expression that precedes or accompanies phenotypic changes. Although this example concerns a different agent, the logic is relevant: in the case of Fe^{2+}, the absence of changes in magnetic susceptibility χ alongside a simultaneous drop in CFU may indicate that key events unfold at the level of cellular regulatory/redox programmes and do not necessarily form a detectable "integral physical signal" in the medium. Applied biotechnology studies aimed at optimising amino acid synthesis conditions are also useful for comparison with the data obtained, as they demonstrate that "optimal conditions" are often the result of a trade-off between growth and production. A.S. Aljaly *et al.* (2023), in a comparative analysis of the conditions for using specific bacterial strains for amino acid production, showed that amino acid yield may depend on medium parameters and cultivation regimes, and that optimisation often does not boil down to maximising biomass. In the context of the data from this study, this supports the conclusion that even with constant growth inhibition (a reduction in CFU), the addition of Fe^{2+} could theoretically alter production fluxes; however, the observed acute toxicity of 1% $FeSO_4$ and the absence of a "neutral" zone at 0.063-0.5% for *Brevibacterium flavum* indicate that, under the selected conditions, iron acted predominantly as a stressor, thereby increasing the technological risk. A separate parallel line of research involves the use of elicitors that alter metabolism and the amino acid profile without directly "supplying" the system with metals. N.A. Sigala-Aguilar *et al.* (2025) demonstrated that multi-walled carbon nanotubes can act as elicitors in tomato seedlings, altering the accumulation of bioactive compounds and amino acids, nutrient uptake, growth and soil biological quality. From a practical point of view, this reinforces the conclusion that excess Fe^{2+} is not a universal tool for "manipulating" amino acid production: under certain conditions, its contribution may be detrimental to growth, whereas controlled elicitors can provide a metabolic effect with a lower risk of toxicity.

As a result, analysis of additional sources further expanded presented findings in two respects. Firstly, the "minerals/ions-microbial process" interaction is fundamentally capable of both enhancing efficiency (through synergistic catalysis in consortia) and inhibiting it (through metal-induced stress), and indirectly underscores the critical importance of controlling ion composition in biotechnology. Secondly, the genus *Brevibacterium* exhibits significant ecological and functional diversity; therefore, the established sensitivity of *Brevibacterium flavum* to Fe^{2+} at the concentrations studied should be interpreted as a strain-specific characteristic relevant to the optimisation of a specific cultivation process.

Conclusions

The study determined that Fe^{2+} ions present in $FeSO_4$, under cultivation conditions on MPB medium, exhibited a marked inhibitory effect on the growth of producers of amino acids of the aspartic acid family, with toxic effects becoming evident even at a mass fraction of $FeSO_4$ as low as 1%. At this concentration, the viability of the cultures decreased to 10^8 cells/cm^3, compared with control values of 10^{10}-10^{11} cells/cm^3. For *Corynebacterium glutamicum*, 9×10^8 cells/cm^3 were obtained in the experiment compared to 15×10^{10} cells/cm^3 in the control (a reduction of approximately 167-fold, ~2.2 log); for *Brevibacterium flavum*, 4×10^8 versus 2×10^{10} cells/cm^3 (a 50-fold reduction, ~1.7 log), and for *Brevibacterium* sp. 90 – 8×10^8 versus 3×10^{10} cells/cm^3 (a reduction of approximately 37.5-fold, ~1.6 log). Together, these data confirmed the universality of the inhibitory effect of Fe^{2+} on the tested strains and the presence of strain-specific variability in sensitivity, which is significant for the biotechnological standardisation of the trace element composition of media.

An in-depth dose-response analysis using a *Brevibacterium flavum* model in the range of 0.063-0.5% $FeSO_4$ revealed the absence of a "growth stimulation window" and the presence of inhibition even at the minimum concentration. Thus, at 0.063% $FeSO_4$, colony formation decreased from 31 to 12 colonies ($\times 10^7$ level; -61%) and from 6 to 3 ($\times 10^8$ level; -50%) compared with the control. An increase in $FeSO_4$ to 0.125% was accompanied by a sharp decline in colony formation (31 → 1 at a level of $\times 10^7$; ~-96.8% and 6 → 2 at a level of $\times 10^8$; -66.7%). At 0.25-0.5%, low values were recorded, with the absence of colonies at certain dilution levels, reflecting the system's approach to the toxicity threshold and an increase in CFU stochasticity at low numbers. Overall, a negative dose-dependent trend was confirmed: as $FeSO_4$ increased, the reproductive capacity of the *Brevibacterium flavum* population was progressively limited.

The study demonstrated that, in the control group, there was an increase in the viable fraction of *Brevibacterium flavum* compared with the inoculum: the initial concentration was estimated at 6×10^4 cells/cm^3, whereas after 24-hour cultivation, an increase in colony formation was recorded, requiring measurement at high dilutions (10^{-7}-10^{-8}). It was established that in the physical block of the study (radio-technical resonance method), the effective magnetic susceptibility χ in the range of 0-0.5% $FeSO_4$ remained at ~10^{-3} for both the MPB and the "*Brevibacterium flavum* cells + MPB" system, which corresponded to a paramagnetic response. The values of χ for the medium and the cell suspension coincided within the margin of error ($\pm 0.4 \times 10^{-3}$) at each concentration point: for example, at 0% $FeSO_4$ – 8.459×10^{-3} versus 8.305×10^{-3}, at 0.25% – 8.282×10^{-3} versus 8.307×10^{-3}, at 0.5% – 8.304×10^{-3} versus 8.028×10^{-3}. No monotonic dependence of χ on the concentration of $FeSO_4$ was detected, which confirmed the distinction between the biological toxic effect of

Fe^{2+} (inhibition of CFU) and the integral physical parameter χ within the sensitivity limits of the method used.

A limitation of the study was the use of CFU as the primary metric of viability without concurrent determination of dry biomass/optical density and without direct measurement of the production of target amino acids, which limits the ability to quantitatively extrapolate the results to metabolite yield levels. Promising avenues for further research include extending the range of Fe^{2+} concentrations to trace levels (below 0.063%) whilst seeking non-toxic, regulatory concentrations; introducing a suite of analytical parameters (OD/dry weight, oxidative stress indicators, residual Fe^{2+}/Fe^{3+} in the medium, amino acid profile in the culture medium); and optimising physical measurements through standardisation of biomass/cell concentration to increase the sensitivity of detecting a possible "cellular" contribution to χ.

Acknowledgements

None.

Funding

None.

Conflict of Interest

None.

References

[1] Aljaly, A.S., Osman, M.A., Badr, S.A., & Shehata, R.M. (2023). Comparative study and the optimum conditions on the use of certain bacterial strains for the production of some amino acids. *Egyptian Journal of Chemistry*, 66(6), 419-429. doi: 10.21608/EJCHEM.2023.185356.7419.

[2] González-Paz, J.R., del Carmen Monterrubio-Badillo, M., Ordaz, A., García-Peña, E.I., & Guerrero-Barajas, C. (2022). Influence of Fe^{2+} and Fe^{3+} on the performance and microbial community composition of a MFC inoculated with sulfate-reducing sludge and acetate as electron donor. *Journal of Chemistry*, 2022(1), article number 5685178. doi: 10.1155/2022/5685178.

[3] Khachatryan, A.C. (2019). Influence of Fe^{2+} and Fe^{3+} on the growth of *Leptospirillum ferriphilum* CC and oxidation of Fe^{2+}. *Biological Journal of Armenia*, 3(71), 83-88.

[4] Khachatryan, A., Vardanyan, N., Vardanyan, A., Zhang, R., & Castro, L. (2021). The effect of metal ions on the growth and ferrous IronOxidation by *Leptospirillum ferriphilum* CC isolated from Armenia mine sites. *Metals*, 11(3), article number 425. doi: 10.3390/met11030425.

[5] Kim, H.J., Lee, M.S., Jeong, S.K., & Lee, S.J. (2023). Transcriptomic analysis of the antimicrobial activity of prodigiosin against *Cutibacterium acnes*. *Scientific Reports*, 13(1), article number 17412. doi: 10.1038/s41598-023-44612-7.

[6] Kovalova, S., Golub, N., & Levtun, I. (2025). The combined effect of ferric ion complexes (Fe^{2+} and Fe^{3+}) and illumination on *Chlorella vulgaris* metabolism. *Journal of Applied Phycology*, 38, 81-98. doi: 10.1007/s10811-025-03711-w.

[7] Krüger, A., Weber, U., & Frunzke, J. (2025). Genome-wide analysis of DtxR and HrrA regulons reveals novel targets and a high level of interconnectivity between iron and heme regulatory networks in *Corynebacterium glutamicum*. *Molecular Microbiology*, 124(2), 115-130. doi: 10.1111/mmi.15376.

[8] Küberl, A., Mengus-Kaya, A., Polen, T., & Bott, M. (2020). The iron deficiency response of Corynebacterium glutamicum and a link to thiamine biosynthesis. *Applied and Environmental Microbiology*, 86(10), article number e00065-20. doi: 10.1128/AEM.00065-20.

[9] Li, D., He, H., Xu, Z., & Deng, H. (2024). Investigation on the effect of Cu^{2+}, Mn^{2+} and Fe^{3+} on biotreatment of Cr (VI) by *Shewanella oneidensis* and *Bacillus subtilis* in bimetallic system. *Surfaces and Interfaces*, 44, article number 103742. doi: 10.1016/j.surfin.2023.103742.

[10] Lin, Y., Shu, L., Chen, H., Duan, X., & Zeng, W. (2025). Poly-γ-glutamic acid production from untreated sugarcane molasses by non-sterilized repeated-batch fermentation with *Bacillus subtilis* GLS-8. *Chemical Engineering Journal Advances*, 24, article number 100900. doi: 10.1016/j.ceja.2025.100900.

[11] Manzoor, S., Abbas, S., Zulfiqar, S., Wang, H.C., Xiao, M., Li, WJ., Arshad, M., & Ahmed, I. (2024). Functional genomics and taxonomic insights into heavy metal tolerant novel bacterium *Brevibacterium metallidurans* sp. nov. NCCP-602T isolated from tannery effluent in Pakistan. *Antonie van Leeuwenhoek*, 117(1), article number 111. doi: 10.1007/s10482-024-02006-3.

[12] Mazur, T., Malik, M., & Bieńko, D.C. (2024). The impact of chelating compounds on Cu^{2+}, $Fe^{2+}/^{3+}$, and Zn^{2+} ions in Alzheimer's disease treatment. *Journal of Inorganic Biochemistry*, 257, article number 112601. doi: 10.1016/j.jinorgbio.2024.112601.

[13] Müller, F. (2020). *Interaction between CO2/HCO3-and the iron homeostasis in Corynebacterium glutamicum*. Stuttgart: Universität Stuttgart.

[14] Murdoch, C.C., & Skaar, E.P. (2022). Nutritional immunity: The battle for nutrient metals at the host-pathogen interface. *Nature Reviews Microbiology*, 20(11), 657-670. doi: 10.1038/s41579-022-00745-6.

[15] Niessen, N., & Soppa, J. (2020). Regulated iron siderophore production of the halophilic archaeon *Haloferax Volcanii*. *Biomolecules*, 10(7), article number 1072. doi: 10.3390/biom10071072.

[16] Pei, S., Niu, S., Xie, F., Wang, W., Zhang, S., & Zhang, G. (2021). *Brevibacterium limosum* sp. nov., *Brevibacterium pigmenatum* sp. nov., and *Brevibacterium atlanticum* sp. nov., three novel dye decolorizing actinobacteria isolated from ocean sediments. *Journal of Microbiology*, 59(10), 898-910. doi: 10.1007/s12275-021-1235-0.

[17] Putri, A.N., Ratnaningsih, R., & Rinanti, A. (2021). Acid mine drainage removal by mixed bacteria culture of *Pseudomonas aeruginosa* and *Brevibacterium* sp. *IOP Conference Series: Materials Science and Engineering*, 1098(5), article number 052072. doi: 10.1088/1757-899X/1098/5/052072.

[18] Raynal, J.T., da Rocha, M.S., da Silva Cavalcanti, N.A., Bastos, B.L., de Farias, A P.., da Costa Silva, M., de Moura-Costa, L., Portela, R., Trindade, S., & Nascimento, R.J. (2022). Influence of iron chelating agents on the in vitro growth curve of *Corynebacterium pseudotuberculosis* strains. *Ensaios e Ciência: Ciências Biológicas, Agrárias e da Saúde*, 26(2), 270-280. doi: 10.17921/1415-6938.2022v26n2p270-280.

[19] Raza, W., Hongsheng, W., & Qirong, S. (2010). Use of response surface methodology to evaluate the effect of metal ions (Ca^{2+}, Ni^{2+}, Mn^{2+}, Cu^{2+}) on production of antifungal compounds by *Paenibacillus polymyxa*. *Bioresource Technology*, 101(6), 1904-1912. doi: 10.1016/j.biortech.2009.10.029.

[20] Sher, S., Ishaq, M.T., Bukhari, D.A., & Rehman, A. (2023). *Brevibacterium* sp. strain CS2: A potential candidate for arsenic bioremediation from industrial wastewater. *Saudi Journal of Biological Sciences*, 30(10), article number 103781. doi: 10.1016/j.sjbs.2023.103781.

[21] Sher, S., Ullah, S., Bukhari, D.A., Hussain, S.Z., & Rehman, A. (2024). Evaluation of interaction among arsenic and *Brevibacterium* sp. strain CS2 and its proteins profiling. *Journal of Hazardous Materials Letters*, 5, article number 100119. doi: 10.1016/j.hazl.2024.100119.

[22] Sigala-Aguilar, N.A., Delgadillo-Martínez, J., Fernández-Luqueño, F., & López, M.G. (2025). Multi-walled carbon nanotubes as elicitors in tomato seedlings (*Solanum lycopersicum* L.): impact on biocompounds and amino acids production, nutrient uptake, growth of seedlings, and biological quality of the soil. *Journal of Soil Science and Plant Nutrition*, 25(3), 8168-8186. doi: 10.1007/s42729-025-02663-x.

[23] Thoma, F., Appel, C., Russ, D., Huber, J., Werner, F., & Blombach, B. (2023). Improving growth properties of *Corynebacterium glutamicum* by implementing an iron-responsive protocatechuate biosynthesis. *Microbial Biotechnology*, 16(5), 1041-1053. doi: 10.1111/1751-7915.14244.

[24] Walter, T., Veldmann, K.H., Götker, S., Busche, T., Rückert, C., Kashkooli, A.B., Paulus, J., Cankar, K., & Wendisch, V.F. (2020). Physiological response of *Corynebacterium glutamicum* to indole. *Microorganisms*, 8(12), article number 1945. doi: 10.3390/microorganisms8121945.

[25] Xia, D., Lv, H., Jian, K., Huang, D., Wang, Y., Wei, G., & Chen, L. (2025). Mechanisms of biogas production under synergistic catalysis between coal and various minerals. *Journal of Environmental Chemical Engineering*, 13(5), article number 117725. doi: 10.1016/j.jece.2025.117725.

[26] Yang, G., Wang, X., Zhou, Y., Ding, X., Huang, J., Qiao, S., Deng, A., & Yu, H. (2025). Decoupling growth phase dependency and metal ion inhibition: A dual engineering strategy for the high-yield biosynthesis of microcin J25 in *Escherichia coli*. *Engineering Microbiology*, 5(4), article number 100230. doi: 10.1016/j.engmic.2025.100230.

[27] Yu, C., Hu, W., Li, X., Lei, Y., Gao, D., Wang, M., Zheng, P., Zhu, Y., & Sun, J. (2025). Elucidating the mechanism of temporal adaptation to hydrogen peroxide-induced oxidative stress in *Corynebacterium glutamicum*. *Microbial Biotechnology*, 18(6), article number e70170. doi: 10.1111/1751-7915.70170.

[28] Zeng, W., *et al.* (2023). *In situ* detection of Cu^{2+}, Fe^{3+} and Fe^{2+} ions at the microbe-mineral interface during bioleaching of chalcopyrite by moderate thermophiles. *Minerals Engineering*, 191, article number 107936. doi: 10.1016/j.mineng.2022.107936.

[29] Zhang, R., Wang, H., Wang, L., & Zheng, Z. (2025). Enhancement of Menaquinone-7 production in *Bacillus subtilis* by optimizing the medium components through response surface methodology. *Bioresources and Bioprocessing*, 12(1), article number 93. doi: 10.1186/s40643-025-00934-0.

[30] Zhao, G., Zhang, D., Li, R., Tang, Y., Wang, J., Hu, X., & Wang, X. (2025). Regulatory mechanism of ferrous ion in enhancing the biosynthesis of L-homoserine, L-threonine, and L-isoleucine in *Corynebacterium glutamicum*. *World Journal of Microbiology and Biotechnology*, 41(10), article number 407. doi: 10.1007/s11274-025-04648-5.

Вплив іонів заліза Fe^{2+} на культивування продуцентів амінокислот аспартатної родини

Ірина Дем'яненко
Кандидат технічних наук, старший викладач
Національний технічний університет України «Київський політехнічний інститут імені Ігоря Сікорського»
03056, просп. Берестейський, 37, м. Київ, Україна
https://orcid.org/0000-0002-0832-3619
Ігор Левтун
Кандидат технічних наук, старший викладач
Національний технічний університет України «Київський політехнічний інститут імені Ігоря Сікорського»
03056, просп. Берестейський, 37, м. Київ, Україна
https://orcid.org/0000-0003-2498-035X

Анотація. Метою дослідження було експериментально оцінити вплив Fe^{2+} (у вигляді $FeSO_4$) на життєздатність і ріст мікроорганізмів-продуцентів амінокислот аспартатної родини. Дослідження виконано в умовах лабораторного культивування з порівнянням контролю і дослідних варіантів; життєздатність визначали за колонієутворюючою здатністю методом послідовних розведень і висіву з перерахунком концентрації клітин, а фізичний компонент оцінювали за ефективною магнітною сприйнятливістю χ, розрахованою з резонансних вимірювань зсуву частоти коливального контуру. Встановлено, що $FeSO_4$ (1 %) спричиняв різке зниження концентрації життєздатних клітин у всіх тестованих штамів: для *Corynebacterium glutamicum* показник зменшувався з 15×10^{10} до 9×10^{8} клітин/см^3, для *Brevibacterium flavum* – з 2×10^{10} до 4×10^{8} клітин/см^3, для *Brevibacterium* sp. 90 – з 3×10^{10} до 8×10^{8} клітин/см^3, що відповідало падінню приблизно на 1,6-2,2 log. Дозозалежний аналіз для *B. flavum* м'ясопептонного бульйону $7{,}97 \times 10^{-3}$-$8{,}459 \times 10^{-3}$, для «клітини + м'ясопептонний бульйон» $8{,}028 \times 10^{-3}$-$8{,}408 \times 10^{-3}$, а відмінності між середовищем і суспензіями з клітинами не виходили за межі $\pm 0{,}4 \times 10^{-3}$. Результати можна безпосередньо використовувати у промислових біотехнологічних та науково-дослідних лабораторіях, які культивують *Corynebacterium/Brevibacterium* для отримання амінокислот, для корекції мікроелементного складу середовищ і оперативного моніторингу життєздатності культур за колонієутворювальною здатністю формувати колонії

Ключові слова: колонієутворювальна здатність; магнітна сприйнятливість; дозозалежний ефект; продуценти; біотехнології

SCIENTIFIC REPORTS OF THE NATIONAL UNIVERSITY OF LIFE AND ENVIRONMENTAL SCIENCES OF UKRAINE

Scientific Journal

Volume 22, No. 2 . 2026

Founded in 2005. Published 6 times a year

Managing editor:
V. Postoi

Publisher's address:
National University of Life and Environmental Sciences of Ukraine
03041, 15 Heroiv Oborony Str., Kyiv, Ukraine
Tel.: +38(044)-258-42-63
E-mail: sr@scireports.com.ua
https://scireports.com.ua/en

НАУКОВІ ДОПОВІДІ НАЦІОНАЛЬНОГО УНІВЕРСИТЕТУ БІОРЕСУРСІВ І ПРИРОДОКОРИСТУВАННЯ УКРАЇНИ

Науковий журнал

Том 22, № 2. 2026

Заснований у 2005 р. Виходить 6 разів на рік

Відповідальний редактор:
В. Постой

Адреса видавництва:
Національний університет біоресурсів і природокористування України
03041, вул. Героїв Оборони, 15, м. Київ, Україна
Тел.: +38(044)-258-42-63
E-mail: sr@scireports.com.ua
https://scireports.com.ua/uk